National Library of Canada
Canadian Theses Service
Ottawa, Canada
K1A 0N4

Bibliothèque nationale du Canada
Service des thèses canadiennes

NOTICE

The quality of this microform is heavily dependent upon the quality of the original thesis submitted for microfilming. Every effort has been made to ensure the highest quality of reproduction possible.

If pages are missing, contact the university which granted the degree.

Some pages may have indistinct print especially if the original pages were typed with a poor typewriter ribbon or if the university sent us an inferior photocopy.

Reproduction in full or in part of this microform is governed by the Canadian Copyright Act, R.S.C. 1970, c. C-30, and subsequent amendments.

AVIS

La qualité de cette microforme dépend grandement de la qualité de la thèse soumise au microfilmage. Nous avons tout fait pour assurer une qualité supérieure de reproduction.

S'il manque des pages, veuillez communiquer avec l'université qui a conféré le grade.

La qualité d'impression de certaines pages peut laisser à désirer, surtout si les pages originales ont été dactylographiées à l'aide d'un ruban usé ou si l'université nous a fait parvenir une photocopie de qualité inférieure.

La reproduction, même partielle, de cette microforme est soumise à la Loi canadienne sur le droit d'auteur, SRC 1970, c. C-30, et ses amendements subséquents.

NL-339 (r. 88/04) c

Canada

University of Alberta

Low-Valent Binuclear Bis(diphenylphosphino)methane-Bridged Complexes of Rhodium and Iridium

by

Ⓒ Robert McDonald

A thesis
submitted to the Faculty of Graduate Studies and Research
in partial fulfilment of the requirements
for the degree of Doctor of Philosophy

Department of Chemistry

Edmonton, Alberta
Fall, 1991

National Library of Canada
Bibliothèque nationale du Canada

Canadian Theses Service
Service des thèses canadiennes

Ottawa, Canada
K1A 0N4

The author has granted an irrevocable non-exclusive licence allowing the National Library of Canada to reproduce, loan, distribute or sell copies of his/her thesis by any means and in any form or format, making this thesis available to interested persons.

The author retains ownership of the copyright in his/her thesis. Neither the thesis nor substantial extracts from it may be printed or otherwise reproduced without his/her permission.

L'auteur a accordé une licence irrévocable et non exclusive permettant à la Bibliothèque nationale du Canada de reproduire, prêter, distribuer ou vendre des copies de sa thèse de quelque manière et sous quelque forme que ce soit pour mettre des exemplaires de cette thèse à la disposition des personnes intéressées.

L'auteur conserve la propriété du droit d'auteur qui protège sa thèse. Ni la thèse ni des extraits substantiels de celle-ci ne doivent être imprimés ou autrement reproduits sans son autorisation.

ISBN 0-315-70093-9

Canada

University of Alberta
Edmonton
Canada T6G 2G2

Department of Chemistry
Faculty of Science
E3-44 Chemistry Bldg., Tel. (403) 492-3254 Fax (403) 492-8231

July 18, 1991

To Whom It May Concern:

Robert McDonald has my permission to use the material contained in Chapters 2 and 3 of his thesis. This material was published with myself and Mr. McDonald as coauthors.

Yours sincerely,

Martin Cowie

Martin Cowie
Professor of Chemistry

:aw

University of Alberta

Release Form

Name of Author:	Robert McDonald
Title of Thesis:	**Low-Valent Binuclear Bis(diphenylphosphino)methane-Bridged Complexes of Rhodium and Iridium**
Degree:	Doctor of Philosophy
Year this Degree Granted:	1991

Permission is hereby granted to the University of Alberta Library to reproduce single copies of this thesis and to lend or sell such copies for private, scholarly or scientific research purposes only.

The author reserves other publication rights, and neither the thesis nor extensive extracts from it may be printed or otherwise reproduced without the author's written permission.

(Signed) Robert McDonald
Robert McDonald

Permanent Address:
#2–Pine Bud Apartments
St. John's, Nfld. A1B 1M5

Date: 19 July 1991

University of Alberta

Faculty of Graduate Studies and Research

The undersigned certify that they have read, and recommend to the Faculty of Graduate Studies and Research for acceptance, a thesis entitled **Low-Valent Binuclear Bis(diphenylphosphino)methane-Bridged Complexes of Rhodium and Iridium** submitted by Robert McDonald in partial fulfilment of the requirements for the degree of Doctor of Philosophy.

Martin Cowie

M. Cowie (Supervisor)

P. J. Crickmore

P. J. Crickmore

N. J. Dovichi

W. A. Graham

W. A. G. Graham

Robert B Jordan

R. B. Jordan

RBJ

L. H. Pignolet

Date: 18 July 1991

To Dad, Mary Catherine and Karen.

Abstract

A series of heterobimetallic RhIr complexes has been synthesized using [RhIrCl$_2$(CO)$_2$(dppm)$_2$] as the main precursor. Reaction with NaBH$_4$ yields [RhIr(CO)$_3$(dppm)$_2$] or [RhIr(H)(CO)$_2$(μ-H)(dppm)$_2$], depending upon whether a CO or H$_2$ atmosphere is employed. Protonation of the tricarbonyl yields, successively, [RhIr(CO)$_3$(μ-H)(dppm)$_2$][BF$_4$] or [RhIr(CO)$_3$(μ-H)$_2$(dppm)$_2$][BF$_4$]$_2$, while [RhIr(H)(CO)$_2$(μ-H)$_2$(dppm)$_2$][BF$_4$] is obtained by protonation of the neutral dihydride. An X-ray structure determination shows [RhIr(CO)$_3$(dppm)$_2$] to have a non-A-frame structure; the coordination geometries about each metal suggest that a dative Ir(-I)→Rh(I) bond is present. As an extension of an earlier study, the related homobimetallic complexes [Ir(CO)(μ-H)(dppm)]$_2$ and [Ir$_2$(CO)$_4$(μ-H)(dppm)$_2$][BF$_4$] were also prepared.

Silanes oxidatively add to [Ir$_2$(CO)$_3$(dppm)$_2$] to give [Ir$_2$(H)$_2$(CO)$_2$(μ-SiRR′)(dppm)$_2$] (RR′ = Me$_2$, Et$_2$, Ph$_2$; R = Ph, R′ = H); these SiR$_2$-bridged complexes are fluxional at room temperature. The X-ray structures of [Ir$_2$(H)$_2$(CO)$_2$(μ-SiPh$_2$)(dppm)$_2$] and [Ir$_2$(H)$_2$(CO)$_2$(μ-SiHPh)(dppm)$_2$] show both to have terminal hydride ligands and cis arrangements of the phosphine ligands at each metal center. The SiPh$_2$-bridged compound has a twisted configuration due to substantial steric interaction between the μ-SiPh$_2$ and dppm groups, whereas the SiHPh-containing species is much less crowded. The similarities of the low-temperature ^{1}H and ^{31}P{^{1}H} NMR spectra of the dialkylsilylene-bridged complexes to those of [Ir$_2$(H)$_2$(CO)$_2$(μ-SiHPh)(dppm)$_2$] at room temperature indicate that a structure similar to

that of the latter compound may be the low-temperature configuration adopted by the $SiMe_2$- and $SiEt_2$-bridged dimers.

The complexes $[M_2(CO)_3(dppm)_2]$ (M = Rh, Ir) react with H_2S to produce $[M_2(CO)_2(\mu\text{-}S)(dppm)_2]$, CO and H_2; the reaction is immediate for M = Rh, while for M = Ir several intermediates of formula $[M_2(H)_2(CO)_2(\mu\text{-}S)(dppm)_2]$ are observed, allowing a mechanism for H_2S addition and H_2 elimination to be proposed. Similar species are observed in the reaction of $[Ir_2(CO)_3(dppm)_2]$ with H_2Se. Exposure of $[RhIr(CO)_3(dppm)_2]$ to H_2S or H_2Se results in formation of $[RhIr(H)(EH)(CO)_2(dppm)_2]$ (E = S, Se), in which the EH ligand bridges the metals in an asymmetric fashion. The reactions of the thiols or selenols REH (E = S, R = Et, Ph; E = Se, R = Ph) with $[Ir_2(CO)_3(dppm)_2]$ yield products of the form $[Ir_2(ER)_2(CO)_2(\mu\text{-}CO)(dppm)_2]$; unlike the reactions involving H_2S or H_2Se, net carbonyl loss does not occur.

Reaction of $[Ir_2(CO)_3(dppm)_2]$ with dimethyl acetylenedicarboxylate (DMAD) initially yields $[Ir_2(CO)_2(\mu\text{-}\eta^1\text{:}\eta^{1'}\text{-DMAD})(dppm)_2]$, which contains a cis-dimetallated olefin unit. This complex undergoes conversion to the more stable form, $[Ir_2(CO)_2(\mu\text{-}\eta^2\text{:}\eta^{2'}\text{-DMAD})(dppm)_2]$, the X-ray structure of which shows the alkyne ligand to now be oriented perpendicular to the metal-metal bond, as part of a dimetallatetrahedrane unit; furthermore, the diphosphine ligands are oriented cis about each metal, in contrast to the trans arrangement in the initial $\mu\text{-}\eta^1\text{:}\eta^{1'}$-alkyne product.

Acknowledgements

Although this section is brief compared to the remainder of this work, I would like to emphasize that the help and friendship of the following people have enabled my stay here to be an enjoyable and rewarding experience.

I thank my supervisor, Martin Cowie, for his guidance, encouragement, **patience** and sense of humour (see: patience) during these past six-plus (!!) years, and for only 'firing' me about once a month. The hospitality that Marty and his wife Gail have shown in hosting numerous group get-togethers (including farewell dinners, World Cup parties and rainy-day barbeques) at their home has been greatly appreciated.

Had I worked alone, I would not have learned or lived as much. I would particularly like to recognize Jim Jenkins, for providing, over several million cups of Java Jive and glasses of Molson's, much valued advice, and for doing something amazing (in a work-related, social, athletic or surreal manner) approximately once a week. Brian Vaartstra is also given a hearty round of applause, for his company during the struggle through the grad school obstacle course, and for not letting religious matters (Oilers vs. Habs) divide us. The friendship of these and other group members, especially (in order of appearance) Steve Sherlock, Thomas Sielisch, Al Hunter (whose group I joined before completion of my thesis writing, and whom I thank for accomodating my 'double life' and for letting me write this thing on his computer), Jianliang Xiao, and Li-Sheng Wang, contributed greatly to making my time in the Cowie group productive and (dare I say it) fun. Of the other friends who made life more enjoyable in and outside of this department, I'd like to single out Bernie Santarsiero, for advice, lunchtime company, Oilers tickets and Christmas dinner; Gary Paul, Keith Lepla, Rob McLaren, Don Mullin, Gord Nicol and Bruce Todd, for their participation in the sports of hockey, softball and 'post-game' (hic); Steve Astley, Mike and Elaine Burke, Evert Ditzel, Dietmar Kennepohl, Gong and Bill Kiel, Richard Krentz, Rob Reed, Lonni Shilliday and John Washington, all of whom helped to create a certain 'esprit de corps' in the Inorganic division; and Laurie and Deb Danielson, John Drover, Dan Raymond and Sabeth Verpoorte, for providing and participating in assorted other good times. I am also indebted to the talented people in the NMR Lab, Spectral Services, the Elemental Analysis Lab, the Machine Shop, the Electronics Shop, the Glass Shop and the General Office, without whose help my work would have been decidedly more difficult.

Despite being four thousand miles (6400 km!) away, my family in Newfoundland has always given me their understanding, interest, faith and encouragement, which have made our separation more bearable. I dedicate this thesis especially to my father, who asked only that I do my best in all things, and to my sister, whose phone calls and letters kept me from feeling too far from home.

The other person to whom this work is dedicated is my fiancée, Karen McLeod, who, although immersed in demanding graduate research of her own, always gave me motivation to overcome various trials and frustrations, and company to celebrate the successes.

Table of Contents

Chapter 1

Introduction ... 1

References and Footnotes ... 15

Chapter 2

Diiridium and Mixed Rhodium-Iridium Hydridocarbonyl Complexes and the Structure of [RhIr(CO)$_3$(dppm)$_2$], a Complex Containing an Ir(-I)→Rh(I) Dative Bond ... 24

Introduction ... 24

Experimental Section ... 25

Preparation of Compounds ... 26

X-ray Data Collection ... 33

Structure Solution and Refinement ... 34

Results and Discussion ... 37

(a) Description of Structure ... 37

(b) Preparation and Characterization of Compounds ... 47

Conclusions ... 67

References and Footnotes ... 69

Chapter 3

Binuclear Oxidative Additions of Silanes to [Ir$_2$(CO)$_3$(dppm)$_2$] ... 74

Introduction ... 74

Experimental Section ... 75

Preparation of Compounds 75

X-ray Data Collection 78

(a) $[Ir_2(H)_2(CO)_2(\mu\text{-}SiPh_2)(dppm)_2]\cdot 2THF$ (4) 78

(b) $[Ir_2(H)_2(CO)_2(\mu\text{-}SiHPh)(dppm)_2]\cdot 2THF$ (5) 82

Structure Solution and Refinement 82

Results and Discussion 84

(a) Description of Structures 84

(i) $[Ir_2(H)_2(CO)_2(\mu\text{-}SiPh_2)(dppm)_2]\cdot 2THF$ (4) 84

(ii) $[Ir_2(H)_2(CO)_2(\mu\text{-}SiHPh)(dppm)_2]\cdot 2THF$ (5) 99

(b) Preparation and Characterization of Compounds 103

Conclusions 121

References and Footnotes 122

Chapter 4

Oxidative Additions of S-H and Se-H Bonds to $[MM'(CO)_3(dppm)_2]$ (MM' = Rh_2, Ir_2, RhIr) 126

Introduction 126

Experimental Section 127

Preparation of Compounds 128

X-ray Data Collection 134

Structure Solution and Refinement 135

Results and Discussion 138

(a) Description of Structure 138

(b) Description of Chemistry 146

Conclusions 168

References and Footnotes 170

Chapter 5

Interconversion Between Isomeric Alkyne-Bridged Diiridium Complexes and the Structure of $[Ir_2(CO)_2(\mu\text{-}\eta^2{:}\eta^{2'}\text{-}DMAD)(dppm)_2]\cdot 2CH_2Cl_2$ 176
Introduction 176
Experimental Section 178
Preparation of $[Ir_2(CO)_2(\mu\text{-}\eta^2{:}\eta^{2'}\text{-}DMAD)(dppm)_2]$ (3) 178
X-ray Data Collection 179
Structure Solution and Refinement 180
Results and Discussion 186
(a) Description of Structure 186
(b) Description of Chemistry 197
Conclusions 203
References and Footnotes 204

Chapter 6

Conclusions 208
References and Footnotes 218

Appendix

Solvents and Drying Agents 219

List of Tables

Chapter 2

Table 2.1 Spectroscopic Data for the Compounds of Chapter 2 27

Table 2.2 Crystallographic Data for [RhIr$(CO)_3(dppm)_2$] (3) 35

Table 2.3 Positional and Thermal Parameters for the Atoms of Complex **3** 38

Table 2.4 Selected Distances (Å) in Complex **3** 41

Table 2.5 Selected Angles (deg) in Complex **3** 42

Chapter 3

Table 3.1 Spectroscopic Data for the Compounds of Chapter 3 76

Table 3.2. Crystallographic Data for [$Ir_2(H)_2(CO)_2(\mu$-$SiPh_2)(dppm)_2$]-•2THF (4) and [$Ir_2(H)_2(CO)_2(\mu$-$SiHPh)(dppm)_2$]•2THF (5) ... 80

Table 3.3. Positional and Thermal Parameters of the Atoms of Complex **4** 85

Table 3.4. Selected Distances (Å) in Complex **4** 87

Table 3.5. Selected Angles (deg) in Complex **4** 88

Table 3.6. Positional and Thermal Parameters of the Atoms of Complex **5** 89

Table 3.7. Selected Distances (Å) in Complex **5** 92

Table 3.8. Selected Angles (deg) in Complex **5** 93

Table 3.9. Free Energies of Activation for the Fluxional Silylene-Bridged Complexes [$Ir_2(H)_2(CO)_2(\mu$-$SiR_2)(dppm)_2$] (2–4) .. 117

Chapter 4

Table 4.1 Infrared Spectroscopic Data for the Compounds of Chapter 4 129

Table 4.2 Nuclear Magnetic Resonance Spectroscopic Data for the Compounds of Chapter 4 130

Table 4.3. Crystallographic Data for $[Ir_2(SPh)_2(CO)_2(\mu\text{-}CO)(dppm)_2]\cdot{}^1/_2CH_2Cl_2$ (17) 136

Table 4.4. Positional and Thermal Parameters of the Atoms of Complex 17 139

Table 4.5. Selected Distances (Å) in Complex 17 141

Table 4.6. Selected Angles (deg) in Complex 17 142

Table 4.7. NMR Spectroscopic Parameters for the Species Observed in the Reaction of 2 with H_2Se 155

Chapter 5

Table 5.1 Crystallographic Data for $[Ir_2(CO)_2(\mu\text{-}\eta^2{:}\eta^{2'}\text{-}DMAD)(dppm)_2]\cdot 2CH_2Cl_2$ (3) 181

Table 5.2. Positional and Thermal Parameters of the Atoms of Complex 3 183

Table 5.3. Selected Distances (Å) in Complex 3 187

Table 5.4. Selected Angles (deg) in Complex 3 188

List of Figures

Chapter 2

Figure 2.1. Perspective view of $[RhIr(CO)_3(dppm)_2]$ (3) showing the numbering scheme........43

Figure 2.2. View of complex 3 approximately along the Rh-Ir bond, omitting the phenyl carbon atoms except those bound to phosphorus........44

Figure 2.3. The $^{31}P\{^1H\}$ NMR spectrum of 3 at 20 °C........54

Figure 2.4. The $^{31}P\{^1H\}$, ^1H and $^1H\{^{31}P\}$ NMR spectra of 6 at 20 °C........61

Figure 2.5. The $^{31}P\{^1H\}$, ^1H and $^1H\{^{31}P\}$ NMR spectra of 7 at 20 °C........65

Chapter 3

Figure 3.1. Perspective view of $[Ir_2(H)_2(CO)_2(\mu\text{-}SiPh_2)(dppm)_2]$ (4) showing the numbering scheme........95

Figure 3.2. View of complex 4 omitting the phenyl carbon atoms except those bound to phosphorus and silicon........96

Figure 3.3. Perspective view of $[Ir_2(H)_2(CO)_2(\mu\text{-}SiHPh)(dppm)_2]$ (5) showing the numbering scheme........100

Figure 3.4. View of complex 5 omitting the dppm phenyl carbon atoms except those bound to phosphorus........101

Figure 3.5. The $^{31}P\{^1H\}$, ^1H and $^1H\{^{31}P\}$ NMR spectra of complex 2 at 20 °C and -60 °C........106

Figure 3.6. The $^{31}P\{^1H\}$, ^1H and $^1H\{^{31}P\}$ NMR spectra of complex 4 at 20 °C and -60 °C........108

Figure 3.7. The $^{31}P\{^{1}H\}$, ^{1}H and $^{1}H\{^{31}P\}$ NMR spectra of complex **5** at 20 °C 110

Chapter 4

Figure 4.1. Perspective view of $[Ir_2(SPh)_2(CO)_2(\mu\text{-}CO)(dppm)_2]$ (**17**) showing the numbering scheme 143

Chapter 5

Figure 5.1. Perspective view of $[Ir_2(CO)_2(\mu\text{-}\eta^2{:}\eta^{2'}\text{-}DMAD)(dppm)_2]\text{-}\bullet 2CH_2Cl_2$ (**3**, molecule A) showing the numbering scheme 190

Figure 5.2. Perspective view of complex **3** (molecule B) 191

Figure 5.3. View of complex **3**, molecule A, omitting all dppm phenyl carbons except those bound to phosphorus 192

Figure 5.4. View of complex **3**, molecule B, omitting all dppm phenyl carbons except those bound to phosphorus 193

List of Schemes

Chapter 2

Scheme 2.1 53

Chapter 4

Scheme 4.1 148

Scheme 4.2 149

Scheme 4.3 159

List of Abbreviations and Symbols

anal	analyses
ca.	circa (approximately)
calcd	calculated
DMAD	dimethyl acetylenedicarboxylate, $CH_3O_2C\text{-}C{\equiv}C\text{-}CO_2CH_3$
dppm	bis(diphenylphosphino)methane, $(C_6H_5)_2PCH_2P(C_6H_5)_2$
Et	ethyl, CH_3CH_2–
h	hour(s)
HFB	hexafluoro-2-butyne, $F_3C\text{-}C{\equiv}C\text{-}CF_3$
IR	infrared
Me	methyl, CH_3–
MeOH	methanol, CH_3OH
mg	milligrams
min	minute(s)
mL	milliliters
mmol	millimoles
NMR	nuclear magnetic resonance
Ph	phenyl, C_6H_5–
s	second(s)
THF	tetrahydrofuran, C_4H_8O
μL	microliters
μmol	micromoles

Crystallographic Abbreviations and Symbols

a, b, c	lengths of the x, y, and z axes, respectively, of the unit cell
B	isotropic thermal parameter
deg (or °)	degrees
F_c	calculated structure factor
F_o	observed structure factor
h, k, l	Miller indices defining lattice planes, where the plane intersects the unit cell axes at $1/h$, $1/k$ and $1/l$ of the respective lengths of a, b and c
p	experimental instability factor (used in the calculation of $\sigma(I)$ to downweight intense reflections)
R	residual index (a measure of agreement between calculated and observed structure factors)
R_w	weighted residual index
V	unit cell volume
w	weighting factor applied to structure factor
Å	Angstrom(s) (1 Å = 10^{-10} meters)
α, β, γ	angles between b and c, a and c, and a and b axes, respectively, of unit cell
β_{ij}	anisotropic displacement parameters
λ	wavelength
ρ	density
σ	standard deviation

Chapter 1

Introduction

Interest in binuclear transition metal complexes has arisen due to their potential to display reactivity patterns and structures not possible for mononuclear complexes; in particular it is anticipated that binuclear species may display cooperative effects between metal centers in close proximity.[1] Such cooperativity may be as simple as the binding of a substrate molecule or fragment in a bridging fashion, but may be significant in stabilizing the coordinated form of the substrate, or affecting the further reactivity of the ligand, compared to the terminally-bound form.[2] Another scenario would involve binding of a ligand by one nucleus while the second center acts as an electron sink or source, resulting in a transfer of electrons between metal centers, facilitating redox reactions that for a mononuclear system would involve too great a change in metal oxidation state.[3] There is also the possibility that a substrate molecule may be activated at one metal center and then be induced to react with molecules or fragments that are coordinated to the adjacent metal.[2]

Credit for the first binuclear complexes that have exploited some or all of the above properties goes not to any particular researcher or group but to nature. Hemerythrin (an oxygen transport protein in several species of marine worms),[4-9] methane monooxygenase (which catalyzes conversion of CH_4 to CH_3OH in several forms of bacteria),[7,9] and ribonucleotide reductase (which catalyzes the formation of deoxyribonucleotide di- and triphosphates, an important first step in DNA synthesis)[8,10] are metalloenzymes each having two iron atoms in close proximity present at the protein's active site, while hemocyanin (the oxygen-transport protein of several crustacean species)[11,12] and superoxide dismutase (which catalyzes diproportionation of O_2^- into O_2 and H_2O_2),[13,14] respectively, possess Cu-Cu and Cu-Zn units at their active sites. The study of the roles and structures of these enzymes is an ongoing concern of many biological and bioinorganic chemists, and the disciplines of "biological" and "inorganic" chemistry are further intertwined by the continuing attempts of coördination chemists to prepare complexes that mimic properties of the metalloproteins.[15]

Compounds containing associated metal centers are also of great interest to synthetic and theoretical inorganic chemistry, not only for the challenges of synthesis of the many forms thus far observed, but also in development of explanations of the bonding between metals. According to the definition propounded by Cotton,[16] metal cluster compounds, i.e. "those containing a finite group of metal atoms that are held together…to a significant extent by bonds directly between the metal atoms, even though some non-metal atoms may be associated intimately with the cluster," would include many binuclear complexes as the simplest form. Understanding the bonding between two metals serves as an important first step towards developing theories that explain bonding interactions within higher-nuclearity metal cluster complexes,[17] which themselves can be regarded as model systems for bulk metals.[18,19]

A great deal of the attention accorded binuclear complexes has been due to the relevance of their chemistry towards catalysis. These are the simplest systems in which interactions between small molecules and more than one metal nucleus can be studied, a situation directly applicable to heterogeneous catalysis, where the bonding between catalyst and substrate is often believed to involve several neighboring metal atoms.[20-24] Although a wealth of methods are employed to study heterogeneous catalytic materials,[21,25-27] the exact modes of metal-substrate coordination are difficult to directly observe, thus models are important in elucidating mechanisms of action of these catalysts.

Since homogeneous catalysts are most often mononuclear species, modelling of their mechanisms of action does not usually involve binuclear complexes. However, binuclear complexes have attracted much attention due to their potential to combine desirable characteristics of homogeneous and heterogeneous catalysts (i.e. the milder reaction conditions and improved selectivities of the former and the cooperative substrate activation of the latter). In some systems, e.g. the reduction of triply-bonded substrates such as carbon monoxide[20] and alkynes,[28] it has been proposed that multinuclear complexes would afford a better chance of substrate activation, due to their increased ability to coordinate both atoms of the triple bond simultaneously. In this manner, these complexes would have the potential of extending Fischer-Tropsch chemistry (the synthesis of multicarbon products from CO and H_2) from the heterogeneous conditions currently employed in industry[24] to homogeneous conditions.[20]

During chemical reactions involving binuclear complexes, changes of oxidation state and coordination geometry can often result in changes in bond order between the two metals, thus bridging ligands are often employed to prevent fragmentation of these complexes into mononuclear species. One ligand system commonly used to maintain metals in a binuclear framework involves dialkyl or diaryl phosphine groups joined by one or more methylene units, with the phosphorus atoms at each end of the $R_2P(CH_2)_nPR_2$ chain coordinating to different metal centers. One of these, bis(diphenylphosphino)methane (dppm), has attracted the attention of numerous research groups since the synthesis of the first dppm-bridged complex, $[\{CpFe(\mu\text{-}CO)\}_2(\mu\text{-}dppm)]$, by Haines and coworkers in 1968.[29] The chemistry of compounds containing dppm has been the subject of several excellent review articles by Puddephatt,[30] Balch[3] and Poilblanc,[31] thus a comprehensive survey will not be attempted here; however, some important general information about diphosphine complexes and some brief details of chemistry relevant to the work discussed in later chapters of this thesis will be given.

One of the reasons for the popularity of dppm in the synthesis of binuclear compounds is its similarity to triphenylphosphine, a ubiquitous ligand in mononuclear coordination chemistry; both are inexpensive, virtually odorless, air-stable solids that readily form complexes with late transition metals. In contrast, bis(dimethylphosphino)methane (dmpm), a similar ligand that would be attractive due to its decreased steric bulk and increased basicity,[32] has been much less utilized. The comparatively high cost and pyrophoric nature of dmpm are significant drawbacks, but, perhaps more importantly, reactions involving this ligand or its complexes tend to be much more difficult to control, due to the tendency of the products to be highly fluxional and prone to subsequent rearrangement.[33] Another advantage of dppm is its marked tendency to bridge two metal centers; although many examples of mononuclear complexes containing chelating dppm groups are known (e.g. [Fe(CO)$_3$-(dppm)],[34a] [RhHCl(dppm)$_2$]$^+$,[34b], [Pt(alkyl)$_2$(dppm)],[34c] [W(N$_2$)$_2$(dppm)$_2$[34d]), crystallographic studies have shown that the four-membered chelate rings present in these compounds tend to be strained. The preference of dppm to adopt bridging over chelated coordination modes not only simplifies syntheses of homobinuclear compounds, but also allows the chelated species to be employed in the production of binuclear complexes containing two different metals, an approach exploited by, among others, Shaw and coworkers. Shaw's group demonstrated that reaction of complexes containing chelated (e.g. [M(CO)(η^2-dppm)$_2$]$^+$, M = Rh, Ir) or "dangling" (e.g. [M(C$\equiv$CPh)(η^1-dppm)$_2$], M = Pd, Pt) diphosphine groups with stoichiometric equivalents of other coordinatively unsaturated or labile metal complexes (e.g. [CuC$\equiv$CPh], [AgCl(PPh$_3$)]$_4$, [Rh$_2$(μ-Cl)$_2$(CO)$_4$]) often results in capture of the second metal, making accessible a wide variety of heterobimetallic compounds.[35] A large number of binuclear dppm complexes studied contain two of the diphosphine bridges, but species having one dppm group spanning the metals are also common;[29,36] tris(dppm)-bridged complexes are rare, but at least one example, [Pt$_2$(dppm)$_3$],[37] has been characterized.

Three arrangements of the diphosphine ligands in the doubly-bridged species have been observed. Most commonly, the dppm groups are oriented trans to each other about each metal center as shown in the leftmost structure below, in which P$\frown$P represents the dppm ligand (the dashed line indicates that a metal-metal bond may or may not be present).

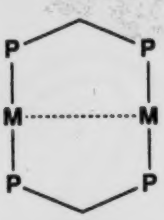

trans,trans

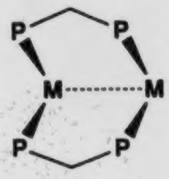

cis,cis

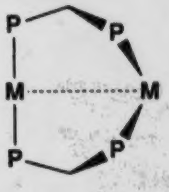

trans,cis

A few examples of structurally-characterized complexes representative of this category include $[Pd_2Cl_2(\mu\text{-}\eta^1\text{:}\eta^{1'}\text{-}CF_3C{\equiv}CCF_3)(dppm)_2]$,[38] $[Rh_2(CO)_2\text{-}(\mu\text{-}\eta^1\text{:}\eta^{2'}\text{-}C{\equiv}CBu^t)(dppm)_2][ClO_4]$[39] and $[(OC)_3MnPdBr(dppm)_2]$.[40] Less often the ligands occupy coordination sites at cis positions at each metal, as observed in the compounds $[Ni_2(CO)_2(\mu\text{-}CO)(dppm)_2]$[41] and $[CoRh(CO)_2\text{-}(\mu\text{-}H)(\mu\text{-}PPh_2)(dppm)_2]$.[42] An even smaller number, including $[Pt_2(CH_3)_3\text{-}(dppm)_2][PF_6]$[43] and $[(PhC{\equiv}C)(OC)IrCuCl(dppm)_2]$,[35i] contain a mixed geometry in which the phosphines are trans to each other at one metal center and cis at the other.

An advantageous property of dppm is its ability to span a wide range of intermetal separations. Metal-metal distances between 2.4 and 3.6 Å are commonly accommodated by bridging dppm ligands; in extreme cases, separations as large as 4.361(1) Å (in the complex *cis,cis*-$[Pt_2Me_4\text{-}(dppm)_2]$[44]) or as small as 2.138(2) Å (in $[Mo_2Cl_4(dppm)_2]$[45]) have been observed. Such flexibility is desirable as it allows the ligands to adjust to changes in the metal's oxidation state and coordination geometry that frequently accompany chemical reactions. In addition, binuclear complexes often undergo formation or cleavage of metal-metal bonds, necessitating shortening or lengthening of internuclear distances. In contrast to the ability of dppm bridges to accommodate such changes, the heterodifunctional ligand 2-(diphenylphosphino)pyridine (Ph_2Ppy),[46] which is similar to dppm in having a one-carbon-atom span between the two ligating atoms (P and N in the case of Ph_2Ppy), has been much less widely employed; its smaller bite distance renders it less able to span binuclear systems in which no formal metal-metal bond is involved.

Another attractive feature of dppm-containing compounds is that they are amenable to characterization in solution via multinuclear nuclear magnetic resonance (NMR) spectroscopy. The presence of four spin-active phosphorus-31 nuclei (100% isotopic abundance) in each bis(dppm)-bridged dimer makes ^{31}P NMR spectroscopy a sensitive probe of the structure of the complex. A homobimetallic bis(dppm)-bridged species in which the coordination spheres of both metal centers are identical possesses four chemically equivalent phosphorus nuclei and thus will give rise to one singlet resonance. If the environments of the metal atoms are in any way different, or if the complex is heterobimetallic, the sets of phosphorus atoms attached to each center will be inequivalent, and two multiplet resonances will be observed. In rare cases, such as in the complex $[IrOs(H)_2(CO)_3(\mu\text{-}\eta^3\text{-}(o\text{-}C_6H_4)PhPCH_2PPh_2)(dppm)]$,[47] which contains an orthometallated phosphine phenyl group as shown below, all four phosphorus environments are inequivalent. The dispositions of

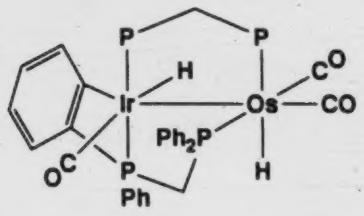

ligands such as hydride or carbonyl groups can be determined from the multiplicities of the resonances in the respective ^1H and $^{13}C\{^1H\}$ NMR spectra (observation and assignment of the latter resonances is aided by use of ^{13}C-enriched carbon monoxide in the preparation of the compound of interest). Furthermore, in the case of asymmetric complexes the attachment of such ligands to one metal center or the other can be established through use of selective heteronuclear decoupling ($^1H\{^{31}P\}$, $^{13}C\{^{31}P\}$) techniques, in which irradiation at the frequency corresponding to the chemical shift of the phosphorus nuclei coordinated to one metal center should produce a simplification of the multiplets observed for other spin-active ligands attached to the same metal center (provided that the couplings between the ligands and the phosphorus nuclei can be observed). These heteronuclear decoupling techniques greatly aid in the characterization of mixtures containing several species, where attempts to correlate combinations of phosphorus, carbon and proton signals based solely on relative peak areas can produce uncertain results.

The ^1H NMR resonances due to the protons of the methylene group bridging the two phosphorus atoms of the dppm ligand can also yield valuable structural information, especially as a probe of possible "front-to-back" asymmetry of the complex. Although the solid-state structure of a complex such as *trans*-$[RhCl(CO)(dppm)]_2$ shows folding of the dppm bridges to produce inequivalent environments for the methylene hydrogens, in solution a "flipping" mechanism of interchange, as shown below,

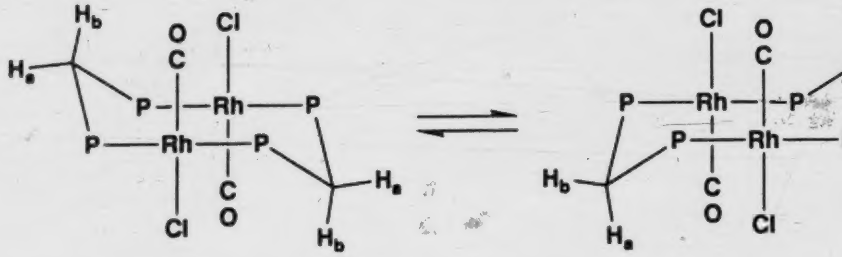
H_b
O
C
Cl
H_a
P
Rh
P
P
Rh
P
C
O
Cl
H_a
H_b
Cl
O
C
H_a
H_b
P
Rh
P
P
Rh
P
H_b
C
O
Cl
H_a

is facile and results in a time-averaged equivalence of these protons (H_a and H_b). A contrasting case is presented by a compound such as $[PdCl_2(\mu\text{-}S)(dppm)_2]$, which in the solid state shows the dppm methylene groups to be preferentially folded over the bridging sulfur as shown in the leftmost structure below. Again, two inequivalent environments for the

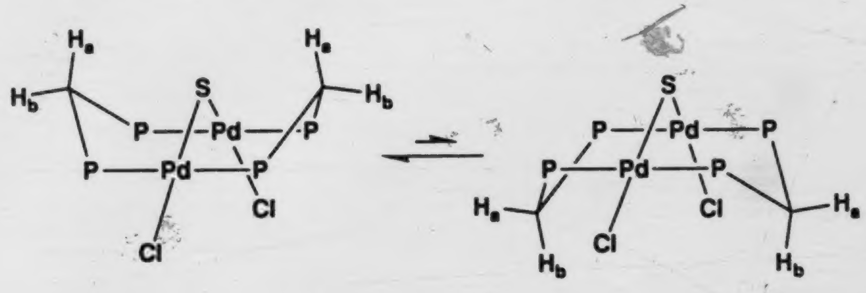
H_a
H_b
S
H_a
H_b
P
Pd
P
P
Pd
P
Cl
Cl
S
P
Pd
P
P
Pd
P
H_a
Cl
Cl
H_a
H_b
H_b

methylene hydrogens are present, but in this case H_a and H_b can never undergo equilibration; in either conformation H_b is always exo to the sulfide bridge, so H_a and H_b remain chemically distinct. The appearance of these resonances can serve as an indication of fluxionality of the complex, especially if only one resonance is seen for a species in which the two sides of the M_2P_4 unit are inherently inequivalent. Using variable-temperature NMR spectroscopy Puddephatt and coworkers have shown that the complex $[Pt_2(H)_2(\mu\text{-}H)(dppm)_2]^+$ [48] undergoes such an equilibration of the methylene proton signals, and have proposed that the interchange pathway involves a "tunnelling" of the bridging hydride between the metals from one side of the Pt_2P_4 to the other, as shown below. A similar mechanism has been proposed to account for the room-temperature equivalence of the dppm methylene protons of $[RhFe(CO)_3(\mu\text{-}H)(dppm)_2]$.[49] An additional advantageous feature of the dppm CH_2 bridge is that, in general, these methylene protons are reasonably inert to deprotonation and substitution reactions, making them a reliable internal standard for assigning the number of hydrides or other proton-bearing groups contained in the complex, as well as for confirming the quantity of solvent of crystallization present in a crystalline solid.

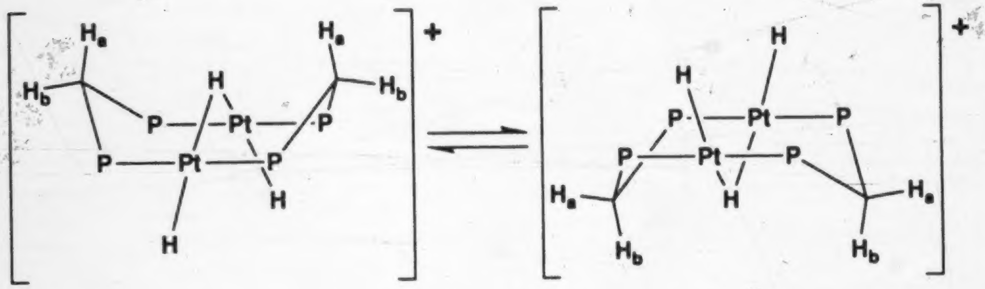

The demonstrated utility of mononuclear complexes containing metals from groups 8, 9 and 10 of the periodic table (the iron, cobalt and nickel triads) to act as effective and economical homogeneous catalysts[50] for such industrially-important processes as hydrogenation,[51,52] hydroformylation,[53,54] alcohol carbonylation,[55,56] alkene hydrosilation,[57] and hydrocyanation[52,58] has inspired investigations into the possible catalytic activity of dppm complexes of these metals. The fact that such catalytically-active compounds as [$HRuCl(PPh_3)_3$], [$RhCl(PPh_3)_3$], [$HRh(CO)(PPh_3)_3$] and [$Ni(P(OPh)_3)_3$] contain relatively simple ligands in their coordination spheres invites comparison with dppm-bridged species like *trans*-[RhCl(CO)(dppm)]$_2$[59,60] and [Rh(CO)(μ-H)(dppm)]$_2$,[61] and suggests that these or related complexes might be capable of similar activity. In fact, studies have shown that the complexes [Rh(CO)(μ-H)(dppm)]$_2$,[61] [$Rh_2(CO)_2(\mu$-H)(μ-CO)(dppm)$_2$]$^+$,[62,63] [$Rh_2(CO)_2(\mu$-OH)(dppm)$_2$]$^+$,[64,65] *trans*-[Rh(CN)(CO)(dppm)]$_2$,[66] [$Rh_2(CO)_2(\mu$-Cl)(dppm)$_2$]$^+$,[67-69] [$Rh_2Cl_2(\mu$-CO)(dppm)$_2$],[70] [PdCl(dppm)]$_2$[71-73] and [$Pt_2(H)_2(\mu$-H)(dppm)$_2$]$^+$ [74] can act as catalysts or catalyst precursors in one or more of such processes as the hydrogenation of alkynes,[63,67,70] olefins[63] or aldehydes,[63] the water-gas shift reaction,[63,64,74] the hydroformylation of olefins,[63] and the cyclotrimerization of alkynes;[38,70,71] however, all of these cases suffer from slow turnover rates and low product yields. Although the related iridium complexes [$Ir_2(CO)_2(\mu$-S)(dppm)$_2$][75,76] and [$Ir_2(H)_2(CO)_2(\mu$-Cl)(dppm)$_2$]$^+$ [77,78] were also found to catalyze the hydrogenation of alkynes and olefins, diiridium species appear on the whole to be much less suitable catalytic agents than do their dirhodium counterparts, mainly due to the greater strengths of Ir-H and Ir-C bonds compared to Rh-H and Rh-C bonds.[79] These properties would tend to work in favor of the formation of adducts between the substrate and the diiridium complex, but would discourage elimination processes leading to the desired products. The stability of such adducts can tremendously aid in the elucidation of catalytic mechanisms, as was done in several studies[64,76-78,80-82] in which the catalytic activity of dirhodium complexes was modelled through the preparation and characterization of series of diiridium analogues of the presumed intermediates. These series were built up through elementary chemical steps believed active in the catalytic processes (e.g. loss or gain of halide ion, CO, H_2, H^+), and could be used to determine the possible roles of both metals acting in concert to accomplish a chemical transformation, as well as to predict which steps would be rate-determining in the actual catalytic process.

Studies of oxidative additions to, and coordination of unsaturated organic substrates by, dppm-bridged binuclear complexes of low-oxidation-state late transition metals are presently less exhaustive than those for similar mononuclear compounds. However, $M_2(dppm)_2$ complexes have been observed to oxidatively add a wide variety of substrates, including dihydrogen,[75,76,81] halogens,[83,84] protonic acids,[62-64,85,86] hydrogen halides,[61,85] silanes,[87,88] hydrogen sulfide,[89-92] thiols,[92-94] disulfides,[92,95] and to coordinate oxygen[96] and alkynes.[38,70,77,78,80,82,97-103] Both one-center and two-center modes of substrate interaction were observed, indicating the versatility of binuclear systems in the activation of small molecules, and illustrating their potential to serve as catalysts or models thereof, since the mechanisms by which catalysts activate and transform substrates involve one and frequently both of these processes.

At the outset, there were two main goals of this thesis project. One objective was to extend the already well-characterized series of homobinuclear rhodium and iridium complexes, containing (apart from the dppm bridges) only hydride and carbonyl ligands, to include heterobinuclear rhodium-iridium systems. This family of hydridocarbonyl complexes can be seen as dimeric analogues of such species as [RhH(CO)-$(PPh_3)_2$], which is believed to be catalytically active in olefin hydrogenation and hydroformylation reactions.[51,53] It was anticipated that the rhodium-iridium compounds would not only combine attractive characteristics due to both types of metals (the catalytic activity of rhodium complexes, the stability of adducts with iridium species) that would aid future investigations into modelling of catalytic cycles, but might also display modes of structure and reactivity not previously seen in the homobimetallic systems. A second goal was to study the reactivity of the formally zerovalent complexes of formula [MM'$(CO)_3(dppm)_2$]. The dirhodium and diiridium compounds (MM' = Rh_2,[63,104] Ir_2[80]) had been previously characterized, while synthesis of the rhodium-iridium analogue (MM' = RhIr) was to be accomplished in connection with the studies of mixed-metal hydridocarbonyl complexes as described above. Despite the possibility of a symmetrical formulation for the homobimetallic tricarbonyl complexes (i.e. [$M_2(CO)_2(\mu\text{-}CO)(dppm)_2$]), the X-ray structure determination of [$Rh_2(CO)_3(dppm)_2$] indicated an asymmetric structure,[104] as illustrated below (with the dashed line indicating a weak semibridging interaction between the metal M and one of the CO ligands attached to

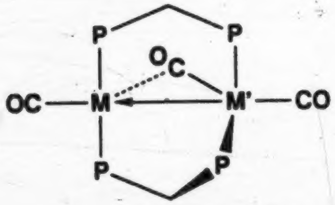

[$Rh_2(CO)_3(dppm)_2$]: M = M' = Rh

[$Ir_2(CO)_3(dppm)_2$]: M = M' = Ir

[$RhIr(CO)_3(dppm)_2$]: M = Rh, M' = Ir

M′). The coordination geometries at the metal centers suggest a mixed-valence dimetal core, with a dative metal-metal bond between the d^{10} M′(-I) center to the d^8 M(I) nucleus. Whatever the oxidation-state formulation for the metals, it was believed that the low oxidation states of both metals, the built-in coordinative unsaturation at one metal, and the presumed lability of the metal-metal bond of these species would make them susceptible to reaction with substrates containing bonds between hydrogen and silicon, sulfur or selenium, and with unsaturated organic substrates. Work towards both of these goals was to consist of synthesis and characterization of new complexes and studies of their further reactivity. To this end, multinuclear NMR spectroscopy, particularly ^{1}H, ^{31}P, and ^{13}C studies, would be the most useful technique for elucidation of the structures of the species observed, especially for unstable reactive intermediates. X-ray structural determinations of some of the compounds would also be undertaken, not only to provide definitive proof for the structures proposed for the particular compounds under study, but also to increase the bank of knowledge concerning the structures of dppm-bridged diiridium and mixed rhodium-iridium complexes.

References and Footnotes

1. Chisholm, M. H. In *Reactivity of Metal-Metal Bonds*; Chisholm, M. H. ed. *ACS Symp. Ser.* **1981**, *155*, 17.
2. Brown, M. P.; Fisher, J. R.; Franklin, S. J.; Puddephatt, R. J.; Thomson, M. A. In *Catalytic Aspects of Molecular Phosphine Complexes*; Alyea, E. C.; Meek, D. W., eds. *Adv. Chem. Ser.* **1982**, *196*, 231.
3. Balch, A. L. In *Homogeneous Catalysis with Metal Phosphine Complexes*; Pignolet, L. H., Ed.; Plenum: New York, 1983; pp. 167-213.
4. Wilkins, R. G.; Harrington, P. C. *Adv. Inorg. Biochem.* **1983**, *5*, 51.
5. Klotz, I. M.; Kurtz, D. M., Jr. *Acc. Chem. Res.* **1984**, *17*, 16.
6. Wilkins, P. C.; Wilkins, R. G. *Coord. Chem. Rev.* **1987**, *79*, 195.
7. Kurtz, D. M., Jr. *Chem. Rev.* **1990**, *90*, 585.
8. Vincent, J. B.; Olivier-Lilley, G. L.; Averill, B. A. *Chem. Rev.* **1990**, *90*, 1447.
9. Que, L., Jr.; True, A. E. *Prog. Inorg. Chem.* **1990**, *38*, 97.
10. Sjoberg, B.-M.; Graslund, A. *Adv. Inorg. Biochem.* **1983**, *5*, 87.
11. Gaykema, W. P. J.; Hol, W. G. J.; Vereijken, J. M.; Soeter, N. M.; Bak, H. J.; Beintema, J. J. *Nature* **1984**, *309*, 23.
12. Linzen, B.; Soeter, N. M.; Riggs, A. F.; Schneider, H.-J.; Schartau, W.; Moore, M. D.; Yokota, E.; Behrens, P. Q.; Nakashima, H.; Takagi, T.; Nemoto, T.; Vereijken, J. M.; Bak, H. J.; Beintema, J. J.; Volbeda, A.; Gaykema, W. P. J. *Science* **1985**, *229*, 519.
13. Argese, E.; Viglino, P.; Rotilio, G.; Scarpa, M.; Rigo, A. *Biochemistry*

1987, *26,* 3224.

14. Roe, J. A.; Butler, A.; Scholler, D. M.; Valentine, J. S.; Marky, L.; Breslauer, K. J. *Biochemistry* **1988,** *27,* 950.
15. Kurtz, D. M., Jr. *Chem. Rev.* **1990,** *90,* 585.
16. Cotton, F. A. *Quart. Rev.* **1966,** *20,* 389.
17. Cotton, F. A.; Wilkinson, G. *Advanced Inorganic Chemistry,* 4th ed.; John Wiley and Sons: New York, 1980; pp. 1109-1110.
18. Cotton, F. A. In *Reactivity of Metal-Metal Bonds;* Chisholm, M. H. ed. *ACS Symp. Ser.* **1981,** *155,* 1.
19. Mingos, D. M. P. *Chem. Soc. Rev.* **1986,** *15,* 31.
20. Muetterties, E. L.; Stein, J. *Chem. Rev.* **1979,** *79,* 479.
21. Roberts, M. W. *Chem. Soc. Rev.* **1977,** *6,* 373.
22. Muetterties, E. L. In *Reactivity of Metal-Metal Bonds;* Chisholm, M. H. ed. *ACS Symp. Ser.* **1981,** *155,* 273.
23. Muetterties, E. L.; Rhodin, R. N.; Band, E.; Brucker, C. F.; Pretzer, W. F. *Chem. Rev.* **1979,** *79,* 91.
24. Rofer-DePoorter, C. S. *Chem. Rev.* **1981,** *81,* 447.
25. Davis, S. C.; Klabunde, K. J. *Chem. Rev.* **1982,** *82,* 153.
26. Somorjai, G. A. *Chem. Soc. Rev.* **1984,** *13,* 321.
27. Castner, D. G.; Somorjai, G. A. *Chem. Rev.* **1979,** *79,* 233.
28. Muetterties, E. L. *Pure Appl. Chem.* **1978,** *50,* 941.
29. Haines, R. J.; du Preez, A. L.; Wittmann, G. T. W. *Chem. Commun.* **1968,** 611.
30. Puddephatt, R. J. *Chem. Soc. Rev.* **1983,** *12,* 99.
31. Chaudret, B.; Delavaux, B.; Poilblanc, R. *Coord. Chem. Rev.* **1988,** *86,*

191.

32. (a) Karsch, H. H.; Milewski-Mahrla, B. *Angew. Chem., Int. Ed. Engl.* **1981,** *20,* 814. (b) King, R. B.; RaghuVeer, K. S. *Inorg. Chem.* **1984,** *21,* 246. (c) Kullberg, M. L.; Lemke, F. R.; Powell, D. R.; Kubiak, C. P. *Inorg. Chem.* **1985,** *24,* 3589. (d) Kullberg, M. L.; Kubiak, C. P. *Inorg. Chem.* **1986,** *25,* 26. (e) Karsch, H. H.; Milewski-Mahrla, B.; Besenhard, J. O.; Hofmann, P.; Stauffert, P.; Albright, T. A. *Inorg. Chem.* **1986,** *25,* 3811. (f) Cotton, F. A.; Falvello, L. R.; Harwood, W. S.; Powell, G. L.; Walton, R. A. *Inorg. Chem.* **1986,** *25,* 3949. (g) Doherty, N. M.; Hogarth, G.; Knox, S. A. R.; Macpherson, K. A.; Melchior, F.; Orpen, A. G. *J. Chem. Soc., Chem. Commun.* **1986,** 540. (h) Wu, J.; Fanwick, P. E.; Kubiak, C. P. *J. Am. Chem. Soc.* **1988,** *110,* 1319. (i) Wu, J.; Fanwick, P. E.; Kubiak, C. P. *J. Am. Chem. Soc.* **1989,** *111,* 7812. (j) Jenkins, J. A. Ph.D. Thesis, University of Alberta, 1991, Chapter 1.
33. Jenkins, J. A. Ph.D. Thesis, University of Alberta, 1991, Chapter 7.
34. See, for example: (a) Cotton, F. A.; Hardcastle, K. I.; Rusholme, G. A. *J. Coord. Chem.* **1973,** *2,* 217. (b) Cowie, M.; Dwight, S. K. *Inorg. Chem.* **1979,** *18,* 1209. (c) Hassan, F. S. M.; MacEwan, D. M.; Pringle, P. G.; Shaw, B. L. *J. Chem. Soc., Dalton Trans.* **1985,** 1501. (d) Dadkham, H.; Dilworth, J. R.; Fairman, K.; Kan, C. T.; Richards, R. L.; Hughes, D. L. *J. Chem. Soc., Dalton Trans.* **1985,** 1523.
35. (a) McEwan, D. M.; Pringle, P. G.; Shaw, B. L. *J. Chem. Soc., Chem. Commun.* **1982,** 859. (b) McDonald, W. S.; Pringle, P. G.; Shaw, B. L. *J. Chem. Soc., Chem. Commun.* **1982,** 861. (c) Pringle, P. G.; Shaw, B.

L. *J. Chem. Soc., Chem. Commun.* **1982**, 956. (d) McEwan, D. M.; Pringle, P. G.; Shaw, B. L. *J. Chem. Soc., Chem. Commun.* **1982**, 1240. (e) Pringle, P. G.; Shaw, B. L. *J. Chem. Soc., Dalton Trans.* **1983**, 889. (f) Langrick, C. R.; Pringle, P. G.; Shaw, B. L. *Inorg. Chim. Acta* **1983**, *76*, L263. (g) Blagg, A.; Hutton, A. T.; Pringle, P. G.; Shaw, B. L. *Inorg. Chim. Acta* **1983**, *76*, L265. (h) Cooper, G. R.; Hutton, A. T.; McEwan, D. M.; Pringle, P. G.; Shaw, B. L. *Inorg. Chim. Acta* **1983**, *76*, L265. (i) Hutton, A. T.; Pringle, P. G.; Shaw, B. L. *Organometallics* **1983**, *2*, 1889.

36. See, for example: (a) Hanson, B. E.; Fanwick, P. E.; Mancini, J. S. *Inorg. Chem.* **1982**, *21*, 3811. (b) Davies, D. L.; Gracey, B. P.; Guerchais, V.; Knox, S. A. R.; Orpen, A. G. *J. Chem. Soc., Chem. Commun.* **1984**, 841. (c) Faraone, F.; Bruno, G.; Lo Schiavo, S.; Bombieri, G. *J. Chem. Soc., Dalton Trans.* **1984**, 533. (d) Al-Resayes, S. I.; Hitchcock, P. B.; Nixon, J. F. *J. Organomet. Chem.* **1984**, *267*, C13. (e) DeLeeuw, G.; Field, J. S.; Haines, R. J.; McCulloch, B.; Meintjies, E.; Monberg, F.; Olivier, G. M.; Ramdial, P.; Sampson, C. N.; Sigwarth, B.; Steen, N. D.; Moodley, K. G. *J. Organomet. Chem.* **1984**, *275*, 95. (f) Lee, K. W.; Pennington, W. T.; Cordes, A. W.; Brown, T. L. *Organometallics* **1984**, *3*, 404. (g) Darensbourg, M. Y.; ElMehdawi, R.; Delord, T. J.; Fronczek, F. R.; Watkins, S. F. *J. Am. Chem. Soc.* **1986**, *106*, 2583. (h) Jacobsen, G. B.; Shaw, B. L.; Thornton-Pett, M. *J. Chem. Soc., Chem. Commun.* **1986**, 13.

37. Ling, S. S. M.; Jobe, I. R.; McLennan, A. J.; Manojlović-Muir, L.; Muir, K. W.; Puddephatt, R. J. *J. Chem. Soc., Chem. Commun.* **1985**,

566.

38. Balch, A. L.; Lee, C.-L.; Lindsay, C. H.; Olmstead, M. M. *J. Organomet. Chem.* **1979**, *177*, C22.

39. Cowie, M.; Loeb, S. J. *Organometallics* **1985**, *4*, 852.

40. Hoskins, B. F.; Steen, R. F.; Turney, T. W. *Inorg. Chim. Acta* **1983**, *77*, L69.

41. Zhang, Z.-Z.; Wang, H.-K.; Wang, H.-G.; Wang, R.-J.; Zhao, W.-J.; Yang, L.-M. *J. Organomet. Chem.* **1988**, *347*, 269.

42. Elliot, D. J.; Ferguson, G.; Holah, D. G.; Hughes, A. N.; Jennings, M. C.; Magnuson, V. R.; Potter, D.; Puddephatt, R. J. *Organometallics* **1990**, *9*, 1336.

43. Brown, M. P.; Cooper, S. J.; Frew, A. A.; Manojlović-Muir, L.; Muir, K. A.; Puddephatt, R. J.; Seddon, K. R.; Thomson, M. A. *Inorg. Chem.* **1981**, *20*, 1500.

44. Manojlović-Muir, L.; Muir, K. W.; Frew, A. A.; Ling, S. S. M.; Thomson, M. A.; Puddephatt, R. J. *Organometallics* **1984**, *3*, 1637.

45. Abbott, E. H.; Bose, K. S.; Cotton, F. A.; Hall, W. T.; Sekutowshi, J. C. *Inorg. Chem.* **1978**, *17*, 3240.

46. (a) Farr, J. P.; Olmstead, M. M.; Balch, A. L. *J. Am. Chem. Soc.* **1980**, *102*, 6654. (b) Maisonnat, A.; Farr, J. P.; Balch, A. L. *Inorg. Chim. Acta* **1981**, *53*, L217. (c) Farr, J. P.; Olmstead, M. M.; Lindsay, C. H.; Balch, A. L. *Inorg. Chem.* **1981**, *20*, 1182. (d) Maisonnat, A.; Farr, J. P.; Olmstead, M. M.; Hunt, C. T.; Balch, A. L. *Inorg. Chem.* **1982**, *21*, 3961. (e) Inoguchi, J.; Milewski-Mahrla, B.; Schmidbaur, H. *Chem. Ber.* **1982**, *115*, 3085. (f) Maisonnat, A.; Farr, J. P.; Olmstead, M. M.; Wood, F. E.;

Balch, A. L. *J. Am. Chem. Soc.* **1983,** *105*, 792. (g) Farr, J. P.; Olmstead, M. M.; Balch, A. L. *Inorg. Chem.* **1983,** 22, 1229. (h) Farr, J. P.; Wood, F. E.; Balch, A. L. *Inorg. Chem.* **1983,** 22, 3387. (i) Farr, J. P.; Olmstead, M. M.; Rutherford, N. M.; Wood, F. E.; Balch, A. L. *Organometallics* **1983,** 2, 1758. (j) Barder, T. J.; Cotton, F. A.; Powell, G. L.; Tetrick, S. M.; Walton, R. A. *J. Am. Chem. Soc.* **1984,** *106*, 1323.

47. Hilts, R. W.; Franchuk, R. A.; Cowie, M. *Organometallics*, in press.
48. Puddephatt, R. J.; Azam, K. A.; Hill, R. H.; Brown, M. P.; Nelson, C. D.; Moulding, R. P.; Seddon, K. R.; Grossel, M. C. *J. Am. Chem. Soc.* **1983,** *105*, 5642.
49. Antonelli, D. M.; Cowie, M. *Organometallics* **1990,** *9*, 1818.
50. Collman, J. P.; Hegedus, L. S.; Norton, J. R.; Finke, R. G. *Principles and Applications of Organotransition Metal Chemistry*; University Science Books: Mill Valley, CA, 1987; Chapters 10-12.
51. James, B. R. *Adv. Organomet. Chem.* **1979,** *17*, 319.
52. James, B. R. In *Comprehensive Organometallic Chemistry*; Wilkinson, G., Stone, F. G. A., Abel, E. W., Eds.; Pergamon Press: Oxford, England, 1982; Chapter 51.
53. Pruett, R. L. *Adv. Organomet. Chem.* **1979,** *17*, 1.
54. Orchin, M. *Acc. Chem. Res.* **1981,** *14*, 259.
55. Forster, D. *Adv. Organomet. Chem.* **1979,** *17*, 255.
56. Dekleva, T. W.; Forster, D. *Adv. Catal.* **1986,** 34, 81.
57. Speier, J. L. *Adv. Organomet. Chem.* **1979,** *17*, 407.
58. Tolman, C. A.; McKinney, R. J.; Seidel, W. C.; Druliner, J. D.; Stevens, W. R. *Adv. Catal.* **1985,** 33, 1.

59. Mague, J. T.; Mitchener, J. P. *Inorg. Chem.* **1969**, *8*, 119.

60. Cowie, M.; Dwight, S. K. *Inorg. Chem.* **1980**, *19*, 2500.

61. Woodcock, C.; Eisenberg, R. *Inorg. Chem.* **1984**, *23*, 4207.

62. Kubiak, C. P.; Eisenberg, R. *J. Am. Chem. Soc.* **1980**, *102*, 3637.

63. Kubiak, C. P.; Woodcock, C.; Eisenberg, R. *Inorg. Chem.* **1982**, *21*, 2119.

64. Sutherland, B. R.; Cowie, M. *Organometallics* **1985**, *4*, 1637.

65. Deraniyagala, S. P.; Grundy, K. R. *Inorg. Chem.* **1985**, *24*, 50.

66. Sanger, A. R. *Can. J. Chem.* **1982**, *60*, 1363.

67. Sanger, A. R. *Prepr.–Can. Symp. Catal.* **1979**, *6*, 37.

68. Cowie, M.; Mague, J. T.; Sanger, A. R. *J. Am. Chem. Soc.* **1978**, *100*, 3628.

69. Cowie, M.; Dwight, S. K. *Inorg. Chem.* **1979**, *18*, 2700.

70. Cowie, M.; Southern, T. G. *Inorg. Chem.* **1982**, *21*, 246.

71. Lee, C.-L.; Hunt, C. T.; Balch, A. L. *Inorg. Chem.* **1981**, *20*, 2498.

72. Manojlović-Muir, L.; Muir, K. W.; Solomun, T. *Acta Cryst.* **1979**, *B35*, 1237.

73. Benner, L. A.; Balch, A. L. *J. Am. Chem. Soc.* **1978**, *100*, 6099.

74. Fisher, J. R.; Mills, A. J.; Sumner, S.; Brown, M. P.; Thomson, M. A.; Puddephatt, R. J.; Manojlović-Muir, L.; Muir, K. W. *Organometallics* **1982**, *1*, 1421.

75. Kubiak, C. P.; Woodcock, C.; Eisenberg, R. *Inorg. Chem.* **1980**, *19*, 2733.

76. Vaartstra, B. A.; O'Brien, K. N.; Eisenberg, R.; Cowie, M. *Inorg. Chem.* **1988**, *27*, 3668.

77. Sutherland, B. R.; Cowie, M. *Organometallics* **1985**, *4*, 1801.

78. Vaartstra, B. A.; Cowie, M. *Organometallics* **1990**, *9*, 1594.

79. Martinho Simões, J. A.; Beauchamp, J. L. *Chem. Rev.* **1990**, *90*, 629.

80. Sutherland, B. R.; Cowie, M. *Organometallics* **1984**, *3*, 1869.

81. Vaartstra, B. A.; Cowie, M. *Inorg. Chem.* **1989**, *28*, 3138.

82. Vaartstra, B. A.; Cowie, M. *Organometallics* **1989**, *8*, 2388.

83. Cotton, F. A.; Eagle, C. T.; Price, A. C. *Inorg. Chem.* **1988**, *27*, 4362.

84. Balch, A. L. *J. Am. Chem. Soc.* **1976**, *98*, 8049.

85. Sutherland, B. R.; Cowie, M. *Inorg. Chem.* **1984**, *23*, 1290.

86. Kubiak, C. P.; Eisenberg, R. *Inorg. Chem.* **1980**, *19*, 2726.

87. Wang, W.-D.; Hommeltoft, S. I.; Eisenberg, R. *Organometallics* **1988**, *7*, 2417.

88. Wang, W.-D.; Eisenberg, R. *J. Am. Chem. Soc.* **1990**, *112*, 1833.

89. Lee, C.-L.; Besenyei, G.; James, B. R.; Nelson, D. A.; Lilga, M. A. *J. Chem. Soc., Chem. Commun.* **1985**, 1175.

90. Besenyei, G.; Lee, C.-L.; Gulinski, J.; Rettig, S. J.; James, B. R. *Inorg Chem.* **1987**, *26*, 3622.

91. Barnabas, A. F.; Sallin, D.; James, B. R. *Can. J. Chem.* **1989**, *67*, 2009.

92. Hadj-Bagheri, N.; Puddephatt, R. J.; Manojlović-Muir, L.; Stefanović, A. *J. Chem. Soc., Dalton Trans.* **1990**, 535.

93. Antonelli, D. A.; Cowie, M. *Inorg. Chem.* **1990**, *29*, 3339.

94. Brown. M. P.; Fisher, J. R.; Puddephatt, R. J.; Seddon, K. R. *Inorg. Chem.* **1979**, *18*, 2808.

95. Balch, A. L.; Labadie, J. W.; Delker, G. *Inorg. Chem.* **1979**, *18*, 1224.

96. Vaartstra, B. A.; Xiao, J.; Cowie, M. *J. Am. Chem. Soc.* **1990**, *112*, 9425.

97. Berry, D. H.; Eisenberg, R. *J. Am. Chem. Soc.* **1985,** *107,* 7181.

98. Berry, D. H.; Eisenberg, R. *Organometallics* **1987,** *6,* 1796.

99. Jenkins, J. A.; Ennett, J. P.; Cowie, M. *Organometallics* **1988,** *7,* 1845.

100. Puddephatt, R. J.; Thomson, M. A. *Inorg. Chem.* **1982,** *21,* 725.

101. Aggarwal, R. P.; Connelly, N. G.; Crespo, M. C.; Dunne, B. J.; Hopkins, P. J.; Orpen, A. G. *J. Chem. Soc., Chem. Commun.* **1989,** 33.

102. Cowie, M.; Dickson, R. S. *Inorg. Chem.* **1981,** *20,* 2682.

103. Hommeltoft, S. I.; Berry, D. H.; Eisenberg, R. *J. Am. Chem. Soc.* **1986,** *108,* 5345.

104. Woodcock, C.; Eisenberg, R. *Inorg. Chem.* **1985,** *24,* 1285.

Chapter 2

Diiridium and Mixed Rhodium-Iridium Hydridocarbonyl Complexes and the Structure of [RhIr(CO)$_3$(dppm)$_2$], a Complex Containing an Ir(-I)→Rh(I) Dative Bond[†]

Introduction

Much of the interest in hydride and carbonyl complexes of the metals of groups 8, 9 and 10 (the iron, cobalt and nickel triads, respectively) has stemmed from their proven or probable functions as intermediates in numerous catalytic processes, notably hydroformylation,[1] olefin hydrogenation,[2] alcohol carbonylation[3] and the water-gas shift reaction.[4] However, to date most studies have concentrated on mononuclear complexes. As part of an ongoing effort to determine the effects of adjacent metal centers upon catalytic processes, the chemistry of binuclear diphosphine-bridged complexes of rhodium[5-8] and iridium[9-15] has been investigated in this research group. In a previous study a series of diiridium complexes was described that, aside from the diphosphine bridges, contained only hydride and carbonyl ligands.[16] A more limited series of analogous dirhodium species has also been studied by other workers.[17,18] The preparation and study of similar heterobimetallic Rh/Ir complexes thus appeared to be a logical extension to these studies. In addition, previous work involving H_2[15] and alkyne[19] addition to mixed rhodium-iridium species had demonstrated some rather interesting differences with respect to the chemistry of the homobimetallic analogues. Thus, it was anticipated that the Rh/Ir hydridocarbonyls would themselves show some unique behavior not previously shown by their Rh_2 and Ir_2 counterparts.

[†] A version of this chapter has been published. See: McDonald, R; Cowie, M. *Inorg. Chem.* **1990**, *29*, 1564.

Experimental Section

All solvents, including deuterated solvents used for NMR experiments, were dried (using the appropriate drying agents listed in the Appendix), degassed and distilled before use and were stored under N_2. Reactions were carried out using standard Schlenk procedures. Dinitrogen was passed through columns of Ridox and 4A molecular sieves to remove traces of oxygen and water, respectively. Carbon monoxide (Matheson) and dihydrogen were used as received. Hydrated rhodium(III) chloride was obtained from Johnson Matthey Ltd., hydrated iridium(III) chloride was purchased from Engelhard Scientific and bis(diphenylphosphino)methane (dppm) was purchased from Organometallics Inc. The compounds $[RhIrCl_2(CO)_2(dppm)_2]$,[15] $[Ir_2(H)(CO)_2(\mu\text{-}H)_2(dppm)_2][BF_4]\bullet CH_2Cl_2$,[13,16] $[Ir_2(CO)_2(\mu\text{-}H)(\mu\text{-}CO)(dppm)_2][BF_4]$[9] and $[Ir_2(CO)_3(dppm)_2]$[9] were prepared as previously reported. All other chemicals were used as received without further purification.

NMR spectra were recorded on a Bruker AM-400 spectrometer operating at 400 MHz for ^1H and $^1H\{^{31}P\}$ spectra and at 161.9 MHz for $^{31}P\{^1H\}$ spectra; $^{13}C\{^1H\}$ spectra were obtained on a Bruker WH-200 instrument operating at 50.32 MHz. In these cases an internal deuterated solvent lock was employed. Phosphorus chemical shifts are reported with respect to external 85% H_3PO_4, while carbon and proton shifts are with respect to TMS with the solvent as internal standard. Reactions were frequently monitored by use of $^{31}P\{^1H\}$ NMR, using a Bruker HFX-90 spectrometer operating at 36.43 MHz and employing an external deuterium lock; here, the sample (in non-deuterated solvent) was placed in a 10-mm sample tube that contained a concentric 5-mm insert filled with acetone-d_6. Infrared spectra were run on a Nicolet 7199 Fourier transform interferometer, as either solids (Nujol mulls on KBr disks) or solutions (KCl cell windows, 0.5-mm path length). A Perkin-Elmer 883 infrared spectrophotometer was also employed to check the progress of some reactions. Spectroscopic parameters for the compounds prepared are found in Table 2.1. Conductivity measurements were carried out using a Yellow Springs Instruments Model 31 conductivity bridge, with solutions of approximately 10^{-3} M concentration. Elemental analyses were performed by the microanalytical service within the department.

Preparation of Compounds. (a) $[Ir_2(CO)_2(\mu\text{-}H)_2(dppm)_2]$ (1). A solution of $[Ir_2(H)(CO)_2(\mu\text{-}H)_2(dppm)_2][BF_4]\cdot CH_2Cl_2$ (100 mg, 72.3 μmol) in THF (10 mL) was chilled to 0 °C; to this was added a THF solution of potassium *tert*-butoxide (8.6 mg, 77 μmol in 1 mL). The solution color immediately changed from golden yellow to deep red. Attempts to isolate this material in the solid state led only to a number of decomposition products, so its characterization was carried out in solution through use of IR and NMR (^1H, $^{31}P\{^1H\}$) spectroscopy.

Table 2.1. Spectroscopic Data[a] for the Compounds of Chapter 2.

	IR, cm^{-1}		NMR		
compound	solid[b]	solution[c]	$\delta(^{31}P\{^1H\})$[d]	$^1J_{Rh-P}$, Hz	$\delta(^1H)$[e]
$[Ir_2(CO)_2(\mu-H)_2(dppm)_2]$ (1)	f	1909 (vs)	12.9 (sing)		7.68-7.16 (mult, 40 H), 4.56 (br, 4 H), -10.12 (q, 2 H, $^2J_{P-H}$ = 6.6 Hz)
$[Ir_2(CO)_4(\mu-H)(dppm)_2][BF_4]$ (2)	f	1998 (s), 1981 (vs), 1959 (vs)	-9.6 (sing)		7.82-7.24 (mult, 40 H), 5.02 (br, 4 H), -9.95 (q, 1 H, $^2J_{P-H}$ = 9.4 Hz)
$[RhIr(CO)_3(dppm)_2]$ (3)	1958 (s), 1940 (vs), 1849 (s)	1950 (s), 1934 (vs), 1861 (w,br)	16.4 (dmult),[g] -16.3 (mult)[h]	129.6	8.05-6.90 (mult, 40 H), 4.84 (mult, 2 H), 2.93 (mult, 2 H)
$[RhIr(H)(CO)_2(\mu-H)(dppm)_2]$ (5)	1942 (s), 1924 (vs), 2033 (w)[i]	1937 (vs), 2033 (w)[i]	32.5 (dmult),[g] 9.9 (mult)[h]	118.2	7.79-7.02 (mult, 40 H), 4.22 (mult, 2 H), 2.51 (mult, 2 H), -11.00 (br, 1 H), 12.73 (br, 1 H)
$[RhIr(CO)_3(\mu-H)(dppm)_2][BF_4]$ (6)	2000 (s), 1974 (vs), 1899 (m)	1986 (vs,br), 1960 (sh), 1893 (w)	22.8 (dmult),[g] -5.5 (mult)[h]	112.2	7.54-7.30 (mult, 40 H), 4.38 (mult, 4 H), -10.19 (mult, 1 H, $^2J_{P(Ir)-H}$ = 12.2 Hz, $^2J_{P(Rh)-H}$ = 9.3 Hz, $^1J_{Rh-H}$ = 19.0 Hz)

(continued)

Table 2.1. (continued)

$[RhIr(CO)_3(\mu\text{-}H)_2(dppm)_2][BF_4]_2$ (7)	2141 (m), 2110 (m), 2001 (vs)	2142 (s), 2110 (s), 2015 (vs)	21.9 (dmult)[g] -10.2 (mult)[h]	102.7	7.57-7.33 (mult, 40 H), 4.63 (mult, 4 H), -11.18 (mult, 2 H, $^2J_{P(Ir)\text{-}H}$ = 11.1 Hz, $^2J_{P(Rh)\text{-}H} \le$ 7 Hz, $^1J_{Rh\text{-}H}$ = 17.3 Hz)
$[RhIr(H)(CO)_2(\mu\text{-}H)_2(dppm)_2][BF_4]$ (8)	2054 (m), 1971 (vs)	2059 (s), 1986 (vs)	27.1 (dmult)[g] -2.7 (mult)[h]	109.5	7.58-7.27 (mult, 40 H), 4.58 (br, 2 H), 3.90 (br, 2 H), -10.58 (br, 1 H), -11.46 (br, 1 H), -11.76 (br, 1 H)

[a] Abbreviations used: w = weak, m = medium, s = strong, vs = very strong, br = broad, sh = shoulder, mult = multiplet, dmult = doublet of multiplets, sing = singlet. [b] Nujol mull on KBr disk. Values are ν(CO) except as noted otherwise. [c] CH_2Cl_2 solution in KCl cells. [d] Vs. 85% H_3PO_4, -40 °C, in CD_2Cl_2 solvent. [e] Vs. TMS, 25 °C, in CD_2Cl_2 solvent. [f] Not isolable in solid state. [g] Rh-*P*. [h] Ir-*P*. [i] ν(Ir-H).

(b) $[Ir_2(CO)_4(\mu\text{-}H)(dppm)_2][BF_4]$ (2). Method A. A solution of $[Ir_2(CO)_2(\mu\text{-}H)(\mu\text{-}CO)(dppm)_2][BF_4]$ was prepared by adding 1 equiv (11.6 μL, 13.1 mg, 80.8 μmol) of $HBF_4{\cdot}OEt_2$ to a CH_2Cl_2 solution of $[Ir_2(CO)_3(dppm)_2]$ (100 mg, 80.8 μmol in 5 mL) under N_2. An atmosphere of CO was then placed over this solution, causing a change of color from deep red-purple to medium red-orange. The solution was taken to dryness under a CO stream, leaving a light red-brown residue. Recrystallization from CH_2Cl_2/Et_2O produced a pale orange powder that immediately turned pink when the CO atmosphere was removed, thus precluding its accurate elemental analysis; however, this species has been characterized in solution using IR and NMR (^1H, $^{31}P\{^1H\}$) spectroscopy. Furthermore, the species giving rise to the pink color was identified by these spectroscopic techniques as being the known compound $[Ir_2(CO)_2(\mu\text{-}H)(\mu\text{-}CO)(dppm)_2][BF_4]$.[9]

Method B. A solution of $[Ir_2(CO)_4(dppm)_2]$ was prepared by bubbling CO through a CH_2Cl_2 solution of $[Ir_2(CO)_3(dppm)_2]$ (100 mg, 80.8 μmol in 5 mL). One equivalent (11.6 μL, 13.1 mg 80.8 μmol) of $HBF_4{\cdot}OEt_2$ was added, causing a color change from bright yellow to red-orange. Isolation of the product proceeded as in method A, and the material obtained was found to be identical in its spectroscopic properties to that prepared above.

(c) $[RhIr(CO)_3(dppm)_2]$ (3). An atmosphere of CO was placed over a mixture of $[RhIrCl_2(CO)_2(dppm)_2]$ (300 mg, 252 μmol) and $NaBH_4$ (60 mg, 1.59 mmol) in THF (15 mL). Addition of methanol (5 mL) resulted in much effervescence and caused a slight deepening of the orange solution color. The mixture was allowed to stir for 2 h, after which degassed water

(1 mL) was added to destroy the excess borohydride. The solution was taken to dryness in vacuo, producing an orange-brown residue that was redissolved in THF (15 mL) and filtered. The filtrate volume was reduced to 5 mL and hexanes (40 mL) added, yielding **3** as an orange powder (258 mg, 89% yield). This complex proved to be a nonelectrolyte in CH_2Cl_2 ($\Lambda(10^{-3}$ M$) = 1.44\ \Omega^{-1}$ cm^2 mol^{-1}).[20] Anal. Calcd for $C_{53}H_{44}IrO_3P_4Rh$: C, 55.45; H, 3.86. Found: C, 54.99; H, 4.03.

(d) [RhIr(H)(CO)$_2$(μ–H)(dppm)$_2$] (5). A slurry of [RhIrCl$_2$(CO)$_2$-(dppm)$_2$] (150 mg, 134 μmol) and $NaBH_4$ (60 mg, 1.59 mmol) in THF (5 mL) was placed under an atmosphere of H_2. The reaction mixture changed from cloudy orange to cloudy yellow in color after 1 h, then to cloudy brown after 24 h. At this point the solvent was evaporated under an H_2 stream, the brown residue extracted with toluene (5 mL), filtered, and hexanes (20 mL) added, resulting in isolation of 107 mg (76% yield) of medium brown powdery solid. Complex **5** was essentially nonconducting in CH_2Cl_2 ($\Lambda(10^{-3}$ M$) = 3.36\ \Omega^{-1}$ cm^2 mol^{-1}).

(e) [RhIr(CO)$_3$(μ-H)(dppm)$_2$][BF$_4$] (6). To a solution of **3** (130 mg, 113 μmol) in CH_2Cl_2 (5 mL) was added one equivalent of $HBF_4{\cdot}OEt_2$ (16.3 μL, 18.3 mg, 113 μmol), resulting in a color change from deep orange to deep red-purple. The solution volume was reduced to 2 mL and ether (15 mL) added, causing the precipitation of a reddish solid. Recrystallization of this material from THF/ether yielded 118 mg (85%) of rust-colored solid. Compound **6** proved to be a 1:1 electrolyte in CH_2Cl_2 ($\Lambda(10^{-3}$ M$) = 56.4\ \Omega^{-1}$ cm^2 mol^{-1}). Anal. Calcd for $BC_{53}F_4H_{45}IrO_3P_4Rh$: C, 51.51; H, 3.67. Found: C, 50.87; H, 3.58.

(f) [RhIr(CO)$_3$(μ-H)$_2$(dppm)$_2$][BF$_4$]$_2$·CH$_2$Cl$_2$ (7). To a solution of 3 (100 mg, 87.1 μmol) in CH$_2$Cl$_2$ (5 mL) was added an excess of HBF$_4$•OEt$_2$ (30 μL, 33.8 mg, 209 μmol), resulting in a change in color from orange to deep red-purple, then to pale yellow, accompanied by the precipitation of a light yellow solid. Ether (10 mL) was added to complete the precipitation, the supernatant liquid drawn off, the solid washed with ether then dried under a stream of N$_2$, affording 99 mg (84% yield) of light yellow product. Compound 7 behaved as a weak electrolyte in CH$_2$Cl$_2$ (Λ(10^{-3} M) = 24.9 Ω^{-1} cm^2 mol^{-1}), whereas it was found to be a normal 2:1 electrolyte in nitromethane (Λ(10^{-3} M) = 189.1 Ω^{-1} cm^2 mol^{-1}). Anal. Calcd for B$_2$C$_{54}$Cl$_2$F$_8$H$_{48}$IrO$_3$P$_4$Rh: C, 46.05; H, 3.50; Cl, 5.03. Found: C, 45.83; H, 3.44; Cl, 4.12 (although this compound is prone to solvent loss yielding variable results for chlorine analyses, the totally-desolvated compound could not be obtained, and significant amounts [>1%] of Cl remained even after being stored under vacuum).

(g) [RhIr(H)(CO)$_2$(μ-H)$_2$(dppm)$_2$][BF$_4$] (8). A suspension of 6 (120 mg, 97.1 μmol) in THF (5 ml) was stirred under an atmosphere of H$_2$ for 3 h, during which time the reaction mixture changed from cloudy and red-orange to clear and golden-yellow. After reduction of the solution volume to 2 mL the product was precipitated by addition of ether (15 mL). Recrystallization of this material from THF/ether produced 98 mg (83%) of golden-yellow powder. Compound 8 proved to be a 1:1 electrolyte in CH$_2$Cl$_2$ (Λ(10^{-3} M) = 57.0 Ω^{-1} cm^2 mol^{-1}). Anal. Calcd for BC$_{52}$F$_4$H$_{47}$IrO$_2$P$_4$Rh: C, 51.63; H, 3.92. Found: C, 51.51; H, 4.18.

Reaction of 1 with HBF$_4$•OEt$_2$. To a solution of 1 in THF (62 μmol in

5 mL; prepared in situ as described above) was added 1 equiv of $HBF_4 \cdot OEt_2$ (8.9 μL, 10.0 mg, 62 μmol), causing an immediate color change from deep red to golden yellow. The product was found to be $[Ir_2(H)(CO)_2(\mu\text{-}H)_2(dppm)_2][BF_4]$[13,16] on the basis of its infrared and $^{31}P\{^1H\}$ NMR spectra.

Reaction of 1 with H_2. Dihydrogen was bubbled through a THF solution of **1** (62 μmol in 5 mL; prepared in situ as described above), causing an immediate color change from deep red to light yellow. The product was found to be $[Ir_2(H)_4(CO)_2(dppm)_2]$[13,16] on the basis of its ^1H and $^{31}P\{^1H\}$ NMR spectra.

Reaction of 5 with CO. A solution of **5** in THF (50 mg, 41.3 μmol in 2 mL) was stirred under an atmosphere of CO for 2 h, after which time **3** was the only species observed in the IR and $^{31}P\{^1H\}$ NMR spectra of the solution.

Reaction of 5 with $HBF_4 \cdot OEt_2$. To a solution of **5** in CH_2Cl_2 (20 mg, 17.8 μmol in 2 mL) was added 1 equivalent of $HBF_4 \cdot OEt_2$ (2.6 μL, 2.9 mg, 17.8 μmol), causing a slight deepening of the yellow color of solution. The product of the reaction was found by $^{31}P\{^1H\}$ NMR and solution IR spectroscopy to be compound **7**.

Reaction of 6 with $HBF_4 \cdot OEt_2$. To a solution of **6** in CH_2Cl_2 (40 mg, 32.4 μmol in 2 mL) was added 1 equivalent of $HBF_4 \cdot OEt_2$ (4.6 μL, 5.2 mg, 32.4 μmol), causing a color change from deep orange-red to light brown. The $^{31}P\{^1H\}$ NMR and solution IR spectra showed **7** to be the only species present after reaction.

Reactions of 6 with $KOC(CH_3)_3$ and $NaBH_4$. Solid potassium *tert*-butoxide (5 mg, 44.6 μmol) was added to a solution of **6** in CH_2Cl_2 (15 mg, 12.1 μmol in 2 mL) and the mixture stirred for 1 h, during which time the color changed from red-orange to light orange. The $^{31}P\{^1H\}$ NMR and IR spectra of the solution showed complete conversion of the starting material to species **3**. Similarly, reaction of a THF solution of **6** (25 mg in 3 mL) with $NaBH_4$ (5 mg) resulted in the formation of the same product.

Reaction of 7 with NEt_3. To a solution of **7** in CH_2Cl_2 (40 mg, 30.2 μmol in 2 mL) was added NEt_3 (10 μL, 7.3 mg, 72.1 μmol), causing an immediate color change from light brown to deep red-orange. The $^{31}P\{^1H\}$ NMR and solution IR spectra showed **6** to be the product formed.

Reaction of 8 with CO. A solution of **8** in CH_2Cl_2 (50 mg, 41.3 μmol in 2 mL) was stirred under an atmosphere of CO for 18 h, resulting in a color change from golden-yellow to red-orange. The $^{31}P\{^1H\}$ NMR and solution IR spectra of the solution showed **6** to be the only species present.

Reactions of 8 with $KOC(CH_3)_3$ and $NaBH_4$. To a solution of **8** in THF (20 mg, 16.5 μmol in 2 mL) was added solid potassium *tert*-butoxide (5 mg, 44.6 μmol). After stirring for 18 h the mixture was found by $^{31}P\{^1H\}$ NMR and IR spectroscopy to contain only compound **5**. The reaction of **8** (40 mg, 33.1 μmol in 4 mL THF) with $NaBH_4$ (5 mg, 132 μmol) similarly gave **5** as the sole product after 1 h reaction time.

X-ray Data Collection. Red-orange crystals of $[RhIr(CO)_3(dppm)_2]$ (**3**) were obtained by slow diffusion of ether into a concentrated CH_2Cl_2 solution of the compound. Several suitable crystals were mounted and flame-sealed in glass capillaries under N_2 and solvent vapor to minimize decomposition. Data were collected on an Enraf-Nonius CAD4 diffractometer using Mo Kα radiation. Unit-cell parameters were obtained from a least-squares refinement of the setting angles of 25 reflections in the range $20.0° \leq 2\theta \leq 24.0°$. The monoclinic diffraction symmetry and the systematic absences ($h0l$, l = odd; $0k0$, k = odd) were consistent with the space group $P2_1/c$.

Intensity data were collected at 22 °C using the $\theta/2\theta$ scan technique to a maximum $2\theta = 50.0°$, collecting reflections with indices of the form $+h$ $+k$ $\pm l$. Backgrounds were scanned for 25% of the peak width on either side of the peak scan. Three reflections were chosen as intensity standards, being remeasured at 120-min intervals of X-ray exposure time. There was no significant systematic decrease in the intensities of these standards thus no decomposition correction was applied. A total of 8686 unique reflections were measured and processed in the usual way, using a value of 0.04 for p[22] to downweight intense reflections; 5208 of these were considered to be observed ($F_o^2 \geq 3\sigma(F_o^2)$) and were used in subsequent calculations. Absorption corrections were applied to the data using the method of Walker and Stuart.[23,24] See Table 2.2 for crystal data and more information on X-ray data collection.

Structure Solution and Refinement. The structure was solved in the space group $P2_1/c$ using standard Patterson and Fourier techniques. Full-matrix least-squares refinements proceeded so as to minimize the function $\Sigma w(|F_o|-|F_c|)^2$, where $w = 4F_o^2/\sigma^2(F_o^2)$. All non-hydrogen atoms were ultimately located. Atomic scattering factors[25,26] and anomalous dispersion terms[27] were taken from the usual tabulations. All hydrogen atoms were included as fixed contributions but not refined. Their idealized positions were calculated from the geometries about the attached carbon

Table 2.2. Crystallographic Data for $[RhIr(CO)_3(dppm)_2]$ (3)

formula	$C_{53}H_{44}IrO_3P_4Rh$
formula weight	1147.95
crystal shape	monoclinic prism
crystal dimensions, mm	0.49 × 0.15 × 0.12
space group	$P2_1/c$ (No. 14)
temperature, °C	22
radiation (λ, Å)	graphite-monochromated Mo Kα (0.71069)
unit cell parameters	
a, Å	20.296 (4)
b, Å	12.190 (7)
c, Å	19.064 (7)
β, deg	95.11 (2)
V, Å^3	4697.9
Z	4
ρ(calcd), g cm^{-3}	1.623
linear absorption coeff (μ), cm^{-1}	33.403
range of transmission factors	0.791-1.354
detector aperture, mm	(3.00 + tan θ) wide × 4.00 high
takeoff angle, deg	3.0
maximum 2θ, deg	50.0
crystal-detector distance, mm	173

(continued)

Table 2.2. (continued)

scan type	$\theta/2\theta$
scan rate, deg/min	between 1.18 and 6.67
scan width, deg	$0.60 + 0.347 \tan\theta$
total unique reflections	8686 ($h\ k\ \pm l$)
total observations (NO)	5208 ($F_o^2 \geq 3\sigma(F_o^2)$)
final no. parameters varied (NV)	559
error in obs. of unit wt. (GOF)[a]	1.543
R[b]	0.047
R_w[c]	0.053

[a] $\mathrm{GOF} = [\sum w(|F_o| - |F_c|)^2/(\mathrm{NO} - \mathrm{NV})]^{1/2}$ where $w = 4F_o^2/\sigma^2(F_o^2)$.

[b] $R = \sum ||F_o| - |F_c|| / \sum |F_o|$. [c] $R_w = [\sum w(|F_o| - |F_c|)^2/\sum wF_o^2]^{1/2}$.

atoms, using a C-H bond length of 0.95 Å, and they were assigned thermal parameters 20% greater than the equivalent isotropic B's of their attached C atoms.

The final model, with 559 parameters refined, converged to values of $R = 0.047$ and $R_w = 0.053$. In the final difference Fourier map the 10 highest residuals (1.3-0.7 e/Å^3) were found to be in the vicinity of the Ir and Rh atoms (a typical carbon atom in an earlier synthesis had an electron density of ca. 4.9 e/Å^3). The positional parameters of all non-hydrogen atoms are given in Table 2.3, while selected bond distances and angles are given in Tables 2.4 and 2.5, respectively.

Results and Discussion

(a) Description of Structure. The title complex, [RhIr(CO)$_3$(dppm)$_2$], has the structure shown in Figure 2.1 in which both diphosphine ligands bridge the metal nuclei in an atypical, non-A-frame manner. This geometry, having the phosphorus atoms on one metal mutually trans and on the other metal mutually cis, is similar to those reported for the closely-related, formally Rh(0) complexes, [Rh$_2$(CO)$_3$(dppm)$_2$][28] and [Rh$_2$(CO)$_3${(PhO)$_2$PN(Et)P(OPh)$_2$}$_2$],[29] to that for the heterobimetallic rhodium-cobalt species [RhCo(CO)$_3$(dppm)$_2$],[30a] and to that presumed for the diiridium analogue [Ir$_2$(CO)$_3$(dppm)$_2$].[9] Figure 2.2 shows a view approximately along the metal-metal axis, in which all phenyl carbons except those bound to phosphorus are omitted.

The coordination spheres about the two metals are quite different. The Rh atom has a coordination number of 4 (excluding the weak inter-

Table 2.3. Positional and Thermal Parameters for the Atoms of $[RhIr(CO)_3(dppm)_2]$ (3)[a]

Atom	*x*	*y*	*z*	*B*, Å^2
Ir	0.22767(2)	0.18475(3)	0.20696(2)	2.43(1)
Rh	0.29649(4)	0.01816(6)	0.14660(4)	2.47(2)
P(1)	0.3071(1)	0.2972(2)	0.1655(1)	2.6(1)
P(2)	0.3935(1)	0.1003(2)	0.1928(1)	2.8(1)
P(3)	0.1413(1)	0.1843(2)	0.1186(1)	2.6(1)
P(4)	0.1993(1)	-0.0319(2)	0.0841(1)	2.7(1)
O(1)	0.2495(4)	-0.0071(6)	0.3079(4)	4.8(2)
O(2)	0.1733(5)	0.3389(7)	0.3123(5)	8.2(3)
O(3)	0.3699(4)	-0.1729(6)	0.0928(5)	5.6(2)
C(1)	0.2427(4)	0.0629(8)	0.2647(5)	3.2(2)
C(2)	0.1927(6)	0.2849(9)	0.2716(6)	4.9(3)
C(3)	0.3419(5)	-0.0999(8)	0.1120(5)	3.9(2)
C(4)	0.3891(5)	0.2505(8)	0.2027(5)	3.0(2)
C(5)	0.1549(5)	0.0894(8)	0.0468(5)	2.9(2)
C(11)	0.3164(4)	0.3118(8)	0.0701(5)	2.9(2)
C(12)	0.3121(5)	0.2197(9)	0.0276(5)	3.3(2)
C(13)	0.3180(5)	0.2299(9)	-0.0446(5)	3.9(3)
C(14)	0.3260(6)	0.329(1)	-0.0746(5)	4.8(3)
C(15)	0.3311(6)	0.423(1)	-0.0329(6)	5.2(3)
C(16)	0.3274(5)	0.4132(9)	0.0390(6)	4.2(3)
C(21)	0.3043(5)	0.4418(8)	0.1919(5)	3.5(2)
C(22)	0.2463(5)	0.4961(9)	0.1781(6)	3.8(2)
C(23)	0.2421(6)	0.6100(9)	0.1891(6)	4.9(3)
C(24)	0.2955(6)	0.6671(8)	0.2150(6)	4.6(3)
C(25)	0.3536(6)	0.6135(9)	0.2323(6)	5.0(3)
C(26)	0.3588(5)	0.5015(9)	0.2188(6)	4.3(3)
C(31)	0.4642(5)	0.0796(9)	0.1401(5)	3.3(2)

(continued)

Table 2.3. (continued)

C(32)	0.5013(5)	-0.0167(9)	0.1500(6)	4.3(3)
C(33)	0.5528(6)	-0.035(1)	0.1095(6)	5.6(3)
C(34)	0.5691(5)	0.039(1)	0.0596(6)	5.1(3)
C(35)	0.5327(6)	0.133(1)	0.0487(6)	5.3(3)
C(36)	0.4786(5)	0.1531(8)	0.0878(5)	3.6(2)
C(41)	0.4282(5)	0.0512(8)	0.2787(5)	3.3(2)
C(42)	0.4089(6)	-0.0504(9)	0.3021(6)	4.6(3)
C(43)	0.4384(6)	-0.095(1)	0.3636(6)	5.7(3)
C(44)	0.4860(6)	-0.037(1)	0.4029(6)	6.5(3)
C(45)	0.5059(6)	0.065(1)	0.3812(6)	5.6(3)
C(46)	0.4764(5)	0.111(1)	0.3194(6)	4.3(3)
C(51)	0.0603(5)	0.1406(8)	0.1437(5)	3.0(2)
C(52)	0.0571(5)	0.0818(8)	0.2059(6)	4.2(3)
C(53)	-0.0044(6)	0.0414(9)	0.2229(6)	4.9(3)
C(54)	-0.0608(6)	0.061(1)	0.1783(7)	5.9(3)
C(55)	-0.0573(5)	0.120(1)	0.1183(7)	5.2(3)
C(56)	0.0022(5)	0.157(1)	0.1004(6)	4.7(3)
C(61)	0.1195(5)	0.3130(8)	0.0729(5)	3.3(2)
C(62)	0.1407(6)	0.3371(9)	0.0071(7)	4.9(3)
C(63)	0.1256(7)	0.444(1)	-0.0213(7)	6.7(4)
C(64)	0.0942(6)	0.521(1)	0.0128(8)	6.9(4)
C(65)	0.0734(6)	0.4968(9)	0.0782(8)	5.9(3)
C(66)	0.0865(6)	0.392(1)	0.1072(6)	4.8(3)
C(71)	0.1358(5)	-0.1091(8)	0.1233(5)	3.6(2)
C(72)	0.1461(6)	-0.1468(8)	0.1918(6)	4.3(3)
C(73)	0.0948(7)	-0.2025(9)	0.2208(7)	6.1(3)
C(74)	0.0345(6)	-0.222(1)	0.1818(8)	6.5(4)
C(75)	0.0241(6)	-0.185(1)	0.1145(8)	6.3(3)
C(76)	0.0750(5)	-0.131(1)	0.0845(6)	4.6(3)
C(81)	0.2131(5)	-0.1129(8)	0.0058(5)	3.4(2)

(continued)

Table 2.3. (continued)

C(82)	0.2313(5)	-0.0612(9)	-0.0557(6)	4.3(3)
C(83)	0.2462(6)	-0.124(1)	-0.1126(6)	5.1(3)
C(84)	0.2455(6)	-0.236(1)	-0.1083(6)	5.8(3)
C(85)	0.2300(7)	-0.289(1)	-0.0476(7)	5.8(3)
C(86)	0.2129(5)	-0.228(1)	0.0090(6)	4.5(3)

[a] Numbers in parentheses are estimated standard deviations in the least significant digits in this and all subsequent tables. Thermal parameters for the anisotropically refined atoms are given in the form of the equivalent isotropic Gaussian displacement parameter defined as $^4/_3\left[a^2\beta_{11} + b^2\beta_{22} + c^2\beta_{33} + ac(\cos\beta)\beta_{13}\right]$.

Table 2.4. Selected Distances (Å) in [RhIr(CO)$_3$(dppm)$_2$] (3)

(a) Bonded

Ir-Rh	2.7722(7)	P(2)-C(31)	1.840(8)
Ir-P(1)	2.309(2)	P(2)-C(41)	1.825(8)
Ir-P(3)	2.321(2)	P(3)-C(5)	1.833(8)
Ir-C(1)	1.857(9)	P(3)-C(51)	1.833(8)
Ir-C(2)	1.916(9)	P(3)-C(61)	1.829(9)
Rh-P(2)	2.312(2)	P(4)-C(5)	1.842(8)
Rh-P(4)	2.295(2)	P(4)-C(71)	1.811(8)
Rh-C(3)	1.861(9)	P(4)-C(81)	1.831(8)
P(1)-C(4)	1.841(8)	O(1)-C(1)	1.186(9)
P(1)-C(11)	1.853(8)	O(2)-C(2)	1.12(1)
P(1)-C(21)	1.835(8)	O(3)-C(3)	1.134(9)
P(2)-C(4)	1.843(8)		

(b) Non-bonded

Rh-C(1)	2.644(7)	P(3)-P(4)	2.983(4)
P(1)-P(2)	2.991(3)		

Table 2.5. Selected Angles (deg) in [RhIr(CO)$_3$(dppm)$_2$] (3)

(a) Bond angles

Rh-Ir-P(1)	84.25(5)	Rh-P(2)-C(31)	114.3(3)
Rh-Ir-P(3)	94.17(5)	Rh-P(2)-C(41)	116.6(3)
Rh-Ir-C(1)	66.3(2)	C(4)-P(2)-C(31)	103.9(4)
Rh-Ir-C(2)	164.5(3)	C(4)-P(2)-C(41)	104.6(4)
P(1)-Ir-P(3)	104.95(7)	C(31)-P(2)-C(41)	100.8(4)
P(1)-Ir-C(1)	126.6(3)	Ir-P(3)-C(5)	113.0(3)
P(1)-Ir-C(2)	98.7(3)	Ir-P(3)-C(51)	116.7(3)
P(3)-Ir-C(1)	120.1(3)	Ir-P(3)-C(61)	118.6(3)
P(3)-Ir-C(2)	99.8(3)	C(5)-P(3)-C(51)	102.1(4)
C(1)-Ir-C(2)	100.3(4)	C(5)-P(3)-C(61)	103.5(4)
Ir-Rh-P(2)	88.18(6)	C(51)-P(3)-C(61)	100.9(4)
Ir-Rh-P(4)	88.22(6)	Rh-P(4)-C(5)	110.9(3)
Ir-Rh-C(3)	175.7(3)	Rh-P(4)-C(71)	122.4(3)
P(2)-Rh-P(4)	167.56(8)	Rh-P(4)-C(81)	112.3(3)
P(2)-Rh-C(3)	92.2(3)	C(5)-P(4)-C(71)	103.6(4)
P(4)-Rh-C(3)	92.3(3)	C(5)-P(4)-C(81)	102.9(4)
Ir-P(1)-C(4)	108.6(3)	C(71)-P(4)-C(81)	102.8(4)
Ir-P(1)-C(11)	121.9(3)	Ir-C(1)-O(1)	171.9(6)
Ir-P(1)-C(21)	115.9(3)	Ir-C(2)-O(2)	176.0(9)
C(4)-P(1)-C(11)	103.9(4)	Rh-C(3)-O(3)	178.2(8)
C(4)-P(1)-C(21)	103.9(4)	P(1)-C(4)-P(2)	108.6(4)
C(11)-P(1)-C(21)	100.8(4)	P(3)-C(5)-P(4)	108.7(4)
Rh-P(2)-C(4)	114.9(3)		

(b) Torsion angles

P(1)-Ir-Rh-P(2)	43.05(9)	P(3)-Ir-Rh-P(4)	20.41(9)

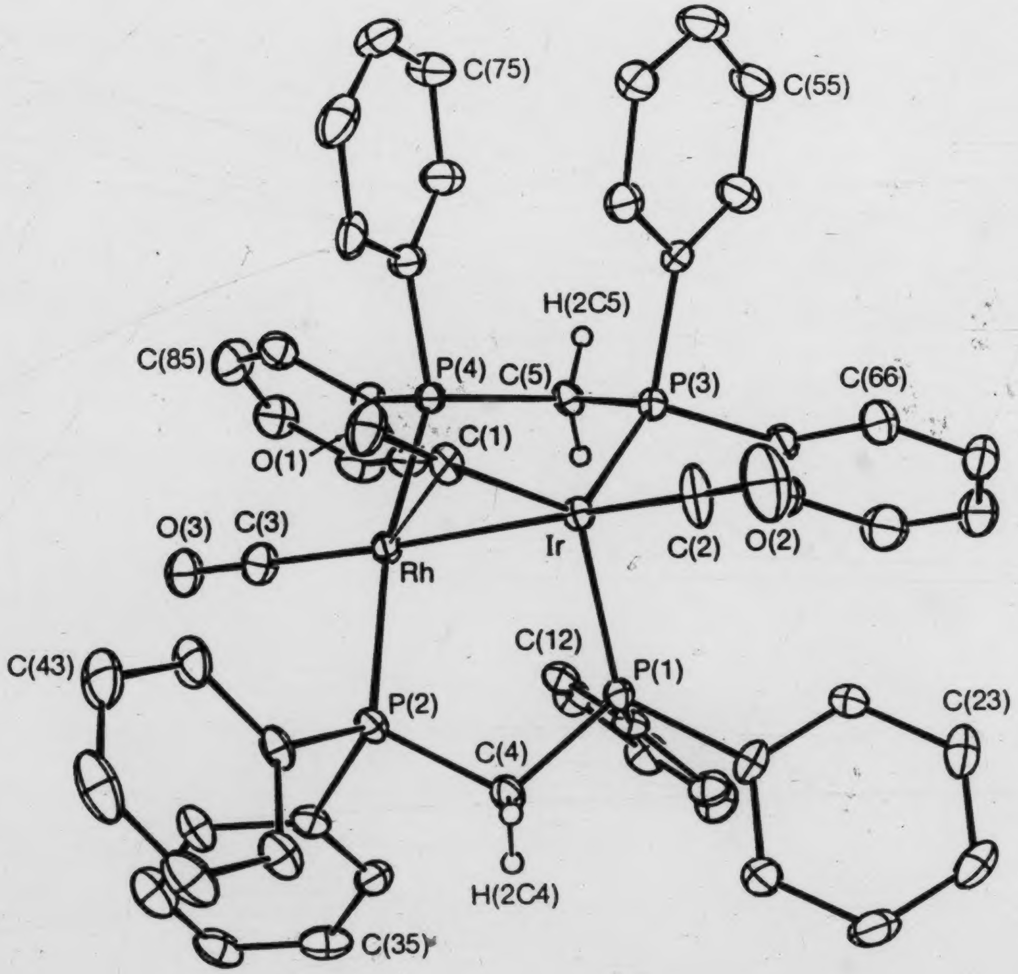
C(75)
C(55)
H(2C5)
C(85)
P(4)
C(5)
P(3)
C(66)
C(1)
O(1)
O(3)
C(3)
Rh
Ir
C(2)
O(2)
C(12)
C(43)
P(1)
P(2)
C(23)
C(4)
H(2C4)
C(35)

Figure 2.1. Perspective view of $[RhIr(CO)_3(dppm)_2]$ (3) showing the numbering scheme. Thermal parameters are shown at the 20% level except for hydrogens, which are shown artificially small for the dppm methylene groups but are not shown for the phenyl groups.

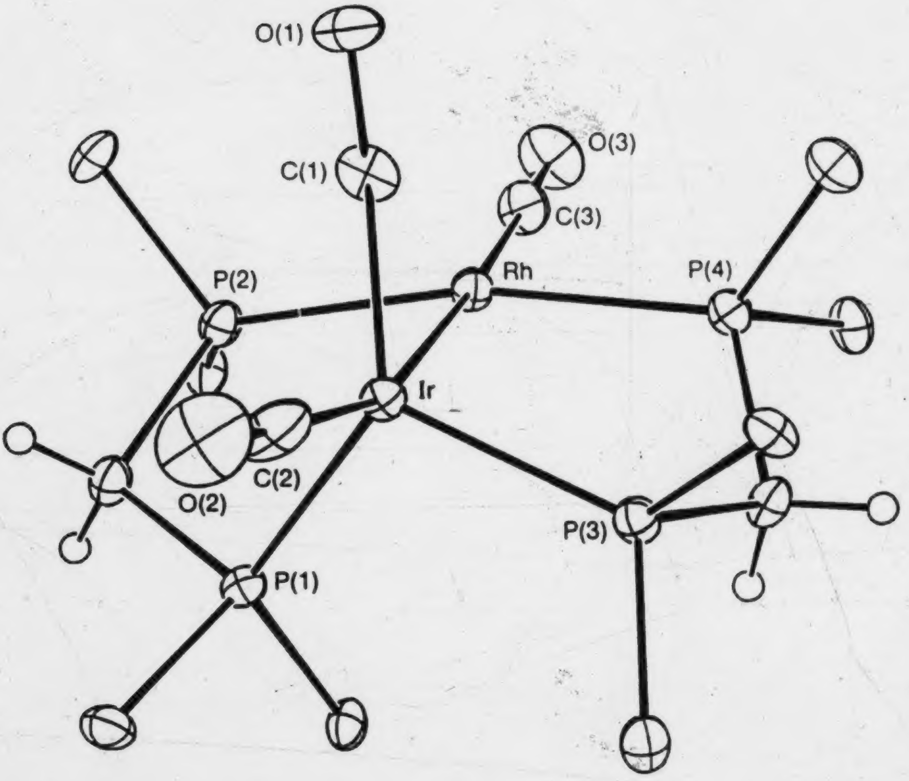
O(1)
C(1)
O(3)
C(3)
P(2)
Rh
P(4)
Ir
C(2)
O(2)
P(3)
P(1)

Figure 2.2. View of complex 3 approximately along the Rh-Ir bond, omitting the phenyl carbon atoms except those bound to phosphorus.

action with C(1)), while the Ir atom is bound to five other atoms (including Rh). This appears to be the general structural form for the complexes $[MM'(CO)_3(dppm)_2]$ (MM' = Rh_2, Ir_2, RhIr, RhCo), even though the homobimetallic species are potentially symmetrical. Instead of viewing these complexes as containing formally zerovalent metal atoms, as would be implied by a symmetrical formulation, it may be more appropriate to regard them as mixed-valence M(I)/M(-I) species, in which the M(-I) atom functions as a pseudohalide that bonds to the other metal via a dative metal-metal bond. This view is consistent with the asymmetric structure observed and the coordination environments about each metal (vide infra). The present compound may therefore be considered as containing an Ir(-I)→Rh(I) dative bond. This formulation is supported by the square-planar geometry at Rh, an arrangement typical of d^8 systems. The dppm phosphorus atoms P(2) and P(4) are approximately trans to each other about Rh (P(2)-Rh-P(4) = 167.66(8)°) as are the carbonyl group C(3)O(3) and the Ir center (Ir-Rh-C(3) = 175.7(3)°). The geometry about Ir, on the other hand, may be described as roughly trigonal bipyramidal, with Rh and C(2) in the axial sites and P(1), P(3) and C(1) in the equatorial positions. However, it must be pointed out that the distortions from this geometry are not negligible. In particular, the Rh-Ir-C(1) angle, at 66.3(2)°, is rather acute and all three equatorial substituents are bent away from C(2) by approximately 100°, such that the Ir center is raised 0.355 Å above the plane defined by P(1), P(3), and C(1). Alternately, if the Ir→Rh bond is not included in the above description, the coordination geometry about Ir in the isolated $Ir(CO)_2P_2$ unit may be described as approximately tetrahedral.

Such a view is consistent with Ir being in the -1 oxidation state, having a d^{10} configuration (cf. $Ir(CO)_4^-$) and suggests a pseudo-halide formulation for this group. The largest distortions from an idealized tetrahedral geometry again appear to result from the formation of the Ir→Rh dative bond and a possible weak interaction between the carbonyl group, C(1)O(1), and Rh (vide infra). The Ir(-I) formulation is supported by the analogous coordination geometries observed for the d^{10} Ni(0) centers in the closely related complexes $[Ni_2(CO)_2(\mu\text{-}CO)(dppm)_2]$[31] and $[Ni_2(CO)_2(\mu\text{-}CO)((CF_3)_2PSP(CF_3)_2)_2]$.[32,33] The structure of 3 is also very similar to that determined for the related species $[(PEt_3)_2RhCo(CO)_5]$[34] and to that proposed for $[RhCo(CO)_7]$,[35] and it is noteworthy that a mixed-valence formulation and a labile Co(-I)→Rh(I) dative bond were also proposed for the former. The fact that facile cleavage of the Co→Rh bond in the closely-related species $[RhCo(CO)_3(dppm)_2]$ (yielding $[Rh(CO)(dppm)_2]^+$ and $[Co(CO)_4]^-$) has been demonstrated[30b] offers further support for mixed-valence formulations for these dppm-bridged species. Compound 3 and the related Rh_2, Ir_2 and RhCo analogues are thus members of a growing class of complexes containing dative M→M' bonds.[30,34,36]

The Ir-Rh distance of 2.7722(7) Å falls within the range typically observed for Rh-Rh (2.52-2.84 Å)[5,7,17,28,29,37] and Ir-Ir (2.77-2.89 Å)[11,13,16,19,38] single bonds in related systems. Compression along the Ir-Rh axis, through mutual attraction of the metals, is borne out through comparison of the Ir-Rh distance with the intraligand P···P separations (2.991(3) Å, 2.983(3) Å). The Ir→Rh dative bond is accompanied by what may be a weakly semibridging carbonyl group, C(1)O(1), bonded primarily to Ir (Ir-

C(1) = 1.857(1) Å) and interacting weakly with Rh (Rh···C(1) = 2.644(7) Å). This group is nearly linear with respect to Ir (Ir-C(1)-O(1) = 171.9(6)°) and is rather strongly bound to this metal, as evidenced by the short Ir-C(1) distance. The C(1)-O(1) distance is longer than those for the other carbonyl groups, possibly resulting from a slight decrease in the C-O bond order due to donation of electron density from Rh into the π^* orbital of C(1)-O(1), in order to alleviate charge buildup at the Rh center due to the dative Ir→Rh bond. The Rh-C(1) distance is longer than the corresponding metal-semibridging carbonyl distance in the dirhodium analogue (2.533(3) Å), indicating a weaker interaction in the present case. The structural parameters for this carbonyl group do not adequately fit the trends described previously for known classes of semibridging carbonyls,[39] implying therefore that the interaction of C(1)O(1) with Rh may be rather weak. This would seem to agree with the lack of coupling between rhodium and either of the Ir-bound carbonyl ligands in the ^{13}C NMR spectrum.

Other parameters in the molecule are essentially as expected. The Ir-P distances are very similar to the Rh-P distances, despite the dissimilar coordination geometries about the metals.

(b) Preparation and Characterization of Compounds. Although the chemistries of dirhodium and diiridium systems can differ appreciably, they frequently do so in a complementary manner. As an example, this research group has shown in several previous studies[9,10,13-15,19,40] that the more stable and less kinetically labile iridium complexes can frequently serve as models for unstable or labile intermediates in analogous rhodium chemistry. It therefore appeared an obvious extension to investigate the related heterobimetallic rhodium-iridium compounds, with the hope that some of these might combine the more desirable characteristics (in terms of reactivity and stability) observed in the dirhodium and diiridium chemistry.

The initial series of dppm-bridged dirhodium hydridocarbonyl complexes was prepared by Eisenberg and coworkers.[17,18] Of the complexes $[Rh_2(CO)_3(dppm)_2]$, $[Rh_2(CO)_2(\mu\text{-}H)(\mu\text{-}CO)(dppm)_2]^+$, $[Rh_2(CO)_2(\mu\text{-}H)(dppm)_2]^+$ and $[Rh(CO)(\mu\text{-}H)(dppm)]_2$, the protonated tricarbonyl and neutral dihydride dicarbonyl species were found to act as catalyst precursors for the water-gas shift reaction and the hydrogenation of unsaturated organic substrates; however, little was known about the intermediates active in these transformations. A wider series of diiridium hydridocarbonyl complexes was later characterized by our research group.[16] Although not catalytically active, these species could be used to infer the structures of possible intermediates involved for the dirhodium-catalyzed systems, an approach that was used in one study to construct a model cycle for the water-gas shift reaction.[9] The greater strength of Ir-H over Rh-H bonds also contributed to the formation of several stable diiridium polyhydride complexes not having dirhodium analogues. One of these was $[Ir_2(H)_4(CO)_2(dppm)_2]$, which was formed via borohydride reduction of *trans*-$[IrCl(CO)(dppm)]_2$ under hydrogen atmosphere; this tetrahydride species served as a starting point for other polyhydride complexes.[16] It was shown that the trihydridic complex $[Ir_2(H)(CO)_2(\mu\text{-}H)_2(dppm)_2][BF_4]$ could be obtained through reaction of the tetrahydride with either $HBF_4{\bullet}OEt_2$

(involving loss of H_2 from a presumed pentahydridic intermediate) or $[Ph_3C^+][BF_4^-]$ (a hydride abstraction). This trihydridic compound serves as the precursor for the complexes $[Ir(CO)(\mu\text{-}H)(dppm)]_2$ (**1**) and $[Ir_2(CO)_4(\mu\text{-}H)(dppm)_2][BF_4]$ (**2**), which are described below.

In the original study[16] the diiridium dihydride complex analogous to $[Rh(CO)(\mu\text{-}H)(dppm)]_2$[18] was not synthesized. However, complex **1** has now been successfully prepared through the deprotonation of $[Ir_2(H)(CO)_2(\mu\text{-}H)_2(dppm)_2]^+$ using the strong base potassium *tert*-butoxide. Although $[Rh(CO)(\mu\text{-}H)(dppm)]_2$ can be prepared directly via reaction of *trans*-$[RhCl(CO)(dppm)]_2$ with $NaBH_4$ under H_2, the corresponding reaction with the diiridium system yields the tetrahydride, $[Ir_2(H)_4(CO)_2(dppm)_2]$ as noted above. Another difference between compound **1** and its dirhodium analogue is that the former cannot be isolated in the solid state; attempted crystallizations from the deep red solutions containing complex **1** led only to isolation of grey products of uncertain composition. However, the diiridium dihydride is stable in solution for several hours, enabling it to be characterized by spectroscopic means. The infrared spectrum shows one strong band at 1909 cm^{-1}, very close to that seen for the rhodium species (1920 cm^{-1} (Nujol)) and supporting a similar structural formulation, as shown below. The $^{31}P\{^1H\}$ NMR spectrum of a solution of **1** is temperature invariant and shows a singlet resonance at δ 12.9, while in the highfield region of the ^1H NMR spectrum is seen a single quintet resonance at δ -10.22 ($^2J_{P\text{-}H}$ = 6.6 Hz) corresponding to two hydrides bridging the metal centers. Species **1** readily reacts with H^+ or H_2, leading to the immediate formation of $[Ir_2(H)(CO)_2(\mu\text{-}H)_2(dppm)_2]^+$ or $[Ir_2(H)_4(CO)_2(dppm)_2]$,

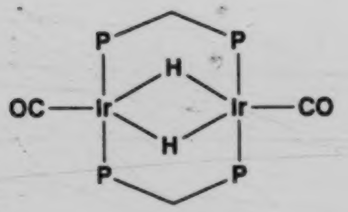

1

respectively, and with CO, through reductive elimination of H_2, to yield $[Ir_2(CO)_4(dppm)_2]$, which has also been previously characterized.[9]

Interconversions between the neutral tetrahydride and tetracarbonyl complexes ($[Ir_2(H)_4(CO)_2(dppm)_2] + 2\ CO \rightleftarrows [Ir_2(CO)_4(dppm)_2] + 2\ H_2$) and between the cationic trihydride and protonated tricarbonyl species ($[Ir_2(H)(CO)_2(\mu\text{-}H)_2(dppm)_2]^+ + CO \rightleftarrows [Ir_2(CO)_2(\mu\text{-}H)(\mu\text{-}CO)(dppm)_2]^+ + H_2$) had previously been observed, but an unexpected byproduct of the reaction of $[Ir_2(H)(CO)_2(\mu\text{-}H)_2(dppm)_2][BF_4]$ with CO was the protonated tetracarbonyl, $[Ir_2(CO)_4(\mu\text{-}H)(dppm)_2][BF_4]$ (**2**). This compound can also be prepared by protonation of $[Ir_2(CO)_4(dppm)_2]$ (see Experimental). No dirhodium analogues of either of the tetracarbonyl species **2** or $[Ir_2(CO)_4(dppm)_2]$ have been reported, consistent with the greater basicity of iridium, which allows it to form complexes containing larger numbers of carbonyl ligands. Like the neutral tetracarbonyl, **2** is quite prone to CO loss (forming $[Ir_2(CO)_2(\mu\text{-}H)(\mu\text{-}CO)(dppm)_2][BF_4]$), thus characterization of this product has been confined to spectroscopic measurements in solutions that are kept under CO atmosphere. The infrared spectrum is consistent with a structure containing only terminal carbonyl groups (ν(CO): 1998, 1981, 1959 cm^{-1}), while a singlet at δ -9.6 in the $^{31}P\{^1H\}$ NMR spectrum confirms a symmetrical formulation, with all phosphorus nuclei being chemically equivalent. In the ^{1}H spectrum a quintet at δ -9.95 ($^2J_{P\text{-}H}$ = 9.4 Hz) is indicative of a hydride bridge, while the single broad resonance for the dppm methylene protons, at δ 5.02, suggests a fluxionality of the hydride, likely via a mechanism as shown; the inequivalent protons (H_a and H_b of each

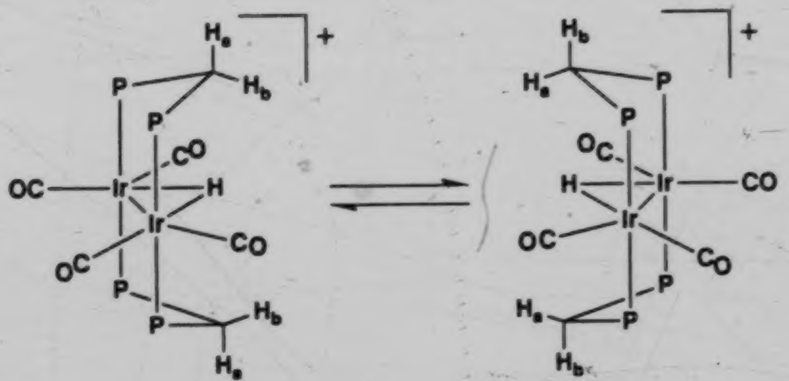

CH_aH_b) on opposite sides of the plane formed by the iridium and phosphorus nuclei would be made equivalent by "tunnelling" of the hydride from one side of the Ir_2P_4 plane to the other, as well as a "flipping" of the orientations of the methylene bridges. Although both of these processes are required to produce the observed signal for the methylene protons, they need not be coupled. The tunnelling process can be visualized as shown below, viewed in the equatorial plane of the complex with the

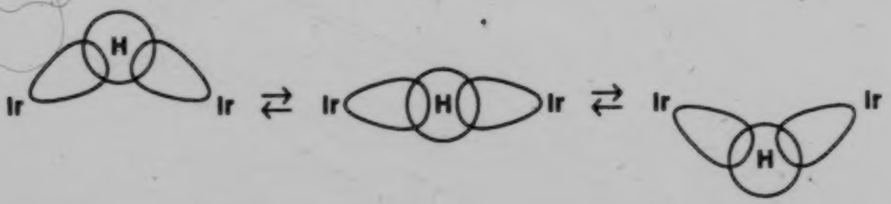

diphosphine and carbonyl ligands omitted for clarity. The complex [Pt_2-$(H)_2(\mu\text{-}H)(dppm)_2]^+$ [41] is believed to undergo interchange in a similar manner (see Chapter 1). The slight increase in metal-metal distance in going from a bent to a linear M-H-M linkage should not be difficult for the bridging dppm ligands to accommodate.

With the preparation of an extensive series of diiridium hydridocarbonyl complexes accomplished, it was next desired to expand the scope of interest to include species containing both rhodium and iridium centers. For the preparation of the heterobimetallic complexes, a useful precursor proved to be [$RhIrCl_2(CO)_2(dppm)_2$], which was first prepared by Shaw and coworkers;[42] the compounds derived from it are shown in Scheme 2.1. The reaction of this mixed-metal starting material with $NaBH_4$ under CO gives rise to the formally zerovalent binuclear species, [$RhIr(CO)_3(dppm)_2$] (3), which is the mixed-metal analogue of the previously-observed dirhodium[17b,28] and diiridium[9] compounds. Its $^{31}P\{^1H\}$ NMR spectrum (see Figure 2.3) is characteristic of those observed for such a mixed-metal dppm-bridged complex, displaying a pattern consistent with an AA'BB'X spin system. The Rh-bound phosphorus resonance appears as a doublet of multiplets (δ 16.4), with each multiplet resembling the Ir-P signal (δ -16.3). No resonance is observed in the highfield region of the ^1H NMR spectrum, indicating that **3** is not a hydrido species. The infrared spectrum of **3** displays bands at 1958, 1940 and 1849 cm^{-1} (Nujol) and is similar to those of the above-mentioned homobimetallic tricarbonyls, suggesting a similar structure, in which one metal is 5-coordinate and the other 4-coordinate. The X-ray structure confirms the non-A-frame structure of the complex and indicates that the "third" CO ligand and the related distortions at the metal center are

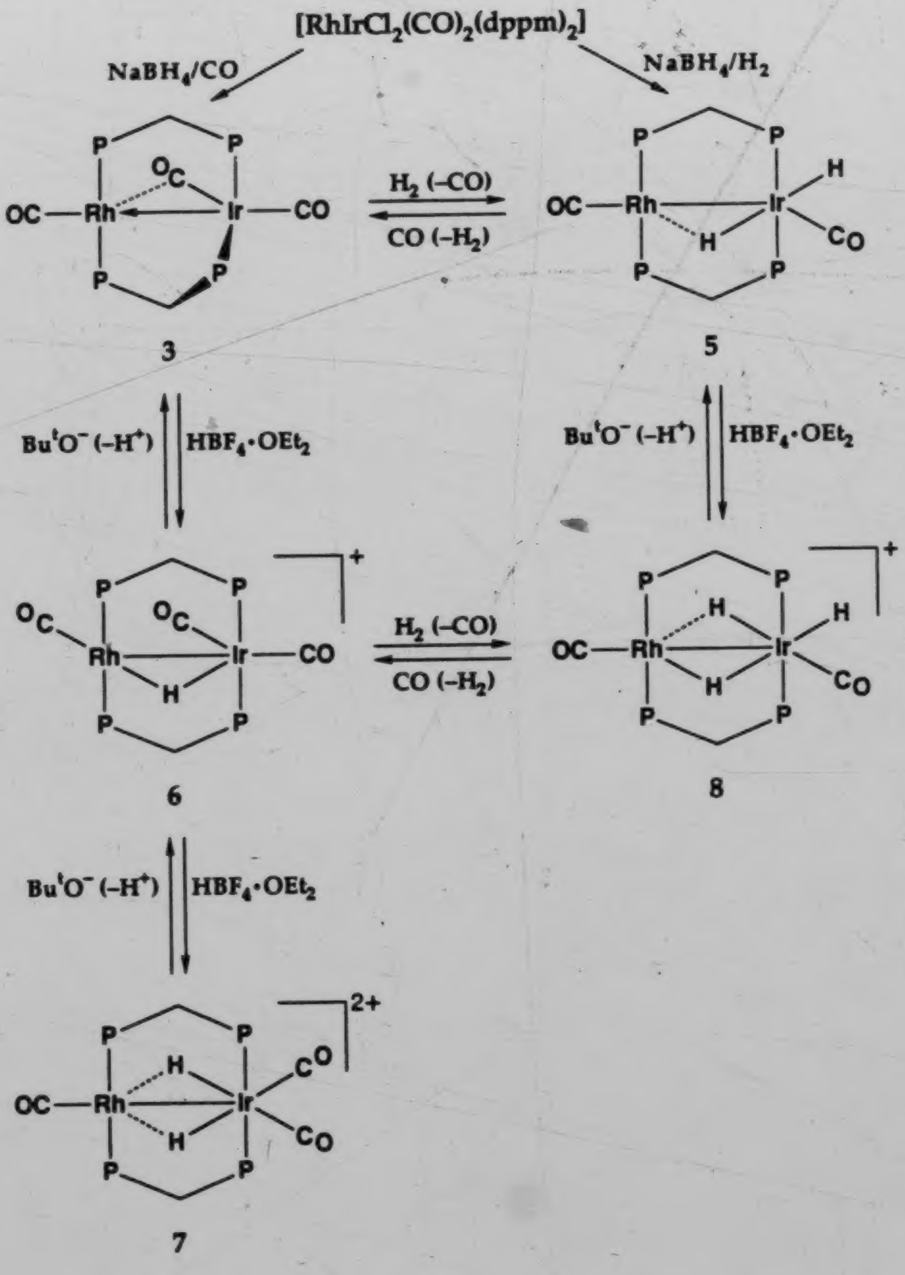
[RhIrCl$_2$(CO)$_2$(dppm)$_2$]
NaBH$_4$/CO
NaBH$_4$/H$_2$
H$_2$ (–CO)
CO (–H$_2$)
3
5
Bu^{t}O$^-$ (–H$^+$)
HBF$_4$·OEt$_2$
Bu^{t}O$^-$ (–H$^+$)
HBF$_4$·OEt$_2$
+
+
H$_2$ (–CO)
CO (–H$_2$)
6
8
Bu^{t}O$^-$ (–H$^+$)
HBF$_4$·OEt$_2$
2+
7

Scheme 2.1.

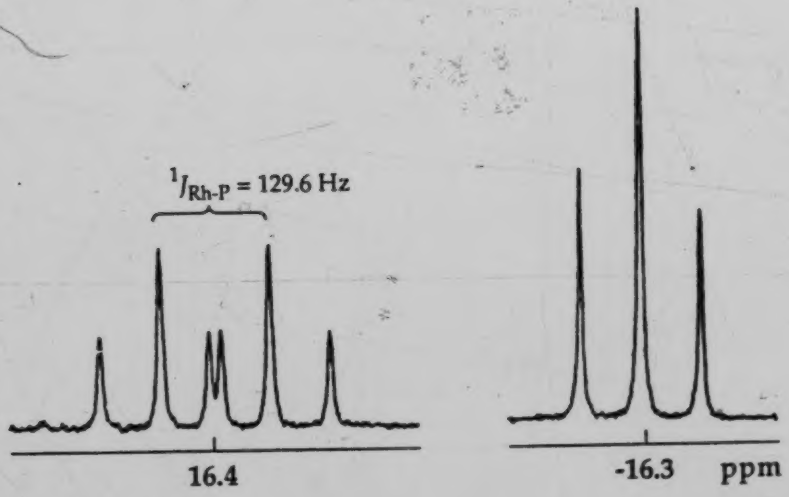

Figure 2.3. The $^{31}P\{^1H\}$ NMR spectrum of complex 3 at 20 °C.

associated with iridium. That the Ir atom should have the M(-I) formulation instead of Rh is consistent with the greater electronegativity of the former.[43]

Like its homobimetallic counterparts, species 3 is fluxional in solution. The room-temperature $^{13}C\{^1H\}$ NMR spectrum shows resonances at δ 188.7 (triplet, $^2J_{P\text{-}C}$ = 18.1 Hz) and 185.1 (doublet of triplets, $^1J_{Rh\text{-}C}$ = 67.9 Hz and $^2J_{P(Rh)\text{-}C}$ = 13.7 Hz) with relative intensities of 2:1, whereas at -80 °C three signals of equal intensity appear at δ 191.9 (triplet, $^2J_{P\text{-}C}$ = 41.7 Hz), 185.0 (broad singlet), and 183.8 (doublet of triplets, $^1J_{Rh\text{-}C}$ = 69.7 Hz and $^2J_{P\text{-}C}$ = 13.4 Hz). The fluxionality at ambient temperature appears to involve interchange between the terminal and semibridging carbonyls attached to iridium, with the rhodium carbonyl remaining unaffected therefore uninvolved in the process. It should also be noted that the $^{31}P\{^1H\}$ NMR spectrum of 3 remains essentially invariant throughout the temperature range studied (+25 to -80 °C), indicating that the mechanism for phosphorus equilibration is independent of that for carbonyl interchange. Unlike the homobimetallic analogues $[Rh_2(CO)_3(dppm)_2]$ and $[Ir_2(CO)_3(dppm)_2]$, two different methylene proton signals are observed in the ^1H NMR spectrum of complex 3, ruling out an intermediate for either interchange process in which the dppm groups are oriented trans to each other at both metal centers. The combination of fluxional processes may be illustrated as shown below. These Newman projections are viewed down the Ir-Rh bond, with the CO ligand coordinated to iridium (which lies approximately along this bond) included to show its role in the interchange. Equilibration of the carbonyl groups bound to Ir is accomplished as

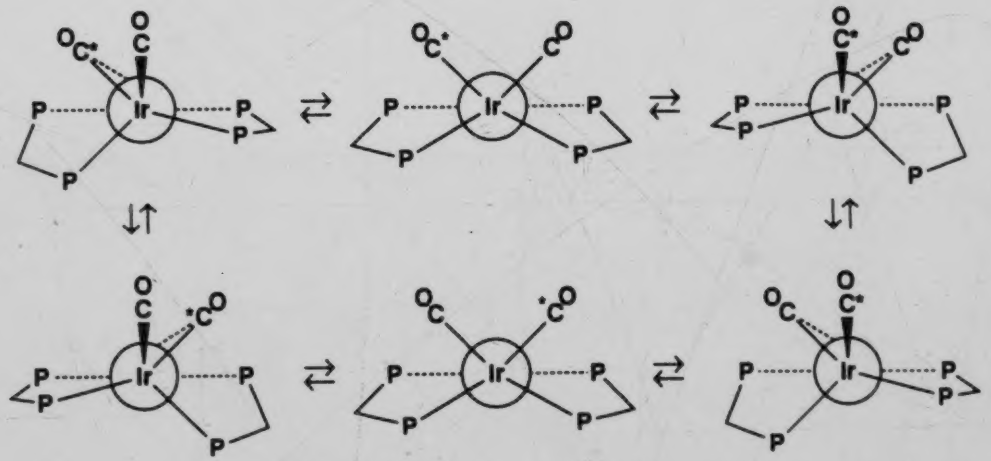

shown by the structures separated by horizontal arrows, and passes through a square pyramidal intermediate in which the Rh atom is at the apex and the phosphine and carbonyl groups form the base. It can be seen that interruption of this process leaves the carbonyl groups inequivalent but still allows the sets of phosphorus atoms to equilibrate via a pivoting of the $IrP_2(CO)$ unit about the Rh-Ir bond, as shown by the vertical arrows. In either case the dppm methylene protons above the "planes" of the $RhIrP_4$ units cannot become chemically equivalent to those below.

The above proposal for the fluxionality of complex 3 assumes that the structure in solution strongly resembles that in the solid state, i.e. the diphosphine ligands are eclipsed in an asymmetric fashion. If the structure observed were actually due to crystal packing effects, complex 3 might assume a more symmetrical configuration in solution, as shown below. Here, pivoting of the semibridging carbonyl and iridium-bound phosphines about the metal-metal bond would not be necessary to maintain two sets of two chemically-equivalent phosphorus atoms, and would

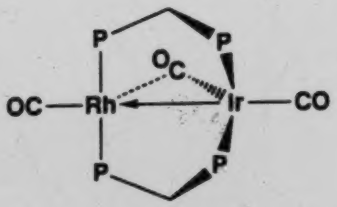

account for the independence of the $^{31}P\{^1H\}$ NMR spectrum with respect to temperature. Equilibration of the iridium-bound carbonyl groups at room temperature could still occur via the intermediate shown in the scheme above in which the iridium center adopts a square pyramidal coordination geometry.

Although facile scrambling of the carbonyl ligands of complex **3** over both metals is not observed at ambient temperatures under N_2 atmosphere, ligand exchange under ^{13}CO is facile, resulting in enrichment of all three positions within $^1/_2$ h. It would appear that a labile tetracarbonyl species, $[RhIr(CO)_4(dppm)_2]$ (**4**), analogous to the labile diiridium species, $[Ir_2(CO)_4(dppm)_2]$,[9] may be involved as an intermediate in the scrambling process. However, its identification is not unambiguous. The infrared spectrum of a solution of **3** under an atmosphere of CO shows two new carbonyl stretches at 1955 and 1926 cm^{-1}, while the $^{31}P\{^1H\}$ NMR spectrum shows the two signals due to **3**, with no apparent evidence of an additional species. However, as the temperature is lowered, two additional resonances appear at δ 3.1 and -12.3. At -60 °C these resonances appear as an unresolved multiplet and a pseudotriplet, respectively, and account for ca. 40% of the total intensity. At the same temperature, the $^{13}C\{^1H\}$ NMR spectrum of a ^{13}CO-enriched sample of **3** under an atmosphere of ^{13}CO shows new broad resonances at δ 188 and 197 as well as one that falls under the δ 192 resonance due to **3**; unfortunately the very poor signal-to-noise ratio for these signals does not allow their unambiguous assignment. Flushing the solution with N_2 results in the disappearance of all new resonances, leaving only those due to **3**. This labile species is believed to be the tetracarbonyl, **4**. Although the NMR studies indicate that this species is fluxional it does not appear to be interconverting with **3** on the NMR time scale since the resonances due to **3** and **4** appear to behave independently as the temperature is varied.

The reaction of $[RhIrCl_2(CO)_2(dppm)_2]$ with sodium borohydride under an atmosphere of H_2 gives rise to complex **5**, $[RhIr(H)(CO)_2(\mu\text{-}H)(dppm)_2]$. Its solution infrared spectrum shows only one carbonyl stretch (1937 cm^{-1}), suggestive of a symmetrical structure similar to the homobimetallic dihydrides $[M_2(CO)_2(\mu\text{-}H)_2(dppm)_2]$ (M = Rh,[18] Ir (**1**)); however, the presence of two carbonyl bands in the solid-state IR spectrum (1942, 1924 cm^{-1}) suggests a less symmetrical structure, and a weak stretch at 2033 cm^{-1} suggests at least one terminal hydride ligand in the complex. Furthermore, the highfield region of the ^{1}H NMR spectrum of **5** shows two different resonances (δ -11.00 and -12.73). Both of these are broad at ambient temperatures, but at -40 °C the latter hydride peak (now at δ -12.84) appears as a triplet. This highfield signal is due to a hydride ligand terminally bound to iridium ($^2J_{P(Ir)\text{-}H}$ = 17.6 Hz), as selective heteronuclear decoupling of the iridium-bound phosphorus resonance causes this signal to collapse into a singlet. At this temperature it is also observed that the lower-field hydride signal (now at δ -11.15) also resolves into a broad doublet when either the iridium-bound or the rhodium-bound phosphorus resonance is selectively irradiated. Although the poor resolution makes it impossible to determine the phosphorus-hydride couplings, the rhodium-hydride coupling may be estimated as approximately 14 Hz. Clearly this lower-field resonance is due to a hydride ligand that bridges the two metals. The value of $^1J_{Rh\text{-}H}$ involving this hydride suggests that the rhodium-hydride interaction is weaker than in similar dirhodium complexes that contain symmetrically-bridging hydride ligands ($^1J_{Rh\text{-}H}$ = 20 Hz for $[Rh_2(CO)_2(\mu\text{-}H)_2(dppm)_2]$,[18] and $^1J_{Rh\text{-}H}$ = ca. 20 Hz for the series $[Rh_2Cl_2X(\mu\text{-}H)(\mu\text{-}CO)(dppm)_2]$ (X = Cl, $OSO_2C_6H_4CH_3$, FBF_3)[37f]). This suggests that compound **5** contains an unsymmetrical Rh-H-Ir bridge in which the hydride interacts more strongly with Ir. Couplings of this magnitude have been noted in other mixed binuclear and trinuclear Rh/Ir complexes containing asymmetrically-bridging hydrides,[15,44] while a $^1J_{Rh\text{-}H}$ coupling of 24.4 Hz has been reported for $[(\eta^4\text{-}C_8H_{12})Rh(\mu\text{-}H)(\mu\text{-}Cl)IrH_2(PPh_3)_2]$, a species containing a more symmetrical hydride bridge.[45] The structure proposed for **5** (see Scheme 2.1) thus differs from that for the homobimetallic dihydrides, in which *both* hydrides bridge the metals symmetrically. In Scheme 2.1, dashed lines between Rh and H are employed to denote this weaker bonding. A trans arrangement of the hydride ligands across the iridium center in **5** would explain the reluctance of this species to reductively eliminate H_2; however, a cis disposition of hydrides cannot unambiguously be ruled out, since even for **7**, for which two hydrides *are* mutually cis, reductive elimination is slow (vide infra). Although it is possibly not surprising that **5** is thermally more stable than the dirhodium analogue, it is surprisingly also more stable than the diiridium species; both homobimetallic complexes decompose within several hours at 20 °C whereas **5** is stable for several days at room temperature.

Compound **3** may be converted to **5** via reaction with H_2 in THF at room temperature over a 24 h period, whereas conversion of **5** to **3** by reaction with CO in THF at room temperature is complete within approximately 2 h.

Compound **3** reacts with one equivalent of $HBF_4{\cdot}OEt_2$, yielding $[RhIr(CO)_3(\mu\text{-}H)(dppm)_2][BF_4]$ (**6**). This compound has the same ligand stoichiometry as the dirhodium[17] and diiridium[9,11] analogues, but possesses a significantly different structure. Whereas the homobinuclear species have A-frame structures in which a hydride *and* a carbonyl ligand bridge the metals, compound **6** has *no* bridging carbonyl group. The lowest CO stretch in the infrared spectrum (1899 cm^{-1}) is significantly higher than those due to the bridging carbonyls in the homobimetallic analogues (1870 cm^{-1} (Rh_2);[17] 1850 cm^{-1} (Ir_2)[9]). The $^{13}C\{^1H\}$ NMR spectrum at room temperature shows signals at δ 186.2 (doublet of triplets, $^1J_{Rh\text{-}C}$ = 73.9 Hz and $^2J_{P(Rh)\text{-}C}$ = 15.0 Hz) and 179.5 (broad) with relative intensities of 1:2, indicating that two carbonyls are located on the iridium center while one is coordinated to rhodium; the ^1H NMR spectrum (see Figure 2.4) shows one highfield resonance, a complex multiplet at δ -10.19 due to the bridging hydride, and one resonance at δ 4.38 (quintet) for the methylene protons of the dppm groups. At -80 °C the carbon NMR spectrum shows that the Rh-bound carbonyl resonance remains unchanged while the broad Ir-carbonyl signal splits into two unresolved ones of equal intensity at δ 184.1 and

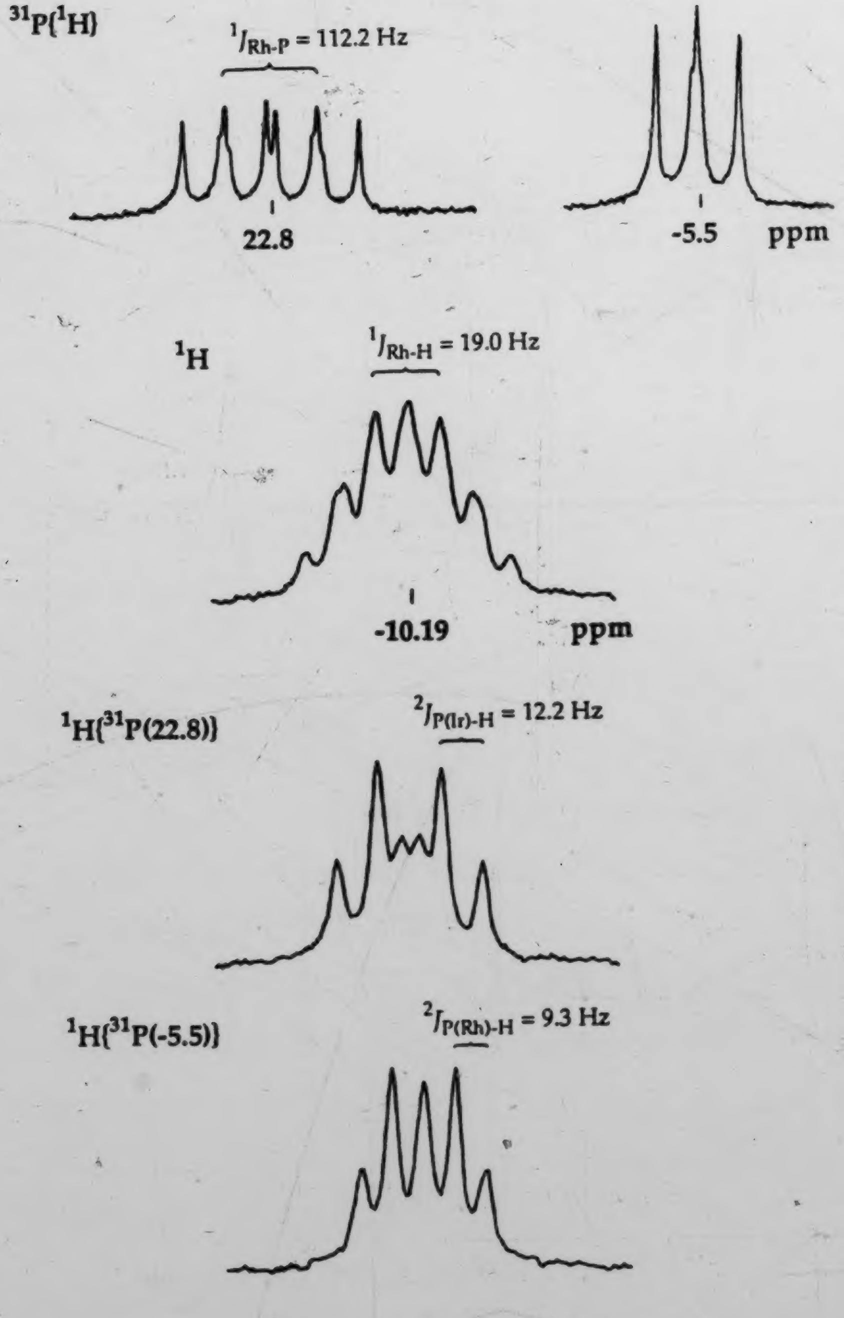

Figure 2.4. The $^{31}P\{^1H\}$, ^1H and $^1H\{^{31}P\}$ NMR spectra of complex 6 at 20 °C.

176.9. In the proton NMR spectrum the hydride resonance is broad at this temperature while the methylene resonance has resolved into two signals at δ 4.54 and 4.07 integrating as two protons each. It appears that a fluxional process such as that shown below equilibrates the iridium-bound carbonyl

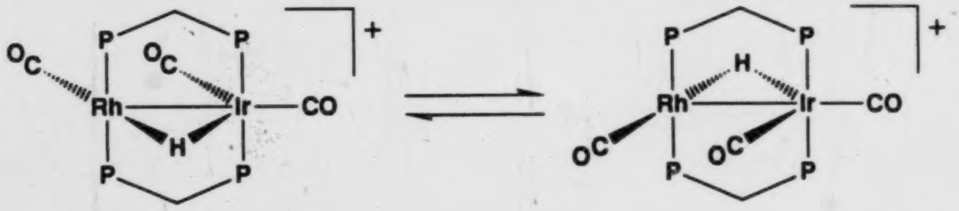

groups at higher temperatures. This interchange may be proposed to occur via tunnelling of the hydride ligand between the metals resulting in a twisting of the $HIr(CO)_2$ unit about the P-Ir-P axis, bringing the hydride from one face of the dimer to the other and interchanging the carbonyls on Ir. Analogous structures and mechanisms of fluxionality have been proposed for the isoelectronic species $[RhM(\mu\text{-}H)(CO)_3(dppm)_2]^{n+}$ (M = Co, n = 1;[30a] M = Fe, n = 0[30b]). Selective decoupling of the two phosphorus environments during observation of the ^1H NMR spectrum at 22 °C enables the magnitudes of the Rh-H and P-H couplings to be determined ($^1J_{Rh\text{-}H}$ = 19.0 Hz, $^2J_{P(Rh)\text{-}H}$ = 9.3 Hz, $^2J_{P(Ir)\text{-}H}$ = 12.2 Hz). The values for the phosphorus-hydrogen couplings might suggest that this hydride is more strongly bound to iridium than rhodium; however the Rh-H coupling, although somewhat smaller, is comparable to those quoted above for hydrido-bridged dirhodium compounds and other symmetrically-bridged species, thus is more in line with a close-to-symmetrical bridge. Compound **6** may be converted back to **3** via reaction with the strong base potassium *tert*-butoxide, but this transformation does not occur when a weaker base such as triethylamine is used.

Complex **6** undergoes facile carbonyl exchange with free CO; in CH_2Cl_2 solution at room temperature under atmospheric pressure of ^{13}CO, **6** is seen to be quantitatively enriched at all positions within 2 h (as observed via solution infrared spectroscopy). This result may be seen as evidence for the involvement of a species formulated as $[RhIr(CO)_4(\mu\text{-}H)(dppm)_2]^+$ (a mixed-metal analogue of **2**) in the exchange process. Such a species, like the neutral tetracarbonyl **4**, would be expected to be unstable, as its formation would require the rhodium center to adopt an 18-electron configuration, a situation found to be disfavored within this series of compounds. The $^{13}C\{^1H\}$ and $^{31}P\{^1H\}$ NMR spectra of a ^{13}CO-enriched sample of **6** under ^{13}CO shows no resonances assignable to a protonated tetracarbonyl species.

Reaction of **6** with one equivalent of $HBF_4{\cdot}OEt_2$ (or reaction of the neutral tricarbonyl, **3**, with two equivalents of $HBF_4{\cdot}OEt_2$) yields the dicationic species $[RhIr(CO)_3(\mu\text{-}H)_2(dppm)_2][BF_4]_2$ (**7**). This product appears to resemble the iridium carbonyl hydrides $[Ir_2(H)_2(CO)_3(dppm)_2][BF_4]_2$ and $[Ir_2(CO)_4(\mu\text{-}H)_2(dppm)_2][BF_4]_2$,[9] in that movement of the hydride ligands of **7** from bridging to terminal sites (one on each metal) would make this complex structurally comparable to the diiridium tricarbonyl species, while addition of one CO ligand at the coordinatively unsaturated Rh center would produce a form parallel to the diiridium tetracarbonyl. These changes would involve the formation of terminal Rh-H and Rh-CO bonds, which are less favored than the equivalent Ir-H and Ir-CO bonds, providing a rationale for the nonobservance of the exact mixed-metal analogues of these Ir_2 systems. Only one hydride signal is seen in the ^1H NMR spectrum of **7** (see Figure 2.5), appearing as a complex multiplet at δ -11.18 and integrating as two protons. Selective irradiation of the resonance due to the Rh-bound phosphorus nuclei causes the hydride signal to collapse to an overlapping doublet of triplets ($^1J_{Rh\text{-}H}$ = 17.3 Hz, $^2J_{P(Ir)\text{-}H}$ = 11.1 Hz). Irradiation of the Ir-P signal resolves the hydride multiplet into a broadened doublet, from which $^2J_{P(Rh)\text{-}H}$ may be estimated as ≤ 7 Hz (the half-width at half-height of either peak of the doublet); broadband phosphorus decoupling further sharpens this doublet, but the resonance is not resolved to baseline and the peaks are still 7 Hz wide at half-height, making the value of $^2J_{P(Rh)\text{-}H}$ difficult to determine accurately. The Rh-H coupling constant suggests a somewhat weaker interaction of the hydride ligands with Rh, which is supported by the failure to resolve coupling to the Rh-bound phosphines; however bonding appears to be more symmetrical than in species **5**. The infrared spectra of this complex indicate that all carbonyl groups are terminally bound. Species **7** may be deprotonated easily by NEt_3 regenerating compound **6**.

Reaction of **5** with one equivalent of $HBF_4{\bullet}OEt_2$ leads to the cationic trihydride **8**, $[RhIr(H)(CO)_2(\mu\text{-}H)_2(dppm)_2][BF_4]$, similar to the result of the protonation of complex **1** but quite unlike the product reported in the rhodium chemistry, where H_2 loss apparently occurs, yielding $[Rh_2(CO)_2(\mu\text{-}H)(dppm)_2]^+$.[17,18] The ^1H NMR spectrum of **8** shows three hydride resonances (δ -10.58, -11.46 and -11.76), all of which are broadened at room temperature. Cooling the sample to -40 °C results in the resolution of the

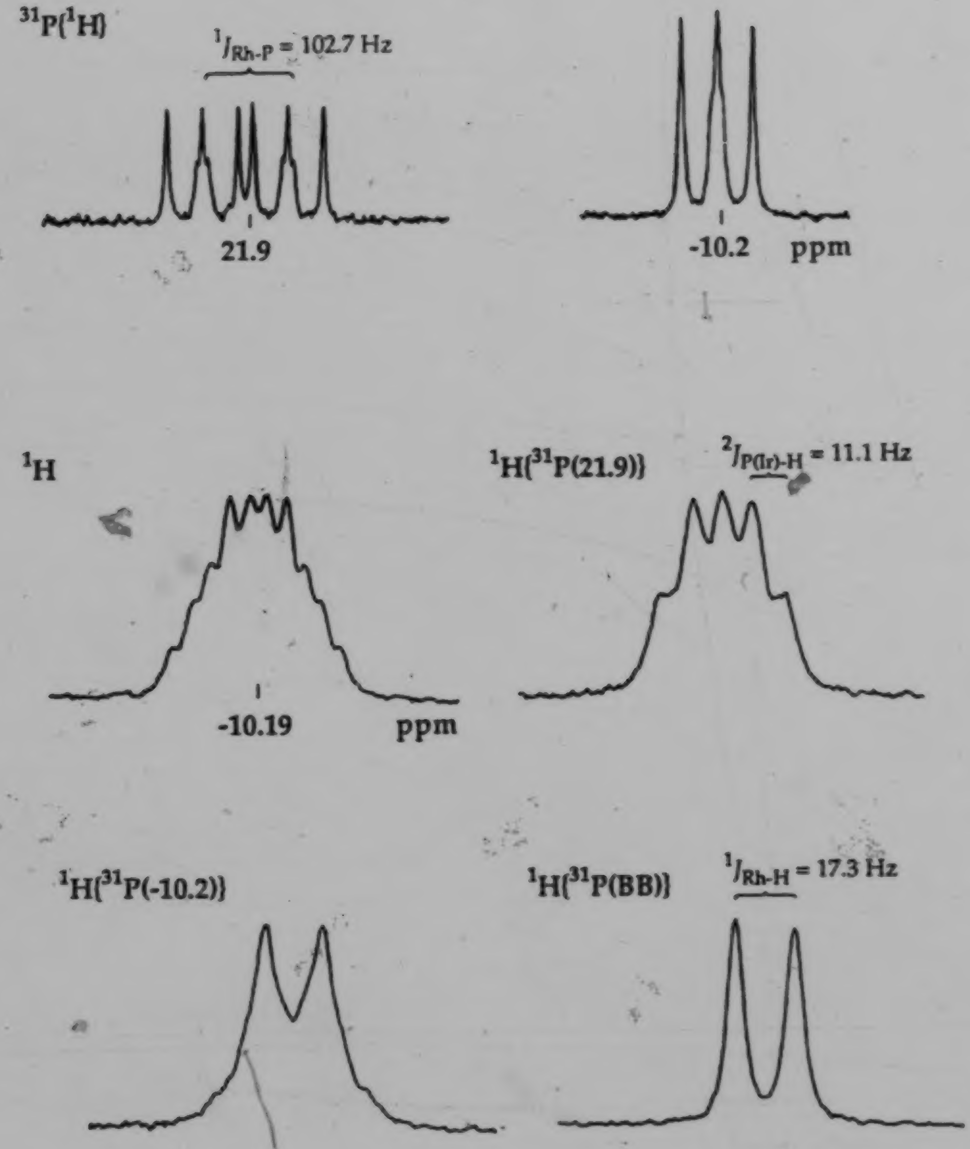

Figure 2.5. The $^{31}P\{^1H\}$, ^1H and $^1H\{^{31}P\}$ NMR spectra of complex **7** at 20 °C.

middle signal into a triplet, which was shown by selective heteronuclear decoupling of the phosphorus resonances to be a terminal hydride attached to iridium ($^{2}J_{P(Ir)-H}$ = 11.8 Hz). The other hydride resonances remained broad, even with selective ^{31}P decoupling; broadband irradiation resolved these into doublets, with $^{1}J_{Rh-H}$ = 10.4 Hz for the former and $^{1}J_{Rh-H}$ = 23.2 Hz for the latter bridging hydride, with no apparent H-H coupling observed. The magnitudes of the rhodium-hydride couplings indicate that unlike complex **7**, the bridging hydrides in **8** are disposed in two different manners; the one with the larger coupling to Rh probably approximates a symmetrical bridge, the other interacts much less strongly with Rh (therefore is more strongly bound to Ir). Although, based on the spectroscopic study, it is not clear which bridging hydride ligand is more symmetrically bound, it is assigned as the one opposite the terminal hydride, as shown in Scheme 2.1. Such a proposal is consistent with the high trans influence of the terminal hydride, resulting in a weakening of the opposite Ir-H bond and a concomitant strengthening of the associated Rh-H bond. The infrared spectra of **8** are quite similar to those observed for $[Ir_2(H)(CO)_2(\mu\text{-}H)_2(dppm)_2][BF_4]$.[13] Whereas exchange between the terminal and one bridging hydride ligand was observed in the diiridium species, none was observed for **8**. This is not surprising since, according to the mechanism previously proposed,[13,16] a species with a terminal hydride on Rh (and none on Ir) would be one of the limiting forms, which should be significantly less stable than that observed owing to the differences between the Ir-H and Rh-H bond energies. Compound **8** may be converted back to **5** by reaction with BH_4^- or Bu^tO^-. Attempts to further protonate **8** to yield a dicationic tetrahydride failed. In fact, no species containing more than three hydrides was observed in this study, in contrast to the diiridium chemistry where several tetrahydride complexes were found.

As described in the Experimental Section, conversion of the protonated tricarbonyl complex **6** to **8** via reaction with H_2 is complete within 3 h, and has been found to be a synthetic route to complex **8** superior to the protonation of the neutral dihydride, **5**. The reverse process (**8** + CO → **6**) requires 24 h.

Conclusions

The work presented in this chapter and in other closely related studies[15,46] illustrates the accessibility of heterobimetallic RhIr compounds. The preparative routes employed, and the potential for new modes of reactivity introduced by the presence of two different types of metal centers in the same complex, have prompted investigations within this research group into the chemistry of other mixed-metal systems (e.g. RhMn,[47] RhRe,[47a,48] RhOs,[47a,49] IrOs[50]). Of particular interest are complexes containing dative bonding interactions between metals of differing oxidation states, as in $[RhIr(CO)_3(dppm)_2]$ (**3**). The unusual non-A-frame structure of **3** illustrates the low oxidation states of both metals, the dative Ir→Rh interaction, and the coordinative unsaturation at the Rh center, properties which suggest that compound **3** and its homobimetallic dirhodium and diiridium analogues may be susceptible to additions of small molecules. Studies of the reactivity of these $[MM'(CO)_3(dppm)_2]$ species (especially for MM' = Ir_2) are the focus of subsequent chapters of this thesis.

At the outset of this thesis project, development of the chemistry of the family of Ir_2 and RhIr hydridic species was a parallel interest, but, due to a shift in emphasis towards the low-valent tricarbonyl compounds, this was not pursued. However, it is notable that, besides the bridging diphosphines, only carbonyl and hydrido ligands are present in the coordination spheres of complexes **1-8**, and that interconversions involving these and related Ir_2 and RhIr species may be accomplished via simple reversible protonation, carbonylation and hydrogenation steps. Such behavior favors the use of these species in the construction of model catalytic cycles for such processes as hydrogenation and hydroformylation (as had been previously done, using related diiridium complexes containing carbonyl, hydrido and hydroxo ligands to model the water-gas shift reaction[9]). Investigations of this type are presently underway in this research group.

References and Footnotes

1. Pruett, R. L. *Adv. Organomet. Chem.* **1979,** *17,* 1.
2. (a) James, B. R. *Homogeneous Hydrogenation;* Wiley: New York, 1974. (b) James, B. R. *Adv. Organomet. Chem.* **1979,** *17,* 319.
3. Forster, D. *Adv. Organomet. Chem.* **1979,** *17,* 255.
4. Yoshida, T.; Okano, T.; Ueda, Y.; Otsuka, S. *J. Am. Chem. Soc.* **1981,** *103,* 3411 and references therein.
5. Cowie, M.; Dickson, R. S.; Hames, B. W. *Organometallics* **1984,** *3,* 1879.
6. Cowie, M.; Loeb, S. J. *Organometallics* **1985,** *4,* 852.
7. Jenkins, J. A.; Ennett, J. P.; Cowie, M. *Organometallics* **1988,** *7,* 1845.
8. McKeer, I. R.; Sherlock, S. J.; Cowie, M. *J. Organomet. Chem.* **1988,** *352,* 205.
9. Sutherland, B. R.; Cowie, M. *Organometallics* **1985,** *4,* 1637.
10. Sutherland, B. R.; Cowie, M. *Organometallics* **1985,** *4,* 1801.
11. Sutherland, B. R.; Cowie, M. *Can. J. Chem.* **1986,** *64,* 464.
12. Cowie, M.; Vasapollo, G.; Sutherland, B. R.; Ennett, J. P. *Inorg. Chem.* **1986,** *25,* 2648.
13. McDonald, R.; Sutherland, B. R.; Cowie, M. *Inorg. Chem.* **1987,** *26,* 3333.
14. Vaartstra, B. A.; O'Brien, K. N.; Eisenberg, R.; Cowie, M. *Inorg. Chem.* **1988,** *27,* 3668.
15. Vaartstra, B. A.; Cowie, M. *Inorg. Chem.* **1989,** *28,* 3138.
16. Sutherland, B. R. Ph.D. Thesis, University of Alberta, 1984, Chapter 6.

17. (a) Kubiak, C. P.; Eisenberg, R. *J. Am. Chem. Soc.* **1980**, *102*, 3637. (b) Kubiak, C. P.; Woodcock, C.; Eisenberg, R. *Inorg. Chem.* **1982**, *21*, 2119.

18. Woodcock, C.; Eisenberg, R. *Inorg. Chem.* **1984**, *23*, 4207.

19. Vaartstra, B. A.; Cowie, M. *Organometallics* **1989**, *8*, 2388.

20. Similar diphosphine-bridged binuclear 1:1 electrolytes[9,13,15,21] have been found to display conductivity values in the range 40-60 Ω^{-1} cm^2 mol^{-1} in CH_2Cl_2 solution. See also: Geary, W. J. *Coord. Chem. Rev.* **1971**, *7*, 81.

21. (a) Cowie, M.; Dwight, S. K. *Inorg. Chem.* **1980**, *19*, 209. (b) Sutherland, B. R.; Cowie, M. *Inorg. Chem.* **1984**, *23*, 2324. (c) Gibson, J. A. E.; Cowie, M. *Organometallics* **1984**, *3*, 722. (d) Sutherland, B. R.; Cowie, M. *Organometallics* **1984**, *3*, 1869.

22. Doedens, R. J.; Ibers, J. A. *Inorg. Chem.* **1967**, *6*, 204.

23. Walker, N., Stuart, D. *Acta Crystallogr., Sect. A: Found. Crystallogr.* **1983**, *A39*, 1581.

24. Programs used were those of the Enraf-Nonius Structure Determination Package by B. A. Frenz, in addition to local programs by R. G. Ball.

25. Cromer, D. T.; Waber, J. T. *International Tables for Crystallography*; Kynoch Press: Birmingham, England, 1974; Vol. IV, Table 2.2A.

26. Stewart, R. F.; Davidson, E. R.; Simpson, W. T. *J. Chem. Phys.* **1965**, *42*, 3175.

27. Cromer, D. T.; Liberman, D. *J. Chem. Phys.* **1970**, *53*, 1891.

28. Woodcock, C.; Eisenberg, R. *Inorg. Chem.* **1985**, *24*, 1285.

29. Haines, R. J.; Meintjies, E.; Laing, M.; Sommerville, P. *J. Organomet. Chem.* **1981**, *216*, C19.

30. (a) Elliot, D. J.; Ferguson, G.; Holah, D. G.; Hughes, A. N.; Jennings, M. C.; Magnusen, V. R.; Potter, D.; Puddephatt, R. J. *Organometallics* **1990**, *9*, 1336. (b) Antonelli, D. M.; Cowie, M. *Organometallics* **1990**, *9*, 1818.

31. Zhang, Z.-Z.; Wang, H.-K.; Wang, H.-G.; Wang, R.-J.; Zhao, W.-J.; Yang, L.-M. *J. Organomet. Chem.* **1988**, *347*, 269.

32. Einspahr, H.; Donohue, J. *Inorg. Chem.* **1974**, *13*, 1839.

33. Burg, A. B.; Sinclair, R. A. *J. Am. Chem. Soc.* **1966**, *88*, 5354.

34. (a) Roberts, D. A.; Mercer, W. C.; Zahurak, S. M.; Geoffroy, G. L.; DeBrosse, C. W.; Cass, M. E.; Pierpont, C. G. *J. Am. Chem. Soc.* **1982**, *104*, 910. (b) Roberts, D. A.; Mercer, W. C.; Geoffroy, G. L.; Pierpont, C. G. *Inorg. Chem.* **1986**, *25*, 1439.

35. Horváth, I. T.; Bor, G.; Garland, M.; Pino, P. *Organometallics* **1986**, *5*, 1441.

36. (a) Meyer, T. J. *Prog. Inorg. Chem.* **1975**, *19*, 1. (b) Hames, B. W.; Legzdins, P. *Organometallics* **1982**, *1*, 116. (c) Barr, R. D.; Marder, T. B.; Orpen, A. G.; Williams, I. D. *J. Chem. Soc., Chem. Commun.* **1984**, 112. (d) Einstein, F. W. B.; Pomeroy, R. K.; Rushman, P.; Willis, A. C. *J. Chem. Soc., Chem. Commun.* **1983**, 854. (e) Einstein, F. W. B.; Jones, T.; Pomeroy, R. K.; Rushman, P. *J. Am. Chem. Soc.* **1984**, *106*, 2707. (f) Einstein, F. W. B.; Pomeroy, R. K.; Rushman, P.; Willis, A. C. *Organometallics* **1985**, *4*, 250.

37. (a) Cowie, M.; Mague, J. T.; Sanger, A. R. *J. Am. Chem. Soc.* **1978**,

100, 3628. (b) Cowie, M. *Inorg. Chem.* **1979**, *18*, 286. (c) Haines, R. J.; Meintjies, E.; Laing, M. *Inorg. Chim. Acta* **1979**, *36*, L403. (d) Cowie, M.; Dickson, R. S. *Inorg. Chem.* **1981**, *20*, 2682. (e) Gibson, J. A. E.; Cowie, M. *Organometallics* **1984**, *3*, 984. (f) Sutherland, B. R.; Cowie, M. *Inorg. Chem.* **1984**, *23*, 1290. (g) Balch, A. L.; Fossett, L. A.; Guimerans, R. R.; Olmstead, M. M. *Organometallics* **1985**, *4*, 781. (h) Cotton, F. A.; Dunbar, K. R.; Verbruggen, M. G. *J. Am. Chem. Soc.* **1987**, *109*, 5498. (i) Berry, D. H.; Eisenberg, R. *Organometallics* **1987**, *6*, 1796. (j) Dulebohn, J. I.; Ward, D. L.; Nocera, D. G. *J. Am. Chem. Soc.* **1988**, *110*, 4054. (k) Ge, Y.-W.; Sharp, P. R. *Organometallics* **1988**, *7*, 2234. (l) Wang, W.-D.; Hommeltoft, S. I.; Eisenberg, R. *Organometallics* **1988**, *7*, 2417. (m) Wang, W.-D.; Eisenberg, R. *J. Am. Chem. Soc.* **1990**, *112*, 1833. (n) Tortorelli, L. J.; Woods, C.; McPhail, A. T. *Inorg. Chem.* **1990**, *29*, 2726.

38. (a) Kubiak, C. P.; Woodcock, C.; Eisenberg, R. *Inorg. Chem.* **1980**, *19*, 2733. (b) Sutherland, B. R.; Cowie, M. *Inorg. Chem.* **1984**, *23*, 2324. (c) Mague, J. T.; Klein, C. L.; Majeste, R. J.; Stevens, E. D. *Organometallics* **1984**, *3*, 1860. (d) Sutherland, B. R.; Cowie, M. *Organometallics* **1984**, *3*, 1869. (e) Wu, J.; Reinking, M. K.; Fanwick, P. E.; Kubiak, C. P. *Inorg. Chem.* **1987**, *26*, 247. (f) Wu, J.; Fanwick, P. E.; Kubiak, C. P. *Organometallics* **1987**, *6*, 1805. (g) Balch, A. L.; Waggoner, K. M.; Olmstead, M. M. *Inorg. Chem.* **1988**, *27*, 4511.

39. Crabtree, R. H.; Lavin, M. *Inorg. Chem.* **1986**, *25*, 805. See also: Cotton, F. A. *Prog. Inorg. Chem.* **1976**, *21*, 1.

40. Vaartstra, B. A.; Cowie, M. *Organometallics* **1990**, *9*, 1594.

41. Puddephatt, R. J.; Azam, K. A.; Hill, R. H.; Brown, M. P.; Nelson, C. D.; Moulding, R. P.; Seddon, K. R.; Grossel, M. C. *J. Am. Chem. Soc.* 1983, *105*, 5642.

42. Hutton, A. T.; Pringle, P. G.; Shaw, B. L. *Organometallics* 1983, *2*, 1637.

43. Little, E. J.; Jones, M. M. *J. Chem. Educ.* 1960, *37*, 231.

44. Balch, A. L.; Davis, B. J.; Neve, F.; Olmstead, M. M. *Organometallics* 1989, *8*, 1000.

45. Hlatky, G. G.; Johnson, B. F. G.; Lewis, J.; Raithby, P. R. *J. Chem. Soc., Dalton Trans.* 1985, 1277.

46. Vaartstra, B. A.; Xiao, J.; Jenkins, J. A.; Verhagen, R.; Cowie, M. *Organometallics*, in press.

47. (a) Antonelli, D. M.; Cowie, M. *Organometallics* 1990, *9*, 1818. (b) Wang, L.-S.; Cowie, M., unpublished observations.

48. (a) Antonelli, D. M.; Cowie, M. *Inorg. Chem.* 1990, *29*, 3339. (b) Antonelli, D. M.; Cowie, M. *Inorg. Chem.* 1990, *29*, 4039.

49. Hilts, R. W.; Franchuk, R. A.; Cowie, M. *Organometallics* 1991, *10*, 304.

50. Hilts, R. W.; Franchuk, R. A.; Cowie, M. *Organometallics*, in press.

Chapter 3

Binuclear Oxidative Additions of Silanes to $[Ir_2(CO)_3(dppm)_2]$†

Introduction

The formation of transition-metal-to-silicon bonds is a fundamental step in several metal-catalyzed processes, including olefin hydrosilation,[1] silane alcoholysis,[2] and the oligomerization of silanes.[3] Among the many approaches taken to promote Si-M bond formation[4] the oxidative addition of Si-H bonds to low-valent metal centers is of interest to this research group in that it may offer insights into C-H bond activation processes[5] promoted by adjacent metals, as well as into the activation of other heteroatom-hydrogen bonds by multicenter complexes. As part of an ongoing study of possible cooperative effects between adjacent metal nuclei in the activation of H-H and heteroatom-hydrogen bonds,[6-9] an examination of the reactions of silanes with the low-valent complex $[Ir_2(CO)_3(dppm)_2]$ was undertaken; closely-related studies involving the dirhodium analogue, $[Rh_2(CO)_3(dppm)_2]$, have recently been reported by Eisenberg and coworkers.[10] Although the metals in these complexes are formally zerovalent, close inspection of the structures reported for $[Rh_2(CO)_3(dppm)_2]$ and $[RhIr(CO)_3(dppm)_2]$ (see Chapter 2) suggests that these complexes are more appropriately formulated as mixed-valence species, in which the metals are involved in a dative M(-I)→M′(I) bond. Whatever the oxidation-state formulation for these complexes, the metals are certainly of low valence, thus should be susceptible to oxidation; in addition, the coordinative unsaturation at one of the metal centers offers the possibility of initial substrate coordination as a prelude to oxidative addition to the complex. In an effort to utilize both metals in substrate activation, the reactivities of H_2X-type molecules (X = S, Se, SiR_2, SiHR), in which both geminal X-H bonds are potentially reactive, have been investigated. It was of particular interest to establish how such substrates interact with the two metal nuclei during the proposed "double activation" process. Herein are reported the results involving studies of the reactions between $[Ir_2(CO)_3(dppm)_2]$ and some primary and secondary alkyl- and arylsilanes.

---

†A version of this chapter has been published. See: McDonald, R.; Cowie, M. *Organometallics* **1990**, *9*, 2468.

Experimental Section

General experimental conditions were as described in Chapter 2. The silane reagents were purchased from Petrarch Systems Inc., while $[Ir_2(CO)_3(dppm)_2]$ (1) was prepared as previously reported.[6] All other chemicals were used as received without further purification. Spectroscopic parameters for the compounds prepared are found in Table 3.1.

Preparation of Compounds. (a) $[Ir_2(H)_2(CO)_2(\mu\text{-}SiMe_2)(dppm)_2]$ (2). Dimethylsilane was slowly bubbled (~0.25 mL/s) through a solution of 1 (150 mg, 121 μmol) in THF (10 mL) for ca. 30 s, producing an immediate color change from orange to light yellow. The reaction mixture was allowed to stir for 10 min, and the solution volume then reduced under

Table 3.1. Spectroscopic Data[a] for the Compounds of Chapter 3.

compound	IR, cm^{-1}		NMR	
	solid[b]	solution[c]	$\delta(^{31}P\{^1H\})$[d]	$\delta(^1H)$[e]
[$Ir_2(H)_2(CO)_2(\mu$-$SiMe_2)(dppm)_2$] (2)	1944 (st), 1935 (vs), 2012 (w)[f]	1945 (sh), 1930 (vs, br), 2010 (w)[f]	-13.3 (s, br)	7.38-6.86 (mult, 40 H), 6.18 (mult, 2 H), 2.98 (mult, 2 H), 0.70 (s, br, 6 H), -11.49 (mult, 2 H)
[$Ir_2(H)_2(CO)_2(\mu$-$SiEt_2)(dppm)_2$] (3)	1942 (st), 1929 (vs), 2007 (w)[f]	1940 (sh), 1926 (vs, br), 2015 (w)[f]	-14.5 (s, br)	7.65-6.83 (mult, 40 H), 6.17 (mult, 2 H), 2.99 (mult, 2 H), 1.13 (t, $^3J_{H\text{-}H}$ = 7.6 Hz, 6 H), 0.88 (q, $^3J_{H\text{-}H}$ = 7.6 Hz, 4 H), -11.69 (mult, 2 H)
[$Ir_2(H)_2(CO)_2(\mu$-$SiPh_2)(dppm)_2$] (4)	1929 (vs), 2098 (w)[f]	1933 (vs, br), 2096 (w)[f]	-17.3 (s, br)	7.69-6.73 (mult, 50 H), 5.76 (br, 2 H), 3.29 (mult, 2 H), -11.99 (mult, 2 H)
[$Ir_2(H)_2(CO)_2(\mu$-$SiHPh)(dppm)_2$] (5)	1942 (vs), 2061 (w),[g] 2108 (w)[f]	1940 (vs, br), 2070 (w),[g] 2108 (w)[f]	-8.4 (s, br), -19.1 (s, br)	8.19-6.79 (mult, 45 H), 6.72 (s, 1 H), 6.39 (mult, 1 H), 6.08 (mult, 1 H), 3.22 (mult, 1 H), 2.82 (mult, 1 H), -11.43 (mult, 2 H)

[a] Abbreviations used: w = weak, m = medium, st = strong, vs = very strong, sh = shoulder, br = broad, s = singlet, t = triplet, q = quartet, mult = multiplet. [b] Nujol mull on KBr disk. Values are ν(CO) except as noted otherwise. [c] CH_2Cl_2 solution in KCl cells. [d] Vs. 85% H_3PO_4, 25 °C, in CD_2Cl_2 solvent. [e] Vs. TMS, 25 °C, in CD_2Cl_2 solvent. [f] ν(Ir-H). [g] ν(Si-H).

an N_2 stream to 2 mL; addition of hexanes (20 mL) caused precipitation of a golden-yellow solid. Recrystallization from THF/ether afforded **2** as a bright yellow powder (131 mg, 86% isolated yield). Anal. Calcd for $C_{54}H_{52}Ir_2O_2P_4Si$: C, 51.09, H, 4.13; Found: C, 50.93, H, 4.13.

(b) $[Ir_2(H)_2(CO)_2(\mu\text{-}SiEt_2)(dppm)_2]$ (3). Diethylsilane (15.6 μL, 10.7 mg, 121 μmol) was added to a solution of **1** (150 mg, 121 μmol) in THF (10 mL). Within 30 min the solution color had changed from orange to light yellow. Reduction of solution volume to 2 mL followed by addition of hexanes (20 mL) produced a golden-yellow solid. Complex **3** was recrystallized from THF/ether to give 121 mg (77%) of yellow powder. Anal. Calcd for $C_{56}H_{56}Ir_2O_2P_4Si$: C, 51.84, H, 4.35; Found: C, 51.38, H, 4.10.

(c) $[Ir_2(H)_2(CO)_2(\mu\text{-}SiPh_2)(dppm)_2]$ (4). To a solution of **1** (150 mg, 121 μmol) in THF (10 mL) was added diphenylsilane (22.4 μL, 22.3 mg, 121 μmol). After 2 h the solution color had changed from orange to light yellow, accompanied by formation of yellow solid. Precipitation was completed via addition of hexanes (20 mL). The product was recrystallized from THF/ether then dried in vacuo, affording **4** as a light yellow solid (139 mg, 82%). Anal. Calcd for $C_{64}H_{56}Ir_2O_2P_4Si$: C, 55.16, H, 4.05; Found: C, 55.37, H, 4.47.

(d) $[Ir_2(H)_2(CO)_2(\mu\text{-}SiHPh)(dppm)_2]$ (5). Addition of phenylsilane (20.2 μL, 17.5 mg, 162 μmol) to a solution of **1** (200 mg, 162 μmol) in THF (5 mL) produced an immediate change in color from orange to yellow; within 1 h a yellow precipitate formed. Diethyl ether (20 mL) was added to complete precipitation; recrystallization from THF/ether and drying under vacuum resulted in the isolation of **5** as a pale yellow solid (178 mg, 84%).

Anal. Calcd for $C_{58}H_{52}Ir_2O_2P_4Si$: C, 52.88, H, 3.98; Found: C, 53.12, H, 4.53.

Reaction of 1 with Me_3SiH. Trimethylsilane was slowly bubbled (~0.25 mL/s) through a rapidly-stirred solution of **1** (65 mg, 52.5 μmol) in THF (3 mL) for 1 min. After 10 min the solution color had changed from orange to light yellow. The product was found by ^1H and $^{31}P\{^1H\}$ NMR spectroscopy to be the previously characterized $[Ir_2(H)_4(CO)_2(dppm)_2]$.[11]

Reaction of $[Ir_2(CO)_2(\mu\text{-}H)_2(dppm)_2]$ with Me_3SiH. A solution of $[Ir_2(CO)_2(\mu\text{-}H)_2(dppm)_2]$ was generated according to the procedure of Chapter 2, by reaction of $[Ir_2(H)(CO)_2(\mu\text{-}H)_2(dppm)_2][BF_4]$ (70 mg, 53.9 μmol) with potassium *tert*-butoxide (6.0 mg, 53.9 μmol) in THF (2 mL) at 0 °C. Trimethylsilane was slowly bubbled (~0.25 mL/s) through this solution for 1 min, during which time the color changed from deep red to medium yellow. The product was found by IR and $^{31}P\{^1H\}$ NMR spectroscopy to be $[Ir_2(H)_4(CO)_2(dppm)_2]$.[11]

Determination of Coalescence Temperatures. The T_c values for complexes **2–4** were determined through use of variable-temperature $^{31}P\{^1H\}$ NMR spectroscopy. Typically 20 mg of the complex was dissolved in 0.5 mL CD_2Cl_2, and the sample spectrum obtained at room temperature, then at 0 °C; thereafter the temperature was lowered in 5° increments, allowed to stabilize (to within ±1° of the desired reading) and the spectrum taken at each step. Coalescence temperature was taken to mean the lowest temperature at which only one single (albeit broadened) resonance was observed for both sets of exchanging nuclei, and was found to be -15 ± 5 °C for **2**, -25 ± 5 °C for **3**, and -20 ± 10 °C for **4**.

X-ray Data Collection. (a) $[Ir_2(H)_2(CO)_2(\mu\text{-}SiPh_2)(dppm)_2]\cdot 2THF$ (4).

Diffusion of ether into a concentrated THF solution of 4 produced colorless crystals of the complex, several of which were mounted and flame-sealed in glass capillaries under N_2 and solvent vapor to minimize decomposition and/or solvent loss. Data were collected on an Enraf-Nonius CAD4 diffractometer using Mo Kα radiation. Unit-cell parameters were obtained from a least-squares refinement of the setting angles of 25 reflections in the range $20.0° \leq 2\theta \leq 24.0°$. The systematic absences ($00l$, $l \neq 3n$) and the $\bar{3}m1$ diffraction symmetry suggested one of the trigonal space groups $P3_121$ or $P3_221$. The space group $P3_121$ was confirmed by the successful solution and refinement of the structure. Refinement of the structure in the enantiomeric space group $P3_221$ gave significantly poorer residuals ($R = 0.056$ and $R_w = 0.067$ for the trial space group vs. $R = 0.038$ and $R_w = 0.040$ for the correct space group at the same stage of refinement).

Intensity data were collected at 22 °C by using the ω scan technique to a maximum $2\theta = 50.0°$, collecting reflections of the form $\pm h +k +l$. Of the data collected 5803 reflections were unique after merging. Backgrounds were scanned for 25% of the peak width on either side of the peak scan. Three reflections were chosen as intensity standards, being remeasured after every 120 min of X-ray exposure time. Each standard lost approximately 15% of its original intensity thus a linear decomposition correction was applied to the data. The data were measured and processed in the usual way, with a value of 0.04 for p[12] employed to downweight intense reflections; 3288 reflections were considered observed ($F_o^2 \geq 3\sigma(F_o^2)$) and were used in subsequent calculations. Absorption corrections were applied to the data according to Walker and Stuart's method.[13,14] See Table 3.2 for

Table 3.2. Crystallographic Data for $[Ir_2(H)_2(CO)_2(\mu\text{-}SiPh_2)(dppm)_2]\cdot 2THF$ (**4**) and $[Ir_2(H)_2(CO)_2(\mu\text{-}SiHPh)(dppm)_2]\cdot 2THF$ (**5**)

compound	**4**	**5**
formula	$C_{72}H_{72}Ir_2O_4P_4Si$	$C_{66}H_{68}Ir_2O_4P_4Si$
formula weight	1537.78	1461.68
crystal shape	hexagonal prism	monoclinic prism
crystal dimensions, mm	0.28 × 0.23 × 0.14	0.27 × 0.22 × 0.18
space group	$P3_121$ (No. 152)	$P2_1/c$ (No. 14)
temperature, °C	22	
radiation (λ, Å)	graphite-monochromated Mo Kα (0.71069)	
unit cell parameters		
a, Å	13.295(3)	12.425(3)
b, Å	—	20.282(4)
c, Å	32.286(4)	26.505(3)
β, deg	—	97.61(1)
V, Å^3	4941(2)	6621(3)
Z	3	4
ρ(calcd), g cm^{-3}	1.550	1.466
linear absorpt. coeff (μ), cm^{-1}	41.799	41.550
range of transmission factors	0.852-1.095	0.660-1.286
detector aperture, mm	(3.00 + tan θ) wide × 4.00 high	
takeoff angle, deg	3.0	

(continued)

Table 3.2. (continued)

maximum 2θ, deg	50.0	
crystal-detector distance, mm	173	
scan type	ω	$\theta/2\theta$
scan rate, deg/min	betw. 1.11 and 6.67	betw. 1.18 and 6.67
scan width, deg	$0.50 + 0.347 \tan\theta$	$0.60 + 0.347 \tan\theta$
total unique reflections	5803	11952 ($h\ k\ \pm l$)
total observations (NO)	3288 ($F_o^2 \geq 3\sigma(F_o^2)$)	4697 ($F_o^2 \geq 3\sigma(F_o^2)$)
final no. params. varied (NV)	229	334
error in obs. of unit wt. (GOF)[a]	1.093	2.174
R[b]	0.038	0.061
R_w[c]	0.039	0.087

[a] $\mathrm{GOF} = [\sum w(|F_o| - |F_c|)^2/(\mathrm{NO} - \mathrm{NV})]^{1/2}$ where $w = 4F_o^2/\sigma^2(F_o^2)$.

[b] $R = \sum ||F_o| - |F_c|| / \sum |F_o|$. [c] $R_w = [\sum w(|F_o| - |F_c|)^2/\sum wF_o^2]^{1/2}$.

crystal data and more information on X-ray data collection.

(b) $[Ir_2(H)_2(CO)_2(\mu\text{-SiHPh})(dppm)_2]\cdot 2THF$ (5). Pale yellow crystals of 5 were obtained by diffusion of hexanes into a THF solution of the complex. Crystals were mounted in glass capillaries under N_2 and solvent vapor. Data collection and derivation of unit-cell parameters proceeded in a manner similar to above. The monoclinic diffraction symmetry and systematic absences ($h0l$, l = odd; $0k0$, k = odd) were consistent with the space group $P2_1/c$.

Intensity data were collected at 22 °C using the $\theta/2\theta$ scan technique to a maximum $2\theta = 50.0°$; reflections with indices of the form $+h$ $+k$ $\pm l$ were collected. The intensity standards were found to lose 20 to 30% of their initial intensity, necessitating application of a linear decomposition correction. Of 11952 unique reflections measured, 4697 were considered observed for the purposes of subsequent calculations, with absorption corrections applied as above.

Structure Solution and Refinement. Both structures were solved in the respective space groups ($P3_121$ for **4**, $P2_1/c$ for **5**) using standard Patterson and Fourier techniques. Full-matrix least-squares refinements proceeded so as to minimize the function $\Sigma w(|F_o| - |F_c|)^2$, where $w = 4F_o^2/\sigma^2(F_o^2)$. Atomic scattering factors and anomalous dispersion terms were taken from the usual tabulations.[15-17] Positional parameters for the hydrogens attached to the carbon atoms of the complexes (as well as to the carbons of the solvent molecules in the structure of **4**, and to the silicon atom of **5**) were calculated from the geometries about the attached carbon (or silicon). These hydrogens were located 0.95 Å from their attached C atoms (1.35 Å in the case of Si-H), given thermal parameters 20% greater than the equivalent isotropic *B*'s of their attached atoms, and included as fixed contributions.

In addition to all non-hydrogen atoms of the complex and its solvent molecules, the hydrogen atoms attached to the Ir centers of **4** were also located with aid of difference Fourier contour maps; these were included in subsequent least-squares cycles and refined acceptably. Only the non-hydrogen atoms of complex **5** were refined; contour maps of the electron density in the vicinity of the solvent molecules indicated these groups to be severely rotationally disordered, and attempts to assign and refine carbon or oxygen atoms were unsuccessful. Instead, all solvent atoms were input as carbon atoms in five-membered rings that most appropriately described the electron density. These atoms were assigned large thermal parameters and were not refined in subsequent least-squares cycles. For this reason the solvent molecules' hydrogen atoms were not included. A difference Fourier map calculated with use of all data displayed peaks in the expected positions of the hydride ligands. However, when only low-angle data ($\sin \theta/\lambda \leq 0.25$) were used in the Fourier synthesis, the peak corresponding to H(2) could no longer be unambiguously identified, although that due to H(1) was observed in its original location. Owing to the uncertainty in the identification of H(2), neither atom was refined; instead, both were included as fixed contributions in the structure factor calculations, in their positions obtained from the full-data Fourier map. Other hydrogens were included in their idealized positions and handled as described for compound **4**.

The final model for complex 4, with 229 parameters varied, converged to values of $R = 0.038$ and $R_w = 0.039$. In the final difference Fourier map the 10 highest residuals (0.8-0.7 e/Å^3) were found in the vicinity of the dppm ligands (a typical carbon in an earlier synthesis had an electron density of 3.4 e/Å^3). For compound 5 the final model, with 334 parameters varied, converged to values of $R = 0.061$ and $R_w = 0.087$. The 10 highest residuals in the final difference Fourier map (1.5-0.9 e/Å^3) were found in the area of the solvent molecules (a typical carbon in an earlier synthesis had an electron density of 2.9 e/Å^3). The badly-disordered solvent molecules prevented more satisfactory refinement of the structure; however the parameters within the complex molecule should not be significantly affected. The positional and thermal parameters for the non-hydrogen atoms of complex 4 are given in Table 3.3, and selected bond lengths and angles are given in Tables 3.4 and 3.5, respectively. For complex 5 the pertinent data are found in Tables 3.6-3.8.

Results and Discussion

(a) Description of Structures. (i) $[Ir_2(H)_2(CO)_2(\mu\text{-}SiPh_2)(dppm)_2]\cdot 2THF$ (4). Complex 4 has the structure shown in Figure 3.1, in which the molecule contains a crystallographic twofold axis of symmetry passing through the Si atom and the center of the Ir-Ir′ bond. The metal nuclei are bridged by the two diphosphine ligands and the diphenylsilylene group, but the most striking feature is the disposition of the dppm ligands about each metal center. Figure 3.2 shows a slightly different spatial orientation, with only the *ipso* carbons of each phenyl ring shown. The atoms P(1) and P(2′)

Table 3.3. Positional and Thermal Parameters of the Atoms of $[\mathrm{Ir_2(H)_2(CO)_2(\mu\text{-}SiPh_2)(dppm)_2}]\cdot 2\mathrm{THF}$ (4)[a]

Atom	*x*	*y*	z	*B*, Å^2
Ir	0.27192(3)	0.09855(3)	-0.14031(1)	3.211(8)
P(1)	0.3883(2)	0.0423(2)	-0.10409(9)	3.61(7)
P(2)	0.1982(2)	-0.1937(2)	-0.13619(9)	3.78(7)
Si	0.0797(3)	0.000	-0.167	3.9(1)
O(1)	0.2681(8)	0.2940(7)	-0.0960(3)	9.0(3)
O(2)	0.446(1)	0.726(1)	0.9579(4)	15.4(6)[b]
C(1)	0.272(1)	0.2221(9)	-0.1141(4)	6.0(4)[b]
C(2)	0.3436(8)	-0.1096(9)	-0.1152(3)	4.2(3)[b]
C(3)	0.473(2)	0.633(2)	0.957(1)	28(1)[b]
C(4)	0.392(3)	0.545(2)	0.9669(9)	28(2)[b]
C(5)	0.376(2)	0.587(2)	1.0085(7)	17(1)[b]
C(6)	0.375(2)	0.692(2)	0.9950(7)	16.0(9)[b]
C(11)	0.3738(8)	0.0425(8)	-0.0466(3)	4.4(3)[b]
C(12)	0.3034(9)	0.0777(9)	-0.0290(4)	5.6(3)[b]
C(13)	0.295(1)	0.078(1)	0.0151(4)	6.6(3)[b]
C(14)	0.361(1)	0.048(1)	0.0380(4)	7.1(4)[b]
C(15)	0.435(1)	0.016(1)	0.0220(4)	7.2(4)[b]
C(16)	0.4416(9)	0.0161(9)	-0.0221(4)	5.5(3)[b]
C(21)	0.5477(8)	0.1149(8)	-0.1093(3)	4.6(3)[b]
C(22)	0.6044(9)	0.2347(9)	-0.1055(4)	5.9(3)[b]
C(23)	0.730(1)	0.300(1)	-0.1076(4)	7.3(4)[b]
C(24)	0.786(1)	0.237(1)	-0.1128(5)	8.5(4)[b]
C(25)	0.731(1)	0.120(1)	-0.1161(5)	8.3(4)[b]
C(26)	0.610(1)	0.058(1)	-0.1153(4)	6.1(3)[b]
C(31)	0.0999(9)	-0.2315(9)	-0.0920(3)	4.4(2)[b]
C(32)	0.136(1)	-0.226(1)	-0.0516(4)	6.3(3)[b]
C(33)	0.048(1)	-0.268(1)	-0.0195(4)	7.1(4)[b]
C(34)	-0.063(1)	-0.315(1)	-0.0286(4)	7.8(4)[b]

(continued)

Table 3.3. (continued)

C(35)	-0.102(1)	-0.328(1)	-0.0686(4)	8.7(4)[b]
C(36)	-0.015(1)	-0.282(1)	-0.1009(4)	6.0(3)[b]
C(41)	0.1825(8)	-0.3374(9)	-0.1457(3)	4.0(2)[b]
C(42)	0.092(1)	-0.415(1)	-0.1691(4)	7.9(4)[b]
C(43)	0.078(1)	-0.527(1)	-0.1772(5)	10.1(5)[b]
C(44)	0.147(1)	-0.560(1)	-0.1613(5)	8.5(4)[b]
C(45)	0.239(1)	-0.485(1)	-0.1391(4)	7.9(4)[b]
C(46)	0.253(1)	-0.368(1)	-0.1312(4)	6.8(4)[b]
C(51)	-0.0423(8)	-0.0553(9)	-0.1279(3)	4.5(2)[b]
C(52)	-0.1561(9)	-0.127(1)	-0.1416(4)	5.3(3)[b]
C(53)	-0.252(1)	-0.163(1)	-0.1156(4)	7.1(3)[b]
C(54)	-0.235(1)	-0.134(1)	-0.0744(5)	7.8(4)[b]
C(55)	-0.126(1)	-0.060(1)	-0.0601(4)	7.4(4)[b]
C(56)	-0.028(1)	-0.0215(9)	-0.0867(4)	6.0(3)[b]
H(1)	0.194(7)	0.024(6)	-0.101(3)	2(2)[b]

[a] Numbers in parentheses are estimated standard deviations in the least significant digits in this and all subsequent tables. Thermal parameters for the anisotropically refined atoms are given in the form of the equivalent isotropic Gaussian displacement parameter defined as $^4/_3[a^2\beta_{11} + b^2\beta_{22} + c^2\beta_{33} + ab(\cos\gamma)\beta_{12} + ac(\cos\beta)\beta_{13} + bc(\cos\alpha)\beta_{23}]$. [b] Refined isotropically.

Table 3.4. Selected Distances (Å) in $[Ir_2(H)_2(CO)_2(\mu\text{-}SiPh_2)(dppm)_2]\cdot 2THF$ (4)

(a) Bonded			
Ir-Ir′	2.8361(9)	P(1)-C(11)	1.87(1)
Ir-P(1)	2.340(3)	P(1)-C(21)	1.85(1)
Ir-P(2′)	2.344(3)	P(2)-C(2)	1.81(1)
Ir-Si	2.371(4)	P(2)-C(31)	1.83(1)
Ir-C(1)	1.85(1)	P(2)-C(41)	1.85(1)
Ir-H(1)	1.63(9)	Si-C(51)	1.88(1)
P(1)-C(2)	1.83(1)	O(1)-C(1)	1.14(1)
(b) Non-bonded			
P(1)···P(2)	3.062(3)	Si···H(1)	2.53(9)

Primed atoms are related to unprimed ones by the crystallographic 2-fold axis passing through Si and the center of the Ir-Ir′ bond.

Table 3.5. Selected Angles (deg) in $[Ir_2(H)_2(CO)_2(\mu\text{-}SiPh_2)(dppm)_2]\cdot 2THF$ (4)

(a) Bond angles

Ir′-Ir-P(1)	94.51(7)	Ir-P(1)-C(21)	123.9(4)
Ir′-Ir-P(2′)	84.50(7)	C(2)-P(1)-C(11)	102.7(5)
Ir′-Ir-Si	53.26(6)	C(2)-P(1)-C(21)	102.4(5)
Ir′-Ir-C(1)	153.1(5)	C(11)-P(1)-C(21)	100.5(5)
Ir′-Ir-H(1)	92(3)	Ir′-P(2)-C(2)	110.8(4)
P(1)-Ir-P(2′)	100.6(1)	Ir′-P(2)-C(31)	119.0(4)
P(1)-Ir-Si	134.82(8)	Ir′-P(2)-C(41)	117.2(4)
P(1)-Ir-C(1)	110.3(4)	C(2)-P(2)-C(31)	105.8(5)
P(1)-Ir-H(1)	75(3)	C(2)-P(2)-C(41)	103.6(5)
P(2′)-Ir-Si	105.78(8)	C(31)-P(2)-C(41)	98.7(5)
P(2′)-Ir-C(1)	100.4(4)	Ir-Si-Ir′	73.5(1)
P(2′)-Ir-H(1)	174(3)	Ir-Si-C(51)	117.3(3)
Si-Ir-C(1)	100.3(5)	Ir-Si-C(51′)	127.7(4)
Si-Ir-H(1)	76(3)	C(51)-Si-C(51′)	96.4(7)
C(1)-Ir-H(1)	84(3)	Ir-C(1)-O(1)	176(1)
Ir-P(1)-C(2)	110.7(4)	P(1)-C(2)-P(2)	114.3(6)
Ir-P(1)-C(11)	114.3(4)		

(b) Torsion angles

P(1)-Ir-Ir′-P(1′)	31.1(1)	H(1)-Ir-Ir′-H(1′)	141(5)

Primed atoms are related to unprimed ones by the crystallographic 2-fold axis passing through Si and the center of the Ir-Ir′ bond.

Table 3.6. Positional and Thermal Parameters of the Atoms of $[Ir_2(H)_2(CO)_2(\mu\text{-SiHPh})(dppm)_2]\cdot 2THF$ (5)[a]

Atom	x	y	z	B, Å^2
Ir(1)	0.17446(8)	-0.03226(5)	0.31990(4)	3.06(2)
Ir(2)	0.33528(8)	0.06018(5)	0.29519(4)	3.28(2)
P(1)	0.0997(5)	-0.0471(3)	0.2347(3)	3.6(2)
P(2)	0.2982(6)	0.0266(4)	0.2109(3)	3.9(2)
P(3)	0.0616(5)	0.0526(3)	0.3408(3)	3.4(2)
P(4)	0.2134(5)	0.1470(3)	0.2960(3)	3.4(2)
Si	0.3269(6)	0.0066(4)	0.3732(3)	3.6(2)
O(1)	0.092(2)	-0.138(1)	0.3824(7)	7.1(6)
O(2)	0.523(1)	0.154(1)	0.3081(8)	7.3(6)
C(1)	0.123(2)	-0.100(1)	0.356(1)	5.3(7)
C(2)	0.456(2)	0.114(1)	0.305(1)	6.0(8)
C(3)	0.154(2)	0.010(1)	0.1916(8)	3.4(6)
C(4)	0.071(2)	0.125(1)	0.3008(8)	2.9(6)
C(11)	-0.049(2)	-0.041(1)	0.2149(9)	4.4(6)[b]
C(12)	-0.096(2)	0.002(1)	0.178(1)	5.6(7)[b]
C(13)	-0.213(3)	0.002(2)	0.164(1)	8.2(9)[b]
C(14)	-0.271(2)	-0.042(2)	0.191(1)	7.1(8)[b]
C(15)	-0.229(2)	-0.081(1)	0.227(1)	5.8(7)[b]
C(16)	-0.116(2)	-0.081(1)	0.239(1)	5.2(7)[b]
C(21)	0.123(2)	-0.128(1)	0.2081(9)	3.6(6)[b]
C(22)	0.175(2)	-0.178(1)	0.239(1)	6.7(8)[b]
C(23)	0.195(3)	-0.238(2)	0.216(1)	8.2(9)[b]
C(24)	0.163(2)	-0.250(1)	0.164(1)	6.8(8)[b]
C(25)	0.109(3)	-0.203(2)	0.136(1)	7.7(9)[b]
C(26)	0.090(2)	-0.140(1)	0.157(1)	5.5(7)[b]
C(31)	0.365(2)	-0.051(1)	0.1929(9)	4.1(6)[b]
C(32)	0.352(2)	-0.067(2)	0.142(1)	6.9(8)[b]
C(33)	0.402(3)	-0.127(2)	0.129(1)	9(1)[b]

(continued)

Table 3.6. (continued)

C(34)	0.461(3)	-0.164(2)	0.162(1)	8.0(9)[b]
C(35)	0.470(3)	-0.145(2)	0.211(1)	8.1(9)[b]
C(36)	0.424(2)	-0.087(1)	0.226(1)	5.9(7)[b]
C(41)	0.336(2)	0.084(1)	0.161(1)	5.1(7)[b]
C(42)	0.446(2)	0.094(2)	0.165(1)	7.2(8)[b]
C(43)	0.485(3)	0.133(2)	0.127(1)	11(1)[b]
C(44)	0.410(3)	0.158(2)	0.093(1)	8(1)[b]
C(45)	0.292(3)	0.151(2)	0.085(1)	9(1)[b]
C(46)	0.263(2)	0.108(2)	0.123(1)	7.2(8)[b]
C(51)	-0.086(2)	0.039(1)	0.3315(9)	4.2(6)[b]
C(52)	-0.127(2)	-0.013(1)	0.362(1)	4.9(6)[b]
C(53)	-0.242(2)	-0.024(1)	0.360(1)	6.3(7)[b]
C(54)	-0.313(2)	0.011(2)	0.325(1)	6.9(8)[b]
C(55)	-0.276(2)	0.056(1)	0.295(1)	6.3(8)[b]
C(56)	-0.162(2)	0.073(1)	0.299(1)	4.2(6)[b]
C(61)	0.078(2)	0.083(1)	0.4085(9)	3.4(5)[b]
C(62)	0.106(2)	0.038(1)	0.446(1)	4.8(6)[b]
C(63)	0.110(2)	0.060(1)	0.496(1)	5.5(7)[b]
C(64)	0.092(2)	0.125(1)	0.508(1)	6.0(7)[b]
C(65)	0.065(2)	0.170(1)	0.469(1)	6.5(8)[b]
C(66)	0.052(2)	0.151(1)	0.417(1)	5.2(7)[b]
C(71)	0.241(2)	0.209(1)	0.3463(9)	3.5(5)[b]
C(72)	0.316(2)	0.197(1)	0.388(1)	4.6(6)[b]
C(73)	0.338(2)	0.242(1)	0.428(1)	6.0(7)[b]
C(74)	0.282(2)	0.300(1)	0.426(1)	6.3(8)[b]
C(75)	0.206(2)	0.312(1)	0.384(1)	5.5(7)[b]
C(76)	0.186(2)	0.267(1)	0.344(1)	4.7(6)[b]
C(81)	0.201(2)	0.201(1)	0.2406(9)	3.9(6)[b]
C(82)	0.107(2)	0.217(1)	0.211(1)	6.2(8)[b]
C(83)	0.100(3)	0.259(2)	0.166(1)	7.9(9)[b]
C(84)	0.192(2)	0.283(2)	0.158(1)	6.6(8)[b]
C(85)	0.287(2)	0.272(1)	0.187(1)	6.2(8)[b]

(continued)

Table 3.6. (continued)

C(86)	0.290(2)	0.231(1)	0.229(1)	5.3(7)[b]
C(91)	0.436(2)	-0.053(1)	0.3971(9)	3.9(6)[b]
C(92)	0.512(2)	-0.038(1)	0.4379(9)	4.4(6)[b]
C(93)	0.596(2)	-0.076(1)	0.462(1)	5.4(7)[b]
C(94)	0.596(2)	-0.137(1)	0.440(1)	6.0(7)[b]
C(95)	0.531(3)	-0.158(2)	0.399(1)	7.2(8)[b]
C(96)	0.444(2)	-0.114(1)	0.379(1)	5.5(7)[b]
C(100)[c,d]	0.332	0.699	0.059	20.0
C(101)[c,d]	0.384	0.633	0.049	20.0
C(102)[c,d]	0.296	0.582	0.033	20.0
C(103)[c,d]	0.204	0.630	0.016	20.0
C(104)[c,d]	0.250	0.699	0.012	20.0
C(110)[c,d]	0.993	0.568	0.487	20.0
C(111)[c,d]	1.001	0.533	0.535	20.0
C(112)[c,d]	1.120	0.533	0.555	20.0
C(113)[c,d]	1.185	0.543	0.510	20.0
C(114)[c,d]	1.106	0.582	0.476	20.0
H(1)[d]	0.2727	-0.0867	0.3145	4.0
H(2)[d]	0.4021	-0.0126	0.2869	4.0

[a] See footnote (a) of Table 3.3. [b] Refined isotropically. [c] Atoms of the rotationally-disordered THF solvent molecules are numbered C(101)-C(104) and C(110)-C(114) (see text). [d] Fixed contribution; not refined.

Table 3.7. Selected Distances (Å) in $[Ir_2(H)_2(CO)_2(\mu\text{-}SiHPh)(dppm)_2]\cdot 2THF$ (5)

(a) Bonded

Ir(1)-Ir(2)	2.879(1)	P(1)-C(21)	1.84(2)
Ir(1)-P(1)	2.344(5)	P(2)-C(3)	1.83(2)
Ir(1)-P(3)	2.331(4)	P(2)-C(31)	1.88(2)
Ir(1)-Si	2.343(5)	P(2)-C(41)	1.87(2)
Ir(1)-C(1)	1.84(2)	P(3)-C(4)	1.82(2)
Ir(1)-H(1)	1.67	P(3)-C(51)	1.85(2)
Ir(2)-P(2)	2.322(5)	P(3)-C(61)	1.88(2)
Ir(2)-P(4)	2.324(5)	P(4)-C(4)	1.84(2)
Ir(2)-Si	2.349(5)	P(4)-C(71)	1.83(2)
Ir(2)-C(2)	1.85(2)	P(4)-C(81)	1.82(2)
Ir(2)-H(2)	1.72	Si-C(91)	1.87(2)
P(1)-C(3)	1.83(2)	O(1)-C(1)	1.13(2)
P(1)-C(11)	1.86(2)	O(2)-C(2)	1.16(2)

(b) Non-bonded

P(1)···P(2)	3.02(1)	Si···H(1)	2.48
P(3)···P(4)	3.04(1)	Si···H(2)	2.61

Table 3.8. Selected Angles (deg) in $[Ir_2(H)_2(CO)_2(\mu\text{-}SiHPh)(dppm)_2]\cdot 2THF$ (5)

(a) Bond angles

Ir(2)-Ir(1)-P(1)	93.6(1)	C(2)-Ir(2)-H(2)	97.6
Ir(2)-Ir(1)-P(3)	91.8(1)	Ir(1)-P(1)-C(3)	112.9(5)
Ir(2)-Ir(1)-Si	52.3(1)	Ir(1)-P(1)-C(11)	121.1(6)
Ir(2)-Ir(1)-C(1)	154.7(6)	Ir(1)-P(1)-C(21)	115.0(6)
Ir(2)-Ir(1)-H(1)	82.8	C(3)-P(1)-C(11)	102.9(8)
P(1)-Ir(1)-P(3)	98.6(2)	C(3)-P(1)-C(21)	103.8(8)
P(1)-Ir(1)-Si	144.0(2)	C(11)-P(1)-C(21)	98.9(8)
P(1)-Ir(1)-C(1)	106.8(6)	Ir(2)-P(2)-C(3)	112.7(5)
P(1)-Ir(1)-H(1)	92.1	Ir(2)-P(2)-C(31)	117.0(6)
P(3)-Ir(1)-Si	94.2(2)	Ir(2)-P(2)-C(41)	117.4(7)
P(3)-Ir(1)-C(1)	99.5(7)	C(3)-P(2)-C(31)	103.1(8)
P(3)-Ir(1)-H(1)	168.4	C(3)-P(2)-C(41)	104.2(8)
Si-Ir(1)-C(1)	104.0(6)	C(31)-P(2)-C(41)	100.5(8)
Si-Ir(1)-H(1)	74.4	Ir(1)-P(3)-C(4)	111.5(5)
C(1)-Ir(1)-H(1)	81.9	Ir(1)-P(3)-C(51)	118.7(6)
Ir(1)-Ir(2)-P(2)	88.4(1)	Ir(1)-P(3)-C(61)	118.3(5)
Ir(1)-Ir(2)-P(4)	91.1(1)	C(4)-P(3)-C(51)	100.6(8)
Ir(1)-Ir(2)-Si	52.1(1)	C(4)-P(3)-C(61)	106.5(7)
Ir(1)-Ir(2)-C(2)	158.3(7)	C(51)-P(3)-C(61)	99.2(7)
P(2)-Ir(2)-Si	133.2(2)	Ir(2)-P(4)-C(4)	116.4(5)
P(2)-Ir(2)-C(2)	111.4(7)	Ir(2)-P(4)-C(71)	117.9(6)
P(2)-Ir(2)-H(2)	70.3	Ir(2)-P(4)-C(81)	115.6(6)
Ir(1)-Ir(2)-H(2)	80.3	C(4)-P(4)-C(71)	102.0(7)
P(2)-Ir(2)-P(4)	100.7(2)	C(4)-P(4)-C(81)	102.8(8)
P(4)-Ir(2)-Si	103.8(2)	C(71)-P(4)-C(81)	99.6(8)
P(4)-Ir(2)-C(2)	93.8(6)	Ir(1)-Si-Ir(2)	75.7(2)
P(4)-Ir(2)-H(2)	167.5	Ir(1)-Si-C(91)	118.8(6)
Si-Ir(2)-C(2)	106.2(7)	Ir(2)-Si-C(91)	118.9(6)
Si-Ir(2)-H(2)	78.1	Ir(1)-C(1)-O(1)	174(2)

(continued)

Table 3.8. (continued)

Ir(2)-C(2)-O(2)	172(2)	P(3)-C(4)-P(4)	112.1(8)
P(1)-C(3)-P(2)	111.9(8)		

(b) Torsion angles

P(1)-Ir(1)-Ir(2)-P(2)	14.7(2)	H(1)-Ir(1)-Ir(2)-H(2)	6.6
P(3)-Ir(1)-Ir(2)-P(4)	12.7(2)		

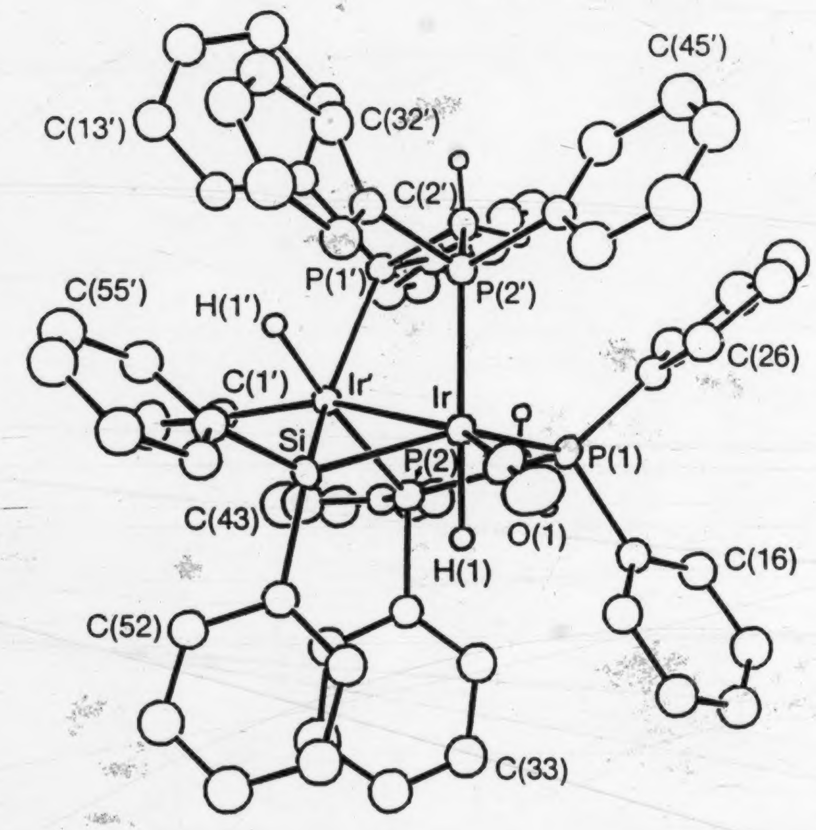
C(45')
C(13')
C(32')
C(2')
P(1')
P(2')
C(55')
H(1')
C(26)
C(1')
Ir'
Ir
Si
P(2)
P(1)
C(43)
O(1)
H(1)
C(16)
C(52)
C(33)

Figure 3.1. Perspective view of $[Ir_2(H)_2(CO)_2(\mu\text{-}SiPh_2)(dppm)_2]$ (4) showing the numbering scheme. Thermal parameters are shown at the 20% level for the non-hydrogen atoms and the iridium-bound hydride groups; the dppm methylene hydrogens are shown artificially small, while the dppm phenyl hydrogens are omitted. Primed atoms are related to unprimed atoms by the crystallographic 2-fold axis passing through Si and the center of the Ir-Ir' bond.

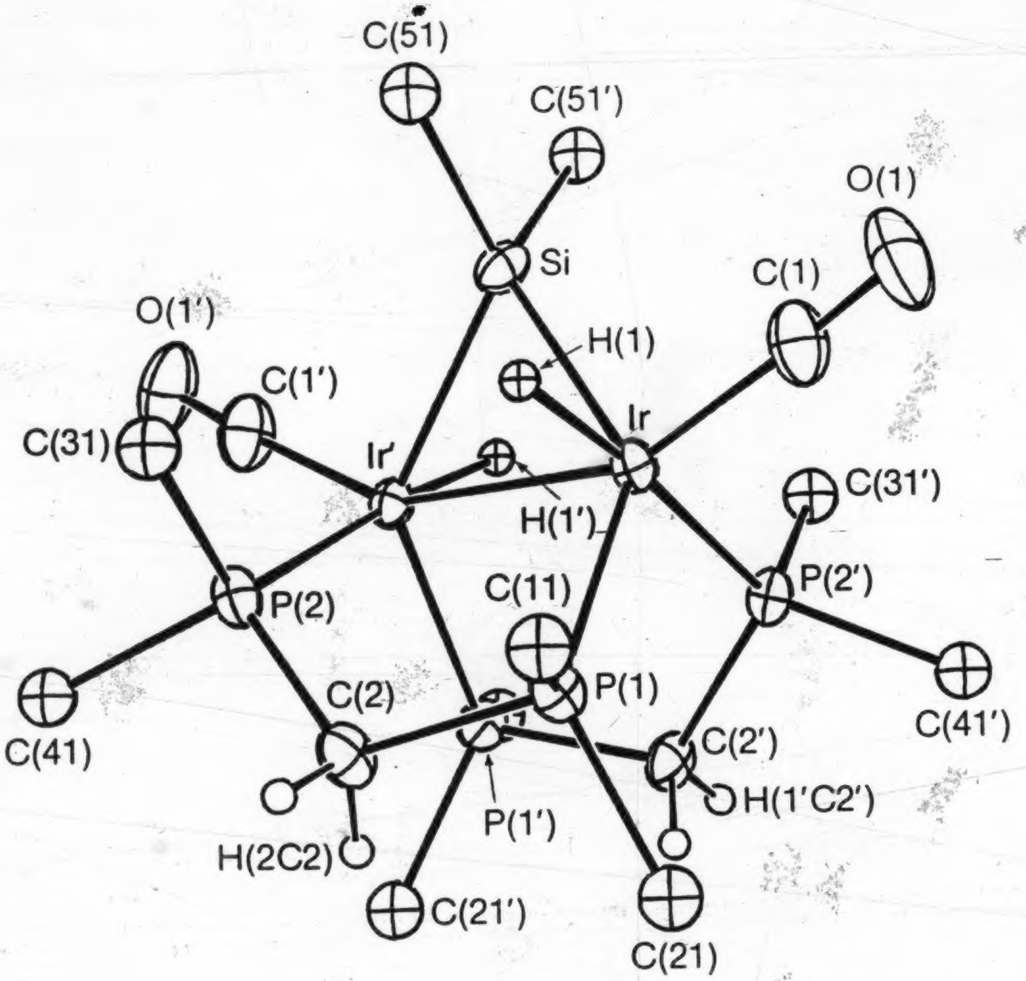
C(51)
C(51')
O(1)
Si
C(1)
O(1')
H(1)
C(1')
Ir
C(31)
Ir'
C(31')
H(1')
P(2')
C(11)
P(2)
P(1)
C(2)
C(41')
C(41)
C(2')
H(1'C2')
P(1')
H(2C2)
C(21')
C(21)

Figure 3.2. View of complex 4 omitting the phenyl carbon atoms except those bound to phosphorus and silicon.

are in an approximately cis arrangement about Ir (P(1)-Ir-P(2′) = 100.6(2)°) with P(1) cis to H(1) (P(1)-Ir-H(1) = 75(3)°) and P(2′) trans to H(1) (P(2′)-Ir-H(1) = 174(3)°). This cis-diphosphine arrangement is in contrast with the trans-diphosphine geometry normally observed for binuclear bis-dppm-bridged species, but is not without precedent. The complexes $[\mathrm{Rh_2(CO)_2(\mu\text{-}SiHR)_2(dppm)_2}]$ (R = Ph,[10a] Et[10b]), $[\mathrm{Rh_2(CO)_2(\mu\text{-}\eta^2{:}\eta^{2'}\text{-}PhCCPh)(dppm)_2}]$,[18] $[\mathrm{Ir_2(CO)_2(\mu\text{-}\eta^2{:}\eta^{2'}\text{-}MeO_2C\text{-}C{\equiv}C\text{-}CO_2Me)(dppm)_2}]$[19] and $[\mathrm{Pt_2Me_4(dRpm)_2}]$ (R = Ph (dppm), Me (dmpm))[20] all possess structures in which the phosphine-metal-phosphine angles deviate significantly from linearity at both metal centers, while $[\mathrm{Pt_2Me_3(dppm)_2}]^+$,[21] $[\mathrm{Rh_2(CO)_3(dppm)_2}]$,[22] $[\mathrm{RhIr(CO)_3(dppm)_2}]$[7] (see Chapter 2) and the related $[\mathrm{Rh_2(CO)_3\{(PhO)_2PN(Et)P(OPh)_2\}_2}]$[23] and $[\mathrm{Rh_2Cl_2(CO)\{(PhO)_2PN(Et)P(OPh)_2\}_2}]$[24] have cis phosphines at one metal center and trans phosphines at the other. The coordination geometry about Ir in complex **4** appears to be roughly octahedral, with the six sites occupied by C(1), Ir′, P(1), P(2′), H(1) and Si. The distortions from the idealized geometry result primarily from the constraints imposed by the bridging diphenylsilylene group (e.g. Ir-Ir′-Si = 53.26(6)°, P(1)-Ir-Si = 134.82(2)°, Si-Ir-H(1) = 76(3)°).

The disposition of the silylene and hydride groups with respect to each other is consistent with a concerted oxidative addition of a silicon-hydrogen bond to each metal center, the Si and H atoms being approximately cis about Ir. The hydrides are disposed roughly trans to each other on adjacent metals with a torsion angle about the Ir-Ir′ bond (H(1)-Ir-Ir′-H(1′)) of 141(5)°, thus are located on opposite faces of the plane defined by the Ir, Ir′ and Si atoms. Unlike some other binuclear silylene-bridged hydride complexes, where three-center two-electron Si-H-M bonding is implicated,[25] compound 4 does not appear to show significant Si-H interactions. Although the Si-H(1) distance (2.53(9) Å) is well within the sum of the van der Waals' radii of these atoms (3.30-3.55 Å),[26] this arrangement appears to be enforced by the pseudooctahedral geometry of the complex and not by any silicon-hydrogen bonding. Schubert has proposed, as a criterion for agostic Si-H bonding, an upper limit of 2.0 Å for the silicon-hydrogen distance.[25] This limit is based on the longest accepted interatomic distances for Si-Si and H-H bonds, and is supported by several crystallographic studies in which the Si-H distances for agostic Si-H···M interactions fall within the range 1.56-1.80 Å. The hydride ligand, H(1), refined acceptably and the resulting Ir-H(1) distance (1.63(9) Å) corresponds to a normal covalent bond. Neither this hydride nor the silylene group appears to be exerting a significant trans influence (the silylene might not be expected to do so, not being oriented strictly trans to P(1) [P(1)-Ir-Si = 134.82(8)°]), as the iridium-phosphorus bond lengths (Ir-P(1) = 2.340(3) Å; Ir-P(2') = 2.344(3) Å) are comparable to those observed in related bis(dppm)-bridged diiridium complexes.[6,9,11,27]

The Ir-Si bond length of 2.371(4) Å is slightly shorter than the range reported for several related silane complexes (2.390(1)-2.454(6) Å),[28] but is not unusual since it appears to be a general phenomenon that metal-silicon distances are shorter in complexes containing bridging silylene groups as compared to those featuring terminal silyl groups.[4] One exception is $[(Me_3P)_3Ir(SiMeCl_2)Cl_2]$, for which the Ir-Si distance (2.299(5) Å)[29] is even shorter than in the present compound. However this is believed to be due to the high electron density on the Ir center of this species, coupled with better π-acceptor ability of the $SiMeCl_2$ group.[29] The acute Ir-Si-Ir′ angle of 73.5(1)° is within the expected range for such a unit that spans a metal-metal bond. Overall the Ir_2Si unit has structural parameters very similar to those found for the Rh_2Si units of the complexes $[Rh(CO)(\mu\text{-}SiHR)(dppm)]_2$ (R = Ph, Et).[10]

Complex **4** is twisted significantly about the Ir-Ir bond, resulting in a staggered arrangement of P(1) and P(2), as shown by the P(1)-Ir-Ir′-P(2) torsion angle of 31.1(1)°. Furthermore, the bridging silylene group is twisted relative to the metals (Ir-Si-C(51) = 117.3(3)°; Ir-Si-C(51′) = 127.7(4)°) such that the phenyl group containing C(51) is rotated into the less congested space in the vicinity of the small hydride ligand, H(1).

The Ir-Ir′ separation (2.8361(9) Å) is consistent with a normal single bond and is within the range observed for similar diiridium systems (2.77-2.89 Å);[6,9,11,27] as a result, the metal-metal distance is compressed with respect to the intraligand P-P separation (P(1)···P(2) = 3.062(3) Å). The carbonyl group, C(1)O(1), does not lie exactly along the metal-metal bond axis (Ir′-Ir-C(1) = 153.1(5)°), presumably reflecting the distortion of the complex by the acute bite of the bridging diphenylsilylene group.

(ii) $[Ir_2(H)_2(CO)_2(\mu\text{-}SiHPh)(dppm)_2]\cdot 2THF$ (5). The structure of **5** is shown in Figure 3.3, while Figure 3.4 presents an alternate orientation, in which only the *ipso* carbons of the dppm phenyls are shown. Similar to the case for complex **4**, the iridium centers are bridged by the phenylsilylene group, while the diphosphine groups have a cis disposition on each metal (P(1)-Ir(1)-P(3) = 98.6(2)°; P(2)-Ir(2)-P(4) = 100.7(2)°). Although, as

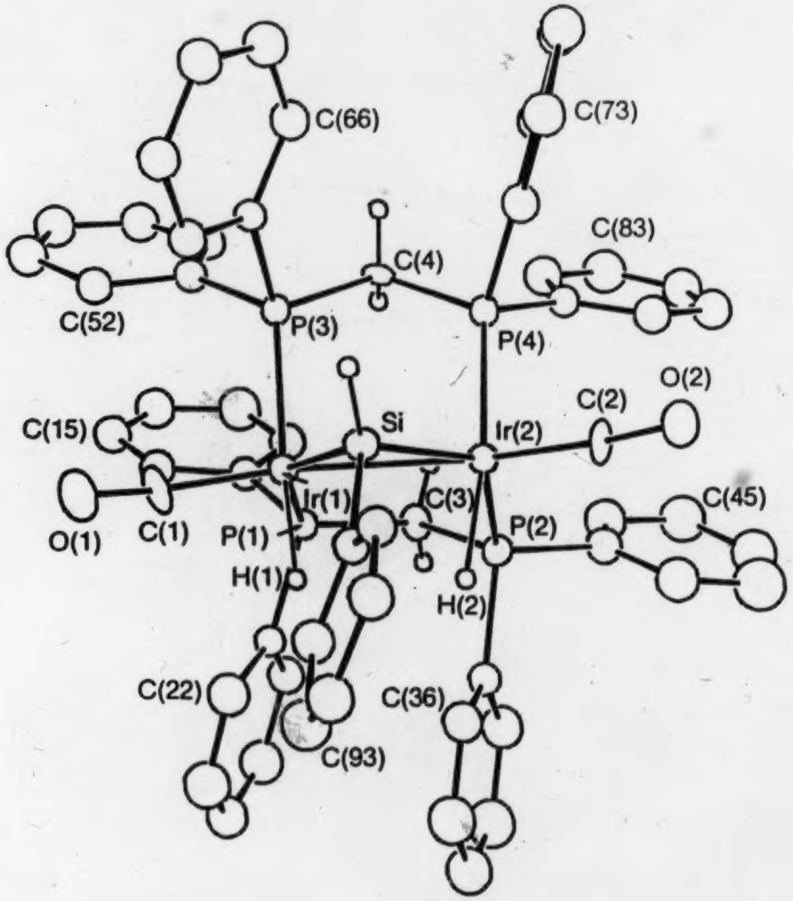
C(66)
C(73)
C(83)
C(4)
C(52)
P(3)
P(4)
O(2)
C(2)
C(15)
Si
Ir(2)
Ir(1)
C(3)
C(45)
O(1)
C(1)
P(1)
P(2)
H(1)
H(2)
C(22)
C(36)
C(93)

Figure 3.3. Perspective view of $[Ir_2(H)_2(CO)_2(\mu\text{-SiHPh})(dppm)_2]$ (5) showing the numbering scheme. Thermal parameters are shown at the 20% level except for hydrogens, which are shown artificially small for the hydride, silylene and dppm methylene groups but are not shown for the phenyl groups.

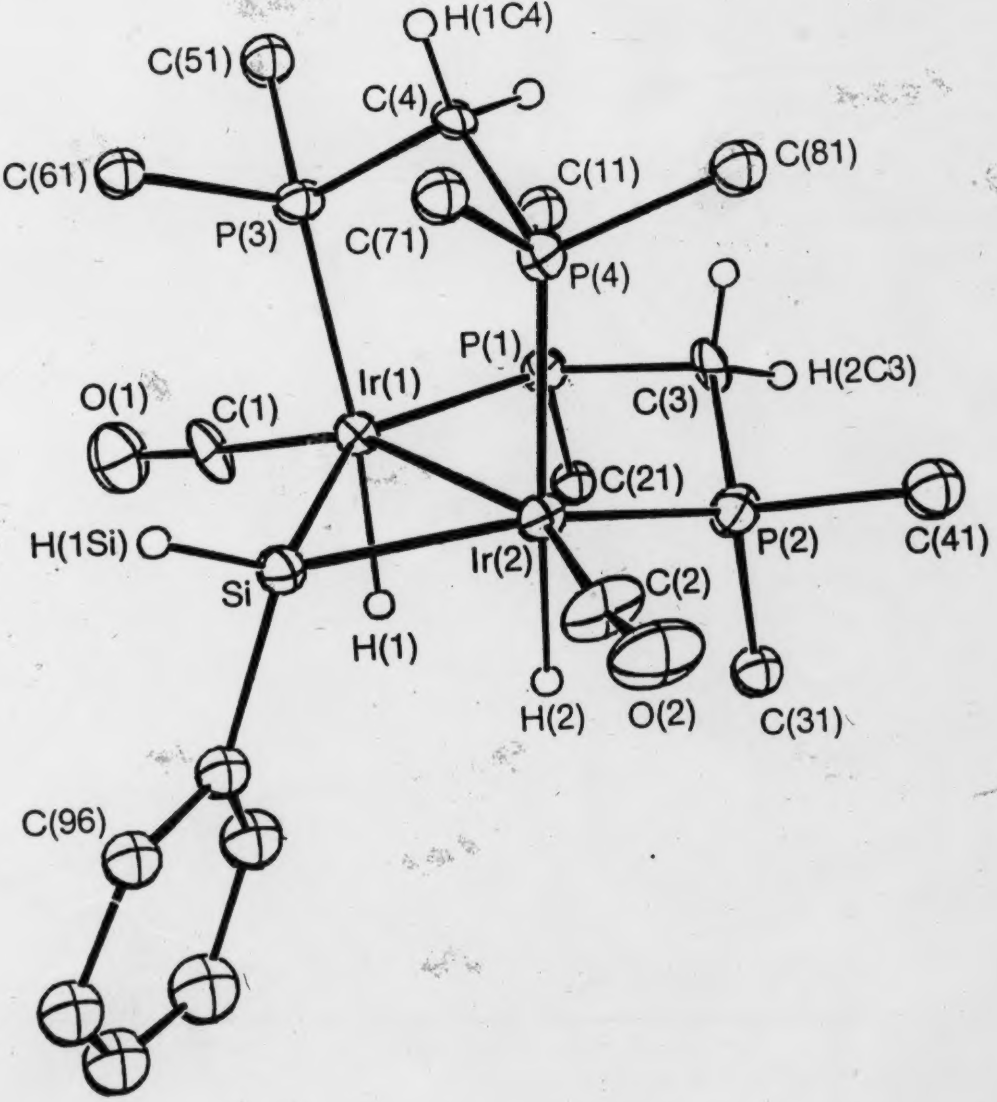
H(1C4)
C(51)
C(4)
C(61)
C(11)
C(81)
P(3)
C(71)
P(4)
P(1)
H(2C3)
O(1)
C(1)
Ir(1)
C(3)
C(21)
H(1Si)
Ir(2)
P(2)
C(41)
Si
C(2)
H(1)
H(2)
O(2)
C(31)
C(96)

Figure 3.4. View of complex 5 omitting the dppm phenyl carbon atoms except those bound to phosphorus. The positions shown for H(1) and H(2) are approximate (see text).

noted earlier, the hydride positions in **5** were not unambiguously located in the X-ray study, they are included in the positions derived from the Fourier map. These positions are in complete agreement with the spectroscopic data (vide infra) and with the locations of the other atoms in the structure, which leave obvious coordination sites in the positions of these hydrides. Their positions on each metal are also consistent with those in complex **4**, for which the hydride parameters were successfully refined. Since the hydride positions in **5** are estimated, bond lengths and angles involving these atoms are necessarily approximate, but are nevertheless in excellent agreement with the corresponding parameters for **4**. One hydride ligand on each metal is located cis to one phosphine (P(1)-Ir(1)-H(1) ≅ 92°; P(2)-Ir(2)-H(2) ≅ 70°) and trans to another (P(3)-Ir(1)-H(1) and P(4)-Ir(2)-H(2) ≅ 168°) as in **4**, and again the metal-phosphorus distances are apparently unaffected by the presence of the hydrides (Ir(1)-P(1) = 2.344(5) Å; Ir(1)-P(3) = 2.331(4) Å; Ir(2)-P(2) = 2.322(5) Å; Ir(2)-P(4) = 2.324(5) Å). The hydride ligands are also situated cis to the bridging phenylsilylene group giving Si-Ir(1)-H(1) and Si-Ir(2)-H(2) angles of ca. 74° and 78°, respectively, and silicon-hydride distances of Si···H(1) ≅ 2.5 Å and Si···H(2) ≅ 2.6 Å. Again the relatively close proximity of the Si and H atoms is not believed to indicate a significant interaction above that imposed by the geometry of the complex. The geometry of the Ir(1)-Si-Ir(2) bridge is rather similar to that of compound **4**, having comparable Ir-Si bond lengths (2.343(5) Å, 2.349(5) Å) and Ir(1)-Si-Ir(2) angle (75.7(2)°). Each metal displays an approximately octahedral coordination geometry, with a CO group, the other iridium center, two phosphines, the phenylsilylene group and a hydride acting as ligands. Deviations from this geometry, especially the offset of the otherwise normal terminal CO's from the Ir(1)-Ir(2) axis (Ir(2)-Ir(1)-C(1) = 154.7(6)°; Ir(1)-Ir(2)-C(2) = 158.3(7)°), appear to again result from the acute bite angle of the silylene bridge.

The phosphorus atoms belonging to the same dppm ligands in **5** are much closer to being eclipsed (P(1)-Ir(1)-Ir(2)-P(2) torsion = 14.7(2)°; P(3)-Ir(1)-Ir(2)-P(4) torsion = 12.7(2)°) than those of **4**, and the hydrides are now on the same side of the Ir(1)-Ir(2)-Si plane, with the Ir-H vectors approximately parallel. In addition, the silylene bridge of **5** appears not to show twisting at the silicon atom (Ir(1)-Si-C(91) = 118.8(6)°; Ir(2)-Si-C(91) = 118.9(6)°), indicating much less steric interaction between the silylene phenyl group and the dppm phenyls than was observed in **4**. It can be seen that while the phenylsilylene group is closer to one dppm group (P(3)-Ir(1)-Si = 94.2(2)°; P(4)-Ir(2)-Si = 103.8(2)°) than the other (P(1)-Ir(1)-Si = 144.0(2)°; P(2)-Ir(2)-Si = 133.2(2)°) its phenyl ring is held on the opposite side of the Ir(1)-Si-Ir(2) plane from the proximal (P(3)-C(4)-P(4)) dppm ligand, and is instead oriented towards the small hydride ligands.

The Ir(1)-Ir(2) distance of 2.879(1) Å is very close to that of **4**, and is again shorter than the intraligand P···P separations (P(1)···P(2) = 3.02(1) Å; P(3)···P(4) = 3.04(1) Å), indicating a mutual attraction of the two metals.

(b) Preparation and Characterization of Compounds. Although the dialkyl-, diphenyl- and phenylsilylene-bridged dimers **2-5** each possess several unique features, it is helpful to first characterize them in terms of their similarities. Each complex is formed via oxidative addition of an Si-H bond of a primary or secondary silane to each of the metal centers of

$[Ir_2(CO)_3(dppm)_2]$, with concomitant loss of a CO ligand. The reactions are facile under ambient conditions, yielding compounds containing terminal carbonyl and hydride groups on each iridium and a silylene bridge between the metals. Structurally these species are reminiscent of the previously-reported series of compounds $[Rh_2(H)_2(CO)_2(\mu\text{-}SiRR')(dppm)_2]$ (R = H, R′ = Et, Ph, *n*-hexyl; R = Me, R′ = Ph; R = R′ = Me, Et)[10] and $[Re_2(CO)_8(H)_2(\mu\text{-}SiPh_2)]$.[30] However, they display some notable differences in reactivity compared to their rhodium analogues. Unlike the Rh species, complexes **2-5** cannot be induced to reductively substitute CO for H_2. These diiridium species remain unchanged under carbon monoxide, even in refluxing THF, and do not yield any carbonyl-bridged, hydride-free products as observed for the dirhodium compounds. This inability to lose H_2 is also in contrast to the behavior of the related A-frame dihydride $[Ir_2(H)_2(CO)_2(\mu\text{-}S)(dppm)_2]$ (formed through oxidative addition of H_2S to $[Ir_2(CO)_3(dppm)_2]$ [see Chapter 4]), which, under reflux in THF or over time under N_2, loses H_2 to form $[Ir_2(CO)_2(\mu\text{-}S)(dppm)_2]$.[31] The $\mu\text{-}SiR_2$ complexes **2–4** are thermally stable in the solid state and in solution, and, unlike their dirhodium counterparts, do not react further by P-C bond cleavage and P-Si bond formation to yield products analogous to $[Rh_2(CO)_2(\mu\text{-}H)(dppm)(Ph_2PCH_2PPhSiRR')]$.[10] In addition, complex **5** is not fluxional and does not react with a second equivalent of $PhSiH_3$, whereas the compounds $[Rh_2(H)_2(CO)_2(\mu\text{-}SiHR)(dppm)_2]$ (R = Et, Ph) rapidly undergo hydride exchange between the Rh and Si centers at room temperature, and react with $RSiH_3$ to yield $[Rh_2(CO)_2(\mu\text{-}SiHR)_2(dppm)_2]$.[10]

Complexes **2-4** *are* fluxional at room temperature, but in a different manner from their dirhodium analogues; furthermore the fluxional process involved for compounds **2** and **3** is somewhat different from that for **4** (vide infra). The signals observed at room temperature in the $^{31}P\{^1H\}$ and highfield region of the ^1H NMR spectra of species **2** are shown in Figure 3.5; the spectra for **3** are quite comparable. The phosphorus NMR spectrum at ambient temperature shows a single broad resonance, implying one time-averaged phosphorus environment, and the proton NMR spectrum shows two different dppm methylene resonances, integrating as two protons each, and one signal in the highfield region, due to the terminal hydrides upon iridium. This highfield resonance appears as a second-order multiplet characteristic of an AA'XX'X''X''' spin system, with intensity corresponding to two hydrogens. The silylene methyl protons of **2** appear as a single broadened resonance at δ 0.70, while the hydrogens of the $SiEt_2$ group of **3** appear as a single triplet-quartet combination at δ 1.13 and 0.88, respectively.

At -60 °C the NMR spectra of these complexes differ substantially from those observed at room temperature. As shown in Figure 3.5, the phosphorus spectrum of the dimethylsilylene-bridged complex **2** shows a splitting of the high-temperature singlet into two broadened singlets at δ -9.2 and -18.0 (a surprising feature of these resonances is the lack of apparent phosphorus-phosphorus coupling). The corresponding proton spectrum shows four different dppm methylene resonances (at δ 6.33, 6.09, 2.85 and 2.69), integrating as one hydrogen each, and the highfield region again shows a second-order, two-proton signal that now appears as a broadened pattern arising from an AA'XX'YY' spin system, and is centered

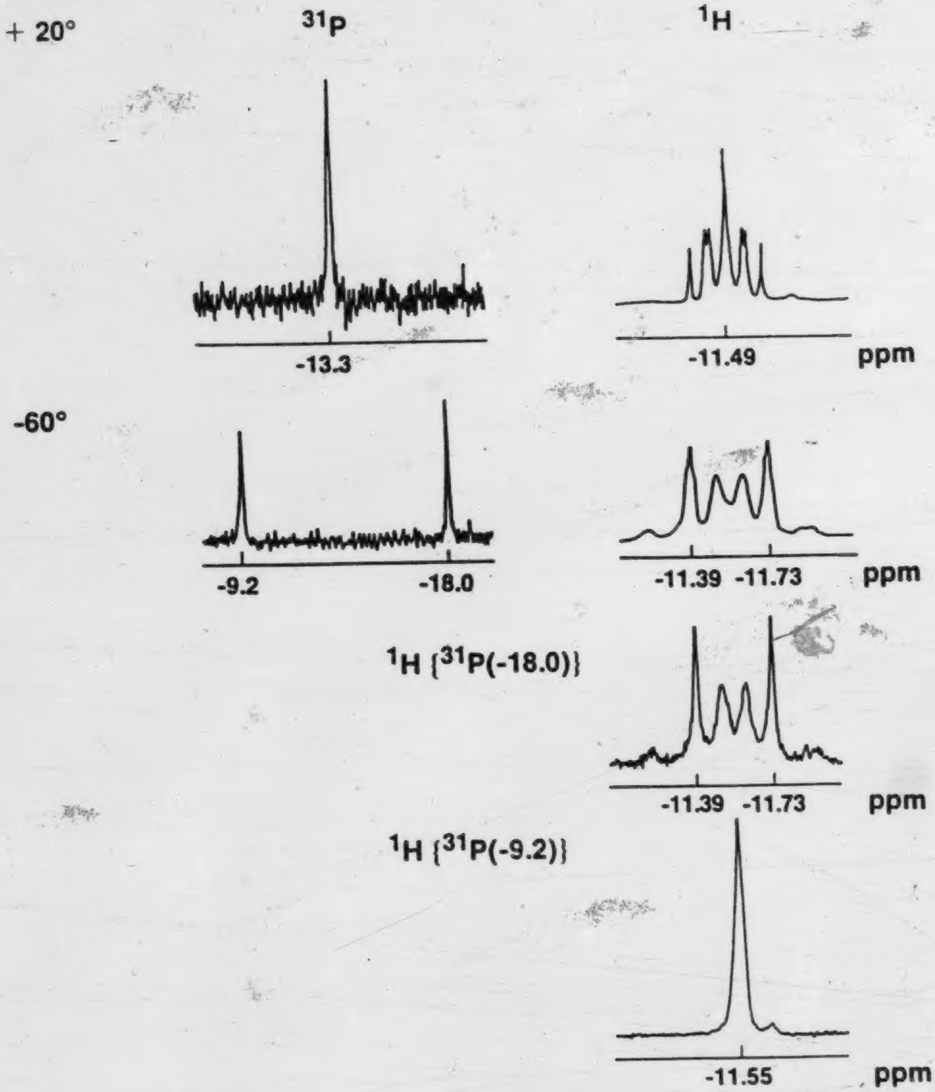

Figure 3.5. The $^{31}P\{^1H\}$, ^1H and $^1H\{^{31}P\}$ NMR spectra of complex 2 at 20 °C and -60 °C.

at δ -11.55. Selective heteronuclear decoupling of the highfield phosphorus resonance produces a sharpening of the spectral lines of the hydride multiplet, while irradiation of the lowfield phosphorus signal causes a collapse of the hydride resonance, indicating a larger coupling of the hydride to the lowfield than to the highfield phosphorus. Similar effects were observed in the low-temperature NMR spectra of complex **3**. The structural features giving rise to these spectroscopic observations, as well as the mechanism of ambient-temperature fluxionality of **2** and **3**, can be more easily explained in light of the spectra and solid-state structures observed for **4** and **5** (vide infra).

At ambient temperature the NMR spectra for **4** are quite similar to those of **2** and **3**. As shown in Figure 3.6, the $^{31}P\{^1H\}$ spectrum shows a broad singlet and in the highfield region of the ^1H spectrum appears a resonance due to a AA'XX'X''X''' spin system. It is important to note that this latter resonance is not a true first-order (1:4:6:4:1) quintet so does not necessarily imply a structure in which the hydrides bridge the metals. This resonance resembles that of **2** (Fig. 5), except that the broader lines adjacent to the central peak in **4** are resolved into two lines each in **2**. A rather analogous spectrum was observed for the closely related species $[Ir_2(H)_2(CO)_2(\mu\text{-}S)(dppm)_2]$,[31] in which one hydride ligand is terminally bound to each metal.

The low-temperature $^{31}P\{^1H\}$ NMR spectrum of **4** (see Figure 3.6) also shows a splitting of the room-temperature singlet, but the pattern observed is now an AA'BB' multiplet, in which the two branches are centered at δ -10.4 and -23.2. Under these conditions, the proton NMR

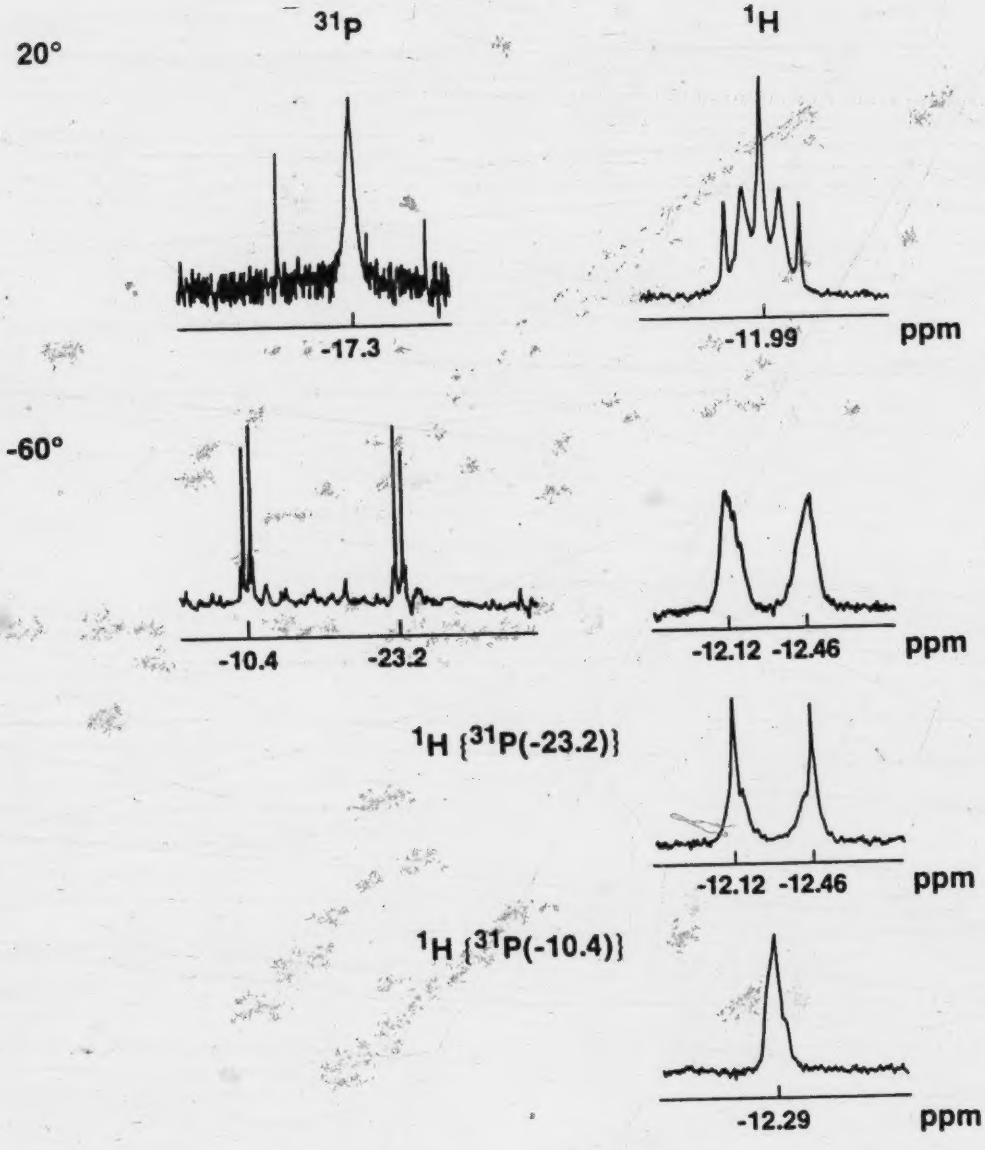

Figure 3.6. The $^{31}P\{^1H\}$, ^1H and $^1H\{^{31}P\}$ NMR spectra of complex 4 at 20 °C and -60 °C.

spectrum shows only two resonances attributable to methylene hydrogens (at δ 6.07 and 2.92); this is in agreement with the solid-state structure of **4**, in that the twofold symmetry of the molecule would still lead to two sets of two equivalent methylene protons. The highfield region of the proton NMR spectrum again shows a multiplet (centered at δ -12.29) due to the AA′ nuclei of an AA′XX′YY′ spin system, but one very different from those seen for **2** and **3**, here resembling two complex unresolved multiplets. Selective heteronuclear phosphorus decoupling again indicates a larger coupling of the hydrides to the lowfield than to the highfield phosphorus atoms, as shown in Figure 3.6. The two different couplings are consistent with the solid-state structure, which shows that each hydride is trans to one phosphorus nucleus, and therefore more strongly coupled to it, and cis to the other, to which it displays a smaller coupling.

The differences between the low-temperature NMR spectra of **2** and **3** and those of **4** imply that the limiting conformations of the dialkylsilylene-bridged species are different from that adopted by the diphenylsilylene complex. In this context, elucidation of the static structures of **2** and **3** is aided by comparison of their low-temperature proton and phosphorus NMR spectra with the corresponding ambient-temperature spectra of the non-fluxional phenylsilylene-bridged compound, **5**, shown in Figure 3.7. The $^{31}P\{^{1}H\}$ NMR spectrum of complex **5** shows two slightly broadened resonances (δ -8.4 and -19.1), while the ^{1}H spectrum shows four different methylene hydrogens (δ 6.39, 6.08, 3.22 and 2.82) and an AA′XX′-YY′-spin-system multiplet for the hydrides (centered at δ -11.43). Heteronuclear decoupling of the highfield phosphorus resonance causes collapse

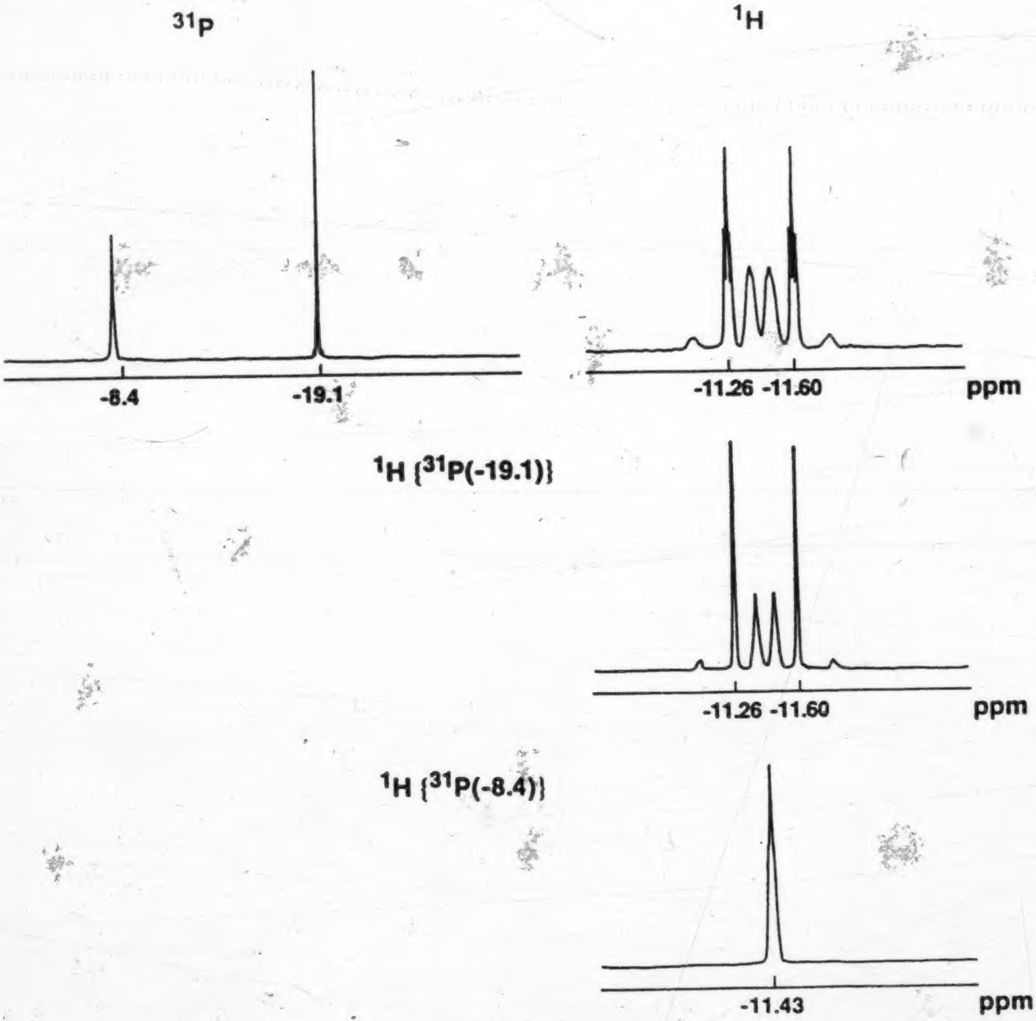

Figure 3.7. The ^{31}P{^{1}H}, ^{1}H and ^{1}H{^{31}P} NMR spectra of complex 5 at 20 °C.

of the hydride signal to a pattern characteristic of an AA'XX' spin system, while irradiation of the lowfield phosphorus resonance changes the hydride peak to a narrow pseudotriplet; these results are in agreement with the solid-state structure of complex **5**, in that the hydrides would be expected to be more strongly coupled to the phosphorus atoms located trans to them at the iridium center than to the phosphorus in the cis position, as was observed for **4**. The ambient-temperature $^{31}P\{^1H\}$, ^1H, and $^1H\{^{31}P\}$ NMR spectra of **5** are very similar to those observed at -60 °C for species **2** and **3**, but are quite different from the corresponding low-temperature spectra of compound **4**. Thus it appears that the dialkylsilylene-bridged complexes, **2** and **3**, adopt *static* configurations directly analogous to the crystallographically-determined structure of **5** (with SiR_2 groups replacing the SiHPh unit). The fluxionality observed for the dialkylsilylene-bridged complexes is proposed to occur via a process as shown, in which the μ-silylene group reversibly migrates from a position

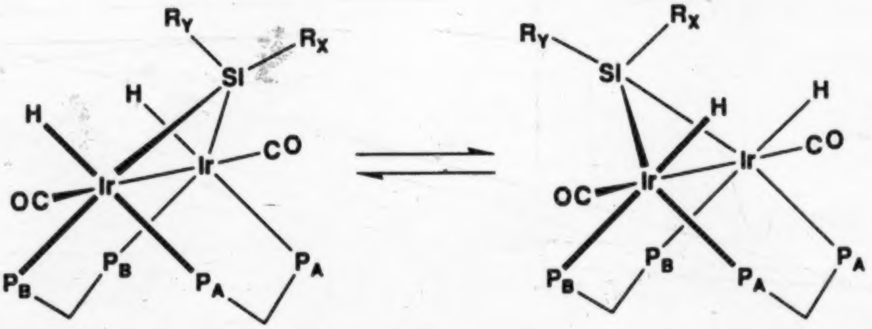

opposite the P_B nuclei to a site opposite the P_A nuclei, while the hydride ligands undergo an analogous but opposite interchange (i.e. from trans to P_A to trans to P_B). Rapid exchange between these two limiting forms would result in equilibration of the P_A and P_B phosphorus nuclei, and also of the R_X and R_Y alkyl groups. When R_X and R_Y are the same (both Me or both Et) the two conformations shown are energetically equivalent. However, when R_Y is a phenyl group and R_X is a hydrogen, as in complex **5**, the structure shown on the left, in which the bulky silylene phenyl group is held towards the small hydride ligands and away from the bulky diphosphine bridges, would be more favored than that on the right. This is the structure adopted by complex **5**, which is not fluxional at room temperature.

Simulations of the ambient-temperature ^{1}H NMR spectra of compounds **2** and **5** have been carried out. The results for **2** yield information about the time-averaged structure in the fluxional process, while those for **5** are characteristic of the static structure. Using the spin system designations as illustrated below, a satisfactory simulation of the hydride resonance of **2** was obtained employing the values $J_{AA'}$ = 1.2 Hz ($^3J_{H\text{-}H}$), $J_{AX} = J_{AX''} = J_{A'X'} = J_{A'X'''}$ = 49.6 Hz ($^2J_{P\text{-}H}$), $J_{AX'} = J_{AX'''} = J_{A'X} = J_{A'X''}$ = 11.0 Hz ($^3J_{P\text{-}H}$), $J_{XX'} = J_{X''X'''}$ = 133 Hz (through-backbone $^2J_{P\text{-}P}$), $J_{XX''} = J_{X'X'''}$ = 29 Hz

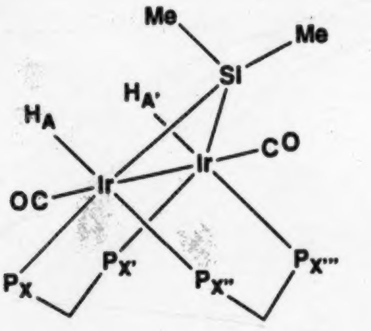

2

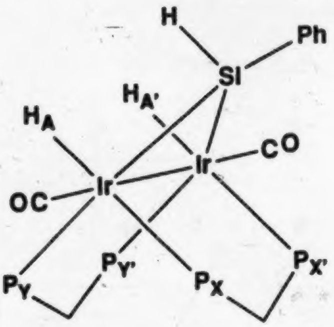

5

(through-metal $^2J_{\text{P-P}}$), and $J_{\text{XX}'''} = J_{\text{X}'\text{X}''}$ = -26 Hz (gauche $^3J_{\text{P-P}}$). The hydride resonance of **5** was simulated according to the above spin designations, and yielded the following values: $J_{\text{AA}'}$ = 4.3 Hz ($^3J_{\text{H-H}}$), $J_{\text{AX}} = J_{\text{A}'\text{X}'}$ = 125.1 Hz (trans $^2J_{\text{P-H}}$), $J_{\text{AX}'} = J_{\text{A}'\text{X}}$ = 12.6 Hz ($^3J_{\text{P-H}}$), $J_{\text{AY}} = J_{\text{A}'\text{Y}'}$ = 7.2 Hz (cis $^2J_{\text{P-H}}$), $J_{\text{AY}'} = J_{\text{A}'\text{Y}}$ = 5.2 Hz ($^3J_{\text{P-H}}$), $J_{\text{XX}'}$ = 123.9 Hz (through-backbone $^2J_{\text{P-P}}$), $J_{\text{XY}} = J_{\text{X}'\text{Y}'}$ = 28.8 Hz (cis $^2J_{\text{P-P}}$), $J_{\text{XY}'} = J_{\text{X}'\text{Y}}$ = -26.2 Hz (gauche $^3J_{\text{P-P}}$), and $J_{\text{YY}'}$ = 141.9 Hz (through-backbone $^2J_{\text{P-P}}$). It should be pointed out that attempted fittings of the spectra of **5** were more successful in the $^1\text{H}\{^{31}\text{P}\}$ cases than for the undecoupled ^{1}H spectrum, since the broadness of some of the observed peaks prevented a closer fit of simulation to data. Simulation of the hydride resonance of **2** at -60° was not attempted due the decreased resolution of this signal; however, its close resemblance to the room-temperature hydride resonance of **5** (see Figures 4.5 and 4.7) implies that the couplings giving rise to the former pattern will be much the same as those found for the latter. In this light, the fact that the nominally two-bond phosphorus-hydrogen coupling for **2** at room temperature (49.6 Hz) is approximately midway between the trans (125.1 Hz) and cis (7.2 Hz) $^2J_{\text{P-H}}$ values for **5** appears to reflect the site exchange taking place, resulting in equivalence of the phosphorus nuclei and averaging of these P-H couplings. According to the mechanism above, the fluxional process occurs via movement of the hydride and silylene groups with respect to the "fixed" Ir_2P_4 core; thus, the values for the through-backbone, through-metal, and gauche P-P couplings should remain relatively constant upon going from the static to the fluxional species, which is indeed the case. Overall the values obtained are in line with previous results for iridium-phosphorus and diphosphine-bridged systems.[10,32]

A slightly different mode of interchange, in which the complex oscillates between enantiomeric forms of the crystallographically-determined structure, would appear to be at work for species 4, and is shown below. Dashed lines are used to indicate bonds within the "rear" half of the molecule. This mechanism involves a twisting of the P-Ir-P units with respect to each other, an oscillation of the $SiPh_2$ bridge about the molecule's twofold axis of symmetry, and movement (while remaining attached to the same metal) of the hydride ligands from positions trans to the P_A phosphorus atoms to opposite the P_B atoms. This is a somewhat more complex mode of interchange than that proposed for 2 and 3, presumably because of the more severe steric interactions involving the large phenyl substituents on Si and the dppm ligands in 4, which result in the differing structures as noted previously. In complex 4 interchange of the hydride and silylene positions, in which the hydride ligands migrate to different sides of the Ir_2Si plane, is also accompanied by twisting of the Ir_2P_4 core and a concomitant pivoting of the silylene group in order to allow the silylene phenyl substituents to occupy the least sterically

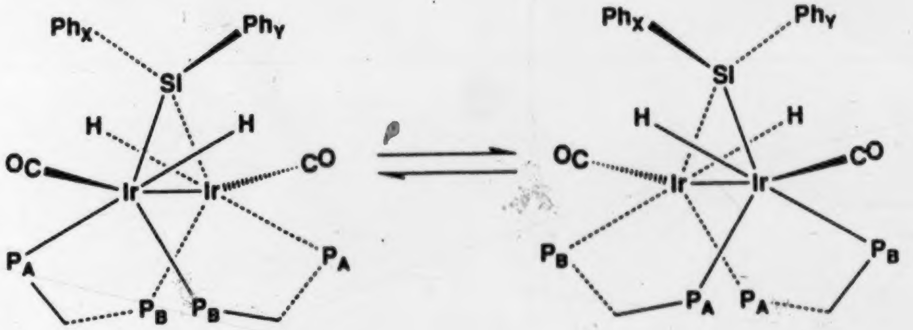

hindered positions. An alternate mechanism that cannot be ruled out would involve the same types of motions of the diphosphine and silylene bridges, but with the hydride ligands exchanging between the metal centers via an intermediate containing two μ-H groups. This would be supported by the slight downfield shift of the hydride resonance (from δ -12.29 to -11.99) upon warming of **4** from -60 °C to room temperature. In previous studies of similar compounds, resonances for bridging hydrides have been found to occur downfield of those for terminal hydrides when both types are contained in the same complex,[6,11] so a mechanism in which rapid hydride exchange occurs via a hydride-bridged intermediate should display a downfield shift for this resonance. In contrast, the hydride resonance for complex **2** remains in essentially the same position over a broad range of temperature (δ -11.49 at 23°, -11.56 at -60°), supporting the mechanism proposed in which both hydrides remain terminal throughout the fluxional process. It would appear that like species **2** and **3**, but unlike **5**, the symmetry of the silylene bridge of **4** means that both limiting conformations shown above are energetically equivalent.

The mechanisms proposed for the room-temperature fluxionality of **2**, **3** and **4** differ from that proposed in the case of $[Rh_2(H)_2(CO)_2(\mu\text{-SiHR})(dppm)_2]$ (R = Et, Ph),[10] where reversible Si-H/Rh-H exchange is believed responsible. For the rhodium dimers, variable-temperature ^1H NMR spectra revealed a scrambling between the rhodium hydrides and the silylene proton under ambient conditions. In the iridium silylene compounds of this study the very slight chemical shift difference for the hydride resonances at ambient and low temperature is not consistent with a mechanism which involves migration of the hydride from the metal to the silyl moiety during the interchange process. Nor is any resonance observed in compounds **2**, **3** or **4** for an Si-H unit. In contrast, an SiHPh-bridged dirhodium analogue displayed a hydride signal at ca. δ -4.1 at room temperature which resolved into two resonances at ca. δ -9.2 and 6.3 in a 2:1 intensity ratio at low temperature.[10] Furthermore, if the fluxionality of the diiridium μ-SiR_2 complexes were similar to that for their dirhodium analogues, the coordinatively-unsaturated Ir(0) center, generated in the reductive elimination of a silicon-hydrogen bond, might be susceptible to oxidative addition by free $PhSiH_3$; in fact, no such reaction is observed (by ^1H and $^{31}P\{^1H\}$ NMR spectroscopy) when $PhSiH_3$ is added to THF-d_8 solutions containing equimolar amounts of **2**, **3** or **4**, even after stirring the mixtures for 24 h at room temperature. As mentioned earlier, the iridium analogue of the above dirhodium complexes, species **5**, is not found to be fluxional, and no evidence of exchange between the iridium- and silicon-bound hydrogens is observed.

As noted in the Experimental section, variable-temperature $^{31}P\{^1H\}$ NMR spectroscopy can be employed to determine coalescence temperatures for the interconverting phosphorus nuclei in each of complexes **2**, **3** and **4**. Coupled with the frequency differences between the resonances for the different environments in the totally decoalesced spectra (obtained in each case at -60 °C), these results may be used in the approximation to the Eyring equation to provide estimates of the free energy of activation of the various fluxional processes. These values are summarized in Table 3.9. Somewhat surprisingly, the $\Delta G^\ddagger$ values are, within experimental error,

Table 3.9. Free Energies of Activation for the Fluxional Silylene-Bridged Complexes $[Ir_2(H)_2(CO)_2(\mu\text{-}SiR_2)(dppm)_2]$ (2–4)[a]

R	$\Delta\nu$ (Hz)	T_c (K)	$\Delta G^\ddagger$ (kJ/mol)
Me (2)	1432.4	258 ± 5	45.6 ± 0.9
Et (3)	1258.5	248 ± 5	44.0 ± 0.9
Ph (4)	2063.6	253 ± 10	43.9 ± 1.8

[a] Calculated using the approximation to the Eyring relationship ($\Delta G^\ddagger = RT_c \ln(\sqrt{2}kT_c/\pi h\Delta\nu)$) where R = the gas constant, T_c = coalescence temperature, k = the Boltzmann constant, h = Planck's constant and $\Delta\nu$ = frequency separation between inequivalent environments of exchanging nuclei).

approximately the same; a clear delineation between activation energies for the dialkylsilylene- and diphenylsilylene-bridged species' interchange processes might have been expected. The corresponding values for the related rhodium dimers ($[Rh_2(H)_2(CO)_2(\mu\text{-}SiHR)(dppm)_2]$) are also similar ($\Delta G^\ddagger$ = 46 ± 4 kJ/mol (R = Et), 50 ± 4 kJ/mol (R = Ph)); however, as explained above, an analogous process for equilibration of phosphorus environments is not believed to be at work for the diiridium systems.

Information about the mechanism by which primary or secondary silanes undergo oxidative addition to $[Ir_2(CO)_3(dppm)_2]$ can be obtained by monitoring the reaction of 1 with Ph_2SiH_2 at low temperature, where two intermediates can be observed before formation of the ultimate product, 4.

At -30 °C an unsymmetrical species is observed, which has been formulated as [$Ir_2(H)(CO)_3(SiHPh_2)(dppm)_2$] (**6**), the result of a single Si-H bond addition at one Ir center. This intermediate appears as two multiplets in the $^{31}P\{^1H\}$ NMR spectrum, at δ -13.6 and -26.7, indicating two inequivalent phosphorus environments, and the $^{13}C\{^1H\}$ NMR spectrum shows two equally-intense signals at δ 193.1 and 182.8. The question of whether **6** is a di- or tricarbonyl complex is complicated by the broad carbonyl resonance (at δ 186.7) due to **1**, which is present in at least a tenfold excess compared to **6** under these conditions, and may be obscuring a third resonance due to **6**. In spite of observing only two ^{13}CO resonances it is likely that **6** contains *three* CO ligands, since related studies on the reactions of H_2S and thiols with the mixed-metal dimer [$RhRe(CO)_4(dppm)_2$], which is isoelectronic with **1**, show that oxidative addition of an S-H bond to the coordinatively-unsaturated Rh center takes place to yield the initial products [$RhRe(H)(SR)(CO)_4(dppm)_2$] (R = H, Et, Ph), with retention of all carbonyl groups, although subsequent CO loss can occur.[8] The ^1H NMR spectrum of **6** shows a triplet in the highfield region at δ -9.40 ($^2J_{P\text{-}H}$ = 13.8 Hz), characteristic of a terminal hydride bound to iridium, and also shows a singlet at δ 5.60 of equal intensity, which may be attributed to a proton attached to silicon. Irradiation of only the lower-field phosphorus signal leads to collapse of the hydride signal to a singlet. Decoupling of the highfield phosphorus resonance causes no change in these two ^1H signals.

If the sample is warmed to -20 °C, another asymmetric species, **7**, is observed, appearing at δ -6.0 and -7.6 in the phosphorus NMR spectrum. The highfield region of the ^1H NMR spectrum shows, in addition to the resonance at δ -9.40 due to **6**, new triplet signals for **7** at -3.84 ($^2J_{P\text{-}H}$ = 6.8 Hz) and -11.86 ($^2J_{P\text{-}H}$ = 11.2 Hz). The latter signal appears to be due to a hydride that is terminally bound to iridium, as it collapses to a singlet when the higher-field phosphorus signal due to **7** is decoupled. The lower-field hydride signal collapses to a singlet when the lower-field phosphorus resonance of **7** is irradiated, indicating that it is interacting with a different metal center than the terminal hydride. The lowfield resonance is assigned as due to the proton of a three-centered Ir-H-Si moiety, which may be visualized as an agostic interaction of the Si-H bond with Ir. Such a proposal is supported by the chemical shift value for this hydrogen, which is intermediate between the values expected for a classical hydride and a silicon-bound hydrogen, and also by the low value of $^2J_{P\text{-}H}$ relative to typical values observed for terminal iridium hydrides; a three-centered Ir-H-Si interaction would be expected to yield smaller phosphorus-hydrogen coupling values owing to the weaker metal-hydride interaction. In the complexes $[Cp_2Ti(\mu\text{-}H)(\mu\text{-}\eta^2\text{-}HSi(H)Ph)TiCp_2]$[33] and $[(dppm)Mn_2(CO)_6(\mu\text{-}\eta^3\text{-}H_2SiPh_2)]$[34] the ^{1}H NMR resonances for the agostic M-H-Si units were also found to be intermediate between those for normal Si-H and M-H groups, whereas the signal for the agostic Ir-H-Si interaction in *cis,cis,trans*-$[Ir(PPh_3)_2(\eta^2\text{-}HSiEt_3)_2(H)_2]^+$ [35] is actually upfield of that for the terminal hydrides, and appears to be an exception. Signals due to intermediate **7** in the $^{13}C\{^1H\}$ NMR spectrum could not be unambiguously assigned, since under these conditions significant amounts of species **1**, **4**, and **6**, as well as $[Ir_2(CO)_4(dppm)_2]$[6] (formed by CO addition to **1**), were found to be present in solution. (The absence of the tetracarbonyl species earlier in the reaction, when **6** was the only observed intermediate, is further evidence that carbonyl loss has not occurred in the transformation of **1** to **6**.) Thus complex **7** is proposed to have the formulation $[Ir_2(H)(CO)_2(\mu\text{-}\eta^2\text{-}SiHPh_2)(dppm)_2]$, in which both the terminal hydride ligand and the diphenylsilyl group are attached to the same metal, with an agostic Si-H interaction with the adjacent metal center. Compound **7** can arise readily from species **6** as shown below, via replacement of a carbonyl

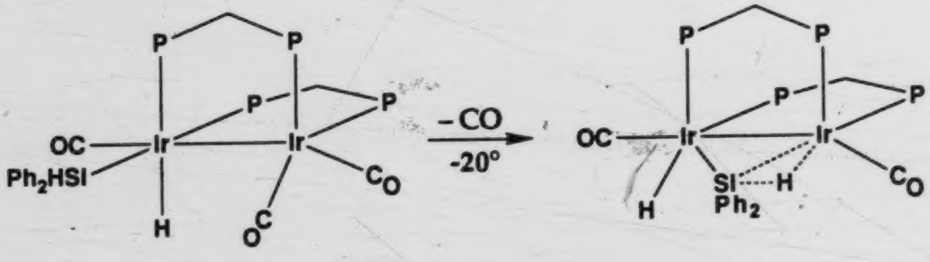

6 **7**

group by an Si-H interaction. Compound **7** then would represent the immediate precursor to the final product, **4**, via Si-H oxidative addition to Ir. When the sample is warmed to room temperature, **4** is the only species observed in the $^{31}P\{^1H\}$ and ^1H NMR spectra. Compounds **6** and **7** are shown with cis diphosphine arrangements, as suggested by the structure determinations of **4** and **5**, as well as that proposed for the precursor, **1**.[7] Although the above structures for **6** and **7** are not entirely consistent with the hydride resonances observed, which suggest that the hydride ligands are coupled to two equivalent phosphorus nuclei in each compound, it is likely that these intermediates, like the final product (**4**), are fluxional.

Attempts to prepare isolable adducts modelling the first oxidative-addition step through reactions of **1** with tertiary silanes were unsuccessful. Triethylsilane does not react with **1** even under reflux in THF, and the reaction of **1** with Me_3SiH leads to the immediate formation of $[Ir_2(H)_4(CO)_2(dppm)_2]$.[11] It is likely that this reaction proceeds via initial Si-H bond addition at Ir, with subsequent β-hydride elimination from the trimethylsilyl fragment. Although β-hydride elimination from a metal-silyl fragment is rare, it has recently been reported for related mononuclear systems.[29,36] The first so-formed hydrogenated product would then be $[Ir_2(CO)_2(\mu\text{-}H)_2(dppm)_2]$,[11] which has been shown to react with Me_3SiH to yield the same ultimate product, conceivably through formation of a diiridium trimethylsilyl trihydride that would again undergo β-hydride elimination to give the final tetrahydride.

Conclusions

The reactivity of complex **1**, $[Ir_2(CO)_3(dppm)_2]$ towards silane substrates illustrates its susceptibility to oxidative addition, as might be expected considering the low oxidation states of the metals. The "built-in" coordinative unsaturation at the Ir(I) center is conducive to precoordination of the substrate as a prelude to addition; having the Ir(-I) center in close proximity allows the activation of both silicon-hydrogen bonds of H_2SiRR'-type molecules to occur readily and in a stepwise fashion, one Si-H bond at a time. The differences between these complexes and their rhodium analogues appear to be mainly due to the greater strength of Ir-H vs. Rh-H bonds; as a result, complexes **2-5** are inert towards reductive substitution of H_2 by CO, and species **2-4** do not undergo reversible Si-H elimination from the Ir centers during their fluxional processes.

References and Footnotes

1. Speier, J. L. *Adv. Organomet. Chem.* **1979**, *17*, 407.
2. (a) Ojima, I.; Kogure, T.; Nihonyanagi, M; Kono, H.; Inaba, S.; Nagai, Y. *Chem. Lett.* **1973**, 501. (b) Corriu, R. J. P.; Moreau, J. J. E. *J. Organomet. Chem.* **1976**, *114*, 135. (c) Blackburn, S. N.; Haszeldine, R. N.; Parish, R. V.; Setchfi, J. H. *J. Organomet. Chem.* **1980**, *192*, 329. (d) Dwyer, J.; Hilal, H. S.; Parish, R. V. *J. Organomet. Chem.* **1982**, *228*, 191. (e) Lukevics, E; Dzintara, M. *J. Organomet. Chem.* **1985**, *295*, 265.
3. (a) Yamamoto, K.; Okinoshima, H.; Kumada, M. *J. Organomet. Chem.* **1971**, *27*, C31. (b) Ojima, I.; Inaba, S.-I.; Kogure, T.; Nagai, Y. *J. Organomet. Chem.* **1973**, *55*, C7. (c) Lappert, M. F.; Maskell, R. K. *J. Organomet. Chem.* **1984**, *264*, 217. (d) Brown-Wensley, K. A. *Organometallics* **1987**, *6*, 1590. (e) Corey, J. Y.; Chang, L. S.; Corey, E. R. *Organometallics* **1987**, *6*, 1595.
4. Mackay, K. M.; Nicholson, B. K. In *Comprehensive Organometallic Chemistry*; Wilkinson, G., Stone, F. G. A., Abel, E. W., Eds.; Pergamon Press: Oxford, England, 1982; Chapter 43.
5. Graham, W. A. G. *J. Organomet. Chem.* **1986**, *300*, 81.
6. Sutherland, B. R.; Cowie, M. *Organometallics* **1985**, *4*, 1637.
7. (a) See Chapter 2 of this thesis. (b) McDonald, R; Cowie, M. *Inorg. Chem.* **1990**, *29*, 1564.
8. Antonelli, D. M.; Cowie, M. *Inorg. Chem.* **1990**, *29*, 3339.
9. Vaartstra, B. A.; Cowie, M. *Inorg. Chem.* **1989**, *28*, 3138.

10. (a) Wang, W.-D.; Hommeltoft, S. I.; Eisenberg, R. *Organometallics* **1988**, *7*, 2417. (b) Wang, W.-D.; Eisenberg, R. *J. Am. Chem. Soc.* **1990**, *112*, 1833.

11. McDonald, R.; Sutherland, B. R.; Cowie, M. *Inorg. Chem.* **1987**, *26*, 3333.

12. Doedens, R. J.; Ibers, J. A. *Inorg. Chem.* **1967**, *6*, 204.

13. Walker, N., Stuart, D. *Acta Crystallogr., Sect. A: Found. Crystallogr.* **1983**, *A39*, 1581.

14. Programs used were those of the Enraf-Nonius Structure Determination Package by B. A. Frenz, in addition to local programs by R. G. Ball.

15. Cromer, D. T.; Waber, J. T. *International Tables for Crystallography*; Kynoch Press: Birmingham, England, 1974; Vol. IV, Table 2.2A.

16. Stewart, R. F.; Davidson, E. R.; Simpson, W. T. *J. Chem. Phys.* **1965**, *42*, 3175.

17. Cromer, D. T.; Liberman, D. *J. Chem. Phys.* **1970**, *53*, 1891.

18. Berry, D. H.; Eisenberg, R. *Organometallics* **1987**, *6*, 1796.

19. See Chapter 5 of this thesis.

20. Manojlović-Muir, L.; Muir, K. A.; Frew, A. A.; Ling, S. S. M.; Thomson, M. A.; Puddephatt, R. J. *Organometallics* **1984**, 3, 1637.

21. Brown, M. P.; Cooper, S. J.; Frew, A. A.; Manojlović-Muir, L.; Muir, K. A.; Puddephatt, R. J.; Seddon, K. R.; Thomson, M. A. *Inorg. Chem.* **1981**, *20*, 1500.

22. Woodcock, C.; Eisenberg, R. *Inorg. Chem.* **1985**, *24*, 1285.

23. Haines, R. J.; Meintjies, E.; Laing, M.; Sommerville, P. *J. Organomet.*

Chem. **1981,** *216,* C19.

24. Haines, R. J.; Meintjies, E.; Laing, M. *Inorg. Chim. Acta* **1979,** *36,* L403.

25. Schubert, U. *Adv. Organomet. Chem.* **1990,** *30,* 151, and references therein.

26. Huheey, J. E. *Inorganic Chemistry,* 3rd ed.; Harper and Row: New York, 1983; pp. 258-259 and references therein.

27. (a) Kubiak, C. P.; Woodcock, C.; Eisenberg, R. *Inorg. Chem.* **1980,** *19,* 2733. (b) Sutherland, B. R.; Cowie, M. *Inorg. Chem.* **1984,** *23,* 2324. (c) Mague, J. T.; Klein, C. L.; Majeste, R. J.; Stevens, E. D. *Organometallics* **1984,** *3,* 1860. (d) Sutherland, B. R.; Cowie, M. *Organometallics* **1984,** *3,* 1869. (e) Wu, J.; Reinking, M. K.; Fanwick, P. E.; Kubiak, C. P. *Inorg. Chem.* **1987,** *26,* 247. (f) Wu, J.; Fanwick, P. E.; Kubiak, C. P. *Organometallics* **1987,** *6,* 1805. (g) Balch, A. L.; Waggoner, K. M.; Olmstead, M. M. *Inorg. Chem.* **1988,** *27,* 4511.

28. (a) Curtis, M. D.; Greene, J.; Butler, W. M. *J. Organomet. Chem.* **1979,** *164,* 371. (b) Auburn, M. J.; Grundy, S. L.; Stobart, S. R.; Zawortko, M. J. *J. Am. Chem. Soc.* **1985,** *107,* 266. (c) Ricci, J. S., Jr.; Koetzle, T. F.; Fernández, M.-J.; Maitlis, P. M.; Green, J. C. *J. Organomet. Chem.* **1986,** *299,* 383. (d) Fernández, M.-J.; Esteruelas, M. A.; Oro, L. A.; Apreda, M.-C.; Foces-Foces, C.; Cano, F. H. *Organometallics* **1987,** *6,* 1751. (e) Rappoli, B. J.; Janik, T. S.; Churchill, M. R.; Thompson, J. S.; Atwood, J. D. *Organometallics* **1988,** *7,* 1939.

29. Zlota, A. A.; Frolow, F.; Milstein, D. *J. Chem. Soc., Dalton Trans.* **1989,** 1826.

30. (a) Hoyano, J. K.; Elder, M.; Graham, W. A. G. *J. Am. Chem. Soc.* **1969,** *91,* 4568. (b) Elder, M. *Inorg. Chem.* **1970,** *9,* 762.

31. Vaartstra, B. A.; O'Brien, K. N.; Eisenberg, R.; Cowie, M. *Inorg. Chem.* **1988,** *27,* 3668.

32. Verkade, J. G.; Quin, L. D., eds. *Phosphorus-31 NMR Spectroscopy in Stereochemical Analysis*; Methods in Stereochemical Analysis 8; VCH Publishers: Deerfield Beach, FL, 1987.

33. Aitken, C. T.; Harrod, J. F.; Samuel, E. *J. Am. Chem. Soc.* **1986,** *108,* 4059.

34. Carreño, R.; Riera, V.; Ruiz, M. A.; Jeannin, Y.; Philoche-Levisalles, M. *J. Chem. Soc., Chem. Commun.* **1990,** 15.

35. Luo, X.-L.; Crabtree, R. H. *J. Am. Chem. Soc.* **1989,** *111,* 2527.

36. Berry, D. H.; Procopio, L. J. *J. Am. Chem. Soc.* **1989,** *111,* 4099.

Chapter 4

Oxidative Additions of S-H and Se-H Bonds to $[MM'(CO)_3(dppm)_2]$ (MM' = Rh_2, Ir_2, RhIr)

Introduction

Much effort has been directed towards understanding the interactions between sulfur-containing substrates and metal catalysts, much of it concerned with establishing how catalyst surfaces are poisoned by these compounds.[1] Other studies have focussed upon chemical transformations of the sulfur-bearing species, including the mechanisms of hydrodesulfurization of sulfur-containing organic compounds present in hydrocarbon feedstock mixtures,[2] and the utilization of hydrogen sulfide as an alternate source of hydrogen.[3,4] In some cases, the presence of sulfur-containing residues in a homogeneous catalyst precursor has been found to actually *enhance* activity of the catalyst.[5]

A fundamental step in the interaction between a catalyst and sulfur-containing substrates, such as hydrogen sulfide or thiols, is the oxidative addition of S-H bonds to metal centers. In the chemistry of mononuclear model complexes it has been found that sulfur tends to promote the formation of multinuclear complexes such that in the resultant products sulfur atoms (as HS^-, RS^- or S^{2-} residues) often bridge two or three metal nuclei.[3,6,7] Complexes in which the sulfur-containing ligands are present as purely terminal groups are far less common.[7a, 8]

Studies of oxidative additions of hydrogen sulfide, thiols and disulfides to low-valent complexes of rhodium and iridium have focussed mainly on mononuclear species;[6f,7,8b,9] fewer studies have involved the interactions of sulfur-containing substrates with binuclear Rh or Ir complexes.[10,11] The reactions of bis(diphenylphosphino)methane-bridged low-oxidation-state di- and triplatinum complexes with H_2S, H_2Se, thiols, selenols, disulfides and diselenides have been the subject of several recent reports from the research group of Puddephatt,[12] while James and coworkers have investigated the kinetics and thermodynamics of the addition of H_2S to $[Pd_2Cl_2(dppm)_2]$, where $[Pd_2Cl_2(\mu\text{-}S)(dppm)_2]$ and H_2 are obtained spontaneously and quantitatively under ambient conditions.[4] Our interest in the binuclear oxidative-addition reactions of the $[MM'(CO)_3(dppm)_2]$ (MM' = Rh_2,[13] Ir_2,[14] RhIr[15]) compounds, which contain rhodium and iridium centers of low oxidation state, prompted investigations into the interactions of these complexes with hydrogen sulfide, hydrogen selenide, thiols and selenols. A primary goal in these studies was to discover how adjacent metals could be involved in the activation of S-H and Se-H bonds.

Experimental Section

General experimental conditions were as described in Chapter 2. The thiol, disulfide, selenol and diselenide reagents were obtained from Aldrich and used as received. The complexes $[Rh_2(CO)_3(dppm)_2]$ (**1**),[13] $[Ir_2(CO)_3(dppm)_2]$ (**2**)[14] and $[RhIr(CO)_3(dppm)_2]$ (**3**)[15] (see Chapter 1) were prepared as previously reported. All other chemicals were used as received without further purification. Infrared and NMR spectroscopic parameters for the compounds prepared are found in Tables 4.1 and 4.2, respectively.

Preparation of Compounds. (a) [RhIr(H)(SH)(CO)$_2$(dppm)$_2$]•CH$_2$Cl$_2$ (7). An atmosphere of H_2S was placed over a solution of **3** (150 mg, 131 μmol) in THF (5 mL), causing a color change from red-orange to deep red-brown. The solution was allowed to stir for 2 h, then was evaporated to dryness under an N_2 stream. The brown residue was extracted with CH_2Cl_2 and the resultant solution filtered and reduced in volume, at which point addition of ether (15 mL) caused precipitation of a medium red-brown powdery solid (91 mg, 56%). Anal. Calcd for $C_{53}Cl_2H_{48}IrO_2P_4RhS$: C, 51.38; H, 3.91. Found: C, 51.42; H, 3.88.

(b) [RhIr(H)(SeH)(CO)$_2$(dppm)$_2$] (8). Hydrogen selenide was placed over a solution of **3** in THF (150 mg, 131 μmol in 5 mL) causing a color change from deep orange to red-brown within 10 min. The solution was stirred for 1 h then evaporated under a stream of N_2 to ca. 2 mL; addition of ether (15 mL) caused precipitation of a dark brown solid. This material was recrystallized from THF/ether, resulting in isolation of 105 mg (67%) of the product as a medium-brown powder. Anal. Calcd for $C_{52}H_{46}IrO_2P_4$-RhSe: C, 52.01; H, 3.86. Found: C, 46.68; H, 3.74.[16]

(c) [Ir$_2$(SEt)$_2$(CO)$_2$(μ-CO)(dppm)$_2$] (11). To a solution of **2** (100 mg, 80.8 μmol) in THF (5 mL) was added ethanethiol (12.0 μmol, 10.0 mg, 162 μmol), causing initially a slight lightening of the orange solution, then a change in color to light yellow within 20 min. The reaction mixture was left to stir for a further 2 h, during which time formation of a light yellow precipitate occurred. The solution volume was reduced to ca. 2 mL, causing a darkening of the supernatant liquid to red-orange. Placing the

Table 4.1. Infrared Spectroscopic Data[a] for the Compounds of Chapter 4.

compound	solid[b]	solution[c]
[RhIr(H)(SH)(CO)$_2$(dppm)$_2$] (7)	1931 (vs), 1906 (vs)	1948 (vs), 1920 (vs)
[RhIr(H)(SeH)(CO)$_2$(dppm)$_2$] (8)	2053 (vs), 2004 (vs)	2047 (s), 2009 (vs)
[Ir$_2$(SEt)$_2$(CO)$_2$(μ-CO)(dppm)$_2$] (11)	1957 (s), 1943 (vs), 1702 (w)	1957 (sh), 1946 (vs, br), 1700 (w)
[Ir$_2$(SPh)$_2$(CO)$_2$(μ-CO)(dppm)$_2$] (16)	1957 (s), 1946 (vs), 1720 (s)	1963 (sh), 1949 (vs), 1721 (s)
[Ir$_2$(SPh)$_2$(CO)$_2$(μ-CO)(dppm)$_2$] (17)	1963 (s), 1951 (vs), 1700 (m)	1964 (vs), 1953 (vs), 1703 (m)
[Ir$_2$(H)$_2$(SPh)$_2$(CO)$_2$(dppm)$_2$] (18)	2152 (w, br),[d] 2044 (s), 1932 (vs)	2152 (w, br),[d] 2050 (vs), 1953 (vs)
[Ir$_2$(SePh)$_2$(CO)$_2$(μ-CO)(dppm)$_2$] (20)	1959 (vs), 1947 (vs), 1708 (s)	1954 (vs, br), 1709 (vs)
[Ir$_2$(H)$_2$(SePh)$_2$(CO)$_2$(dppm)$_2$] (21)		2162 (w, br),[d] 2049 (vs), 1987 (s)

[a] Abbreviations used: w = weak, m = medium, s = strong, vs = very strong, sh = shoulder, br = broad. [b] Nujol mull on KBr disk. Values are ν(CO) except when indicated otherwise. [c] CH_2Cl_2 solution in KCl cells. [d] ν(Ir-H).

Table 4.2. Nuclear Magnetic Resonance Spectroscopic Data[a] for the Compounds of Chapter 4.

compound	$\delta(^{31}P\{^1H\})$[b]	$\delta(^{13}C\{^1H\})$[c]	$\delta(^1H)$[c]
$[Ir_2(H)(\mu\text{-}SH)(CO)_2(dppm)_2]$ (5)	-16.5 (m), -27.1 (m)[d]	173.2 (s, br, 1 C), 164.8 (s, br, 1 C)[d]	-1.07 (s, br, 1 H), -13.03 (t, 1 H, $^2J_{P\text{-}H}$ = 9.8 Hz)[d]
$[RhIr(H)(\mu\text{-}SH)(CO)_2(dppm)_2]$ (7)	-5.04 (dm, $^2J_{Rh\text{-}P}$ = 103.8 Hz),[e] -19.49 (m)[f]	183.4 (dt, 1 C, $^1J_{Rh\text{-}C}$ = 55.7 Hz, $^2J_{P(Rh)\text{-}C}$ = 8.4 Hz), 167.2 (t, 1 C, $^2J_{P(Ir)\text{-}C}$ = 6.4 Hz)	8.07-6.91 (m, 40 H), 6.52 (m, 2 H), 4.21 (m, 2 H), -2.91 (t, 1 H, $^2J_{P(Rh)\text{-}H}$ = 6.4 Hz), -10.74 (t, 1 H, $^2J_{P(Ir)\text{-}H}$ = 12.8 Hz)
$[RhIr(H)(\mu\text{-}SeH)(CO)_2(dppm)_2]$ (8)	-11.04 (dm, $^2J_{Rh\text{-}P}$ = 103.5 Hz),[e] -23.41 (m)[f]	181.0 (dt, 1 C, $^1J_{Rh\text{-}C}$ = 57.3 Hz, $^2J_{P(Rh)\text{-}C}$ = 8.3 Hz), 165.5 (s, br, 1 C)	8.06-6.98 (m, 40 H), 6.71 (m, 2 H), 4.06 (m, 2 H), -4.90 (t, 1 H, $^2J_{P(Rh)\text{-}H}$ = 6.8 Hz), -11.80 (t, 1 H, $^2J_{P(Ir)\text{-}H}$ = 12.4 Hz)
$[Ir_2(SEt)_2(CO)_2(\mu\text{-}CO)(dppm)_2]$ (11)	-13.94 (s)	221.6 (m, 1 C), 176.4 (t, 2 C, $^2J_{P\text{-}C}$ = 7.0 Hz)	7.61-6.97 (m, 40 H), 6.08 (m, 2 H), 5.34 (m, 2 H), 0.21 (t, 6 H, $^3J_{H\text{-}H}$ = 7.2Hz), -0.49 (qrt, 4 H, $^3J_{H\text{-}H}$= 7.2 Hz)
$[Ir_2(H)_2(SEt)_2(CO)_2(dppm)_2]$ (12)	-6.1 (s)[g]	171.3 (m, br, 2 C)[g]	5.42 (m, 2 H), 4.20 (m, 2 H), -9.10 (qnt)[g]
$[Ir_2(H)_2(SEt)_2(CO)_2(dppm)_2]$ (13)	-8.4 (m), -12.8 (m)[g]	160.7 (br, 1 C), 159.9 (br, 1 C)[g]	5.66 (m, 2 H), 5.48 (m, 2 H), -9.37 (t, 1 H, $^2J_{P\text{-}H}$ = 14.4 Hz), -13.06 (t, 1 H, $^2J_{P\text{-}H}$ = 14.4 Hz)[g]

(continued)

Table 4.2. (continued)

[Ir$_2$(H)(SEt)(CO)$_2$(μ-CO)(dppm)$_2$] (14)	-1.7 (m), -11.1 (m)[h]	*i*	-10.20 (t, 1 H, $^2J_{P\text{-}H}$ = 14.0 Hz)[h]
[Ir$_2$(SEt)$_2$(CO)$_2$(μ-CO)(dppm)$_2$] (15)	-15.4 (m), -29.0 (m)[h]	*i*	*i*
[Ir$_2$(SPh)$_2$(CO)$_2$(μ-CO)(dppm)$_2$] (16)	-13.39 (m), -26.96 (m)	227.4 (m, 1 C), 182.3 (dt, 1 C, $^2J_{C\text{-}C}$ = 24.9 Hz, $^2J_{P\text{-}C}$ = 12.4 Hz), 177.3 (t, 1 C, $^2J_{P\text{-}C}$ = 19.3 Hz)	7.68-6.04 (m, 50 H), 4.76 (m, 2 H), 4.45 (m, 2 H)
[Ir$_2$(SPh)$_2$(CO)$_2$(μ-CO)(dppm)$_2$] (17)	-15.06 (s)	216.7 (m, 1 C), 177.3 (t, 2 C, $^2J_{P\text{-}C}$ = 6.8 Hz)	7.70-6.73 (m, 50 H), 5.86 (m, 2 H), 4.91 (m, 2 H)
[Ir$_2$(H)$_2$(SPh)$_2$(CO)$_2$(dppm)$_2$] (18)	-5.31 (s)	171.1 (t, 1 C, $^2J_{P\text{-}C}$ = 5.4 Hz)	7.62-6.76 (m, 50 H), 6.54 (br, 2 H), 4.10 (br, 2 H), -11.58 (qnt, 2 H)
[Ir$_2$(H)(SPh)(CO)$_2$(μ-CO)(dppm)$_2$] (19)	0.5 (m), -11.4 (m)[g]	232.7 (m, 1 C), 180.3 (t, 1C, $^2J_{P\text{-}C}$ = 11.5 Hz), 176.3(t, 1C, $^2J_{P\text{-}C}$ = 7.5 Hz)[g]	-9.98 (t, 1 H, $^2J_{P\text{-}H}$ = 10.0 Hz)[g]

(continued)

Table 4.2. (continued)

$[Ir_2(SePh)_2(CO)_2(\mu\text{-}CO)(dppm)_2]$ (20)	-17.68 (s)	215.7 (m, 1 C), 176.1 (t, 2 C, $^2J_{P\text{-}C} = 6.5$ Hz)	7.70-6.08 (m, 50 H), 6.03 (m, 2 H), 5.21 (m, 2 H)
$[Ir_2(H)_2(SePh)_2(CO)_2(dppm)_2]$ (21)	-6.77 (s)	171.5 (t, 1 C, $^2J_{P\text{-}C} = 5$ Hz)	7.82-6.72 (m, 50 H), 6.12 (m, 2 H), 4.29 (m, 2 H), -11.58 (qnt, 2 H)

[a] Abbreviations used: br = broad, s = singlet, d = doublet, t = triplet, qrt = quartet, qnt = quintet, m = multiplet. Data were obtained in CD_2Cl_2 solvent at 25 °C unless otherwise noted. [b]Vs. 85% H_3PO_4. [c]Vs. TMS.[d]At -60° in THF-d_8. [e]Rh-*P*. [f]Ir-*P*. [g]At -20° in CD_2Cl_2. [h]At -20° in THF-d_8. [i]Data not obtained for this unstable intermediate.

mixture under a CO atmosphere resulted in regeneration of the light yellow color. Addition of hexanes (20 mL) under CO completed precipitation of the light yellow product, which was dried under an N_2 stream, then briefly under vacuum, to give 79 mg (72% yield) of lemon-yellow powder. Anal. Calcd for $C_{57}H_{54}Ir_2O_3P_4S_2$: C, 50.36; H, 4.00. Found: C, 50.10; H, 4.38. (This compound has been found to be susceptible to decomposition via CO loss, more so in solution than in the solid state.)

(d) $[Ir_2(SPh)_2(CO)_2(\mu\text{-}CO)(dppm)_2]$ (16). Thiophenol (16.6 μL, 17.8 mg, 162 μmol) was added to a solution of **2** in THF (100 mg, 80.8 μmol in 5 mL), causing an immediate color change from orange to golden yellow. The reaction was stirred for a further 2 h, allowing formation of a yellow precipitate. Addition of hexanes (20 mL) completed precipitation, and the product was washed with hexanes then dried under a stream of N_2, resulting in isolation of 83 mg (71%) of golden-yellow powder. Anal. Calcd for $C_{65}H_{54}Ir_2O_3P_4S_2$: C, 53.64; H, 3.74. Found: C, 52.47; H, 4.18.[16]

(e) $[Ir_2(SePh)_2(CO)_2(\mu\text{-}CO)(dppm)_2]$ (20). A THF solution of diphenyl diselenide (25.2 mg, 80.8 μmol in 1 mL) was added to a solution of **2** (100 mg, 80.8 μmol) in THF (5 mL). The reaction mixture immediately changed from clear and orange to cloudy and lighter orange. The mixture was stirred for 1 h, after which precipitation of the product was completed via addition of ether (15 mL). Yield was 87 mg (69%) of light orange-yellow powder. Anal. Calcd for $C_{65}H_{54}Ir_2O_3P_4Se_2$: C, 50.39; H, 3.51. Found: C, 49.55; H, 3.81.[16]

Reaction of 1 with H_2S. Hydrogen sulfide was placed over a solution of **1** (150 mg, 142 μmol) in CH_2Cl_2 (15 mL), resulting in an immediate change in the solution color from red-orange to brown. The mixture was stirred for a further 2 h, then evaporated to 5 mL, and the product precipitated via addition of hexanes (20 mL). The brown solid isolated was shown by $^{31}P\{^1H\}$ and infrared spectroscopy to be the previously-characterized complex $[Rh_2(CO)_2(\mu\text{-}S)(dppm)_2]$.[17a]

Reaction of 2 with H_2S at Room Temperature. Hydrogen sulfide was placed over a solution of **2** (30 mg, 24.2 μmol) in THF-d_8 (0.6 mL) in an NMR tube, and the sample shaken vigorously. The solution immediately underwent a color change from orange to light yellow; $^{31}P\{^1H\}$, ^1H and $^1H\{^{31}P\}$ experiments showed the sample to contain a mixture of isomers of $[Ir_2(H)_2(CO)_2(\mu\text{-}S)(dppm)_2]$[17b,18] (as confirmed by comparison of these spectra with those obtained from a study of H_2 addition to $[Ir_2(CO)_2(\mu\text{-}S)(dppm)_2]$[18]), $[Ir_2(CO)_2(\mu\text{-}S)(dppm)_2]$[17b] and $[Ir_2(CO)_2(\mu\text{-}S)(\mu\text{-}CO)(dppm)_2]$.[17b]

X-ray Data Collection. Diffusion of ether into a concentrated CH_2Cl_2 solution containing a mixture of complexes **16** and **17** produced red-orange crystals of **17**, several of which were mounted and flame-sealed in glass capillaries under N_2 and solvent vapor to minimize decomposition and/or solvent loss. Data were collected on an Enraf-Nonius CAD4 diffractometer using Mo $K\alpha$ radiation. Unit-cell parameters were obtained from a least-squares refinement of the setting angles of 25 reflections in the range $20.0° \leq 2\theta \leq 24.0°$. The monoclinic diffraction symmetry and the systematic absences (hkl, $h + k \neq 2n$; $h0l$, $l \neq 2n$) were consistent with the space groups Cc or $C2/c$ (the latter was confirmed as the correct space group by the successful solution and refinement of the structure).

Intensity data were collected at 22 °C by using the $\theta/2\theta$ scan technique, covering reflections with indices of the form $+h$ $+k$ $\pm l$ to a maximum $2\theta = 50.0°$. Of the data collected 6718 reflections were unique after merging. Backgrounds were scanned for 25% of the peak width on either side of the peak scan. Three reflections were chosen as intensity standards, being remeasured after every 120 min of X-ray exposure time. The intensities of these standards remained approximately constant over the duration of data collection thus no decomposition correction was applied. The data were measured and processed in the usual way, with a value of 0.04 for p[19] employed to downweight intense reflections; 3319 reflections were considered observed ($F_o^2 \geq 3\sigma(F_o^2)$) and were used in subsequent calculations. Absorption corrections were applied to the data according to the method of Walker and Stuart.[20,21] See Table 4.3 for crystal data and more information on X-ray data collection.

Structure Solution and Refinement. The structure of compound **17** was solved in the space group $C2/c$ using standard Patterson and Fourier techniques. Full-matrix least-squares refinements proceeded so as to minimize the function $\Sigma w(|F_o| - |F_c|)^2$, where $w = 4F_o^2/\sigma^2(F_o^2)$. Atomic scattering factors and anomalous dispersion terms were taken from the usual tabulations.[22-24] Positional parameters for the hydrogens attached to the carbon atoms of the complex were calculated from the geometries about the attached carbon. These hydrogens were located 0.95 Å from their attached C atoms, given thermal parameters 20% greater than the equivalent isotropic B's of their associated carbons, and included as fixed contributions. Peaks due to the Cl atoms of the solvent molecule were found to be symmetrically disposed about the crystallographic twofold axis

Table 4.3. Crystallographic Data for $[Ir_2(SPh)_2(CO)_2(\mu\text{-}CO)(dppm)_2]\cdot{}^1/_2CH_2Cl_2$ (17)

formula	$C_{65.5}ClH_{55}Ir_2O_3P_4S_2$
formula weight	1498.06
crystal shape	irregular monoclinic prism
crystal dimensions, mm	0.41 × 0.31 × 0.22
space group	$C2/c$ (No. 15)
temperature, °C	22
radiation (λ, Å)	graphite-monochromated Mo Kα (0.71069)
unit cell parameters	
a, Å	19.532 (7)
b, Å	22.030 (6)
c, Å	14.333 (6)
β, deg	102.82 (4)
V, Å^3	6014 (7)
Z	4
ρ(calcd), g cm^{-3}	1.654
linear absorption coeff (μ), cm^{-1}	46.650
range of transmission factors	0.854–1.174
detector aperture, mm	(3.00 + tan θ) wide × 4.00 high
takeoff angle, deg	3.0
maximum 2θ, deg	50.0

(continued)

Table 4.3. (continued)

crystal-detector distance, mm	173
scan type	$\theta/2\theta$
scan rate, deg/min	between 1.18 and 6.67
scan width, deg	$0.60 + 0.347 \tan\theta$
total unique reflections	6718 ($h\ k \pm l$)
total observations (NO)	3319 ($F_o^2 \geq 3\sigma(F_o^2)$)
final no. parameters varied (NV)	349
error in obs. of unit wt. (GOF)[a]	1.643
R^b	0.040
R_w^c	0.053

[a] $\mathrm{GOF} = [\sum w(|F_o| - |F_c|)^2/(\mathrm{NO} - \mathrm{NV})]^{1/2}$ where $w = 4F_o^2/\sigma^2(F_o^2)$.

[b] $R = \sum ||F_o| - |F_c|| / \sum |F_o|$. [c] $R_w = [\sum w(|F_o| - |F_c|)^2 / \sum wF_o^2]^{1/2}$.

of symmetry $^1/_2, y, ^1/_4$, and were found to have electron density roughly half of that expected (being comparable to the typical value for a carbon atom). This suggested one-half molecule of dichloromethane per complex molecule, thus Cl was input at half occupancy, and refined satisfactorily. The central carbon atom of the CH_2Cl_2 molecule was located on the twofold axis at a distance and angle appropriate for a Cl-C-Cl unit, as found through use of difference-Fourier electron density maps; however, this carbon atom did not refine well, so was included as a fixed contribution. For this reason the solvent molecule's hydrogen atoms were not included. There was no evidence for secondary extinction therefore no extinction correction was applied.

The final model for complex **17**, with 349 parameters varied, converged to values of $R = 0.040$ and $R_w = 0.053$. In the final difference Fourier map the 10 highest residuals (1.6-0.9 e/Å^3) were found in the area of the solvent molecule and the thiophenolate group (a typical carbon in an earlier synthesis had an electron density of 3.5 e/Å^3). The positional and thermal parameters for the non-hydrogen atoms of complex **17** are given in Table 4.4, and selected bond lengths and angles are given in Tables 4.5 and 4.6, respectively.

Results and Discussion

(a) Description of Structure. The structure of complex **17** is shown in Figure 4.1; the molecule possesses a twofold axis of symmetry passing through the center of the metal-metal bond and the atoms C(2) and O(2). The metal nuclei are bridged by the dppm ligands and a carbonyl group,

Table 4.4. Positional and Thermal Parameters of the Atoms of $[\mathrm{Ir_2(SPh)_2(CO)_2(\mu\text{-}CO)(dppm)_2}]\cdot{}^1/_2\mathrm{CH_2Cl_2}$ (17)[a]

Atom	*x*	*y*	*z*	*B*, Å^2
Ir	0.06143(2)	0.20069(2)	0.32402(3)	2.642(7)
Cl	0.4817(7)	-0.0186(7)	0.160(1)	14.8(4)[b]
S	0.0756(1)	0.0889(1)	0.3345(2)	3.66(7)
P(1)	-0.0017(1)	0.1875(1)	0.4435(2)	3.09(6)
P(2)	-0.1322(1)	0.1972(1)	0.2874(2)	3.01(6)
O(1)	0.1726(4)	0.2694(4)	0.4635(6)	5.8(2)
O(2)	0.000	0.3212(4)	0.250	4.0(3)
C(1)	0.1318(5)	0.2415(5)	0.4110(7)	3.6(3)
C(2)	0.000	0.2680(6)	0.250	2.6(3)
C(3)	-0.0893(5)	0.1562(5)	0.3936(7)	3.4(2)
C(11)	0.0391(6)	0.1379(5)	0.5407(8)	4.0(3)
C(12)	0.0971(7)	0.1576(6)	0.6057(9)	5.7(3)
C(13)	0.1286(7)	0.1263(6)	0.6836(9)	6.5(4)
C(14)	0.1027(7)	0.0699(7)	0.6976(8)	6.6(4)
C(15)	0.0439(7)	0.0452(6)	0.6338(9)	6.0(3)
C(16)	0.0127(6)	0.0802(6)	0.5536(8)	4.9(3)
C(21)	-0.0200(5)	0.2530(5)	0.5120(8)	3.7(3)
C(22)	-0.0489(6)	0.2444(6)	0.5917(8)	5.1(3)
C(23)	-0.0670(7)	0.2910(7)	0.6415(9)	6.5(4)
C(24)	-0.0564(7)	0.3483(7)	0.6174(9)	7.3(4)
C(25)	-0.0290(7)	0.3594(6)	0.541(1)	6.3(4)
C(26)	-0.0090(6)	0.3101(5)	0.4850(8)	4.1(3)
C(31)	-0.2160(5)	0.1581(5)	0.2485(7)	3.5(2)
C(32)	-0.2725(6)	0.1893(5)	0.2013(9)	4.4(3)
C(33)	-0.3369(6)	0.1604(6)	0.1669(9)	5.2(3)
C(34)	-0.3420(6)	0.0994(7)	0.1815(9)	6.1(3)
C(35)	-0.2849(7)	0.0660(6)	0.230(1)	6.9(4)
C(36)	-0.2208(6)	0.0951(6)	0.2638(9)	5.3(3)

(continued)

Table 4.4. (continued)

C(41)	-0.1599(5)	0.2684(5)	0.3272(7)	3.2(2)
C(42)	-0.1531(6)	0.3204(5)	0.2779(8)	3.9(3)
C(43)	-0.1775(6)	0.3768(6)	0.3051(9)	5.3(3)
C(44)	-0.2063(6)	0.3805(6)	0.3838(9)	5.9(3)
C(45)	-0.2131(7)	0.3291(7)	0.4335(9)	6.6(4)
C(46)	-0.1899(6)	0.2710(6)	0.4054(9)	5.1(3)
C(51)	0.1523(8)	0.0645(7)	0.427(1)	7.1(4)
C(52)	0.1643(8)	0.0013(6)	0.463(1)	8.3(4)
C(53)	0.2076(7)	-0.0185(5)	0.5125(9)	5.9(3)
C(54)	0.2710(9)	0.0216(7)	0.555(1)	10.7(5)
C(55)	0.2685(8)	0.0776(7)	0.5364(9)	7.4(4)
C(56)	0.2102(8)	0.0998(8)	0.472(1)	8.5(5)
C(101)	0.500	-0.052	0.250	14.0[c]

[a] Numbers in parentheses are estimated standard deviations in the least significant digits in this and all subsequent tables. Thermal parameters for the anisotropically refined atoms are given in the form of the equivalent isotropic Gaussian displacement parameter defined as $^4/_3\left[a^2\beta_{11} + b^2\beta_{22} + c^2\beta_{33} + ac(\cos\beta)\beta_{13}\right]$. [b] Refined isotropically. [c] Fixed contribution; not refined.

Table 4.5. Selected Distances (Å) in $[Ir_2(SPh)_2(CO)_2(\mu\text{-}CO)(dppm)_2]\cdot{}^1/{}_2CH_2Cl_2$ **(17)**

(a) Bonded

Ir-Ir′	2.8286(6)	P(1)-C(11)	1.810(9)
Ir-S	2.480(2)	P(1)-C(21)	1.825(9)
Ir-P(1)	2.339(2)	P(2)-C(3)	1.809(9)
Ir-P(2)	2.333(2)	P(2)-C(31)	1.825(9)
Ir-C(1)	1.868(9)	P(2)-C(41)	1.792(9)
Ir-C(2)	2.049(9)	O(1)-C(1)	1.15(1)
S-C(51)	1.84(1)	O(2)-C(2)	1.17(1)
P(1)-C(3)	1.837(8)		

(b) Non-bonded

P(1)···P(2)	3.003(3)	S···S′	3.378(4)

Primed atoms are related to unprimed ones via the crystallographic 2-fold axis passing through C(2)O(2) and the center of the Ir-Ir′ bond.

Table 4.6. Selected Angles (deg) in $[Ir_2(SPh)_2(CO)_2(\mu\text{-}CO)(dppm)_2]\cdot{}^1/_2CH_2Cl_2$ (17)

(a) Bond angles

Ir′-Ir-S	96.32(5)	Ir-P(1)-C(3)	111.0(3)
Ir′-Ir-P(1)	92.97(6)	Ir-P(1)-C(11)	115.1(3)
Ir′-Ir-P(2′)	91.12(5)	Ir-P(1)-C(21)	119.5(3)
Ir′-Ir-C(1)	151.2(3)	C(3)-P(1)-C(11)	106.6(4)
Ir′-Ir-C(2)	46.3(2)	C(3)-P(1)-C(21)	103.3(4)
S-Ir-P(1)	84.35(8)	C(11)-P(1)-C(21)	99.7(4)
S-Ir-P(2′)	86.24(8)	Ir′-P(2)-C(3)	111.1(3)
S-Ir-C(1)	112.5(3)	Ir′-P(2)-C(31)	115.7(3)
S-Ir-C(2)	142.6(2)	Ir′-P(2)-C(41)	117.2(3)
P(1)-Ir-P(2′)	170.10(8)	C(3)-P(2)-C(31)	103.7(4)
P(1)-Ir-C(1)	90.0(3)	C(3)-P(2)-C(41)	106.6(4)
P(1)-Ir-C(2)	97.22(6)	C(31)-P(2)-C(41)	101.3(4)
P(2′)-Ir-C(1)	90.7(3)	Ir-C(1)-O(1)	176.2(9)
P(2′)-Ir-C(2)	92.12(6)	Ir-C(2)-Ir′	87.4(5)
C(1)-Ir-C(2)	104.9(4)	Ir-C(2)-O(2)	136.3(2)
Ir-S-C(51)	113.3(4)	P(1)-C(3)-P(2)	110.9(5)

(b) Torsion angles

S-Ir-Ir′-S′	3.59(9)	P(1)-Ir-Ir′-P(2)	5.3(1)

Primed atoms are related to unprimed ones via the crystallographic 2-fold axis passing through C(2)O(2) and the center of the Ir-Ir′ bond.

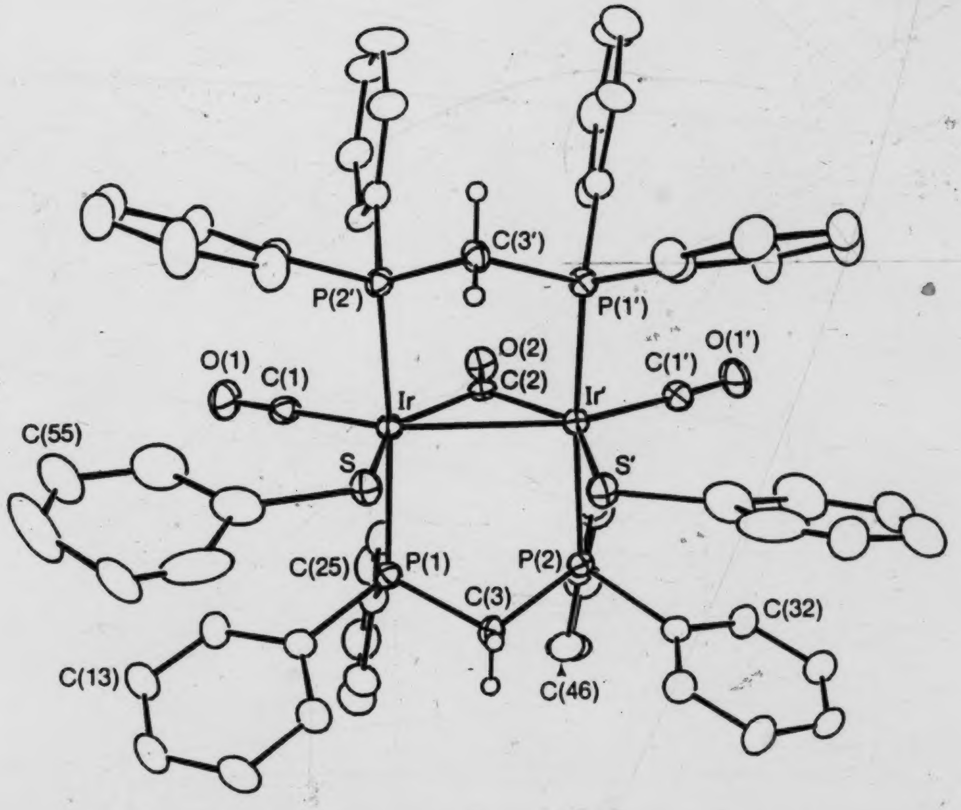
C(3')
P(2')
P(1')
O(1)
C(1)
O(2)
C(2)
C(1')
O(1')
Ir
Ir'
C(55)
S
S'
C(25)
P(1)
P(2)
C(3)
C(32)
C(13)
C(46)

Figure 4.1. Perspective view of $[Ir_2(SPh)_2(CO)_2(\mu\text{-}CO)(dppm)_2]$ (17) showing the numbering scheme. Thermal parameters are shown at the 20% level except for hydrogens, which are shown artificially small for the dppm methylene groups but are not shown for the phenyl groups. Primed atoms are related to unprimed atoms by the crystallographic 2-fold axis passing through C(2)O(2) and the center of the Ir-Ir′ bond.

and one carbonyl and one thiophenolate ligand are coordinated terminally to each metal. As is typical of most other binuclear dppm-bridged systems, the diphosphine groups are oriented trans to each other about the iridium centers (P(1)-Ir-P(2′) = 170.10(8)°), and are both cis to the other atoms coordinated to Ir. The coordination geometry about Ir can be described as distorted trigonal bipyramidal (neglecting the Ir-Ir′ bond), with P(1) and P(2′) occupying axial sites and S, C(1) and C(2) in equatorial positions. Distortions from this model arise from the presence of the metal-metal bond, the bridging nature of the carbonyl group C(2)O(2), and the mutual repulsion between the sulfur atoms S and S′. The latter feature appears to be exerting the largest effect, and is reflected in the large S···S′ distance (3.378(4) Å), which, although less than the sum of the van der Waals radii of these atoms (3.60 Å),[28] is substantially larger than the intraligand P(1)···P(2) separation (3.003(3) Å). This interaction results in an expanded S-Ir-C(2) angle (142.6(2)°); the compressed C(1)-Ir-C(2) angle (104.9(4)°) appears to be due to greater repulsion between the thiophenolate group and the terminal carbonyl C(1)O(1) (S-Ir-C(1) = 112.5(3)°) than between the terminal and bridging CO ligands. The geometry about the bridging carbonyl group is comparable in Ir-C(2) distance (2.049(9) Å) and Ir-C(2)-Ir′ angle (87.4(5)°) to that of other dppm-bridged diiridium compounds containing the same unit.[17b,25-27] Despite the interactions between the sulfur atoms, no significant twisting of the complex about the Ir-Ir′ bond occurs, as seen from the small S-Ir-Ir′-S′ and P(1)-Ir-Ir′-P(2) torsion angles (3.59(9)° and 5.3(1)°, respectively).

This complex is very similar, in appearance and parameters, to the syn isomer of $[Ir_2Cl_2(CO)_2(\mu\text{-}CO)(dppm)_2]$[27] (which cocrystallized with the major [anti] isomer in 1:3 ratio), in which the SPh units of **17** have been replaced by Cl ligands. One interesting difference is the shortness of the Ir-S bond (2.480(2) Å) with respect to the Ir-Cl bonds (2.504 Å [average]) in the former species, despite the fact that sulfur has a larger covalent radius than chlorine.[28a] The same trend has also been noted by Cotton and coworkers in their determinations of the structures of $[Ir(\mu\text{-}Cl)(COD)]_2$[29] and $[Ir(\mu\text{-}SPh)(COD)]_2$,[11] and has been ascribed to the higher degree of π-overlap in Ir-S bonds compared to Ir-Cl bonds; another contributor might be the more favorable interaction between the soft-acid Ir center and the soft-base PhS ligand than between Ir and the harder base Cl.[28b] The difference between the Ir-S and Ir-Cl bond lengths was found to be three times as great for the $[Ir(\mu\text{-}X)(COD)]_2$ dimers as for the $[Ir_2X_2(CO)_2(\mu\text{-}CO)(dppm)_2]$ systems, which would be consistent with the relative electron deficiency of the 16-electron iridium centers of the former vs. the 18-electron nuclei in the dppm-containing complexes. The iridium-sulfur distance in **17** is within the rather broad range observed for other sulfur-containing iridium complexes (2.33-2.53 Å);[7,8b,11,30,31] however, a more meaningful comparison may be made to the range of distances between iridium and sulfur atoms not bridging metal centers (2.41-2.51 Å).[7a,8b,31]

Other parameters in this compound appear normal. The Ir-Ir′ distance (2.8286(6) Å) is well within the range observed in similar systems containing an Ir-Ir bond (2.77-2.89 Å).[17b,25-27,32,33,36] This distance is significantly longer than that observed in the dichloro analogue (2.779(1) Å),[27] possibly reflecting the greater steric requirements of the SPh vs. Cl ligands in forcing the metal centers apart; however it is still less than the intraligand P(1)···P(2) separation (vide supra). The Ir-P distances (2.339(2) Å, 2.333(2) Å) are also typical for these systems.

(b) Description of Chemistry. When hydrogen sulfide is passed through a THF solution of $[Rh_2(CO)_3(dppm)_2]$ (**1**) at room temperature, the previously-synthesized $[Rh_2(CO)_2(\mu\text{-}S)(dppm)_2]$[17a] is the only product observed. Oxidative addition of both S-H bonds of H_2S to **1** has apparently taken place, with concomitant loss of CO and H_2 to give the final species. A similar transformation, the reaction of $[Pd_2Cl_2(dppm)_2]$ with H_2S to yield $[Pd_2Cl_2(\mu\text{-}S)(dppm)_2]$ and H_2, has been thoroughly investigated by James and coworkers.[4] Both of these systems are important in illustrating how adjacent metal centers can work in concert to activate two H-X bonds belonging to the same substrate, and it is of interest to obtain information pertaining to the involvement of each metal in the overall process. Monitoring the reaction of **1** with H_2S by using variable-temperature $^{31}P\{^1H\}$ NMR spectroscopy has failed to uncover evidence of other reactive intermediates; as the mixture is warmed in 10° increments from -80 °C to room temperature, signals due to **1** decrease in intensity while those due to $[Rh_2(CO)_2(\mu\text{-}S)(dppm)_2]$ increase, with conversion being complete by the time the temperature reaches -50 °C. The lack of observable intermediates is not totally surprising, as previous studies of attempted addition of H_2 to $[Rh_2(CO)_2(\mu\text{-}S)(dppm)_2]$ revealed no new hydridic species;[17a] furthermore, dppm-bridged dirhodium complexes containing hydride ligands are found to be fewer in number and generally less stable[13a,37] than similar diiridium species.[14,15a,17b,18,25,32a,33,35,36] Owing to our failure to observe intermediates in the reaction between H_2S and **1**, we turned to the analogous diiridium system in attempts to obtain models for possible intermediates in the "double oxidative addition" of H_2S and the subsequent reductive elimination of H_2.

The complex $[Ir_2(CO)_3(dppm)_2]$ (**2**) reacts with hydrogen sulfide in an analogous fashion, but the course of the reaction can be followed spectroscopically and several intermediates can be identified before formation of the ultimate product, the previously-synthesized sulfide-bridged A-frame complex $[Ir_2(CO)_2(\mu\text{-}S)(dppm)_2]$.[17b] When H_2S is bubbled through a THF solution of **2** at room temperature, several species may be identified in the $^{31}P\{^1H\}$ and ^1H NMR spectra of the mixture, including the sulfide-bridged dicarbonyl dihydride adducts **4a-c** shown in Scheme 4.1. Identification of species **4a-c** was facilitated by comparison of the spectra obtained in this study with those obtained during an earlier investigation of H_2 addition to $[Ir_2(CO)_2(\mu\text{-}S)(dppm)_2]$.[18] Intermediate **4a** can be seen to be the result of the oxidative addition of two S-H bonds to complex **2**, one to each metal, with concomitant loss of CO, while structures **4b** and **4c** are the products of a series of hydride migrations about the bimetallic core, a process for which the mechanism, shown in Scheme 4.2, has been elsewhere described.[35] The complexes $[Ir_2(CO)_2(\mu\text{-}S)(dppm)_2]$ and $[Ir_2(CO)_2(\mu\text{-}S)(\mu\text{-}CO)(dppm)_2]$ are also present in minor amounts, the former evolving via H_2 elimination from **4c**, with the latter the result of CO uptake by the sulfide A-frame complex (the CO being present in solution as a byproduct of the initial reaction of **2** with H_2S to produce **5**). If this THF solution is refluxed for 2 h under a slow N_2 stream, or if it is allowed to stir under N_2 at room temperature for

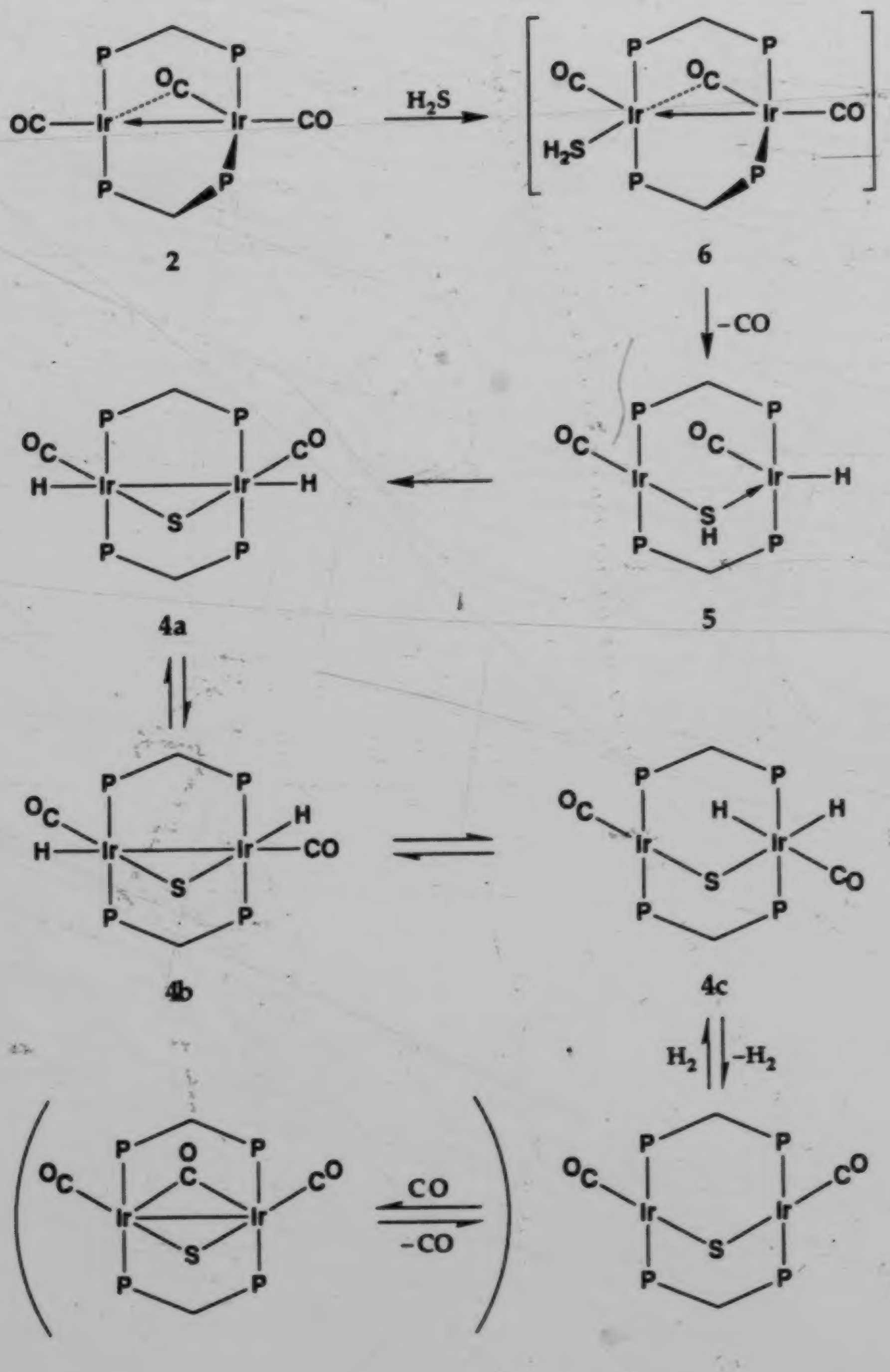
2
H2S
6
-CO
5
4a
4b
4c
H2
-H2
CO
-CO

Scheme 4.1.

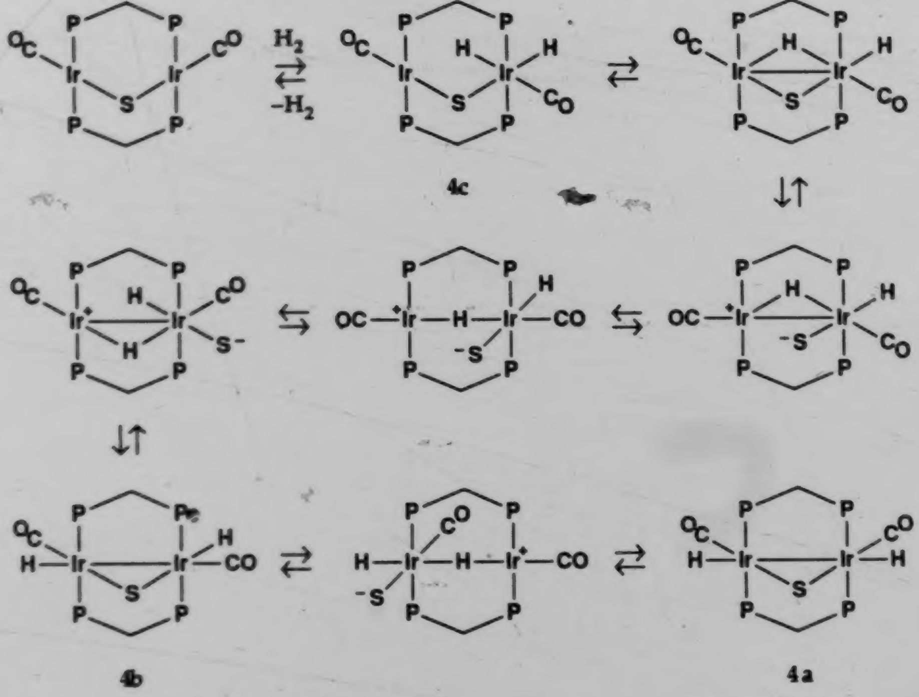

Scheme 4.2. (adapted from reference 34)

two days, conversion of all species to $[Ir_2(CO)_2(\mu\text{-}S)(dppm)_2]$ results. As mentioned earlier, the reductive elimination of H_2 is reversible, as addition of H_2 to $[Ir_2(CO)_2(\mu\text{-}S)(dppm)_2]$ has been shown to regenerate the dihydride complexes **4a-c**.[18]

Monitoring the reaction of **2** with H_2S using variable-temperature multinuclear NMR spectroscopy provides insight into the initial steps of activation of the S-H bonds, and an intermediate that has been formulated as $[Ir_2(H)(CO)_2(\mu\text{-}SH)(dppm)_2]$ (**5**) may be observed and characterized. When H_2S is bubbled through a solution of **2** in THF-d_8 at -60 °C, **5** is seen in the $^{31}P\{^1H\}$ NMR spectrum as the major species; the pseudotriplet resonances at δ -16.5 and -27.1 indicate that **5** possesses two different sets of chemical environments for the phosphorus nuclei, indicative of an asymmetric structure. The highfield region of the ^{1}H NMR spectrum shows two signals, a broad singlet at δ -1.07 and a triplet at δ -13.03 ($^2J_{P\text{-}H}$ = 9.8 Hz). In the spectra obtained using selective heteronuclear ^{1}H{^{31}P} decoupling, the latter resonance collapses to a singlet only upon irradiation of the lower-field phosphorus resonance, confirming it to be a terminally-bound iridium hydride. Although the δ -1.07 resonance is unaffected when either of the phosphorus resonances is irradiated, implying no discernible coupling to either set of phosphorus nuclei, it is likely due to a sulfhydryl group bridging the two metals. Resonances similar in appearance and chemical shift to this one have been observed in the ^{1}H NMR spectra of the series of complexes $[Ir_2(H)_2(\mu\text{-}SH)(\mu\text{-}SR)(\mu\text{-}H)(PPh_3)_4]^{n+}$ (R = H, Pr^i: n =1; R = vacant: n = 0),[7b] which have been shown by X-ray crystallography to contain bridging SH units. The ^{13}C{^{1}H} NMR spectrum at -60° of a sample of **5** prepared in the same manner as above (except using ^{13}CO-enriched compound **2**) shows, in addition to less-intense signals due to **2** and the hydridic products **4a-c**, two resonances of equal intensity (broadened singlets at δ 173.2 and 164.8) attributable to this intermediate. Comparison of these low-temperature spectra with those obtained after the sample has been warmed to room temperature shows that all of the signals due to intermediate **5** disappear, being replaced by those due to the same species produced when the reaction is performed under ambient conditions.

On the basis of the spectra and products observed, the reaction of $[Ir_2(CO)_3(dppm)_2]$ (**2**) with H_2S to give $[Ir_2(CO)_2(\mu\text{-}S)(dppm)_2]$, H_2 and CO may be proposed to proceed as shown in Scheme 4.1. Intermediate **6**, unlike the other species illustrated, was not characterized in this study; however, the structural formulation shown is supported by related investigations of the oxidative additions of H_2S and thiols to the isoelectronic heterobimetallic complex $[RhRe(CO)_4(dppm)_2]$,[34] with the initial adduct observed at low-temperature assigned the structure shown below. An

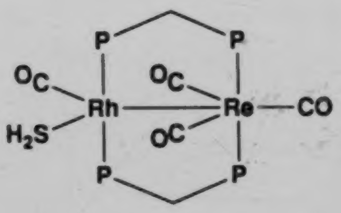

analogous intermediate is likely involved in the present case, as the vacant coordination site on one of the metals of $[Ir_2(CO)_3(dppm)_2]$ (see Chapter 2) would be susceptible to uptake of a σ-donor H_2S ligand as a prelude to oxidative addition of the first S-H bond. It does not appear likely that this reaction takes place via acid/base dissociation of hydrogen sulfide, i.e. involving initial protonation of the tricarbonyl **1** or **2** followed by reaction of the so-formed protonated complex with SH^- to give the dihydride species. Hydrogen sulfide is a weak acid in aqueous solution (first dissociation constant = 9.1×10^{-8}) and would be expected to be even weaker in THF. Furthermore, although the reaction of $[Ir_2(CO)_2(\mu\text{-H})(\mu\text{-CO})(dppm)_2][BF_4]$[14] with NaSH at room temperature does proceed to give a mixture of $[Ir_2(H)_2(CO)_2(\mu\text{-S})(dppm)_2]$ isomers and $[Ir_2(CO)_2(\mu\text{-S})(dppm)_2]$, the reaction time required is 24 h, which is clearly inconsistent with the rapid rate observed for the reaction of **2** with H_2S.

It was believed that further insight into the reactivity of hydrogen sulfide towards compounds **1** and **2** would be gained by studies of the reaction of H_2S with the heterobimetallic [RhIr(CO)$_3$(dppm)$_2$] (**3**). Unlike the transformation observed for the homobimetallic tricarbonyls, this reaction does not ultimately yield the sulfide-bridged, hydride-free dicarbonyl derivative; instead, the only product observed is [RhIr(H)-(μ-SH)(CO)$_2$(dppm)$_2$] (**7**). The infrared and $^{13}C\{^1H\}$ NMR spectra of this complex indicate that two terminal CO groups are present. The highfield region of the ^1H NMR spectrum shows two triplet resonances, at δ -2.91 ($^2J_{P\text{-}H}$ = 6.4 Hz) and -10.74 ($^2J_{P\text{-}H}$ = 12.8 Hz). Decoupling of the iridium-bound phosphorus nuclei causes the latter signal to collapse to a singlet, leaving the other unaffected; decoupling of the rhodium-bound phosphorus nuclei causes the lower-field triplet to collapse to a singlet without altering the appearance of the higher-field triplet. Thus the latter signal is consistent with a hydride ligand that is terminally bound to iridium, whereas the former resonance appears to be due to a sulfhydryl ligand interacting with the rhodium center. The question of whether this SH unit is terminally coordinated to Rh or bridging the metal centers arises; despite the lack of observable coupling between the sulfhydryl and the iridium-bound phosphorus atoms, we believe the latter mode of coordination to be present. Although the magnitude of the $^2J_{P(Rh)\text{-}H}$ coupling and the chemical shift of the sulfhydryl resonance are reminiscent of those observed for other complexes containing terminal SH groups, a structure such as VII below, containing a hydride bound to iridium and sulfhydride coordinated solely to rhodium, would give both metals 16-electron configurations; in related studies involving other

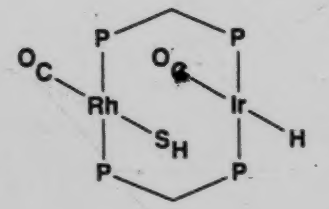

VII

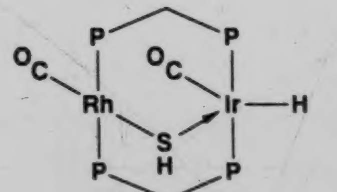

7

heterobimetallic RhIr complexes[33,35,38,39] it has been found that, whenever possible, the rhodium and iridium centers respectively adopt 16- and 18-electron configurations. In this case the bridging S-H group would compensate for the loss of a donor electron pair upon removal of CO from iridium. A selenium-containing analogue of 7, [RhIr(H)(μ-SeH)$(CO)_2$-$(dppm)_2$] (8), has been prepared in much the same manner, and is found to possess spectroscopic parameters very similar to those for the sulfur-containing species (see Table 4.2).

As noted above, complex 7 does not undergo any further hydride rearrangements and does not reductively eliminate H_2. The fact that only one S-H bond of H_2S is activated by **3** is in distinct contrast not only to the reactions of hydrogen sulfide with the homobimetallic Rh_2 and Ir_2 analogues, **1** and **2**, but also to H_2S addition to the abovementioned [RhRe$(CO)_4$$(dppm)_2$], in which the hydrido sulfhydryl intermediate [RhRe$(CO)_4$(SH)(μ-H)$(dppm)_2$] underwent facile H_2 loss to yield [RhRe-$(CO)_4$(μ-S)$(dppm)_2$].[34] It is of interest to note that although [RhIr$(CO)_2$(μ-S)-$(dppm)_2$] (theoretically the result of dehydrogenation of 7), does react reversibly with H_2 to form [RhIr$(H)_2$$(CO)_2$($\mu$-S)$(dppm)_2$],[35] this product does not undergo a hydride migration process as observed for its diiridium analogue; instead, both hydrides remain attached to iridium and oriented cis to each other. For the homobimetallic complex, the mechanism proposed for rearrangement of the hydride ligands involves a swinging of the sulfido group in and out of the bridging position on and off of each metal, as well as formation of isomeric forms containing terminal hydrides on both metals and alternation of each metal center between 16- and 18-electron configurations.[35] These transformations appear to be disfavored for compound 7, as previous studies[15,35] of heterobimetallic RhIr complexes have demonstrated a tendency for rhodium and iridium to retain their respective 16- and 18-electron configurations and for iridium to more readily accept purely terminal hydride ligands.

Hydrogen selenide was also found to react with complexes 1 and 2. The addition of H_2Se to $[Rh_2(CO)_3(dppm)_2]$ (1) yields several products, but their characterization via NMR techniques is difficult due to the broadened and overlapping nature of the resonances. The previously-described selenide A-frame, $[Rh_2(CO)_2(\mu\text{-Se})(dppm)_2]$,[17a] was not obtained, even after refluxing the mixture, purging it with N_2, or leaving it under N_2 for several days. Such a product might have been expected based on the ease of formation of $[Rh_2(CO)_2(\mu\text{-S})(dppm)_2]$ from 1 and H_2S.

Similar to its behavior towards H_2S, treatment of $[Ir_2(CO)_3(dppm)_2]$ (2) with H_2Se yields several species in the initial reaction mixture that can be identified and characterized using $^{31}P\{^1H\}$, ^1H and $^1H\{^{31}P\}$ NMR spectroscopy. The spectroscopic results, and tentative structures (with the bridging diphosphine ligands omitted for clarity) for the species giving rise to the resonances listed, are shown in Table 4.7. Complexes 9a-e and 10 are

Table 4.7. NMR Spectroscopic Parameters for the Species Observed in the Reaction of $[Ir_2(CO)_3(dppm)_2]$ (**2**) with H_2Se

		$\delta(^{31}P\{^1H\})$	$\delta(^1H)$
9a	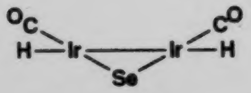 OC H—Ir Ir—H CO Se	-7.33 (s)	-9.86 (pseudoquintet)
9b	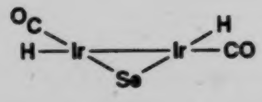 OC H—Ir Ir—CO H Se	-8.62 (m), -14.35 (m)	-9.79 (t, $^2J_{P\text{-}H}$ = 12.0 Hz), -12.70 (t, $^2J_{P\text{-}H}$ = 13.8 Hz)
9c	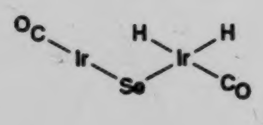 OC Ir H Ir H Se CO	-7.06 (s)	-11.04 (pseudoquintet)
9d	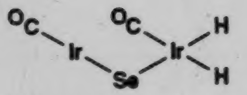 OC Ir OC Ir H H Se	-4.81 (m), -12.04 (m)	-9.48 (dt, $^2J_{P\text{-}H}$ =13.8 Hz, $^2J_{H\text{-}H}$ = 5.6 Hz), -12.03 (dt, $^2J_{P\text{-}H}$ = 18.0 Hz, $^2J_{H\text{-}H}$ = 5.6 Hz)
9e	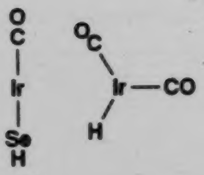 OC Ir Se H OC Ir—CO H	-12.58 (m), -21.83 (m)	-5.34 (t, $^2J_{P\text{-}H}$ = 5.5 Hz), -11.22 (t, $^2J_{P\text{-}H}$ = 13.4 Hz)
9f	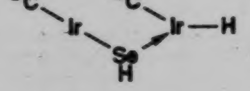 OC Ir OC Ir—H Se H	-17.45 (m), -28.65 (m)	-3.61 (br), -12.59 (t, $^2J_{P\text{-}H}$ = 11.2 Hz)
10	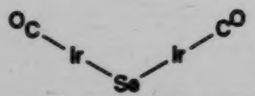 OC Ir Ir CO Se	-6.83 (s)	

The bridging dppm groups above and below the equatorial plane have been omitted for clarity.

observed when the reaction is carried out at room temperature, while complex **9f**, like **5** above, is observed only at temperatures below -30 °C. Species **9a**, **9b**, **9c** and **9f** are assigned structures similar to complexes **4a**, **4b**, **4c** and **5**, respectively, based upon the similarities in chemical shifts and appearances of their phosphorus and proton resonances to those seen in the reaction of H_2S with **2**. The magnitude of the H-H coupling (5.6 Hz) between the hydride ligands of species **9d** is consistent with their being located cis to each other on the same metal. Confirmation was provided upon heteronuclear decoupling of the phosphorus signal at δ -4.81, which caused both hydride resonances to collapse to doublets, while irradiation at the frequency of the phosphorus signal at δ -12.04 did not affect the appearance of these hydride peaks. The chemical shifts of the highfield ^1H resonances belonging to species **9e** suggest that a terminal hydride and a terminal selenohydryl group are present; their behavior upon selective heteronuclear decoupling of each phosphorus resonance suggests that these ligands are coordinated to different iridium centers. Species **10** was found by $^1H\{^{31}P\}$ experiments to possess no associated hydridic signals. Although it was difficult to assign resonances in the $^{13}C\{^1H\}$ NMR spectrum of the reaction mixture to individual species (due to the large number of peaks observed), no peaks characteristic of bridging CO ligands were observed; this result, coupled with the symmetrical nature of **10** as established by its singlet $^{31}P\{^1H\}$ resonance, suggests the formulation for **10** to be the dicarbonyl A-frame, $[Ir_2(CO)_2(\mu\text{-}Se)(dppm)_2]$, rather than $[Ir_2(CO)_2(\mu\text{-}Se)(\mu\text{-}CO)(dppm)_2]$. Despite formation of a small amount of the nonhydridic species, **10**, H_2 loss from the other intermediates is not particularly facile; with heating, or over longer periods of time, decomposition of the above species occurs.

As can be seen above, the reactions of **1** and **2** with both S-H bonds of H_2S (and of **2** with the Se-H bonds of H_2Se) are quite facile under ambient conditions. Although intermediate **5** could be assigned the structure indicated with a fair degree of confidence, the isolation of complexes modelling this first-bond addition product that would be stable at room temperature was still a goal. The instability of **5** is presumably due to the availability of the second S-H bond for oxidative addition to the second low-valent metal center; thus thiols and selenols, possessing only one S(e)-H bond, were considered to be well suited for the preparation of stable first-bond-addition analogues.

The reaction of compound **2** with ethanethiol under an atmosphere of N_2 yields $[Ir_2(SEt)_2(CO)_2(\mu\text{-}CO)(dppm)_2]$ (**11**, below), the net result of

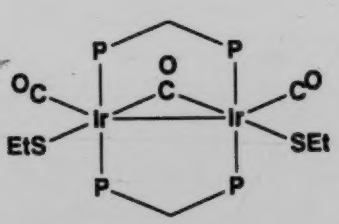

11

addition of two equivalents of thiol followed by loss of H_2. One bridging and two terminal carbonyl groups are indicated by the infrared and $^{13}C\{^1H\}$ NMR spectra of **11**, in distinct contrast to the dicarbonyl products formed in the reactions of **2** with H_2S, H_2Se and H_2SiRR' (R = R' = Me, Et, Ph; R = H, R' = Ph; see Chapter 3).[33] The ^1H NMR spectrum of **11** shows no resonances due to hydride ligands, indicating that, in contrast to the reaction of 2 with H_2S, H_2 loss from any hydridic intermediates formed as precursors to 11 is quite facile. Unlike the results for the reactions of $[RhRe(CO)_4(dppm)_2]$ with thiols, where products of the form $[RhRe(CO)_3(\mu\text{-}H)(\mu\text{-}SR)(dppm)_2]$ (R = Et, Ph) have been characterized,[34] adducts formed by addition of only one equivalent of EtSH to 2 cannot be isolated at room temperature. Complex 11 is the only product observed at ambient temperature even if conditions of high dilution of reaction mixture or slow addition of thiol are employed. However, such 1:1 adducts may be characterized at lower temperatures using NMR spectroscopy (vide infra).

Compound 11 is susceptible to decomposition, presumably via CO loss. Therefore, solutions of this complex under N_2 turn from yellow to deep red-orange within a few hours, with concomitant loss of intensity of the infrared band due to the bridging carbonyl group of 11. Although a deep red solid can be isolated from such solutions, the $^{31}P\{^1H\}$ NMR spectrum of this material is inconclusive, showing only broad unresolved resonances and implying a mixture of products. Attempts to obtain species containing hydride and ethanethiolate ligands that are stable under ambient conditions were equally unsuccessful, as mixtures of products are again observed when the reaction between 2 and EtSH is performed under a hydrogen atmosphere, or if a solution of 11 is stirred under H_2.

The reaction of ethanethiol with 2 has also been studied using variable-temperature multinuclear NMR spectroscopy; the intermediates observed and the likely course of the reaction are summarized in Scheme 4.3. Starting at -80 °C, the $^{31}P\{^1H\}$ spectrum of a mixture of 2 and EtSH in

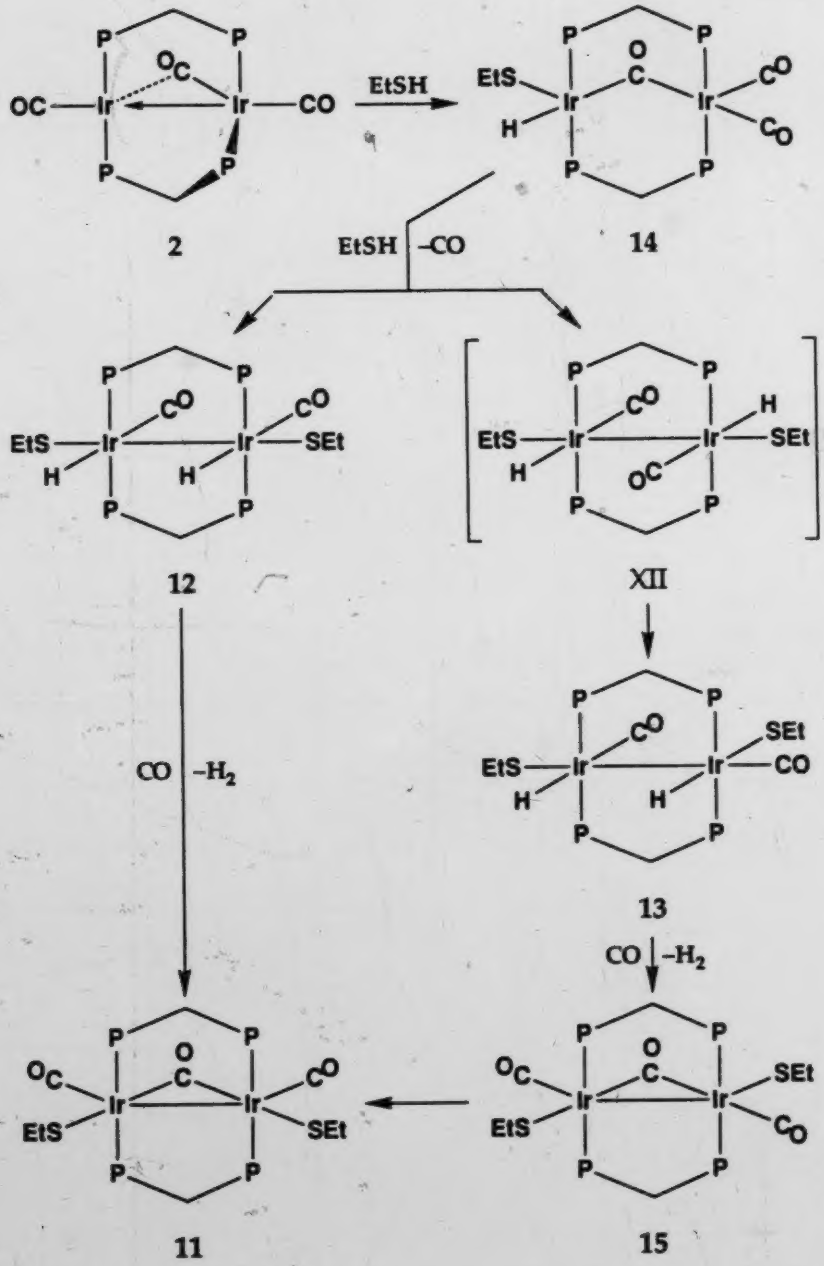
EtSH
EtSH
-CO
CO
-H$_2$
CO
-H$_2$
2
14
12
XII
13
11
15
P
Ir
OC
CO
EtS
SEt
H

Scheme 4.3.

CD_2Cl_2 does not show signals for species other than **2** until the solution temperature has been raised to -20 °C. At this point, besides signals due to **2**, $[Ir_2(CO)_4(dppm)_2]$ (formed by CO uptake by **2**) and a small amount of **11**, phosphorus resonances at δ -6.1 (singlet) and δ -8.4, -12.8 (multiplets) due to one symmetric (**12**) and one asymmetric species (**13**), respectively, are observed. The $^{13}C\{^1H\}$ and ^1H NMR spectroscopic data (see Table 4.2) indicate that both **12** and **13** are dicarbonyl dihydride species. The presence of two resonances, at δ 5.42 and 4.20, for the dppm methylene protons of **12** rules out a formulation such as structure XII, in which both sides of the Ir_2P_4 plane are equivalent (although, as noted later, such a species cannot be ruled out as a short-lived intermediate). It is also less likely that the hydride ligands of **12** are disposed along the Ir-Ir bond, since the elimination of H_2 from such a structure would be much more difficult; furthermore, this orientation would cause greater steric interactions between the ethanethiolate groups than is seen between the thiophenolate residues of the structurally-characterized complex **17** (vide supra). Species **12** is believed to possess a structure similar to those assigned to complexes **18** and **22** (vide infra), despite its instability at elevated temperatures relative to the thiophenolate- and benzeneselenolate-containing analogues.

Selective heteronuclear $^{13}C\{^{31}P\}$ and $^1H\{^{31}P\}$ decoupling experiments for species **13** establish that one hydride and one carbonyl ligand are attached to each of the iridium centers of this intermediate. The structure proposed for **13** is similar to that for $[Ir_2(H)_2Cl_2(CO)_2(dppm)_2]$,[36] and differs from that for **12** in that the ethanethiolate and carbonyl groups on one iridium have been transposed. Formation of such a structure, containing an EtS group trans to a hydride, may not be entirely straightforward, and may involve the intermediacy of a species such as XII. Rearrangement of XII to **13** may occur via a tunnelling of a hydride ligand through the Ir-Ir bond, from one side of the Ir_2P_4 plane to the other, as has been previously proposed in related species.[15,18,34,35,38d,40]

Species **12** and **13** are also observed by $^{31}P\{^1H\}$ NMR spectroscopy when the reaction of **2** with EtSH is carried out at low temperature in THF-d_8; in addition, intermediates **14** and **15** are also seen in this solvent. Selective heteronuclear $^1H\{^{31}P\}$ decoupling experiments show that species **14** also gives rise to one highfield resonance at δ -10.20 (triplet, $^2J_{P\text{-}H}$ = 14.0 Hz), corresponding to a terminal hydride attached to iridium. Although $^{13}C\{^1H\}$ NMR data for this reaction mixture were not acquired, **14** is assigned the structure shown based on the similarities between its $^{31}P\{^1H\}$ and ^1H spectroscopic parameters and those for the analogous thiophenolate-containing species, **19**, for which $^{13}C\{^1H\}$ and $^{13}C\{^{31}P\}$ data have been obtained (vide infra). The nonhydridic intermediate **15** shows $^{31}P\{^1H\}$ spectroscopic parameters similar to the more fully characterized thiophenolate analogue, **16**, thus is believed to possess a similar structure. When the reaction mixture is warmed to room temperature, signals due to all of these intermediates disappear, being replaced by those due to the final product, **11**.

It is notable that although both the starting material, **2**, and the final product, **11**, are tricarbonyl complexes, intermediates **12** and **13** possess only two CO groups each, implying that, like the addition of the second S-H bond of H_2S to **2**, the reaction of **14** with another equivalent of EtSH is accompanied by CO loss. It is likely that the CO evolved in this step, which would then be present in solution either uncoordinated or bound to the labile [$Ir_2(CO)_4(dppm)_2$], is readily scavenged by the products of H_2 loss from **12** and **13**, leading to formation of **11** and **15**. The isomerization of the asymmetric **15** to the symmetrical **11** may occur via reversible CO loss and recoordination, which is consistent with the tendency of **11** to decompose via loss of CO (vide supra).

Under ambient conditions, thiophenol also reacts with complex **2** in 2:1 ratio yielding a species that contains three carbonyl groups and two thiolate residues. Like those of **11**, the infrared spectra of **16** are consistent with a structure containing one bridging and two terminal carbonyl groups, and no resonances are seen in the highfield region ($\delta < 0$) of the ^1H NMR spectrum, showing that net H_2 loss has taken place. Unlike species **11**, the $^{31}P\{^1H\}$ spectrum of **16**, with multiplet resonances at δ -13.39 and -26.96, shows the presence of two inequivalent phosphorus environments, indicating that this complex possesses an asymmetric structure. The $^{13}C\{^1H\}$ NMR spectrum shows resonances due to three inequivalent carbonyl ligands, one bridging (δ 227.4 [multiplet]) and two terminal (δ 182.3 [doublet of triplets, $^2J_{C\text{-}C}$ = 24.9 Hz, $^2J_{P\text{-}C}$ = 12.4 Hz] and 177.3 [triplet, $^2J_{P\text{-}C}$ = 19.3 Hz]). Selective $^{13}C\{^{31}P\}$ heteronuclear decoupling experiments show that the terminal CO groups are bound to different iridium centers. Broadband $^{13}C\{^{31}P\}$ heteronuclear decoupling shows a $^2J_{C\text{-}C}$ coupling of 24.9 Hz between the higher-field terminal carbonyl and the bridging CO, which is comparable to values previously observed for similar systems containing carbonyl groups oriented trans across a metal center.[38] On the basis of the spectroscopic data the two structures shown below are possible.

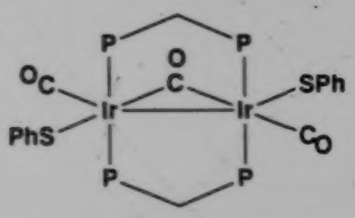

16

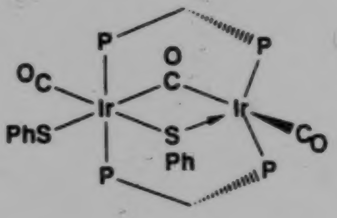

XVI

Complex **16** is also obtained as the immediate and sole product of the reaction of **2** with diphenyl disulfide, which, based on a concerted oxidative-addition mechanism, would appear to favor formulation XVI (containing one bridging and one terminal thiophenolate group and a mixed-valence Ir(III)-Ir(I) metal core). However, it is suggested that the formulation shown for **16** is actually correct. The infrared spectra of similar dppm-bridged compounds show that carbonyls that bridge metals in the absence of a metal-metal bond possess significantly lower stretching frequencies than those in the presence of such a bond. Besides being an isomeric form of the structurally-characterized compound **17** (vide supra), complex **16** is reminiscent of the *anti* isomer of $[Ir_2Cl_2(CO)_2(\mu\text{-}CO)(dppm)_2]$,[27] and shows a similar bridging CO stretching frequency (1720 cm^{-1} vs. 1728 cm^{-1} for the dichloro analogue). In addition, transannular oxidative addition of trifluoromethyl disulfide to $[Rh_2(CNMe)_4(dppm)_2]^{2+}$ has been noted by Balch and coworkers,[10] so the structure proposed for **16**, in which the thiolate groups are *not* mutually cis, is not unprecedented.

If compound **16** is allowed to stir in CH_2Cl_2 solution for several hours, a new symmetrical product, $[Ir_2(SPh)_2(CO)_2(\mu\text{-}CO)(dppm)_2]$ (**17**), can

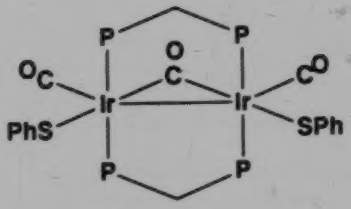

17

be observed spectroscopically. The IR spectrum shows new bands at 1963, 1951 and 1700 cm^{-1}, indicative of retention of the three carbonyl ligands. The $^{31}P\{^1H\}$ NMR spectrum shows a singlet resonance at δ -15.06, while in the $^{13}C\{^1H\}$ NMR spectrum two signals are observed (δ 216.7 (multiplet), 177.9 (triplet, $^2J_{P\text{-}C}$ = 6.8 Hz)) in 1:2 ratio, respectively. The ^1H NMR spectrum shows the expected distribution of phenyl and methylene protons, with no highfield resonances present. The isomerization process is not quantitative; equilibrium mixtures are usually formed in which **16** is present in significant quantities (~40% of total concentration). From such mixtures have been isolated single crystals of complex **17**, enabling the characterization of the compound by X-ray crystallography (vide supra). The structure established in the solid state is consistent with the spectroscopic properties of this species in solution and is in agreement with the formulation for the ethanethiolate-containing analogue, **11**.

Reaction of hydrogen with **16** or **17** leads to loss of CO and uptake of one equivalent of H_2 to form $[Ir_2(H)_2(SPh)_2(CO)_2(dppm)_2]$ (**18**). Loss of the bridging carbonyl ligand is indicated by the infrared spectrum (ν(CO): 2044, 1932 cm^{-1}), specifically by the disappearance of bands near 1700 cm^{-1}. The highfield region of the ^1H NMR spectrum shows an apparent quintet resonance at δ -11.58 corresponding to two hydrides. Although the appearance of this resonance suggests that complex **18** contains hydrides that are bridging the metal centers, this species is believed to have the structure shown below, in which terminal Ir-H groups are present. The five-line

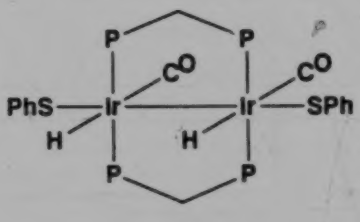

18

multiplet could be produced by the second-order coupling effects inherent in an AA'XX'X''X''' spin system, or by rapid exchange of these hydrides between the metal centers, producing a time-averaged A_2X_4 spin system. The latter view is supported by the broadening of the resonance that occurs as the temperature is lowered, possibly due to slowing of the exchange process. However, a totally decoalesced spectrum could not be observed, even at -80 °C. Complex **18** appears to be a thiophenolate-containing analogue of species **12**, the symmetrical dihydridic intermediate in the reaction of **2** with EtSH, but differs from **12** in being stable at room temperature and unreactive towards CO.

The reaction of thiophenol with **2** in CD_2Cl_2 was also monitored using variable-temperature NMR spectroscopy. At -20 °C an asymmetric species, **19**, is observed at δ 0.5, -11.4 in the $^{31}P\{^1H\}$ spectrum of the reaction mixture; associated with this species is a highfield triplet in the ^1H spectrum at δ -9.98 ($^2J_{P\text{-}H}$ = 10.0 Hz). The $^{13}C\{^1H\}$ spectrum shows one bridging and two terminal carbonyl groups to be associated with **19**, and selective heteronuclear $^{13}C\{^{31}P\}$ decoupling experiments indicate that both terminal carbonyls are coordinated to the same metal center. Intermediate **19** is assigned a structure directly analogous to that of species **14**, the monohydridic intermediate observed in the reaction of ethanethiol with **2**. The presence of a bridging carbonyl group in the structure of **19** is in contrast to the case for [RhRe(H)(SR)(CO)$_4$(dppm)$_2$] (shown above; R = H, Et, Ph), the postulated initial result of oxidative addition of RSH to [RhRe(CO)$_4$(dppm)$_2$], in which all carbonyls appear to remain terminal.[34] A small amount of the dicarbonyl dihydride, **18**, is also observed under these conditions, but, unlike the reaction between ethanethiol and **2**, it is likely present as a byproduct, not an intermediate, since no conversion of **18** to either of the tricarbonyls, **16** or **17**, is observed when a solution of the dihydride is stirred under CO. Furthermore, when a dilute solution of **2** in THF is stirred under a rapid stream of N$_2$ and a THF solution containing one equivalent of thiophenol is slowly added, infrared spectroscopy shows that the only product is **16**. These results taken together suggest that complex **18** is stable in the presence of excess CO, and is not the observed product under conditions that would minimize the amount of free

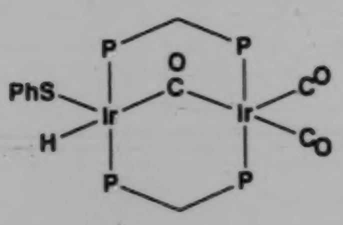

19

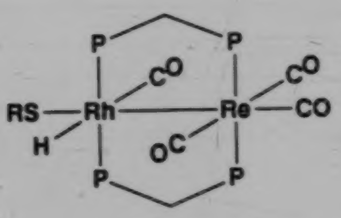

(dissociated) CO present in solution. A bis(thiophenolate) analogue of species **13** is not observed in the course of this reaction, but, given the preference for the formation of the asymmetric **16** over the symmetrical **17**, it is likely that such an intermediate is involved. When the sample is warmed to room temperature, the monohydridic intermediate disappears, with the major species produced being **16** and **17**. Roughly the same amount of **18** as was earlier observed remains in the final mixture.

The reaction of compound **2** with benzeneselenol also follows a 2:1 stoichiometry. Spectroscopic evidence, particularly the infrared and $^{13}C\{^1H\}$ NMR data, suggests that the major product, $[Ir_2(SePh)_2(CO)_2(\mu\text{-}CO)(dppm)_2]$ (**20**), has the same structure as the structurally-characterized species **17**,

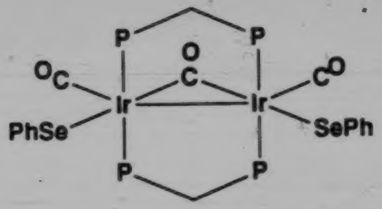

20

with selenium atoms taking the place of sulfurs. This symmetrical complex has been more directly prepared via the reaction of diphenyl diselenide with **2**, a result in marked contrast to the reaction of **2** with $(PhS)_2$, where the product is the asymmetric species, **16**.

Complex **20** is not the sole product of the reaction between benzeneselenol and **2**, as a dihydridic product of formula $[Ir_2(H)_2(SePh)_2(CO)_2(dppm)_2]$ (**21**) is also observed. The $^{31}P\{^1H\}$ NMR spectrum of this dihydride shows a singlet resonance at δ -6.77, while in the ^1H spectrum is seen a multiplet at δ -11.58 characteristic of an AA′XX′X″X‴ spin system, of intensity appropriate to two hydride ligands (compared with the signals for the dppm methylene protons). The ^{1}H, $^{31}P\{^{1}H\}$ and $^{13}C\{^{1}H\}$ NMR spectroscopic parameters for this compound are quite similar to those observed for species **18**, and suggest that complex **21** is also a dicarbonyl dihydride. Rapid exchange between the metal centers may also be implicated, as broadening of the hydride resonance occurs as the temperature is lowered, possibly due to slowing of the exchange process; again, as for **18**, a totally decoalesced spectrum could not be observed, even at -80 °C. Species **21** can also be formed when a solution of **20** is allowed to react with H_2, but attempts to prepare this material in pure form were unsuccessful, as complex **21** is prone to decomposition over time at room temperature.

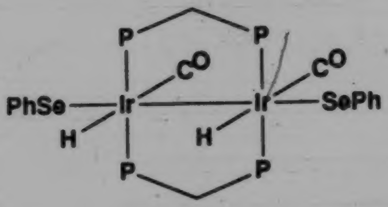

21

Conclusions

The reactivity of $[Ir_2(CO)_3(dppm)_2]$ towards substrates containing sulfur-hydrogen and selenium-hydrogen bonds is characterized by the marked preference of this complex to react with two S-H or Se-H bonds. For the reactions with H_2S and H_2Se this is not surprising, since, as was the case for primary and secondary silanes (see Chapter 3) the close proximity and low oxidation states of the metals favors the facile stepwise "double activation" process. Another common thread between the H_2S and H_2SiRR' reactions with the $[M_2(CO)_3(dppm)_2]$ complexes is that the hydridic adducts formed are more stable for M = Ir than for M = Rh, again pointing up the effects of the greater strength of Ir-H vs. Rh-H bonds. A difference is that no sulfur-bridged dirhodium hydride species can be observed; however, given the wealth of sulfur- and selenium-bridged hydridic diiridium species seen, the rapid elimination of H_2 from the Rh_2 system can be explained via a series of rearrangement steps. These appear to depend on the ability of the sulfur atom to swing in and out of its bridging position, which may explain the reluctance of the H_2S and H_2Se adducts of $[RhIr(CO)_3(dppm)_2]$ to eliminate H_2. The reactivity of $[Ir_2(CO)_3$-$(dppm)_2]$ towards thiols and selenols is consistent with the tendency demonstrated in the reactions with H_2S and H_2Se towards reaction with two S-H or Se-H bonds. This is somewhat of a departure from the behavior of $[RhRe(CO)_4(dppm)_2]$, which also contains a dative metal-metal interaction; the rhodium-rhenium tetracarbonyl was found to react with only one equivalent of thiol, and only the Rh center appeared to be involved in the oxidative-addition process. The results observed in this study may be due to the greater electron-richness of the d^8-d^{10} Ir(I)-Ir(-I) system compared to a d^8-d^8 Rh(I)-Re(-I) core, and the greater ease of CO loss (to generate coordinative unsaturation) from an Ir(-I) than from an Re(-I) center. These characteristics make the diiridium species receptive to a *two* oxidative additions, one at each Ir center.

References and Footnotes

1. (a) Bonzel, H. P.; Ku, R. *J. Chem. Phys.* **1973**, *58*, 4617. (b) Bartholemew, C. H.; Agrawal, P. K.; Katzer, J. R. *Adv. Catal.* **1982**, *31*, 135. (c) Billy, J.; Abon, M. *Surf. Sci.* **1984**, *146*, L525. (d)Trenary, M.; Uram, K. J.; Yates, J. T., Jr. *Surf. Sci.* **1985**, *157*, 512. (e) Wong, P. C.; Zhou, M. Y.; Hui, K. C. Mitchell, K. A. R. *Surf. Sci.* **1985**, *163*, 172. (f) Protopopoff, E.; Marcus, P. *Surf. Sci.* **1986**, *169*, L237. (g) Koestner, R. J.; Salmeron, M.; Kollin, E. B.; Gland, J. L. *Surf. Sci.* **1986**, *172*, 668.
2. (a) Angelici, R. J. *Acc. Chem. Res.* **1988**, *21*, 387. (b) Friend, C. M.; Roberts, J. T. *Acc. Chem. Res.* **1988**, *21*, 394.
3. (a) Bianchini, C.; Mealli, C.; Meli, A.; Sabat, M *Inorg. Chem.* **1986**, *25*, 4617. (b) Bottomley, F.; Drummond, D. F.; Egharevba, G. O.; White, P. S. *Organometallics* **1986**, *5*, 1620.
4. (a) Lee, C.-L.; Besenyei, G.; James, B. R.; Nelson, D. A.; Lilga, M. A. *J. Chem. Soc., Chem. Commun.* **1985**, 1175. (b) Besenyei, G.; Lee, C.-L.; Gulinski, J.; Rettig, S. J.; James, B. R. *Inorg Chem.* **1987**, *26*, 3622. (c) Barnabas, A. F.; Sallin, D.; James, B. R. *Can. J. Chem.* **1989**, *67*, 2009.
5. (a) Kalck, P.; Poilblanc, R.; Martin, R. P.; Rovera, A.; Gaset, A. *J. Organomet. Chem.* **1980**, *195*, C9. (b) Kalck, P.; Frances, J. M.; Pfister, P. M.; Southern, T. G.; Thorez, A. *J. Chem. Soc., Chem. Commun.* **1983**, 510. (c) Kalck, P. *Polyhedron* **1988**, *7*, 2441. (d) Bayón, J. C.; Esteban, P.; Real, J.; Claver, C.; Ruiz, A. *J. Chem. Soc., Dalton Trans.* **1989**, 1579. (e) Bayón, J. C.; Real, J.; Claver, C.; Polo, A.; Ruiz, A. *J. Chem. Soc., Chem. Commun.* **1990**, 1056. (f) Rakowski DuBois, M.

Chem. Rev. **1989**, *89*, 1.

6. (a) Escaffre, P.; Thorez, A.; Kalck, P.; Besson, B.; Perron, R.; Colleuille, Y. *J. Organomet. Chem.* **1986**, *302*, C17. (b) Kalck, P.; Senocq, F.; Siani, M.; Thorez, A. *J. Organomet. Chem.* **1988**, *350*, 77. (c) Bianchini, C.; Meli, A.; Laschi, F.; Vacca, A.; Zanello, P. *J. Am. Chem. Soc.* **1988**, *110*, 3913. (d) Shaver, A. L.; Uhm, H. L.; Singleton, E.; Liles, D. C. *Inorg. Chem.* **1989**, *28*, 847. (e) Wei, G.; Liu, H.; Huang, Z.; Kang, B *J. Chem. Soc., Chem. Commun.* **1989**, 1839. (f) Carlton, L.; Bulbulia, Z. *J. Organomet. Chem.* **1990**, *389*, 139.

7. (a) Mueting, A. M.; Boyle, P. D.; Pignolet, L. H. *Inorg. Chem.* **1984**, 23, 44. (b) Mueting, A. M.; Boyle, P. D.; Wagner, R.; Pignolet, L. H. *Inorg. Chem.* **1988**, *27*, 271.

8. (a) Kuehn, C. G.; Taube, H. *J. Am. Chem. Soc.* **1976**, *98*, 689. (b) Milstein, D.; Calabrese, J. C.; Williams, I. D. *J. Am. Chem. Soc.* **1986**, *108*, 6387. (c) Liaw, W.-F.; Kim, C.; Darensbourg, M. Y.; Rheingold, A. L. *J. Am. Chem. Soc.* **1989**, *111*, 3591. (d) Boyd, S. E.; Field, L. D.; Hambley, T. W.; Young, D. J. *Inorg. Chem.* **1990**, *29*, 1496. (e) Darensbourg, M. Y.; Longridge, E. M.; Payne, V.; Reibenspies, J.; Riordan, C. G.; Springs, J. J.; Calabrese, J. C. *Inorg. Chem.* **1990**, *29*, 2721.

9. (a) Cooke, J.; Green, M.; Stone, F. G. A. *J. Chem. Soc. A* **1968**, 170. (b) Singer, H.; Wilkinson, G. *J. Chem. Soc. A* **1968**, 2516. (c) Bolton, E. S.; Havlin, R.; Knox, G. R. *J. Organomet. Chem.* **1969**, *18*, 153. (d) Senoff, C. V. *Can. J. Chem.* **1970**, *48*, 2444. (e) Kemmit, R. D. W.; Rimmer, D. *J. Inorg. Nucl. Chem.* **1973**, *35*, 3155. (f) Gaines, T.; Roundhill, D. M. *Inorg. Chem.* **1974**, *13*, 2521. (g) Collman, J. P.; Rothrock, R. K.; Stark,

R. A. *Inorg. Chem.* **1977**, *16*, 437.

10. Balch, A. L.; Labadie, J. W.; Delker, G. *Inorg. Chem.* **1979**, *18*, 1224.

11. Cotton, F. A.; Lahuerta, P.; Latorre, J.; Sanaú, M.; Solana, I.; Schwotzer, W. *Inorg. Chem.* **1988**, *27*, 2131.

12. (a) Jennings, M. C.; Payne, N. C.; Puddephatt, R. J. *Inorg Chem.* **1987**, *26*, 3776. (b) Jennings, M. C.; Puddephatt, R. J. *Inorg Chem.* **1988**, *27*, 4280. (c) Hadj-Bagheri, N.; Puddephatt, R. J.; Manojlović-Muir, L.; Stefanović, A. *J. Chem. Soc., Dalton Trans.* **1990**, 535.

13. (a) Kubiak, C. P.; Woodcock, C. P.; Eisenberg, R. *Inorg. Chem.* **1982**, *21*, 2119. (b) Woodcock, C.; Eisenberg, R. *Inorg. Chem.* **1985**, *24*, 1285.

14. Sutherland, B. R.; Cowie, M. *Organometallics* **1985**, *4*, 1637.

15. (a) See Chapter 2 of this thesis. (b) McDonald, R; Cowie, M. *Inorg. Chem.* **1990**, *29*, 1564.

16. The purity of several of the solid compounds obtained could not be confirmed by elemental analysis; although hydrogen percentages were satisfactory, carbon results were consistently ~1% below the calculated values. Nevertheless the compounds were spectroscopically pure, as found by NMR and IR spectroscopy.

17. (a) Kubiak, C. P.; Eisenberg, R. *Inorg. Chem.* **1980**, *19*, 2726. (b) Kubiak, C. P.; Woodcock, C.; Eisenberg, R. *Inorg. Chem.* **1980**, *19*, 2733.

18. (a) Vaartstra, B. A.; O'Brien, K. N.; Eisenberg, R.; Cowie, M. *Inorg. Chem.* **1988**, *27*, 3668. (b) Vaartstra, B. A. Ph.D. Thesis, University of Alberta, 1989, Chapter 5.

19. Doedens, R. J.; Ibers, J. A. *Inorg. Chem.* **1967**, *6*, 204.

20. Walker, N., Stuart, D. *Acta Crystallogr., Sect. A: Found. Crystallogr.* **1983,** *A39,* 1581.

21. Programs used were those of the Enraf-Nonius Structure Determination Package by B. A. Frenz, in addition to local programs by R. G. Ball.

22. Cromer, D. T.; Waber, J. T. *International Tables for Crystallography;* Kynoch Press: Birmingham, England, 1974; Vol. IV, Table 2.2A.

23. Stewart, R. F.; Davidson, E. R.; Simpson, W. T. *J. Chem. Phys.* **1965,** *42,* 3175.

24. Cromer, D. T.; Liberman, D. *J. Chem. Phys.* **1970,** *53,* 1891.

25. Sutherland, B. R.; Cowie, M. *Can. J. Chem.* **1986,** *64,* 464.

26. Vaartstra, B. A.; Cowie, M. *Organometallics* **1989,** *8,* 2388.

27. Sutherland, B. R.; Cowie, M. *Inorg. Chem.* **1984,** 23, 2324.

28. Huheey, J. E. *Inorganic Chemistry,* 3rd ed.; Harper and Row: New York, 1983. (a) pp. 258-259 and references therein. (b) pp. 312-315 and references therein.

29. Cotton, F. A.; Lahuerta, P.; Sanaú, M.; Schwotzer, W. *Inorg. Chim. Acta* **1986,** *120,* 153.

30. (a) Bonnet, J.-J.; Thorez, A.; Maisonnat, A.; Galy, J.; Poilblanc, R. *J. Am. Chem. Soc.* **1979,** *101,* 5940. (b) Devillers, J.; Bonnet, J.-J.; de Montauzon, D.; Galy, J.; Poilblanc, R. *Inorg. Chem.* **1980,** *19,* 154. (c) Kalck, P.; Bonnet, J.-J. *Organometallics* **1982,** *1,* 1211. (d) Devillers, J.; de Montauzon, D.; Poilblanc, R. *Nouv. J. Chim.* **1983,** *7,* 545. (e) El Amane, M.; Maisonnat, A.; Dahan, F.; Pince, R.; Poilblanc, R. *Organometallics* **1985,** *4,* 773. (f) Sielisch, T.; Cowie, M.

Organometallics **1988**, *7*, 707. (g) Balch, A. L.; Waggoner, K. M.; Olmstead, M. M. *Inorg. Chem.* **1988**, *27*, 4511. (h) Blake, A. J.; Gould, R. O.; Holder, A. J.; Hyde, T. I.; Reid, G.; Schröder, M. *J. Chem. Soc., Dalton Trans.* **1990**, 1759.

31. (a) Kalck, P.; Bonnet, J.-J.; Poilblanc, R. *J. Am. Chem. Soc.* **1982**, *104*, 3069. (b) Stephan, D. W. *Inorg. Chem.* **1984**, *23*, 2207. (c) Del Zotto, A.; Mezzetti, A.; Dolcetti, G.; Rigo, P.; Pahor, N. B. *J. Chem. Soc., Dalton Trans.* **1989**, 607.
32. (a) Mague, J. T.; Klein, C. L.; Majeste, R. J.; Stevens, E. D. *Organometallics* **1984**, *3*, 1860. (b) Sutherland, B. R.; Cowie, M. *Organometallics* **1984**, *3*, 1869. (c) Wu, J.; Reinking, M. K.; Fanwick, P. E.; Kubiak, C. P. *Inorg. Chem.* **1987**, *26*, 247. (d) McDonald, R.; Sutherland, B. R.; Cowie, M. *Inorg. Chem.* **1987**, *26*, 3333. (e) Wu, J.; Fanwick, P. E.; Kubiak, C. P. *Organometallics* **1987**, *6*, 1805.
33. (a) See Chapter 3 of this thesis. (b) McDonald, R.; Cowie, M. *Organometallics* **1990**, *9*, 2468.
34. Antonelli, D. M.; Cowie, M. *Inorg. Chem.* **1990**, *29*, 3339.
35. Vaartstra, B. A.; Cowie, M. *Inorg. Chem.* **1989**, *28*, 3138.
36. Sutherland, B. R.; Cowie, M. *Organometallics* **1985**, *4*, 1801.
37. (a) Kubiak, C. P.; Eisenberg, R. *J. Am. Chem. Soc.* **1980**, *102*, 3637. (b) Kubiak, C. P.; Woodcock, C.; Eisenberg, R. *Inorg. Chem.* **1982**, *21*, 2119. (c) Sutherland, B. R.; Cowie, M. *Inorg. Chem.* **1984**, *23*, 1290. (d) Woodcock, C.; Eisenberg, R. *Inorg. Chem.* **1984**, *23*, 4207. (e) Wang, W.-D.; Hommeltoft, S. I.; Eisenberg, R. *Organometallics* **1988**, *7*, 2417. (f) Wang, W.-D.; Eisenberg, R. *J. Am. Chem. Soc.* **1990**, *112*, 1833.

38. (a) Mague, J. T.; Sanger, A. R. *Inorg. Chem.* **1979,** *18,* 2060. (b) Mague, J. T.; DeVries, S. H. *Inorg. Chem.* **1980,** *19,* 3743. (c) Mague, J. T. *Organometallics* **1986,** *5,* 918. (d) Antonelli, D. M.; Cowie, M. *Inorg. Chem.* **1990,** *29,* 4039. (e) Jenkins, J. A. Ph.D. Thesis, University of Alberta, 1991, Chapter 6.

39. Vaartstra, B. A.; Xiao, J.; Jenkins, J. A.; Verhagen, R.; Cowie, M. *Organometallics,* in press.

40. (a) Puddephatt, R. J.; Azam, K. A.; Hill, R. H.; Brown, M. P.; Nelson, C. D.; Moulding, R. P.; Seddon, K. R.; Grossel, M. C. *J. Am. Chem. Soc.* **1983,** *105,* 5642. (b) Antonelli, D. M.; Cowie, M. *Organometallics* **1990,** *9,* 1818.

Chapter 5

Interconversion Between Isomeric Alkyne-Bridged Diiridium Complexes and the Structure of $[Ir_2(CO)_2(\mu\text{-}\eta^2:\eta^{2'}\text{-DMAD})(dppm)_2]\cdot 2CH_2Cl_2$

Introduction

The ability of homogeneous and heterogeneous transition metal catalysts to facilitate the functionalization, hydrogenation, oligomerization, or polymerization of unsaturated organic substrates has provoked much interest in complexes containing coordinated alkynes.[1] Such complexes can not only serve to support proposed intermediates in catalytic cycles, but are also of great importance in deriving bonding models for the interactions between metals and small molecules containing multiple bonds.[2] The bonding of alkyne ligands to single metal centers has been explained in terms of the Dewar-Chatt-Duncanson model,[3] in which the RCCR unit is viewed as a two-electron donor to the metal, with the limiting forms, as shown below, being an η^2-coordinated alkyne or a metallacyclopropene ring. These modes of coordination are also possible for alkynes as ligands in binuclear systems, but the additional possibility of

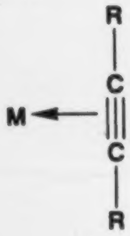

η^2-alkyne

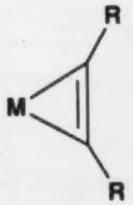

metallacyclopropene

interaction with both metal centers allows the alkyne to orient itself parallel to the metal-metal axis (μ-η^1:$\eta^{1'}$-coordination, the RCCR unit now being referred to as a cis-dimetallated olefin), or perpendicular (μ-η^2:$\eta^{2'}$-coordination). As was pointed out in the landmark review by Hoffmann

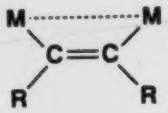

μ-η^1:$\eta^{1'}$

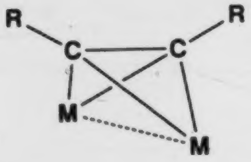

μ-η^2:$\eta^{2'}$

and coworkers[4] the preference for one mode of orientation or the other is a function of the electronic requirements of the metal centers. The parallel-bound alkyne can be considered to be a dianionic four-electron donor, while in the perpendicular disposition it is viewed as functioning as a neutral four-electron donor to the complex.

Reactions of alkynes with diphosphine-bridged homobinuclear complexes of rhodium and iridium have been of long-standing and continuing interest to this research group;[5-12] more recently, heterobimetallic (RhIr,[11] RhOs,[13] RhRe[14]) systems have been investigated. Much of this work has been directed towards the preparation and characterization of stable complexes modelling presumed intermediates involved in the activation and further functionalization of the alkyne substrates. Structure determinations of alkyne-containing complexes have aided understanding of the proposed intermediates and the effects of complexation upon the geometry of the alkyne. The vast majority of these diphosphine-bridged complexes characterized have been found to contain the alkyne as a cis-dimetallated olefin unit. As part of the study of interactions of the low-valent complex $[Ir_2(CO)_3(dppm)_2]$ with small molecules, the reactions of this compound with alkynes were investigated; previous studies involving the rhodium analogue[15,16] had revealed that some of the adducts formed were catalyst precursors for alkyne hydrogenation.

Experimental Section

General experimental conditions were as described in Chapter 2. Dimethyl acetylenedicarboxylate (DMAD) was obtained from Aldrich and stored under N_2 over molecular sieves in the dark. The complex $[Ir_2(CO)_3(dppm)_2]$ (**1**) was prepared as previously reported.[17] All other chemicals were used as received without further purification.

Preparation of $[Ir_2(CO)_2(\mu\text{-}\eta^2{:}\eta^{2'}\text{-DMAD})(dppm)_2]$ (3). To a solution of **1** (100 mg, 80.8 μmol) in toluene (10 mL) was added one equivalent of DMAD (9.9 μL, 11.5 mg, 80.8 μmol). An immediate darkening of the orange reaction mixture occurred, with a change to dark green within 5 min. The solution was then refluxed for 10 min, during which time the color changed to dark blue then to lighter green. Upon slow cooling of the mixture to room temperature the green color faded to light yellow, accompanied by formation of a pale yellow microcrystalline solid. Ether (20 mL) was added to complete precipitation, and the yellow solid obtained was recrystallized from CH_2Cl_2/Et_2O. The pale yellow powder was dried under an N_2 stream then under vacuum, yielding 69 mg (64% isolated yield) of product. NMR (CD_2Cl_2, 22 °C): $^{31}P\{^1H\}$: δ -12.6 (singlet); ^1H: δ 7.45-

6.87 (multiplet, 40 H, phenyl hydrogens), 5.70, 3.39 (multiplets, each 2 H, dppm methylenes), 3.61 (singlet, 6 H, DMAD methyls); $^{13}C\{^{1}H\}$: δ 173.8 (singlet, Ir-CO). IR: (Nujol mull) 1938 (vs, Ir-CO), 1682 (s, ester CO) cm^{-1}; (CH_2Cl_2 solution) 1943 (vs), 1690 (s) cm^{-1}. Anal. Calcd for $C_{58}H_{50}Ir_2O_6P_4$: C, 51.55; H, 3.73. Found: C, 51.78; H, 3.94.

X-ray Data Collection. Diffusion of ether into a concentrated CH_2Cl_2 solution of complex **3** produced crystals in the form of yellow plates, several of which were mounted and flame-sealed in glass capillaries under N_2 and solvent vapor to minimize decomposition and/or solvent loss. Data were collected on an Enraf-Nonius CAD4 diffractometer using Mo $K\alpha$ radiation. Unit-cell parameters were obtained from a least-squares refinement of the setting angles of 25 reflections in the range $20.0° \leq 2\theta \leq 24.0°$. The monoclinic diffraction symmetry and the systematic absences ($h0l$, $l \neq 2n$) were consistent with the space groups *Pc* or *P*2/*c* (the latter was confirmed as the correct space group by the successful solution and refinement of the structure).

Intensity data were collected at 22 °C by using the $\theta/2\theta$ scan technique to a maximum $2\theta = 50.0°$, collecting reflections of the form $+h$ $+k$ $\pm l$. Of the data obtained, 10849 reflections were unique after merging. Backgrounds were scanned for 25% of the peak width on either side of the peak scan. Three reflections were chosen as intensity standards, being remeasured after every 120 min of X-ray exposure time. Although one of these standards lost 10% of its original intensity, the other two remained constant; recentering the crystal did not lead to a significant change in intensities. Since this intensity loss was not uniform a decomposition correction was not applied to the data. The data were measured and processed in the usual way, with a value of 0.04 for p^{18} employed to down-weight intense reflections; 6752 reflections were considered observed ($F_o^2 \geq 3\sigma(F_o^2)$) and were used in subsequent calculations. Absorption corrections were applied to the data according to Walker and Stuart's method.[19,20] See Table 5.1 for crystal data and more information on X-ray data collection.

Structure Solution and Refinement. The structure of **3** was solved in the space group $P2/c$ using standard Patterson and Fourier techniques. The unit cell was found to contain two independent molecules of **3**, each located on a crystallographic twofold axis (vide infra). Full-matrix least-squares refinements proceeded in order to minimize the function $\Sigma w(|F_o|-|F_c|)^2$, where $w = 4F_o^2/\sigma^2(F_o^2)$. Atomic scattering factors and anomalous dispersion terms were taken from the usual tabulations.[21-23] Positional parameters for the hydrogens attached to the carbon atoms of the complex and solvent molecules were calculated from the geometries about the attached carbon. These hydrogens were assigned positions 0.95 Å from their attached C atoms, given thermal parameters 20% greater than the equivalent isotropic B's of their attached atoms, and included as fixed contributions.

The final model for complex **3**, with 675 parameters varied, converged to values of $R = 0.037$ and $R_w = 0.043$. In the final difference Fourier map the 10 highest residuals (0.9-0.6 e/Å^3) were found in the area of the iridium atoms and solvent molecules (a typical carbon atom in an earlier synthesis had an electron density of 2.5 e/Å^3). The positional and thermal parameters for the non-hydrogen atoms of complex are given in Table 5.2,

Table 5.1. Crystallographic Data for $[Ir_2(CO)_2(\mu\text{-}\eta^2{:}\eta^{2'}\text{-DMAD})(dppm)_2]$-$\bullet 2CH_2Cl_2$ (3)

formula	$C_{60}Cl_4H_{54}Ir_2O_6P_4$
formula weight	1521.23
crystal shape	monoclinic plate
crystal dimensions, mm	0.82 × 0.22 × 0.05
space group	*P*2/*c* (No. 13)
temperature, °C	22
radiation (λ, Å)	graphite-monochromated Mo Kα (0.71069)
unit cell parameters	
a, Å	26.088 (5)
b, Å	9.896 (4)
c, Å	23.954 (3)
β, deg	109.27 (1)
V, Å^3	5838 (5)
Z	4
ρ(calcd), g cm^{-3}	1.731
linear absorption coeff (μ), cm^{-1}	48.783
range of transmission factors	0.858-1.341
detector aperture, mm	(3.00 + tan θ) wide × 4.00 high
takeoff angle, deg	3.0
maximum 2θ, deg	50.0

(continued)

Table 5.1. (continued)

crystal-detector distance, mm	173
scan type	$\theta/2\theta$
scan rate, deg/min	between 1.18 and 6.67
scan width, deg	$0.60 + 0.347 \tan \theta$
total unique reflections	10849 ($h\ k\ \pm l$)
total observations (NO)	6752 ($F_o^2 \geq 3\sigma(F_o^2)$)
final no. parameters varied (NV)	675
error in obs. of unit wt. (GOF)[a]	1.283
R[b]	0.037
R_w[c]	0.043

[a] $\mathrm{GOF} = [\sum w(|F_o| - |F_c|)^2/(\mathrm{NO} - \mathrm{NV})]^{1/2}$ where $w = 4F_o^2/\sigma^2(F_o^2)$.

[b] $R = \sum ||F_o| - |F_c|| / \sum |F_o|$. [c] $R_w = [\sum w(|F_o| - |F_c|)^2/\sum wF_o^2]^{1/2}$.

Table 5.2. Positional and Thermal Parameters of the Atoms of $[Ir_2(CO)_2(\mu\text{-}\eta^2{:}\eta^{2'}\text{-DMAD})(dppm)_2]\cdot 2CH_2Cl_2$ (3)[a]

(a) Molecule A

Atom	*x*	*y*	*z*	*B*, Å^2
Ir(1)	-0.04273(1)	0.10107(4)	-0.23109(1)	2.260(7)
P(1)	-0.00013(9)	0.2376(2)	-0.14986(9)	2.56(5)
P(2)	0.08991(9)	0.2678(2)	-0.20455(9)	2.54(5)
O(1)	-0.1355(3)	-0.0157(8)	-0.1972(3)	6.4(2)
O(3)	-0.0101(3)	-0.2519(8)	-0.3246(4)	6.7(2)
O(4)	-0.0904(3)	-0.1555(7)	-0.3477(3)	5.5(2)
C(1)	-0.1003(3)	0.0282(9)	-0.2130(4)	3.3(2)
C(3)	0.0478(3)	0.3543(9)	-0.1678(3)	2.6(2)
C(5)	-0.0190(3)	-0.0428(8)	-0.2801(3)	2.4(2)
C(6)	-0.0376(3)	-0.1615(9)	-0.3182(4)	3.1(2)
C(7)	-0.1128(6)	-0.263(1)	-0.3897(6)	8.0(4)
C(11)	-0.0368(3)	0.350(1)	-0.1153(4)	3.1(2)
C(12)	-0.0252(4)	0.484(1)	-0.1029(5)	7.3(3)
C(13)	-0.0542(5)	0.562(1)	-0.0738(6)	9.1(4)
C(14)	-0.0944(4)	0.502(1)	-0.0583(4)	5.6(3)
C(15)	-0.1073(4)	0.368(1)	-0.0717(5)	5.9(3)
C(16)	-0.0792(4)	0.298(1)	-0.1011(5)	5.0(3)
C(21)	0.0404(3)	0.1468(9)	-0.0833(4)	2.9(2)
C(22)	0.0261(4)	0.018(1)	-0.0738(4)	3.9(2)
C(23)	0.0546(5)	-0.048(1)	-0.0218(5)	5.5(3)
C(24)	0.0976(4)	0.009(1)	0.0196(4)	5.3(3)
C(25)	0.1135(4)	0.138(1)	0.0105(5)	5.5(3)
C(26)	0.0838(4)	0.205(1)	-0.0410(4)	4.4(3)
C(31)	0.1500(3)	0.224(1)	-0.1412(4)	3.2(2)
C(32)	0.1678(4)	0.092(1)	-0.1317(4)	4.3(3)
C(33)	0.2132(4)	0.056(1)	-0.0807(5)	5.7(3)
C(34)	0.2388(4)	0.159(1)	-0.0422(5)	5.6(3)

(continued)

Table 5.2. (continued)

C(35)	0.2210(4)	0.292(1)	-0.0525(5)	4.7(3)
C(36)	0.1773(4)	0.325(1)	-0.1024(4)	4.3(3)
C(41)	0.1173(3)	0.4083(9)	-0.2346(4)	2.8(2)
C(42)	0.0962(4)	0.537(1)	-0.2424(5)	5.3(3)
C(43)	0.1202(5)	0.640(1)	-0.2658(5)	6.2(3)
C(44)	0.1649(4)	0.616(1)	-0.2819(5)	5.0(3)
C(45)	0.1849(4)	0.488(1)	-0.2759(5)	6.4(3)
C(46)	0.1625(4)	0.384(1)	-0.2519(5)	4.7(3)

(b) Molecule B

Atom	*x*	*y*	*z*	B, Å^2
Ir(2)	0.50242(1)	0.21756(3)	0.30636(1)	1.981(6)
P(3)	0.56096(8)	0.0477(2)	0.20410(9)	2.19(5)
P(4)	0.58085(8)	0.0858(2)	0.33674(9)	2.31(5)
O(2)	0.4971(3)	0.3364(8)	0.4206(3)	6.1(2)
O(5)	0.4374(3)	0.5734(6)	0.1960(3)	4.9(2)
O(6)	0.3936(2)	0.4679(7)	0.2486(3)	4.1(2)
C(2)	0.4999(4)	0.2897(9)	0.3770(4)	3.1(2)
C(4)	0.5803(3)	-0.0324(8)	0.2776(3)	2.4(2)
C(8)	0.4709(3)	0.3652(8)	0.2418(3)	2.1(2)
C(9)	0.4335(3)	0.4767(9)	0.2256(3)	2.7(2)
C(10)	0.3529(4)	0.572(1)	0.2323(5)	5.2(3)
C(51)	0.6270(3)	0.0868(9)	0.1962(4)	2.9(2)
C(52)	0.6643(3)	-0.019(1)	0.1982(4)	3.8(2)
C(53)	0.7153(4)	0.010(1)	0.1949(5)	5.4(3)
C(54)	0.7294(4)	0.141(1)	0.1892(5)	5.2(3)
C(55)	0.6929(4)	0.246(1)	0.1865(5)	6.0(3)
C(56)	0.6419(3)	0.216(1)	0.1897(4)	4.3(2)
C(61)	0.5416(3)	-0.0956(9)	0.1535(3)	2.3(2)
C(63)	0.5190(4)	-0.169(1)	0.0524(4)	3.7(2)
C(64)	0.5110(4)	-0.300(1)	0.0688(4)	4.5(3)

(continued)

Table 5.2. (continued)

C(62)	0.5347(4)	-0.0683(9)	0.0947(4)	3.3(2)
C(65)	0.5179(4)	-0.326(1)	0.1271(4)	4.2(2)
C(66)	0.5326(4)	-0.224(1)	0.1693(4)	3.5(2)
C(71)	0.6439(3)	0.180(1)	0.3534(4)	3.1(2)
C(72)	0.6899(4)	0.130(1)	0.3438(4)	4.1(3)
C(73)	0.7377(4)	0.204(1)	0.3607(5)	5.6(3)
C(74)	0.7395(4)	0.329(1)	0.3878(5)	5.8(3)
C(75)	0.6953(4)	0.379(1)	0.3973(5)	5.0(3)
C(76)	0.6479(4)	0.308(1)	0.3802(4)	3.8(2)
C(81)	0.5993(3)	-0.0215(9)	0.4024(3)	2.6(2)
C(82)	0.6099(4)	0.038(1)	0.4575(4)	3.8(2)
C(83)	0.6272(4)	-0.035(1)	0.5092(4)	4.6(3)
C(84)	0.6323(4)	-0.170(1)	0.5067(4)	5.0(3)
C(85)	0.6208(4)	-0.236(1)	0.4526(4)	4.9(3)
C(86)	0.6045(4)	-0.161(1)	0.4016(4)	3.6(2)

(c) Solvent molecules

Atom	x	y	z	B, Å^2
Cl(1)	0.7667(2)	-0.3035(6)	0.4817(2)	11.6(2)
Cl(2)	0.7571(2)	-0.1967(6)	0.3671(3)	13.6(2)
Cl(3)	0.7035(2)	0.3707(6)	0.6474(2)	12.2(2)
Cl(4)	0.6313(3)	0.4311(6)	0.5299(3)	15.5(2)
C(101)	0.7549(7)	-0.159(2)	0.4374(7)	10.6(5)[b]
C(102)	0.6483(9)	0.348(3)	0.594(1)	16.7(9)[b]

[a] Numbers in parentheses in this and subsequent tables are estimated standard deviations in the least significant digits. Thermal parameters for the anisotropically refined atoms are given in the form of the equivalent isotropic Gaussian displacement parameter defined as $^4/_3\left[a^2\beta_{11} + b^2\beta_{22} + c^2\beta_{33} + ac(\cos\beta)\beta_{13}\right]$. [b] Refined isotropically.

and selected bond lengths and angles are given in Tables 5.3 and 5.4, respectively.

Results and Discussion

(a) Description of Structure. Along with two dichloromethane molecules of crystallization, the asymmetric unit in the structure of complex **3** contains half of each of two crystallographically independent molecules; the molecules are essentially mirror images of each other. Molecule A is generated by rotation of the unique moiety containing Ir(1) about the twofold axis at $0, y, {}^{-1}/_{4}$, while rotation of the corresponding unit containing Ir(2) about the twofold axis at ${}^{1}/_{2}, y, {}^{1}/_{4}$ generates molecule B. The tables of bond lengths and angles list parameters for molecule A side-by-side with the corresponding values for molecule B; it can be seen that there are no significant differences between the geometries of the two enantiomers, thus what is said in describing molecule A is consistent with the structure of molecule B.

The structure of complex **3**, molecule A is shown in Figure 5.1; a view of the complex in an alternate orientation, in which only the *ipso* phenyl carbons of the dppm ligands are shown, is presented in Figure 5.3 (Figures 5.2 and 5.4 show similar views for molecule B). The molecule contains a twofold axis of symmetry passing through the centers of the metal-metal and acetylenic carbon-carbon bonds, and is structurally reminiscent of the previously-characterized compounds $[Rh_2(CO)_2(\mu\text{-}\eta^2{:}\eta^{2'}\text{-}PhCCPh)(dppm)_2]$,[16] $[Co_2(CO)_2(\mu\text{-}\eta^2{:}\eta^{2'}\text{-}MeCCMe)(dppm)_2]$,[24] $[Co_2(CO)_2(\mu\text{-}\eta^2{:}\eta^{2'}\text{-}PhCCPh)(dpam)_2]$[25] (dpam = bis(diphenylarsino)methane), [Co$_2$-

Table 5.3. Selected Distances (Å) in $[Ir_2(CO)_2(\mu\text{-}\eta^2{:}\eta^{2'}\text{-DMAD})(dppm)_2]$-
$\cdot 2CH_2Cl_2$ (3)

(a) Bonded

Molecule A		Molecule B	
Ir(1)-Ir(1′)	2.6694(6)	Ir(2)-Ir(2′)	2.6613(6)
Ir(1)-P(1)	2.329(2)	Ir(2)-P(4)	2.332(2)
Ir(1)-P(2′)	2.316(2)	Ir(2)-P(3′)	2.313(2)
Ir(1)-C(1)	1.875(9)	Ir(2)-C(2)	1.859(9)
Ir(1)-C(5)	2.066(7)	Ir(2)-C(8)	2.089(7)
Ir(1)-C(5′)	2.099(7)	Ir(2)-C(8′)	2.115(7)
P(1)-C(3)	1.854(8)	P(4)-C(4)	1.833(8)
P(1)-C(11)	1.834(8)	P(4)-C(81)	1.827(8)
P(1)-C(21)	1.832(8)	P(4)-C(71)	1.819(8)
P(2)-C(3)	1.832(8)	P(3)-C(4)	1.843(7)
P(2)-C(31)	1.839(8)	P(3)-C(51)	1.835(8)
P(2)-C(41)	1.818(8)	P(3)-C(61)	1.826(8)
O(1)-C(1)	1.151(9)	O(2)-C(2)	1.165(9)
O(3)-C(6)	1.19(1)	O(5)-C(9)	1.216(9)
O(4)-C(6)	1.33(1)	O(6)-C(9)	1.332(9)
O(4)-C(7)	1.46(1)	O(6)-C(10)	1.44(1)
C(5)-C(5′)	1.45(1)	C(8)-C(8′)	1.44(1)
C(5)-C(6)	1.47(1)	C(8)-C(9)	1.44(1)

(b) Non-bonded

P(1)···P(2)	3.058(3)	P(3)···P(4)	3.069(3)

Some distances for Molecule B are listed out of order in order to more clearly correspond to the related parameters for Molecule A. Primed atoms are related to unprimed atoms by the crystallographic 2-fold axis passing through the centers of the C(5)-C(5′) and Ir(1)-Ir(1′) bonds for molecule A, and about the axis passing through the centers of the C(8)-C(8′) and Ir(2)-Ir(2′) bonds for molecule B.

Table 5.4. Selected Angles (deg) in [$Ir_2(CO)_2(\mu\text{-}\eta^2\text{:}\eta^{2'}\text{-DMAD})(dppm)_2$]$\bullet 2CH_2Cl_2$ (3)

(a) Bond angles

Molecule A		Molecule B	
Ir(1′)-Ir(1)-P(1)	93.54(5)	Ir(2′)-Ir(2)-P(4)	93.42(5)
Ir(1′)-Ir(1)-P(2′)	95.39(5)	Ir(2′)-Ir(2)-P(3′)	95.58(5)
Ir(1′)-Ir(1)-C(1)	157.2(3)	Ir(2′)-Ir(2)-C(2)	157.0(2)
Ir(1′)-Ir(1)-C(5)	50.7(2)	Ir(2′)-Ir(2)-C(8)	51.2(2)
Ir(1′)-Ir(1)-C(5′)	49.7(2)	Ir(2′)-Ir(2)-C(8′)	50.3(2)
P(1)-Ir(1)-P(2′)	98.34(8)	P(3′)-Ir(2)-P(4)	98.60(7)
P(1)-Ir(1)-C(1)	101.9(3)	P(4)-Ir(2)-C(2)	102.9(3)
P(1)-Ir(1)-C(5)	136.4(2)	P(4)-Ir(2)-C(8)	135.4(2)
P(1)-Ir(1)-C(5′)	98.8(2)	P(4)-Ir(2)-C(8′)	98.3(2)
P(2′)-Ir(1)-C(1)	98.9(3)	P(3′)-Ir(2)-C(2)	98.1(3)
P(2′)-Ir(1)-C(5)	107.8(2)	P(3′)-Ir(2)-C(8)	109.6(2)
P(2′)-Ir(1)-C(5′)	141.7(2)	P(3′)-Ir(2)-C(8′)	142.6(2)
C(1)-Ir(1)-C(5)	107.7(3)	C(2)-Ir(2)-C(8)	106.4(3)
C(1)-Ir(1)-C(5′)	110.7(3)	C(2)-Ir(2)-C(8′)	110.3(3)
C(5)-Ir(1)-C(5′)	40.9(4)	C(8)-Ir(2)-C(8′)	39.9(4)
Ir(1)-P(1)-C(3)	109.9(3)	Ir(2)-P(4)-C(4)	109.5(2)
Ir(1)-P(1)-C(11)	123.6(3)	Ir(2)-P(4)-C(81)	123.3(2)
Ir(1)-P(1)-C(21)	115.0(3)	Ir(2)-P(4)-C(71)	114.7(3)
C(3)-P(1)-C(11)	102.7(4)	C(4)-P(4)-C(81)	103.2(4)
C(3)-P(1)-C(21)	105.5(4)	C(4)-P(4)-C(71)	105.8(4)
C(11)-P(1)-C(21)	98.1(4)	C(71)-P(4)-C(81)	98.6(4)
Ir(1′)-P(2)-C(3)	112.5(3)	Ir(2′)-P(3)-C(4)	112.1(2)
Ir(1′)-P(2)-C(31)	120.1(3)	Ir(2′)-P(3)-C(51)	119.8(3)
Ir(1′)-P(2)-C(41)	118.3(3)	Ir(2′)-P(3)-C(61)	117.5(2)
C(3)-P(2)-C(31)	101.4(4)	C(4)-P(3)-C(51)	102.6(4)
C(3)-P(2)-C(41)	102.1(4)	C(4)-P(3)-C(61)	103.2(4)
C(31)-P(2)-C(41)	99.6(4)	C(51)-P(3)-C(61)	99.1(3)
C(6)-O(4)-C(7)	116.6(8)	C(9)-O(6)-C(10)	116.7(7)

(continued)

Table 5.4. (continued)

Molecule A		Molecule B	
Ir(1)-C(1)-O(1)	179.5(7)	Ir(2)-C(2)-O(2)	178.2(8)
P(1)-C(3)-P(2)	112.2(4)	P(3)-C(4)-P(4)	113.2(4)
Ir(1)-C(5)-Ir(1′)	79.7(3)	Ir(2)-C(8)-Ir(2′)	78.5(2)
Ir(1)-C(5)-C(5′)	70.8(4)	Ir(2)-C(8)-C(8′)	71.0(4)
Ir(1)-C(5)-C(6)	143.6(6)	Ir(2)-C(8)-C(9)	143.2(6)
Ir(1′)-C(5)-C(5′)	68.4(4)	Ir(2′)-C(8)-C(8′)	69.1(4)
Ir(1′)-C(5)-C(6)	134.8(6)	Ir(2′)-C(8)-C(9)	134.3(5)
C(5′)-C(5)-C(6)	126.4(5)	C(8′)-C(8)-C(9)	129.4(4)
O(3)-C(6)-O(4)	122.1(8)	O(5)-C(9)-O(6)	121.3(7)
O(3)-C(6)-C(5)	126.3(8)	O(5)-C(9)-O(8)	125.6(7)
O(4)-C(6)-C(5)	111.6(8)	O(6)-C(9)-C(8)	113.1(7)

(b) Torsion angles

P(1)-Ir(1)-Ir(1′)-P(2)	10.16(8)	P(3)-Ir(2′)-Ir(2)-P(4)	12.82(8)
C(5)-Ir(1)-Ir(1′)-C(5′)	13(1)	C(8)-Ir(2)-Ir(2′)-C(8′)	14(1)

Some angles for Molecule B are listed out of order in order to more clearly correspond to the analogous quantities for Molecule A. Primed atoms are related to unprimed atoms by the crystallographic 2-fold axis passing through the centers of the C(5)-C(5′) and Ir(1)-Ir(1′) bonds for molecule A, and about the axis passing through the centers of the C(8)-C(8′) and Ir(2)-Ir(2′) bonds for molecule B.

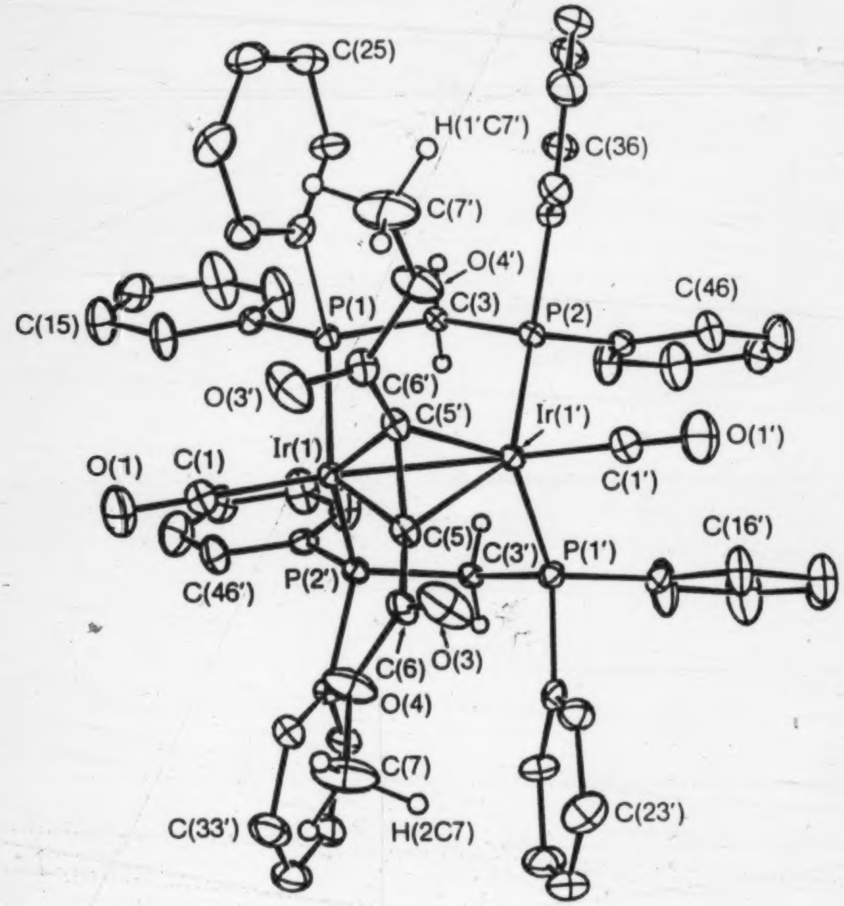
C(25)
H(1'C7')
C(36)
C(7')
O(4')
C(46)
C(15)
P(1)
C(3)
P(2)
O(3')
C(6')
C(5')
Ir(1')
O(1')
O(1)
C(1)
Ir(1)
C(1')
C(16')
C(5)
C(3')
P(1')
C(46')
P(2')
C(6)
O(3)
O(4)
C(7)
C(33')
H(2C7)
C(23')

Figure 5.1. Perspective view of $[Ir_2(CO)_2(\mu\text{-}\eta^2:\eta^{2'}\text{-DMAD})(dppm)_2]$ (3, molecule A) showing the numbering scheme. Thermal parameters are shown at the 20% level except for hydrogens, which are shown artificially small for the DMAD methyl and dppm methylene groups but are not shown for the phenyl groups. Primed atoms are related to unprimed atoms by the crystallographic 2-fold axis passing through the centers of the C(5)-C(5') and Ir(1)-Ir(1') bonds.

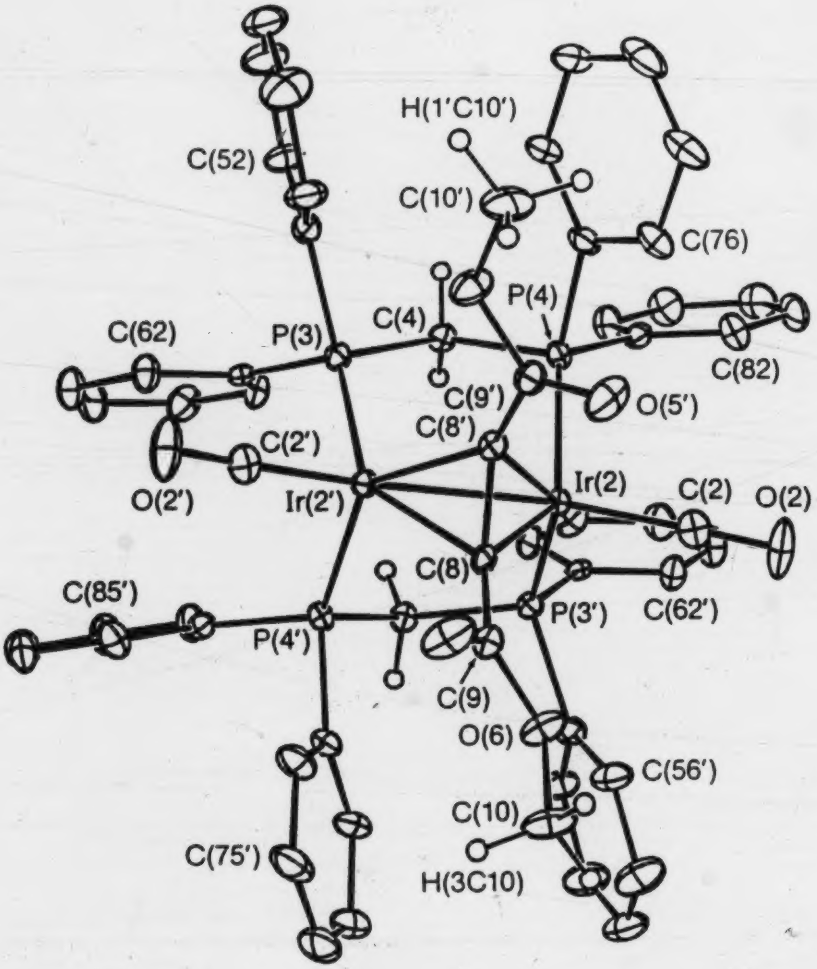
H(1'C10')
C(52)
C(10')
C(76)
P(4)
C(4)
C(62)
P(3)
C(82)
C(9')
O(5')
C(8')
C(2')
Ir(2)
C(2)
O(2)
O(2')
Ir(2')
C(8)
C(85')
P(3')
C(62')
P(4')
C(9)
O(6)
C(56')
C(10)
C(75')
H(3C10)

Figure 5.2. Perspective view of complex 3 (molecule B).

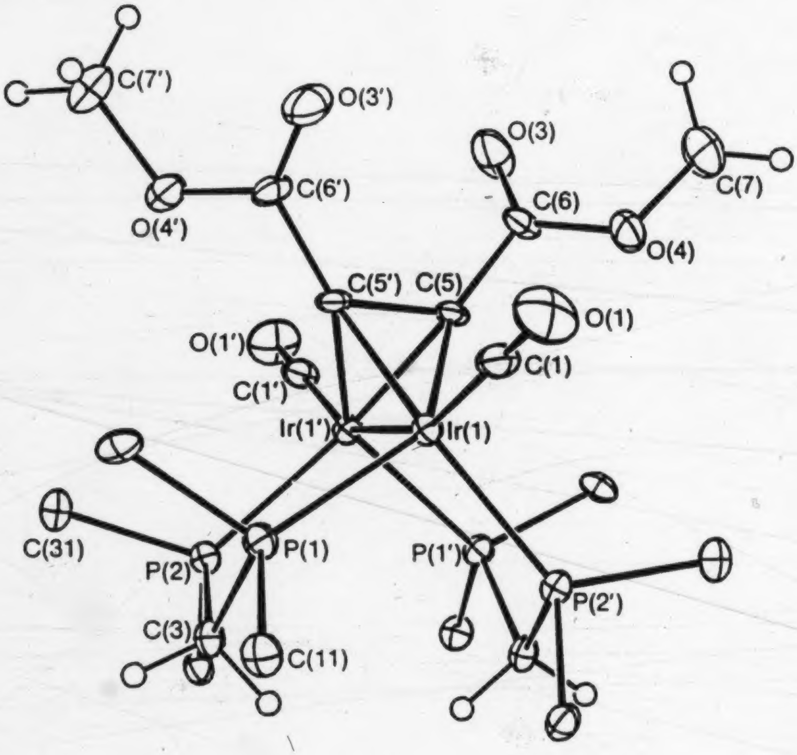
C(7')
O(3')
O(3)
C(7)
C(6')
C(6)
O(4')
O(4)
C(5')
C(5)
O(1')
O(1)
C(1')
C(1)
Ir(1')
Ir(1)
C(31)
P(2)
P(1)
P(1')
P(2')
C(3)
C(11)

Figure 5.3. View of complex 3, molecule A, omitting all dppm phenyl carbons except those bound to phosphorus.

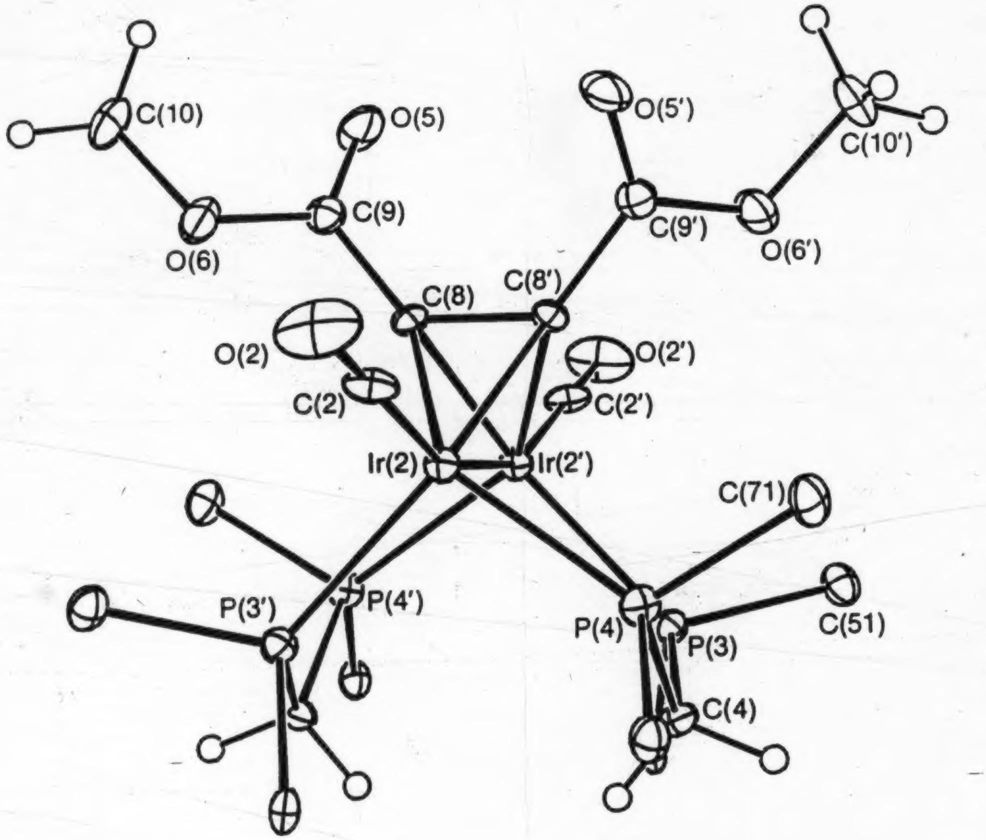
C(10)
O(5)
O(5')
C(10')
C(9)
O(6)
C(9')
O(6')
C(8)
C(8')
O(2)
O(2')
C(2)
C(2')
Ir(2)
Ir(2')
C(71)
P(3')
P(4')
P(4)
P(3)
C(51)
C(4)

Figure 5.4. View of complex 3, molecule B, omitting all dppm phenyl carbons except those bound to phosphorus.

$(CO)_4(\mu\text{-}\eta^2\text{:}\eta^{2'}\text{-PhCCPh})(dppm)]$[25] and $[Co_2(CO)_6(\mu\text{-}\eta^2\text{:}\eta^2\text{-RCCR})]$ (R = Ph,[26a] Bu^t [26b]). Like these complexes, the metal nuclei of **3** are bridged by the dppm and alkyne ligands, with the central C-C bond of the latter oriented in a direction perpendicular to the metal-metal bond (the C(5)-C(5′) and Ir(1)-Ir(1′) bond vectors are rotated 88.0(4)° with respect to each other); in addition, one carbonyl group is terminally bound to each metal. The binding mode of the DMAD ligand is accommodated by a bending-back of the diphosphine ligands (P(1)-Ir-P(2′) = 98.34(8)°); this cis disposition of the diphosphines at both metals has been observed in several of the above alkyne-bridged species, as well as in the complexes $[Ir_2(H)_2(CO)_2(\mu\text{-SiRPh})(dppm)_2]$[27] (R = H, Ph), $[Rh_2(CO)_2(\mu\text{-SiHR})_2(dppm)_2]$[28] (R = Et, Ph), $[Rh_2Cl_2(\mu\text{-X})_2(dppm)_2]$ (X = Cl, CH_3CO_2, $Ph_2P(C_6H_4)$),[29] $[(Rh(PNP))_2(\mu\text{-}\eta^1\text{:}\eta^{1'}\text{-DMAD})(\mu\text{-PNP})_2]$ (PNP = $(MeO)_2PN(Me)P(OMe)_2$)[30] and $[Pt_2Me_4(dRpm)_2]$ (dRpm = dppm, dmpm [bis(dimethylphosphino)methane]).[31] Before determination of this structure no examples of dppm-bridged diiridium complexes containing cis phosphines at both metal centers had been known (although two examples were subsequently reported[27]), and the disposition of the dppm groups about the metals in **3** could not be assigned based solely on spectroscopic data.

The coordination geometry about Ir(1) can be best described as distorted trigonal bipyramidal, with C(1) and Ir(1′) acting as axial ligands while P(1), P(2′) and the C(5)-C(5′) unit (the latter being viewed as a neutral two-electron π-donor to each of Ir and Ir′) occupy the equatorial sites. Distortions from this model, especially the severely acute Ir(1′)-Ir(1)-C(5) and Ir(1′)-Ir(1)-C(5′) angles (50.7(2)° and 49.7(2)°, respectively) and the offset of the terminal carbonyl group C(1)O(1) from the Ir-Ir axis (Ir(1′)-Ir(1)-C(1) = 157.2(3)°), appear to result from the tendency of the bridging alkyne to put the equatorial planes about the metal centers at nearly right angles to each other (dihedral angle between planes containing Ir(1), C(5), C(5′) and Ir(1′), C(5), C(5′) = 86.3(2)°), an effect counteracted by the bridging dppm ligands in linking the equatorial planes (dihedral angle between planes containing Ir(1), P(1), P(2′) and Ir(1′), P(1′), P(2) = 13.8(2)°). The net effect is to force a "bent" interaction between the metal centers, i.e. by forcing the bonding orbitals on each Ir away from the metal-metal axis, as represented below. It may be that this bent metal-metal bond results in a shorter Ir-Ir distance than is usually observed in similar cases (vide infra), since the metals must move closer together to maintain a favorable degree of metal-metal overlap.

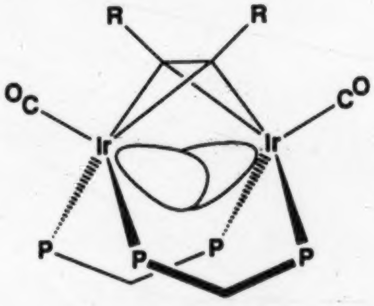

As expected, coordination to the metal centers has changed the geometry of the DMAD group. The acetylenic C(5)-C(5′) distance of 1.45(1) Å is the longest thus far observed for binuclear complexes containing bridging alkyne ligands.[4,16,24] This distance is now comparable to that between the acetylenic and carboxylate carbons (C(5)-C(6) = 1.47(1) Å), suggesting an increase in back donation from Ir into the π^* orbitals of the alkyne bridge and apparent reduction of the C-C bond order. The C(5′)-C(5)-C(6) angle of 126.4(5)° is distinctly more acute than is usually observed (133-145°); only $[Co_2(CO)_6(\mu\text{-}\eta^2\text{:}\eta^{2'}\text{-}C_6F_6)]$[32] ($C_6F_6$ = 3,4,5,5,6,6-hexafluorocyclohexa-1-yne-3-ene) possesses smaller C_{ac}-C_{ac}-R angles (118(2)°, 122(2)°), probably due to their endocyclic nature. In contrast to **3**, the closely-related compound $[Rh_2(CO)_2(\mu\text{-}\eta^2\text{:}\eta^{2'}\text{-}PhCCPh)(dppm)_2]$[16] shows a separation of only 1.33(1) Å between the acetylenic carbons, and the C_{ac}-C_{ac}-R angles (133.0(8)° and 134.2(8)°) are normal. Overall the Ir_2C_2 core of **3** can be described as a dimetallatetrahedrane unit, with the distortions from this model (especially from the ideal bond angles of 60°) mainly arising due to the inherent inequity of the Ir-Ir, Ir-C and C-C bond lengths.

The methoxycarbonyl groups of the DMAD bridge lie in planes essentially perpendicular to each other (dihedral angle between planes of O(3)-C(6)-C(6′) and C(6)-C(6′)-O(3′) = 82.1(6)°), a phenomenon also observed for complexes containing the same alkyne in the cis-dimetallated form.[5,6,33] Avoidance of steric hindrances between the carboxyl oxygens of the two CO_2Me groups, and between these groups and the dppm phenyls, appears to be the main driving force for this twisting.

The Ir(1)-Ir(1′) distance of 2.6694(6) Å is the shortest so far observed within the class of similar diphosphine-bridged systems, where the metal-metal distances usually fall within the range 2.77-2.89 Å;[6,11,27,33,34] the distance observed herein is more comparable to that found in another perpendicular-alkyne bridged complex, $[Ir_2(CO)_4(PPh_3)_2(\mu\text{-}\eta^2\text{:}\eta^{2'}\text{-}PhCCH)]$ (Ir-Ir = 2.691(1) Å),[35] and to the Rh-Rh distance of 2.644(1) Å in $[Rh_2(CO)_2(\mu\text{-}\eta^2\text{:}\eta^{2'}\text{-}PhCCPh)(dppm)_2]$.[16] Presumably the short metal-metal separation is a consequence of the bite imposed by the alkyne bridge, which requires a decreased Ir-Ir distance in order to maximize Ir-Ir and Ir-C overlaps, as mentioned above. In spite of the short metal-metal separation and the long distance between acetylenic carbons (vide supra), the Ir-C(5) and Ir-C(5′) distances (2.066(7) Å and 2.099(7) Å) are within the range previously observed (2.05-2.13 Å) for iridium atoms bound to alkyne residues in related systems.[6,8,11,12] The Ir-P distances (2.329(2) Å, 2.316(2) Å) are similar to those observed in other $Ir_2(dppm)_2$ complexes, and despite the short Ir-Ir distance in the present case the intraligand P(1)⋯P(2) separation (3.058(3) Å) is normal.

(b) Description of Chemistry. The addition of one equivalent of dimethyl acetylenedicarboxylate to a solution of $[Ir_2(CO)_3(dppm)_2]$ (1) in toluene produces an initially deep blue-green solution containing $[Ir_2(CO)_2(\mu\text{-}\eta^1\text{:}\eta^{1'}\text{-DMAD})(dppm)_2]$ (2), which has been assigned the structure shown below. The $^{31}P\{^1H\}$ NMR spectrum of this species shows a singlet

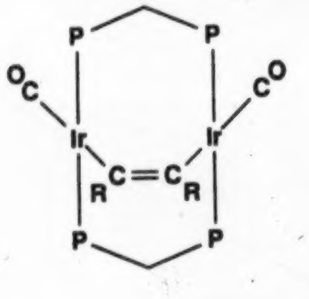

R = CO_2Me

2

resonance at δ 5.18, indicative of only one type of phosphorus chemical environment in the molecule. The ^1H NMR spectrum shows signals for two different types of methylene protons (multiplets at δ 4.36 and 3.42) and a singlet at δ 2.61 for the methyl protons of the alkyne ligand, with a 1:1:3 ratio of intensities, implying (with the $^{31}P\{^1H\}$ NMR data) that the alkyne unit is coordinated symmetrically to both metal centers. The $^{13}C\{^1H\}$ spectrum of species **2** (prepared from addition of DMAD to ^{13}CO-enriched compound **1**) shows a singlet at δ 191.0, with no resolved coupling to the phosphorus atoms bound to iridium ($^2J_{P\text{-}C}$ < 2 Hz). No resonances are observed at lower field, confirming that **2** contains only terminal CO groups. Assignment of the solution infrared spectrum of this complex is more difficult, as the bands are broadened; a stretch due to the acetylenic carbons of the cis-dimetallated olefin (which would usually be observed in the region 1550-1650 cm^{-1}) could not be unambiguously identified. Although these data alone do not distinguish between a formulation for the complex in which the alkyne is coordinated as a cis-dimetallated olefin or one containing a dimetallatetrahedrane unit, characterization of complex **3** by X-ray crystallography eliminated the latter possibility. Species **2** is thus an isoelectronic analogue of the structurally-characterized compound $[Pd_2Cl_2(\mu\text{-}\eta^1:\eta^{1'}\text{-HFB})(dppm)_2]$ (HFB = hexafluoro-2-butyne).[36]

Compound **2** is unusual in that although diphosphine-bridged rhodium or iridium A-frame complexes containing two terminal carbonyls and a dianionic bridge are well known (e.g. $[MM'(CO)_2(\mu\text{-}S)(dppm)_2]$, MM' = Rh_2,[37] Ir_2,[34a] RhIr[38]), this is one of the few cases in which an alkyne is spanning the metals with no metal-metal bond or other bridging group (e.g. CO) other than the diphosphine ligands present. Besides $[Pd_2Cl_2(\mu\text{-}\eta^1:\eta^{1'}\text{-HFB})(dppm)_2]$,[36] the deep blue complex $[Rh_2(CO)_2(\mu\text{-}\eta^1:\eta^{1'}\text{-PhCCH})(dppm)_2]$ has been reported by Eisenberg and coworkers.[39]

Although the latter species has a structure analogous to **2**, it was obtained via reaction of $[Rh_2(CO)_2(\mu\text{-}H)_2dppm)_2]$ with two equivalents of phenylacetylene, yielding styrene as the second product. The same research group has carried out studies of the reactivity of $[Rh_2(CO)_3(dppm)_2]$ (the dirhodium analogue of **1**) towards alkynes, but no mention has been made of whether products containing cis-dimetallated olefin units have been obtained from the tricarbonyl starting material. Related bis(dimethylphosphino)methane-bridged dirhodium complexes of formula $[Rh_2(CO)_2(\mu\text{-}\eta^1\text{:}\eta^{1'}\text{-}RCCR)(dmpm)_2]$ (R = CO_2Me, CF_3)[40a,b] have been synthesized within this research group, via borohydride reduction of the $[Rh_2Cl_2(CO)_2(\mu\text{-}\eta^1\text{:}\eta^{1'}\text{-}RCCR)(dmpm)_2]$[9] precursors. It is interesting to note that direct reaction of DMAD or HFB with $[Rh_2(CO)_3(dmpm)_2]$ (an analogue of **1**) led to products containing two or even three RCCR units, two of which, $[Rh_2(CO)_2(\mu\text{-}\eta^1\text{:}\eta^{1'}\text{-}HFB)_2(dmpm)_2]$ and $[Rh_2(CO)_2(\mu\text{-}\eta^1\text{:}\eta^{1'}\text{-}DMAD)(\mu\text{-}\eta^1\text{:}\eta^{1'}\text{-}HFB)(dmpm)_2]$, have been characterized by X-ray crystallography.[40b,c]

Compound **2** is stable in solution for several hours, but if it is left overnight, the deep blue solution color fades to light orange-yellow, with precipitation of a fine light yellow solid. Attempts to isolate **2** in the solid state via addition of ether or hexanes to the blue solution result in formation of a light green flocculent solid that turns orange-yellow upon standing. In both cases, the solids obtained have been identified as $[Ir_2(CO)_2(\mu\text{-}\eta^2\text{:}\eta^{2'}\text{-}DMAD)(dppm)_2]$ (**3**), the structure of which was described earlier. The infrared and NMR spectroscopic results are consistent with the X-ray structure. Although, as was the case for complex **2**, an infrared stretching frequency for the central acetylenic carbons cannot be unam-

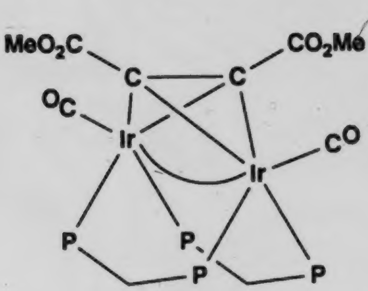

3

biguously assigned, the crystal structure shows that this bond has been substantially weakened, thus the frequency for this vibration may lie in the region where it may be obscured by bands due to other C-C stretches. The progression from species **2** to **3** is similar to the behavior of the abovementioned dirhodium analogue of **2**, $[Rh_2(CO)_2(\mu\text{-}\eta^1\text{:}\eta^{1'}\text{-PhCCH})\text{-}(dppm)_2]$, which slowly converts to $[Rh_2(CO)_2(\mu\text{-}\eta^2\text{:}\eta^{2'}\text{-PhCCH})(dppm)_2]$.[39]

It was surprising to find that the coordination geometry proposed for **2** was not the most stable one since it has the iridium atoms in the favored (+1) oxidation state with the usual square planar geometry. However, it appears that the driving force for conversion of the bridging alkyne ligand from a parallel to a perpendicular binding mode may be the formation of a greater number of bonds. Although this transformation results in a formal decrease of the acetylenic C-C bond order by one, an additional two Ir-C bonds are formed (considering a localized σ-bonding model) along with the strong Ir-Ir bond. The mechanism by which this "twist" of the DMAD group into its final orientation is accomplished may not be as straightforward as it appears. Through calculations using the model systems $[Co_2(H)_6(\mu\text{-}\eta^1\text{:}\eta^{1'}\text{-}C_2H_2)]^{6-}$ and $[Co_2(H)_6(\mu\text{-}\eta^2\text{:}\eta^{2'}\text{-}C_2H_2)]^{6-}$, which possess structures directly analogous to **2** and **3**, respectively, Hoffmann[4] has shown that a simple 90° rotation of the bridging alkyne would result in the bonding orbital combination becoming antibonding, and vice versa, a level crossing of highest occupied and lowest unoccupied molecular orbitals that is forbidden by rules of molecular symmetry. Thus conversion of the cis-dimetallated complex into the dimetallatetrahedrane form may proceed via an intermediate in which the alkyne is coordinated to only one of the metals. This species, formulated as $[Ir_2(CO)_2(\eta^2\text{-DMAD})(dppm)_2]$ (**4**) with the structure shown below, would be an analogue of **1** in

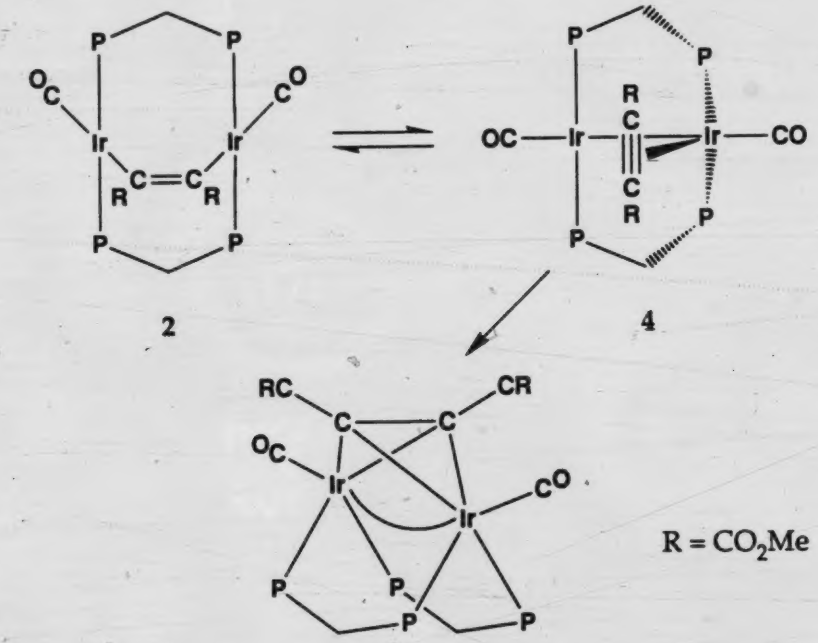

2

4

3

R = CO_2Me

which the alkyne has replaced a carbonyl group as a two-electron donor to one of the metals. Such an intermediate would contain a coordinatively unsaturated iridium center, which would be susceptible to recoordination of the alkyne in either of the μ-η^1:$\eta^{1'}$ or μ-η^2:$\eta^{2'}$ binding modes, with the latter path leading to the stable final product, **3**. Binuclear dppm-bridged species in which alkyne ligands are bound to only one of the metals have been proposed as intermediates in previous studies,[6,12,40c] and one example has been confirmed by an X-ray structure determination.[11]

The conversion of complex **2** to **3** is not thermally reversible, as reflux in toluene leaves **3** unaffected. Reversible interconversions between μ-η^1:$\eta^{1'}$- and μ-η^2:$\eta^{2'}$-bound alkynes have been reported by Dickson ($[(C_5H_5)_2Rh_2(CO)_2(\mu\text{-}\eta^1:\eta^{1'}\text{-}CF_3C{\equiv}CCF_3)] \rightleftarrows [(C_5H_5)_2Rh_2(\mu\text{-}CO)(\mu\text{-}\eta^2:\eta^{2'}\text{-}CF_3\text{-}C{\equiv}CCF_3)] + CO$)[41] and Takats ($[(OC)_4Ru(\mu\text{-}\eta^1:\eta^{1'}\text{-}CF_3C{\equiv}CCF_3)Co(CO)(C_5Me_5)] \rightleftarrows [(OC)_3Ru(\mu\text{-}\eta^2:\eta^{2'}\text{-}CF_3C{\equiv}CCF_3)(\mu\text{-}CO)Co(C_5Me_5)] + CO$),[42] but these processes were effected by loss or gain of CO. The irreversible transformation of $[(C_5H_5)_2Rh_2(\mu\text{-}\eta^1:\eta^{1'}\text{-}CF_3C{\equiv}CCF_3)(\mu\text{-}CO)(\mu\text{-}CF_3CH)]$ to $[(C_5H_5)_2Rh_2(\mu\text{-}\eta^2:\eta^{2'}\text{-}CF_3C{\equiv}CCF_3)(\mu\text{-}CF_3CH)]$, observed by Dickson, is also accompanied by CO loss.[43] Compound **3** does not react with carbon monoxide, which may not be surprising considering that the metal centers are already coordinatively saturated. Formation of a carbonyl-bridged product would thus require attack of CO at the other side of the Ir-Ir bond from the coordinated alkyne, at a site protected by the steric bulk of the dppm bridges. For the same reasons the failure of **3** to react with H_2 is not unexpected. Reaction of Species **2** does react with CO, but the result is a mixture of unidentified products.

The preparations of other alkyne-bridged derivatives of compound **1** were attempted but were not successful. Reactions of **1** with phenylacetylene and diphenylacetylene did not proceed beyond starting materials, and the use of hexafluoro-2-butyne led only to a multitude of unidentified products. This is surprising (and somewhat disappointing) considering that $[Rh_2(CO)_3(dppm)_2]$ was reported to have formed adducts with acetylene, phenylacetylene and diphenylacetylene, and that the HCCH- and PhCCH-containing species served as catalyst precursors for the hydrogenation of the coordinated alkynes.[15,16]

Conclusions

Despite its greater electron richness compared to $[Rh_2(CO)_3(dppm)_2]$, $[Ir_2(CO)_3(dppm)_2]$ is less prone than its dirhodium analogue to react with alkynes. This has unfortunately curtailed attempts to model the intermediates, especially hydridic species, of the alkyne-hydrogenation processes undergone by the dirhodium complex. However, this is a rare example, along with the dirhodium-phenylacetylene adduct, where a switch from parallel to perpendicular orientation of the bridging alkyne group occurs without any change in the number or identities of other ligands. In both of the diiridium and dirhodium cases, a shift to perpendicular coordination of the alkyne yields a more thermodynamically stable complex. Although this process involves a reduction in the bond order between the acetylenic carbons of the alkyne residue and a significant reorganization of the metals' coordination spheres, it may be favored due to the formation of new Ir-C and Ir-Ir bonds. The presence and relative stability of the intermediate containing the cis-dimetallated olefin unit does, however, illustrate that the attainment of the more favorable coordination geometry is not a trivial process, despite the fact that in previous studies alkyne migration about the bimetallic core had been shown to be extremely facile.

References and Footnotes

1. Collman, J. P.; Hegedus, L. S.; Norton, J. R.; Finke, R. G. *Principles and Applications of Organotransition Metal Chemistry*; University Science Books: Mill Valley, CA, 1987; Chapters 11 and 18, and references therein.
2. (a) Muetterties, E. L. *Bull. Soc. Chim. Belg.* **1975**, *84*, 953. (b) Muetterties, E. L. *Bull. Soc. Chim. Belg.* **1976**, *85*, 451. (c) Muetterties, E. L. *Angew. Chem., Int. Ed. Engl.* **1978**, *17*, 545. (d) Muetterties, E. L.; Rhodin, R. N.; Band, E.; Brucker, C. F.; Pretzer, W. R. *Chem. Rev.* **1979**, *79*, 91. (e) Sappa, E.; Tiripicchio, A.; Braunstein, P. *Chem. Rev.* **1983**, *83*, 203.
3. (a) Dewar, M. J. S. *Bull. Soc. Chim. Fr.* **1951**, *18*, C79. (b) Dewar, M. J. S. *Annu. Rep. Chem. Soc.* **1951**, *48*, 112. (c) Chatt, J.; Duncanson, L. A. *J. Chem. Soc.* **1953**, 2339. (d) Dewar, M. J. S.; Haddon, R. C.; Komornicki, A.; Rzepa, H. *J. Am. Chem. Soc.* **1977**, *99*, 377. (e) Dewar, M. J. S.; Ford, G. P. *J. Am. Chem. Soc.* **1979**, *101*, 783.
4. Hoffman, D. M.; Hoffmann, R.; Fisel, C. R. *J. Am. Chem. Soc.* **1982**, *104*, 3858.
5. Cowie, M.; Southern, T. G. *Inorg. Chem.* **1982**, *21*, 246.
6. Sutherland, B. R.; Cowie, M. *Organometallics* **1984**, *3*, 1869.
7. Cowie, M.; Dickson, R. S.; Hames, B. W. *Organometallics* **1984**, *3*, 1879.
8. Sutherland, B. R.; Cowie, M. *Organometallics* **1985**, *4*, 1801.
9. Jenkins, J. A.; Ennett, J. P.; Cowie, M. *Organometallics* **1988**, *7*, 1845.

10. McKeer, I. R.; Sherlock, S. J.; Cowie, M. *J. Organomet. Chem.* **1988**, *352*, 205.

11. Vaartstra, B. A.; Cowie, M. *Organometallics* **1989**, *8*, 2388.

12. Vaartstra, B. A.; Cowie, M. *Organometallics* **1990**, *9*, 1594.

13. Hilts, R. W.; Franchuk, R. A.; Cowie, M. *Organometallics* **1991**, *10*, 304.

14. Antonelli, D. M.; Cowie, M. *Inorg. Chem.* **1990**, *29*, 4039.

15. Kubiak, C. P.; Woodcock, C.; Eisenberg, R. *Inorg. Chem.* **1982**, *21*, 2119.

16. Berry, D. H.; Eisenberg, R. *Organometallics* **1987**, *6*, 1796.

17. Sutherland, B. R.; Cowie, M. *Organometallics* **1985**, *4*, 1637.

18. Doedens, R. J.; Ibers, J. A. *Inorg. Chem.* **1967**, *6*, 204.

19. Walker, N., Stuart, D. *Acta Crystallogr., Sect. A: Found. Crystallogr.* **1983**, *A39*, 1581.

20. Programs used were those of the Enraf-Nonius Structure Determination Package by B. A. Frenz, in addition to local programs by R. G. Ball.

21. Cromer, D. T.; Waber, J. T. *International Tables for Crystallography*; Kynoch Press: Birmingham, England, 1974; Vol. IV, Table 2.2A.

22. Stewart, R. F.; Davidson, E. R.; Simpson, W. T. *J. Chem. Phys.* **1965**, *42*, 3175.

23. Cromer, D. T.; Liberman, D. *J. Chem. Phys.* **1970**, *53*, 1891.

24. Aggarwal, R. P.; Connelly, N. G.; Crespo, M. C.; Dunne, B. J.; Hopkins, P. J.; Orpen, A. G. *J. Chem. Soc., Chem. Commun.* **1989**, 33.

25. Bird, P. H.; Fraser, A. R.; Hall, D. N. *Inorg. Chem.* **1977**, *16*, 1923.

26. (a) Sly, W. G. *J. Am. Chem. Soc.* **1959,** *81*, 18. (b) Cotton, F. A.; Jamerson, J. D.; Stults, B. R. *J. Am. Chem. Soc.* **1976,** *98*, 1774.

27. (a) See Chapter 3 of this thesis. (b) McDonald, R.; Cowie, M. *Organometallics* **1990,** *9*, 2468.

28. (a) Wang, W.-D.; Hommeltoft, S. I.; Eisenberg, R. *Organometallics* **1988,** *7*, 2417. (b) Wang, W.-D.; Eisenberg, R. *J. Am. Chem. Soc.* **1990,** *112*, 1833.

29. Cotton, F. A.; Dunbar, K. R.; Verbruggen, M. G. *J. Am. Chem. Soc.* **1987,** *109*, 5498.

30. Mague, J. T. *Inorg. Chem.* **1989,** *28*, 2215.

31. Manojlović-Muir, L.; Muir, K. A.; Frew, A. A.; Ling, S. S. M.; Thomson, M. A.; Puddephatt, R. J. *Organometallics* **1984,** *3*, 1637.

32. Bailey, N. A.; Mason, R. *J. Chem. Soc. A* **1968,** 1293.

33. Mague, J. T.; Klein, C. L.; Majeste, R. J.; Stevens, E. D. *Organometallics* **1984,** *3*, 1860.

34. (a) Kubiak, C. P.; Woodcock, C.; Eisenberg, R. *Inorg. Chem.* **1980,** *19*, 2733. (b) Sutherland, B. R.; Cowie, M. *Inorg. Chem.* **1984,** *23*, 2324. (c) Sutherland, B. R.; Cowie, M. *Can. J. Chem.* **1986,** *64*, 464. (d) Wu, J.; Reinking, M. K.; Fanwick, P. E.; Kubiak, C. P. *Inorg. Chem.* **1987,** *26*, 247. (e) McDonald, R.; Sutherland, B. R.; Cowie, M. *Inorg. Chem.* **1987,** *26*, 3333. (f) Wu, J.; Fanwick, P. E.; Kubiak, C. P. *Organometallics* **1987,** *6*, 1805. (g) Balch, A. L.; Waggoner, K. M.; Olmstead, M. M. *Inorg. Chem.* **1988,** *27*, 4511. (h) See Chapter 4 of this thesis.

35. Angoletta, M.; Bellon, P. L.; Demartin, F.; Sansoni, M. *J. Organomet. Chem.* **1981,** *208*, C12.

36. Balch, A. L.; Lee, C.-L.; Lindsay, C. H.; Olmstead, M. M. *J. Organomet. Chem.* **1979**, *177*, C22.

37. Kubiak, C. P.; Eisenberg, R. *Inorg. Chem.* **1980**, *19*, 2726.

38. Vaartstra, B. A.; Cowie, M. *Inorg. Chem.* **1989**, *28*, 3138.

39. Hommeltoft, S. I.; Berry, D. H.; Eisenberg, R. *J. Am. Chem. Soc.* **1986**, *108*, 5345.

40. (a) Jenkins, J. A.; Cowie, M., manuscript in preparation. (b) Jenkins, J. A. Ph.D. Thesis, University of Alberta, 1991, Chapter 4. (c) *Ibid.*, Chapter 5.

41. Dickson, R. S.; Pain, G. N. *J. Chem. Soc., Chem. Commun.* **1979**, 277.

42. Gagné, M. R.; Takats, J. *Organometallics* **1988**, *7*, 561.

43. Dickson, R. S.; Fallon, G. D.; Jenkins, S. M.; Nesbit, R. J. *Organometallics* **1987**, *6*, 1240.

Chapter 6

Conclusions

One of the original goals of this thesis project was to prepare and characterize heterobimetallic rhodium-iridium compounds that, aside from two bridging dppm ligands, contained only hydride and carbonyl ligands; our interest was in determining how the characteristics of the two different metals would influence the overall properties of the complexes. A series of RhIr complexes has been prepared that, as may have been expected (based on the greater strength of Ir-H and Ir-CO vs. Rh-H and Rh-CO bonds), has a greater number of members than the related Rh_2 series (which was limited to the four species $[Rh_2(CO)_3(dppm)_2]$, $[Rh_2(CO)_2(\mu\text{-H})(dppm)_2]^+$, $[Rh_2(CO)_2(\mu\text{-H})(\mu\text{-CO})(dppm)_2]^+$ and $[Rh_2(CO)_2(\mu\text{-H})_2(dppm)_2]$) but is not as extensive as the family of Ir_2 carbonyls and hydridocarbonyls (which consists of twelve compounds, ranging from the tetra- and pentacarbonyls $[Ir_2(CO)_4(dppm)_2]$ and $[Ir_2(CO)_4(\mu\text{-CO})(dppm)_2]^{2+}$ to the tetrahydride dicarbonyls $[Ir_2(H)_4(CO)_2(dppm)_2]$ and $[Ir_2(H)_4(CO)_2(dppm)_2]^{2+}$). In this and other closely-related studies on heterobimetallic rhodium-iridium compounds it has been found that the rhodium center almost always assumes a sixteen-electron configuration with a square-planar coordination geometry. The iridium center, usually eighteen-electron, is less constrained in terms of available coordination environments. In these carbonyl and hydridocarbonyl complexes the greater basicity of iridium and the greater strength of Ir-H compared to Rh-H bonds promotes formation of the $16e^-$-Rh/$18e^-$-Ir core configurations, and leads the iridium center to, whenever possible, coordinate more carbonyl or hydride ligands than the rhodium atom in the same complex. This can result in the heterobimetallic compounds taking on significantly different structures than are observed for the homobimetallic analogues, as can be clearly seen by comparing the complexes $[M_2(CO)_3(\mu\text{-}H)(dppm)_2]^+$ and $[M_2(CO)_2(\mu\text{-}H)_2\text{-}(dppm)_2]$ (M = Rh, Ir) with the respective heterobimetallic analogues, $[RhIr(CO)_3(\mu\text{-}H)(dppm)_2]^+$ and $[RhIr(H)(CO)_2(\mu\text{-}H)(dppm)_2]$. The Rh_2 and Ir_2 species possess mirror symmetry (i.e. the same number, type and disposition of ligands at both metal centers), while the Rh and Ir centers of the mixed-metal compounds assume dissimilar coordination environments, an apparent consequence of the stronger bonding of CO and H ligands to Ir, favoring terminal Ir-H and Ir-CO groups over Rh-H-Ir and Rh-CO-Ir bridges.

The strong tendency of the rhodium center of these mixed RhIr complexes to remain coordinatively unsaturated is an advantageous feature that we had planned to exploit, since it presents an incoming unsaturated organic substrate (e.g. olefin or alkyne) with an open coordination site on the complex. Whether the coordinative unsaturation on Rh could then allow access to the saturated Ir center was a matter of interest. The importance of the rhodium center in this regard is clearly seen in the CO scrambling displayed by $[RhIr(CO)_3(dppm)_2]$ and $[RhIr(CO)_3(\mu\text{-}H)\text{-}(dppm)_2]^+$. Although neither of these species is observed to undergo facile carbonyl exchange at ambient temperatures in the absence of excess carbon monoxide, under excess CO facile scrambling takes place, presumably through the respective carbonyl adducts [RhIr(CO)$_4$(dppm)$_2$] and [RhIr(CO)$_4$(μ-H)(dppm)$_2$]$^+$. Although neither of these species is stable in the absence of CO (with the tetracarbonyl hydride not actually observed, only inferred) they are both necessary to explain the scrambling observed. These adducts suggest that the first step in reactions between small molecules and RhIr species, such as those discussed herein, involves coordination at the rhodium center. The captured substrate (e.g. an alkyne or olefin) is then in a favorable position to react with ligands associated with the iridium center (e.g. one or more hydrides). Thus, although the two metal centers would not necessarily be bound simultaneously to the substrate molecule, activation of substrate can still be a cooperative process.

Although an original objective of this work had been to study the reactivity of the diiridium and mixed rhodium-iridium hydridocarbonyl species (especially towards unsaturated organic substrates), a parallel investigation of the chemistry of the formally zero-valent tricarbonyl species [MM'(CO)$_3$(dppm)$_2$] (MM' = Rh$_2$, Ir$_2$, RhIr) proved to be particularly interesting, and was ultimately pursued at the expense of the chemistry of the diiridium and rhodium-iridium hydridic species. These tricarbonyl compounds were readily obtained from the neutral hydridocarbonyl complexes mentioned earlier by reaction with CO. Shortly after commencement of this work the structure of [Rh$_2$(CO)$_3$(dppm)$_2$] was published by Eisenberg and coworkers, showing it to be quite unlike the "A-frame" configurations commonly seen in the chemistry of bis(dppm)-bridged binuclear compounds. This structure, and that of [RhIr(CO)$_3$(dppm)$_2$], determined in this work, suggest that these complexes possess mixed-valence M(I)-M′(-I) cores, built-in coordinative unsaturation at the M(I) centers, and dative M′(-I)→M(I) bonds. The low oxidation states at both metals and the open coordination site at one center suggested that these species would be especially susceptible to oxidative-addition reactions, which might yield useful information about the roles of adjacent metals in such processes. We had already determined that the Ir_2 and RhIr compounds oxidatively add H_2 to yield the aforementioned hydridic species, so investigations of oxidative additions of substrates of the form H_2X (X = S, Se, SiRR′) seemed to be a natural extension to this work. Our primary interest was to attempt to utilize both metals to activate both geminal X-H bonds, and to establish how the adjacent centers were involved in such activation.

Through use of variable-temperature multinuclear NMR spectroscopy, it has been shown that reactions between H_2X-type molecules and $[Ir_2(CO)_3(dppm)_2]$ (the best-studied member of the series) appear to have a common initial step, that being the attack of one X-H bond upon the coordinatively-unsaturated Ir(I) center to form the unstable intermediate, $[Ir_2(H)(XH)(CO)_3(dppm)_2]$. In the case of H_2S or H_2Se it is reasonable to propose that coordination of the intact substrate to the Ir(I) center through a donor electron pair (to form $[Ir_2(XH_2)(CO)_3(dppm)_2]$) occurs as a prelude to the oxidative-addition process. In the initial stages of the reaction the adjacent, coordinatively saturated Ir(-I) center seems to act as a source of electron density; the dative Ir(-I)→Ir(I) bond appears to especially enhance the ability of the Ir(I) center to undergo X-H bond addition, making this nucleus more electron-rich than it would normally be. Involvement of the second metal (the original Ir(-I)) requires loss of a carbonyl ligand, and the coordinative unsaturation thus generated can be readily alleviated by interaction with the substrate moiety already attached to the adjacent center. Oxidative addition at the second metal then rapidly follows. In the case of addition of H_2S to $[Rh_2(CO)_3(dppm)_2]$ the hydrido intermediates are not observed, presumably due to the lability of these species and the apparently facile reductive elimination of H_2. However, the diiridium system, for which several hydridic intermediates were spectroscopically characterized, would appear to serve as a good model of the rapid addition, rearrangement and elimination processes undergone by the dirhodium analogue.

The significant differences between the chemistry of the heterobinuclear species and that of the homobinuclear analogues are clearly seen in the reactivity of $[RhIr(CO)_3(dppm)_2]$ towards H_2S, H_2Se and silanes. The homobinuclear complexes undergo facile oxidative addition of both geminal heteroatom-hydrogen bonds to yield the respective sulfido-, selenido- and silylene-bridged products. In contrast, oxidative addition of only one S-H or Se-H bond of H_2S or H_2Se to the RhIr species occurs, yielding sulfhydryl hydride and selenohydryl hydride products. Oxidative addition at Ir has apparently taken place in each case, although oxidative addition at Rh followed by facile rearrangement cannot be ruled out. If oxidative addition *has* occurred at Ir, the question arises as to how the required coordinative unsaturation at this metal is generated. The labile tetracarbonyl $[RhIr(CO)_4(dppm)_2]$ (the CO adduct of $[RhIr(CO)_3(dppm)_2]$) was found to scramble carbonyls over both metal centers, and this species is isoelectronic with [RhIr(H_2S)$(CO)_3$$(dppm)_2$], the proposed initial H_2S adduct of [RhIr$(CO)_3$$(dppm)_2$]. Exchange of hydrogen sulfide and one carbonyl between the metals would place H_2S on Ir in a position to undergo S-H activation by this metal. The second sulfur-hydrogen bond remains unactivated by the rhodium center, which may be due to the fact that in the final product, [RhIr(H)$(CO)_2$(μ-SH)$(dppm)_2$], Rh has attained its preferred sixteen-electron square-planar configuration.

The reactions of [RhIr$(CO)_3$$(dppm)_2$] with silanes were also very different from those involving the dirhodium and diiridium analogues, which cleanly yielded silylene-bridged products in most cases. With the RhIr species complex mixtures of products were obtained in all cases. This is not unlike the results of silane addition to [RhRe$(CO)_4$$(dppm)_2$], which also gave a multitude of products.[1] The reasons for these differences are as yet unclear, and given the ease of reactivity these reactions should be reinvestigated at low temperatures.

The reactions of [$Ir_2$$(CO)_3$$(dppm)_2$] with thiols and selenols were undertaken in an attempt to isolate and characterize stable adducts modelling early intermediates in the reaction with H_2S or H_2Se that contain only one oxidatively-added S-H or Se-H bond. Such species were not observed under ambient conditions, and the products formed contained two thiolates or selenolates, three carbonyls and no hydride groups. Variable-temperature NMR studies have indicated that attack of the substrate at the d^8 Ir(I) nucleus is again the initial step. The electron-richness of the second Ir center is now important in that the intermediate thus formed, [Ir_2(H)(XR)$(CO)_2$(μ-CO)$(dppm)_2$] (X = S, Se), is receptive to the addition of a second X-H bond that, unlike the case for the H_2X substrates, is not already incorporated in the complex; however, this center is still coordinatively saturated and must still undergo loss of CO before the second addition can take place. This infers the formation of a dicarbonyl intermediate, which was never observed, even at low temperature. Stable analogous rhodium thiolate complexes, $[Rh_2(SR)_2(CO)_2(\mu\text{-}CO)(dppm)_2]$, were not obtained, which may not be surprising since such species might be expected to be even more prone to decomposition via CO loss than the compound $[Ir_2(SEt)_2(CO)_2(\mu\text{-}CO)(dppm)_2]$ has proven to be.

Although the initial species in the reaction between the activated alkyne, dimethyl acetylenedicarboxylate (DMAD), to $[Ir_2(CO)_3(dppm)_2]$ were not observed as were those in the oxidative additions of silanes and sulfur/selenium-hydrogen substrates, it seems reasonable to propose that the initial steps of this reaction are similar. The first intermediate would be formed by coordination of the alkyne in an η^2 fashion at the Ir(I) center; such a species, $[Ir_2(CO)_3(\eta^2\text{-}DMAD)(dppm)_2]$, would likely possess a static structure comparable to those of $[Co_2(CO)_4\{(MeO)_2PN(Me)P(OMe)_2\}_2]$,[2] $[Co_2(CO)_4\{(CH_2O)_2PN(Et)P(OCH_2)_2\}_2]$[3] and $[Ir_2(CO)_4(dmpm)_2]$,[4] which are very similar to those of $[Rh_2(CO)_3(dppm)_2]$ and $[RhIr(CO)_3(dppm)_2]$ except that an extra CO ligand is bound to the M(I) center, resulting in an eighteen-electron trigonal bipyramidal configuration at this metal. It has been shown that, in solution, $[Ir_2(CO)_4(dmpm)_2]$ undergoes interchange of the four inequivalent terminal carbonyl ligands via formation of a doubly-bridged intermediate, $[Ir_2(CO)_2(\mu\text{-}CO)_2(dmpm)_2]$;[4] rearrangement of the species $[Ir_2(CO)_3(\eta^2\text{-}DMAD)(dppm)_2]$ in an analogous fashion to form [Ir_2-

$(CO)_2(\mu\text{-}CO)(\mu\text{-}\eta^1{:}\eta^{1'}\text{-}DMAD)(dppm)_2]$, followed by elimination of the bridging carbonyl, would yield the first product observed, $[Ir_2(CO)_2(\mu\text{-}\eta^1{:}\eta^{1'}\text{-}DMAD)(dppm)_2]$. The lack of reaction between nonactivated alkynes and $[Ir_2(CO)_3(dppm)_2]$ is unlike the reactivity, described by Eisenberg and coworkers, of these substrates towards $[Rh_2(CO)_3(dppm)_2]$. In the present case, elimination of coordinated alkyne from the tricarbonyl intermediates mentioned above may be a more favorable process than loss of a carbonyl ligand, unless the alkyne is sufficiently π-acidic to bond as strongly to iridium as does CO. Presumably the carbonyl ligands are less tightly bound to the less basic rhodium atoms, and would therefore be more susceptible to substitution by even poor π-acceptor ligands.

An important overall result of this study has been the crystallographic characterization of several complexes displaying the dppm ligands in coordination modes other than the most commonly-observed form, trans at both metal centers. Of the five compounds in this thesis for which structures were determined, three were found to have the diphosphines disposed cis at both metals, while one showed cis diphosphine coordination at one nucleus and trans at the other. Before commencement of this project, no examples of dirhodium and diiridium dppm complexes containing *cis,cis-* or *trans,cis*-$M_2(dppm)_2$ frameworks were known, but the structures described herein, as well as those of $[Rh_2(CO)_3(dppm)_2]$, $[Rh_2(CO)_2(\mu\text{-}\eta^2{:}\eta^{2'}\text{-}PhCCPh)(dppm)_2]$ and $[Rh_2(CO)_2(\mu\text{-}SiHR)_2(dppm)_2]$ (R = Et, Ph) as determined by Eisenberg and coworkers, illustrate the accessibility of such configurations in this family of complexes.

This study has clearly shown that the low-valent complexes of interest are active towards oxidative addition and that *both* metals can be involved in the double activation of either geminal X-H bonds (of H_2S, H_2Se and H_2SiRR') or of X-H bonds of two substrate molecules (RSH, RSeH). The idea that the starting complexes can be formulated as mixed-valence M(I)/M'(-I) systems seems quite reasonable. Throughout this work it had been the idea that the metal in the -1 oxidation state functioned as a good donor of electron density to the adjacent M(I) center, enhancing the susceptibility of the latter towards oxidative addition. This view has recently found support from the results of the reaction of $[Ir_2(CO)_3(dppm)_2]$ with the strong alkylating agent methyl triflate ($CH_3SO_3CF_3$). Rather than yielding the expected cationic methyl compound, an unusual example of C-H activation of the methyl group has taken place to yield $[Ir_2(H)(CO)_3(\mu\text{-}CH_2)(dppm)_2]^+$, which contains a bridging methylene group and a terminal hydride ligand.[5] Although the mechanistic details of this activation are unknown, it is assumed that the methyl group is carbon-bound to one metal while activation of a C-H bond by the adjacent metal occurs, presumably through an agostic C-H-Ir interaction. Activation of C-H bonds of neutral organic molecules, however, would be expected to be much less favored (with orthometallation of a dppm phenyl ring, as was the case for the compound $[IrOs(H)_2(CO)_3(\mu\text{-}\eta^3\text{-}(o\text{-}C_6H_4)PhPCH_2PPh_2)(dppm)]$, a more likely result), but the reactivity of the $[MM'(CO)_3(dppm)_2]$ compounds towards substrates containing carbon- or silicon-halogen bonds is worthy of investigation. Further studies of the reactivity of the hydridocarbonyl species, especially the coordinatively unsaturated dihydrides $[Ir_2(CO)_2(\mu\text{-}H)_2(dppm)_2]$ and $[RhIr(H)(CO)_2(\mu\text{-}H)(dppm)_2]$, towards olefins and alkynes should also be pursued, particularly in light of the ability of [Rh_2-$(CO)_2(\mu$-$H)_2(dppm)_2$] to hydrogenate such substrates. A potentially more challenging direction would be to extend the chemistry of the diiridium and rhodium-iridium hydridocarbonyls from these dppm-bridged species to systems containing the more basic dmpm ligand. Such chemistry would build upon that already developed within this group and by Kubiak and coworkers,[4] and would provide the opportunity of studying oxidative-addition reactions and coordination and conversion of unsaturated organic molecules with a more electron-rich, less sterically hindered binuclear framework.

References and Footnotes

1. Antonelli, D. M.; Cowie, M., unpublished observations.
2. Brown, G. M.; Finholt, J. E.; King, R. B.; Bibber, J. W. *Inorg. Chem.* **1982**, *21*, 2139.
3. De Leeuw, G.; Field, J. S.; Haines, R. J. *J. Organomet. Chem.* **1989**, *359*, 245.
4. (a) Reinking, M. K. Ph.D. Thesis, Purdue University, 1989, Chapter 3. (b) Kubiak, C. P., private communication.
5. Antwi-Nsiah, F.; Cowie, M., unpublished observations.

Appendix

Solvents and Drying Agents

Benzene	Sodium metal
Dichloromethane	Phosphorus pentoxide
Diethyl ether	Sodium benzophenone ketyl
Hexanes	Sodium-potassium alloy
Methanol	Sodium metal
Nitromethane	4A Molecular sieves
Tetrahydrofuran	Sodium benzophenone ketyl
Toluene	Sodium metal